Applications of the Coupled Cluster Method to Pairing Problems

A thesis submitted to the University of Manchester
for the degree of Doctor of Philosophy in the
Faculty of Engineering and Physical Sciences
2010

Christopher Snape

School of Physics and Astronomy

Contents

1 Introduction and Literature Review **13**

1.1 Introduction 13

1.1.1 The Origins of Quantum Theory 13

1.1.2 The Quantum Many-Body Problem 17

1.2 Quantum Many-Body Methods 20

1.2.1 Perturbation Theory 20

1.2.1.1 Time-Independent Perturbation Theory 21

1.2.1.2 Time-Dependent Perturbation Theory 27

1.2.2 The Variational Method 29

1.2.2.1 The Hartree-Fock Approximation 31

1.2.3 Independent Cluster Methods 33

1.2.3.1 The Configuration Interaction Method 35

1.2.3.2 The Coupled Cluster Method 36

1.3 Outline of Thesis 39

1.4 Literature Review 40

1.4.1 Origins of the CCM 40

1.4.2 Formal Developments of the CCM 41

1.4.3 Pairing in Atomic and Nuclear Many-Body Systems 45

2 The Coupled Cluster Method Formalism **51**

2.1 The Normal Coupled Cluster Method 52

2.1.1 The Model State 52

2.1.2 Ket Ground-State Wave Function 55

2.1.3 Ground-State Energy 56

2.1.4 Bra Ground-State Wave Function 58

2.1.5 NCCM Equations 60

2.1.6 Time-Independent Bivariational Principle 61

2.1.7 Excited-States (Emrich Scheme) 62

2.1.8 Time-Dependent Bivariational Principle 64

2.1.9 Excited-State Energies (RPA Scheme) 65

2.1.10 Truncation and Approximation 69

2.2 The Extended Coupled Cluster Method . . . 71
2.2.1 Ground-State Energy Functional . . . 71
2.2.2 ECCM Equations . . . 72
2.2.3 Equations of Motion . . . 73
2.3 Applications to Many-Fermion Systems with Pairing . . . 75
2.3.1 Hamiltonian for s-wave Pairing . . . 75
2.3.2 SUB(1) ECCM Calculation . . . 76
2.3.2.1 Hartree-Fock Model State . . . 77
2.3.2.2 Pairing Cluster Correlation Operators . . . 77
2.3.2.3 Ground-State Energy Functional . . . 78
2.3.2.4 The Hartree-Fock-Bogoliubov Method . . . 80
2.3.2.5 Ground-State Energy Functional Revisited . . . 82
2.3.2.6 SUB(1) ECCM Result . . . 83
2.3.2.7 BCS Solutions and the Gap Equation . . . 87
2.3.2.8 SUB(1) ECCM Solutions . . . 88
2.3.3 Quasi-Particle Basis . . . 91

3 Illustrative Applications of the Coupled Cluster Method to Simple Models 93
3.1 The Quartic Anharmonic Oscillator . . . 93
3.1.1 Normal Coupled Cluster Method . . . 96
3.1.1.1 SUB(1) Calculation . . . 97
3.1.1.2 SUB(2) Mathematica Code . . . 102
3.1.1.3 Binomial Routine . . . 110
3.1.1.4 Excited-State Energies . . . 113
3.1.2 Extended Coupled Cluster Method . . . 116
3.1.2.1 SUB(1) Calculation . . . 117
3.1.2.2 SUB(2) Calculation . . . 118
3.2 The Double-Well Quartic Anharmonic Oscillator . . . 120
3.2.1 Normal Coupled Cluster Method . . . 124
3.2.1.1 SUB(n) Calculations . . . 125
3.2.1.2 Alternative Approaches . . . 130
3.2.2 Extended Coupled Cluster Method . . . 133
3.2.2.1 SUB(1) and SUB(2) Calculations . . . 133
3.3 Discussion . . . 135

4 Single-Shell Pairing 136
4.1 The Model . . . 136
4.1.1 SU(2) Quasi-Spin Algebra . . . 138
4.1.2 Exact Ground-State Solution . . . 140

4.2 Extended Coupled Cluster Method 141
4.2.1 Particle SUB(1) Calculation 141
4.2.2 Particle SUB(n) Calculation 144
4.2.3 Quasi-Particle QPSUB(2) Calculation 148
4.2.4 Quasi-Particle QPSUB(n) Calculation 155
4.2.5 RPA Calculation (Solution Stability Analysis) 158
4.2.5.1 Time Derivatives 159
4.2.5.2 RPA Results 161
4.3 Discussion 163

5 Pairing between Fermionic Atoms of an Ultracold Dilute Gas confined in an Ellipsoidal Harmonic Trap 165
5.1 The Model 166
5.1.1 One-Body Term $\hat{H}_0$ 167
5.1.2 Two-Body Term $\hat{H}_1$ 170
5.2 Extended Coupled Cluster Method 172
5.2.1 SUB(1) Calculation 172
5.2.1.1 Normal Density 173
5.2.1.2 Abnormal Densities 174
5.2.1.3 Ground-State Energy Functional and ECCM Equations 175
5.2.1.4 C++ Code (Solving the ECCM Equations) 177
5.2.1.5 Mathematica Code (Diagonal Approximation) 178
5.2.1.6 Diagonal Approximation Results 180
5.3 Collective Modes 184
5.3.1 SUB(2) Calculation 184
5.4 Discussion 185

6 Summary and Conclusions 187

Word Count: 50,183

List of Figures

1.1 All first and second order Goldstone diagrams which contribute to ΔE in a uniform Fermi system. 24

1.2 Example of a disconnected second order Goldstone diagram for a uniform Fermi system. 27

1.3 Example of a disconnected third order Goldstone diagram for a uniform Fermi system. 27

1.4 Pictorial representation of the BCS-BEC crossover in an ultracold dilute gas of fermionic atoms. The left hand side shows the BCS-like state, where atomic Cooper pairs are separated by distances much greater than the mean interparticle spacing of the atoms in the gas (thus many such pairs may overlap in this regime). The right hand side shows the BEC state of tightly bound diatomic molecules - in the so-called "deep BEC" limit it is practically impossible to resolve any internal structure of these molecules, thus they essentially behave as point-like bosons of spin 0. The directional arrows in between the two regimes represent the process is tunable, i.e. it is possible to tune the system back and forth between the two regimes. This picture has been adapted from the front cover of [102]. 48

3.1 Plot of $E_0(\lambda)$ vs λ using the SUB(1) NCCM approximation. 101

3.2 Plot of $E_0(\lambda)$ vs λ using the SUB(2) NCCM approximation. 103

3.3 Plot of $E_0(\lambda)$ vs λ using the SUB(4) NCCM approximation. 108

3.4 Plot of $E_0(\lambda)$ vs λ using the SUB(7) NCCM approximation. 111

3.5 Plot of the double-well potential $V(x) = \frac{1}{2}(-kx^2 + x^4)$ for $k = 0$ (blue), $k = 1$ (red), $k = 2$ (yellow) and $k = 5$ (green). 121

3.6 Plot of the shifted double-well potential $V_s(x) = \frac{1}{2}\left(x^2 - \frac{1}{2}k\right)^2$ for $k = 0$ (blue), $k = 1$ (red), $k = 2$ (yellow) and $k = 5$ (green). 122

3.7 Plot of $E_0(k)$ vs k using the SUB(1) NCCM approximation. 126

3.8 Plot of $E_0(k)$ vs k using the SUB(3) NCCM approximation. 126

3.9 Plot of $E_0(k)$ vs k using the SUB(5) NCCM approximation. 127

4.1 Plot of E_0 vs N_0 for the exact (dashed) and BCS/SUB(1) ECCM (red) solutions using $\Omega = 10$ and $G = 1$. 144
4.2 Plot of E_0 vs N_0 (upper panels) and particle number fluctuation ΔN^2 vs N_0 (lower panels) for the exact (dotted) and particle SUB(1)-SUB(4) ECCM solutions using $\Omega = 4$ and $G = 1$. 146
4.3 Plot of E_0 vs N_0 (upper panels) and particle number fluctuation ΔN^2 vs N_0 (lower panels) for the exact (dotted) and particle SUB(2) ECCM solutions using various values of Ω and $G = 1$. 147
4.4 Plot of $\Delta E = E_0 - E_0^{exact}$ vs N_0 for particle SUB(1)-SUB(4) ECCM solutions using $\Omega = 10$ and $G = 1$. We compare different orders of approximation using either empty ($\big|0\big\rangle$) or full ($\big|\mathrm{HF}\big\rangle$) model states. . . 148
4.5 Plot of E_0 vs N_0 for the exact (dashed), BCS/SUB(1) ECCM (red) and quasi-particle QPSUB(2) ECCM (blue) solutions using $\Omega = 10$ and $G = 1$.154
4.6 Plot of E_0 vs N_0 (upper panels) and particle number fluctuation ΔN^2 vs N_0 (lower panels) for the exact (dotted) and quasi-particle QPSUB(2) ECCM solutions using various values of Ω and $G = 1$. 155
4.7 Plot of E_0 vs N_0 (upper panels) and particle number fluctuation ΔN^2 vs N_0 (lower panels) for the exact (dotted) and quasi-particle QPSUB(2) NCCM solutions using various values of Ω and $G = 1$. 155
4.8 Plot of E_0 vs N_0 for quasi-particle QPSUB(2)-QPSUB(5) ECCM solutions using $\Omega = 10$ and $G = 1$. We compare different orders of approximation using either empty ($\big|0\big\rangle$) or full ($\big|\mathrm{HF}\big\rangle$) model states. 156
4.9 Plot of $\Delta E = E_0 - E_0^{exact}$ vs N_0 for quasi-particle QPSUB(2)-SUB(5) ECCM solutions using $\Omega = 10$ and $G = 1$. We compare different orders of approximation using either empty ($\big|0\big\rangle$) or full ($\big|\mathrm{HF}\big\rangle$) model states. . 157
4.10 Plot of E_0 vs N_0 for quasi-particle QPSUB(2)-QPSUB(5) NCCM solutions using $\Omega = 10$ and $G = 1$. We compare different orders of approximation using either empty ($\big|0\big\rangle$) or full ($\big|\mathrm{HF}\big\rangle$) model states. 157
4.11 Plot of RPA frequencies ω vs N_0 for particle SUB(2)-SUB(5) ECCM solutions using $\Omega = 10$ and $G = 1$. 162
4.12 Plot of RPA frequencies ω vs N_0 for quasi-particle QPSUB(2)-QPSUB(5) ECCM solutions using $\Omega = 10$ and $G = 1$. 162

5.1 Plot of a disk shaped trap potential $\hat{V}_{\mathrm{ho}} = \frac{1}{2}m\big(\omega_\perp^2 x^2 + \omega_\perp^2 y^2 + \omega_z^2 z^2\big) = 1$, with $m = 1$, $\omega_\perp = \frac{1}{10}$ and $\omega_z = 4$. 169
5.2 Plot of a cigar shaped trap potential $\hat{V}_{\mathrm{ho}} = \frac{1}{2}m\big(\omega_\perp^2 x^2 + \omega_\perp^2 y^2 + \omega_z^2 z^2\big) = 1$, with $m = 1$, $\omega_\perp = 4$ and $\omega_z = \frac{1}{10}$. 170

5.3 Plot of Gaussian potential strength $-V_0\sigma^2$ vs the s-wave scattering length σ/a_s for $\sigma = 0.01$. For a predetermined value of a_s we can find the corresponding strength V_0 from this graph. 180
5.4 Plot of occupation probability v_k^2 vs single-particle energy ϵ_k in a cigar shaped trap ($\omega_\perp = 1.6$, $\omega_z = 0.251$, $\lambda = 0.16$) for $N_0 = 100$ particles and $\sigma = 0.05$. The top picture shows the BCS regime ($\sigma/a_s = -0.5$), the middle picture shows the BEC regime shortly after crossover ($\sigma/a_s = 1$) and the bottom picture shows the deep BEC regime ($\sigma/a_s = 100$). . . 182
5.5 Plot of occupation probability v_k^2 vs single-particle energy ϵ_k in a disk shaped trap ($\omega_\perp = 0.61$, $\omega_z = 1.6$, $\lambda = 2.62$) for $N_0 = 100$ particles and $\sigma = 0.05$. The top picture shows the BCS regime ($\sigma/a_s = -0.5$), the middle picture shows the BEC regime shortly after crossover ($\sigma/a_s = 1$) and the bottom picture shows the deep BEC regime ($\sigma/a_s = 100$). . . 183

List of Tables

3.1 SUB(1) NCCM ground-state energy $E_0(\lambda)$ for various values of λ. . . 101
3.2 Ground-state energy $E_0(\lambda)$ and cluster amplitudes s_2 and s_4 for various values of small λ along the unphysical SUB(2) solution branch. 105
3.3 Ground-state energy $E_0(\lambda)$ and cluster amplitudes s_2 and s_4 for various values of small λ along the physical SUB(2) solution branch. 106
3.4 SUB(2)-SUB(5) NCCM ground-state energy $E_0(\lambda)$ for various values of λ. 109
3.5 SUB(6)-SUB(10) NCCM ground-state energy $E_0(\lambda)$ for various values of λ. 112
3.6 SUB(2)-SUB(5) NCCM excited-state energies ε_2 and ε_4 for various values of λ. 116
3.7 SUB(1) ECCM ground-state energy $E_0(\lambda)$ for various values of λ. . . . 118
3.8 SUB(2) ECCM ground-state energy $E_0(\lambda)$ for various values of λ. . . . 120
3.9 SUB(1)-SUB(5) NCCM ground-state energy $E_0(k)$ for various values of k. 128
3.10 SUB(1)-SUB(5) NCCM ground-state energy $E_0(k)$ for various values of k using squeezed vacuum state $|0_\alpha\rangle$. 132
3.11 SUB(1) and SUB(2) ECCM ground-state energy $E_0(k)$ for various values of k. 134

Abstract

The University of Manchester

Faculty of Engineering and Physical Sciences

ABSTRACT OF THESIS submitted by **Christopher Snape** for the degree of **Doctor of Philosophy** and entitled **Applications of the Coupled Cluster Method to Pairing Problems**.

Date of submission: **17/02/10**

The phenomenon of pairing in atomic and nuclear many-body systems gives rise to a great number of different physical properties of matter, from areas as seemingly diverse as the shape of stable nuclei to superconductivity in metals and superfluidity in neutron stars. With the experimental realisation of the long sought BCS-BEC crossover observed in trapped atomic gases - where it is possible to fine tune the s-wave scattering length a_s of a many-fermion system between a dilute, correlated BCS-like superfluid of Cooper pairs and a densely packed BEC of composite bosons - pairing problems in atomic physics have found renewed interest in recent years. Given the high precision techniques involved in producing these trapped gas condensates, we would like to employ a suitably accurate many-body method to study such systems, preferably one which goes beyond the simple mean-field picture.

The Coupled Cluster Method (CCM) is a widely applied and highly successful *ab initio* method in the realm of quantum many-body physics and quantum chemistry, known to be capable of producing extremely accurate results for a wide variety of different many-body systems. It has not found many applications in pairing problems however, at least not in a general sense. Our aim, therefore, is to study various models of pairing using a variety of CCM techniques - we are interested in studying the generic features of pairing problems and in particular, we are especially interested in probing the collective modes of a system which exhibits the BCS-BEC crossover, in either the BCS or BEC limit. The CCM seems a rather good candidate for the job, given the high precision results it can produce.

Declaration

No portion of the work referred to in the thesis has been submitted in support of an application for another degree or qualification of this or any other university or other institute of learning.

Copyright Statement

1. The author of this thesis (including any appendices and/or schedules to this thesis) owns certain copyright or related rights in it (the "Copyright") and s/he has given the University of Manchester certain rights to use such Copyright, including for administrative purposes.

2. Copies of this thesis, either in full or in extracts and whether in hard or electronic copy, may be made **only** in accordance with the Copyright, Designs and Patents Act 1988 (as amended) and regulations issued under it or, where appropriate, in accordance with licensing agreements which the University has from time to time. This page must form part of any such copies made.

3. The ownership of certain Copyright, patents, designs, trade marks and other intellectual property (the "Intellectual Property") and any reproductions of copyright works in the thesis, for example graphs and tables ("Reproductions"), which may be described in this thesis, may not be owned by the author and may be owned by third parties. Such Intellectual Property and Reproductions cannot and must not be made available for use without the prior written permission of the owner(s) of the relevant Intellectual Property and/or Reproductions.

4. Further information on the conditions under which disclosure, publication and commercialisation of this thesis, the Copyright and any Intellectual Property and/or Reproductions described in it may take place is available in the University IP Policy (see http://www.campus.manchester.ac.uk/medialibrary/policies/intell - ectualproperty.pdf), in any relevant Thesis restriction declarations deposited in the University Library, The University's regulations (see http://www.manchester. - ac.uk/library/aboutus/regulations) and in The University's policy on presentation of Theses.

Acknowledgments

First and foremost I would like to express my gratitude and thanks towards my Ph.D. supervisor Prof. Niels Walet. Without his guidance and support over the past four years this thesis would not have been possible. I am indebted to him for all the help he has given me in realising this body of work and thank him for his dedication and patience.

I thank all of the staff in the Theoretical Physics department at Manchester. It has been a pleasure to work alongside you and I thank you all for your help along the way, regardless of how big or small it may have been.

Thanks go to my friends (in particular, Chris and Mike for helping to keep me sane - Andy's raised his prices by how much? E set with salmon and tuna? Rainbow rolls? Refill?) and family who have stood by me over the last four years. Some years have simply flown by and some have been a hard fought struggle. I thank you all for your belief in me and the words of encouragement you have offered.

Finally, an extra special thank you must go to Tejal for her continued and unyielding support throughout the duration of my Ph.D. - particularly over the past year or so where situations have been their most trying. I hope I was able to offer you at least some support whilst you were writing too and wish you the best of luck in the future.

Chapter 1

Introduction and Literature Review

1.1 Introduction

A little over one hundred years ago, the field of physics which studies systems and interactions which take place on the very small scale[1] had yet to be formally developed. The areas of physics that today we call quantum mechanics and quantum field theory did not exist. It was certain perplexities of the time, which could not be readily explained by the known principles of classical physics, which were to lead down the path of a radical rewriting of physics notions and ultimately the birth of *quantum theory*.

1.1.1 The Origins of Quantum Theory

With the advent of Einstein's explanation of the photoelectric effect in 1905 [1] (a phenomenon discovered experimentally by Hertz in 1887 [2]) physicists of the time gradually began to realise that traditional Newtonian laws that governed the physics of every day situations could no longer be applied to situations happening on extremely small scales. In fact it would soon become apparent that the classical view of the world would seemingly have no connection to that of interacting atoms, molecules and elementary particles, besides providing a sensible limit as to how a small system should behave if it were somehow blown up to our every day proportions (the so-called *correspondence principle* - all quantum systems must tend towards a classical picture at extremely large size [2]).

Einstein's description of light being comprised of small particles called *photons*, which each contained a small, discrete, *quantised* amount of energy was completely at odds with Maxwell's classical wave description of electromagnetic radiation, a sound and widely accepted theory at the time. In fact, Einstein had utilised elements of Planck's earlier study of black-body radiation, published in 1901 [3], in which Planck

[1] where we quantify "small" to be *submicroscopic* or equivalently at the *atomic level.*

himself suggested that light behaves as a stream of small packets of specific energy. Planck's theory, which also introduced the fixed number h (a number Planck believed was a fundamental and universal constant, something which has since become known as *Planck's constant*) was an attempt to explain the so-called "ultraviolet catastrophe"[2] which had arisen in the latter half of the 19^{th} Century as a consequence of trying to understand black body radiation on the basis of classical wave mechanics.

By modeling light as being made up of a stream of massless particles, where each individual particle contained the quantised amount of energy $E = h\nu$, (where ν is the frequency of the light source) Einstein's theory of the photoelectric effect correctly explained why the photo-electrons emitted from a metal sheet when irradiated by a light source of fixed frequency have a *range* of kinetic energies, as opposed to all having the same energy (as classical wave theory would predict). The photo-electrons emitted from the metal are liberated with a spectrum of energies, dependent on how deep they are located away from the surface of the metal [2]. All of the electrons within the metal receive the same initial amount of energy from each photon ($h\nu$) but after this energy absorption, the photo-electron must do work in order to be liberated from the metal. This work, commonly known as the work function ϕ, varies depending on how far the initial electron is away from the surface of the metal. Thus we can write the kinetic energy of emitted photo-electrons T_e as

$$T_e = h\nu - \phi,$$

where ϕ is particular to the metal used. This description explains why there is a threshold frequency ν_0, below which no photo-electron emission will be observed - the value of $h\nu$ must obviously be greater than that of ϕ for emission to take place, hence we may write the work function explicitly as $\phi = h\nu_0$ and thus

$$T_e = h\left(\nu - \nu_0\right).$$

The spectrum of emitted photo-electron kinetic energies is *not* dependent on the intensity of the incident light since increasing the intensity simply increases the *amount* of photons impinging on the metal, which in turn will only increase the *amount* of photo-electrons liberated [2].

Einstein's theoretical predictions were later verified by experimental evidence and for this work he earned himself the Nobel Prize for physics in 1921 (Planck was to receive it in 1918 for his initial study of black body radiation). Thus, the period of time between Hertz's discovery of the photoelectric effect in 1887 and Einstein's correct theoretical description of it in 1905 is widely regarded as the genesis of what we call

[2] a problem concerning the power spectrum radiated by black bodies [2].

quantum theory today. In solving the peculiarities of the photo-electric effect, Einstein had rigorously shown that on small scales, atomic and elementary particles possess the strange property of wave-particle duality, i.e. they simultaneously possess properties of both waves and particles, something which appears completely contradictory. Furthermore, Einstein had therefore shown that Maxwell's electromagnetic wave equations *also* describe the dynamics of atomic and elementary particles.

Nowadays it is perhaps hard to imagine how revolutionary this new branch of physics appeared at the time. This strange, unintuitive and radically different approach to physics was not met with universal optimism however, indeed many did not believe Einstein's theory of the photoelectric effect until its predictions could be proven experimentally. Along with black body radiation and the photoelectric effect, further examples of quantum theory were discovered shortly, and contributions from Bohr [4, 5] (who formulated a somewhat naive first quantum model of Hydrogen and studied the emission of line-spectra from Hydrogen), Compton [6] (whose work with X-ray scattering led to the discovery of the so-called Compton effect - the deflection of x-rays through crystal structures, further proof of the particle-like nature of electromagnetic radiation) and de Broglie [7] (who proposed that all matter possessed wave-particle duality on the submicroscopic level) would further verify Planck's and Einstein's initial work in the field.

Soon enough, the formal implications of this new theory of small systems were expressed and collectively written down in a joint collaboration between Heisenberg, Born and Jordan [8], in which they extended ideas put forth by Bohr and produced the "matrix mechanics" formulation of quantum systems. Shortly afterward, Schrödinger produced his own description of quantum systems in the form of "wave mechanics" and the Schrödinger equation [9] (a differential equation for the so-called *wave function* of a quantum particle, which would calculate the allowed energy eigenvalues and eigenstates of such a particle). In the same year as his publication on wave mechanics (1926), Schrödinger also showed that his interpretation of quantum mechanics was identical to that of Heisenberg's [10]. Dirac [11] would further cement this theory by his introduction of abstract Hilbert space formalism and use of his entirely general "Dirac notation", although this was not formally presented until 1939 [12].

Dirac's abstract Hilbert space formalism as well as the matrix and wave mechanics of Heisenberg, Born, Jordan and Schrödinger respectively, coherently became grouped under the general title of "quantum theory". It became an inescapable fact that matter behaved completely differently on the quantum level compared to that of the classical realm and as such, required an entirely different mathematical formalism, based on postulates, operators, probabilities, observables and many other nonclassical concepts. Not long after Schrödinger's formulation of wave mechanics, Dirac managed to successfully unite special relativity with quantum mechanics in his work on the electron

[13] - the result being the quantum theory of fields rather than particles, something we usually call quantum field theory today. His equations also seemed to predict something described as antimatter - this was to be discovered a few years later in the form of the positron, the antiparticle of the electron [14].

With the core groundwork established for quantum mechanics and quantum field theory in the early half of the 20^{th} century, further experimental and theoretical advances in both of these fields continued unabated into the latter half of the 20^{th} century. The Standard Model (SM) of modern particle physics[3], is essentially built upon the field theories of quantum electrodynamics (or QED - the study of electromagnetic interactions between electrons, positrons and photons) and to a lesser extent quantum chromodynamics (or QCD - the study of strong nuclear interactions between quarks and gluons) [15]. At large enough energy scales of the SM, the electromagnetic and weak nuclear interaction may be unified into a single formalism, the so-called *electroweak* theory [15]. One of the current goals for high-energy physicists is "grand unification" - which seeks to reconcile the elementary forces of gravity, electromagnetism, the weak and strong nuclear forces respectively, into a single *unified* formalism.

A unification of *general relativity* and quantum mechanics, similar to that between special relativity and quantum mechanics which gave birth to quantum field theory, is extremely problematic however [15]. The curved space-time metrics of general relativity seem to be completely at odds with the linearity of quantum mechanics and so ideas of grand unification in physics look towards higher dimensional space-time theories such as "string theory" or "Kaluza-Klein theory", or as yet undiscovered but hypothesised symmetric particles of nature in "super symmetry" (SUSY) [15]. Such searches which seek to go beyond the SM have resulted in the construction of the most powerful particle accelerator to date, in an attempt to reproduce the conditions a fraction of a second after the universe was created and it is hypothesised that all four forces of nature were unified.

A fundamental theme that all of these quantum-based theories possess is that at the core level, they are all describing the interactions which happen between a system of many particles (or "fields") - where we quantify the term "many" here to be any number greater than one [16]. No matter how simple a model we construct to describe a physical process, we are essentially *always* dealing with a so-called "quantum many-body system" - the interactions between nucleons in the nucleus, electron configurations of an atom, the interactions between quarks and gluons which make up nucleons, even the bare particle vacuum of quantum field theory itself has an infinite structure of virtual interactions taking place *in perpetuum*. In order to make any progress in such a far reaching and widely observed problem, we develop theories and methods designed solely to understand the physics of quantum many-body systems.

[3] which describes three of the four fundamental forces of nature.

1.1.2 The Quantum Many-Body Problem

This thesis represents a body of work produced from the study of pairing problems utilising a quantum-many body method known as the Coupled Cluster Method (CCM). The CCM is currently regarded as one of the most powerful and one of the most general *ab initio* methods in the realm of quantum many-body physics and quantum chemistry [17, 18] - it has been applied across many different branches of physics to a large number of different many-body systems and has been found capable of producing extremely accurate results on a consistent basis [17]. However, it has found relatively few applications in the study of pairing forces - the cases where it has been applied [19, 20, 21, 22] are rather specific and perhaps not as general as we would like. This has provided us with a motivation towards studying pairing problems using various forms of the CCM.

Before we can embark on a discussion of the CCM, or in fact *any* quantum many-body method, we must first address one of the most fundamental concepts of quantum many-body physics, namely what is referred to in general terms as the "quantum many-body problem". Simply put, this is the predicament of being able to accurately describe a quantum system consisting of a large number of particles - possibly of different species - and their interactions with one another and the environment in which they are contained [23]. This problem plays an integral role in quantum physics since in the real world, the macroscopic system properties which may result from a collection of quantum particles can *not* be understood solely based on an understanding of the individual particles which make up a system. Perhaps the greatest example of this point is the Bardeen, Cooper and Schrieffer or "BCS theory" of superconductivity [24, 25].

The complications inherent to the quantum many-body problem are perhaps best illustrated by a simple example. Suppose we consider a system of N identical particles, confined within a box of fixed volume V and held at zero temperature. We assume that the particles move slowly enough to neglect any relativistic effects. We do not specify whether these particles are bosons or fermions - it does not matter for our general argument. Any internal properties such as spin or isospin are neglected for convenience.

One of the most important physical quantities we would like to calculate for this many-body system is the ground-state energy E_0, i.e. the total energy of the system when it is in equilibrium. Our starting point is to write down the N-body, time-independent Schrödinger equation

$$\hat{H}\Psi_0\left(\mathbf{r}_1, \mathbf{r}_2, \ldots \mathbf{r}_N\right) = E_0\Psi_0\left(\mathbf{r}_1, \mathbf{r}_2, \ldots \mathbf{r}_N\right). \tag{1.1}$$

Here, $\Psi_0\left(\mathbf{r}_1, \mathbf{r}_2, \ldots \mathbf{r}_N\right)$ is the N-body wave function of the system and the vector $\mathbf{r}_i$ is the 3-dimensional position vector of the i^{th} particle in the system. In the absence

of any spin-, isospin- or momentum-dependent forces, the N-body Hamiltonian $\hat{H}$ for this system will be something of the form [14]

$$\hat{H} = -\sum_{i=1}^{N} \frac{\hbar^2}{2m_i} \nabla_i^2 + \hat{V}\left(\mathbf{r}_1, \mathbf{r}_2, \ldots \mathbf{r}_N\right). \tag{1.2}$$

The first term of the Hamiltonian is the N-body kinetic energy operator, where m_i is the mass of the i^{th} particle in the system and the reduced Planck's constant $\hbar$ is defined as $\frac{h}{2\pi}$. It is the sum of the individual kinetic energies possessed by the N particles. The second term is the N-body potential energy operator - this object must describe the entire range of interactions between all of the N particles in the system, as well as any external potentials which may be effecting the system (for example, gravitational or electromagnetic fields [2]).

In the presence of an external potential and provided the interactions which take place between the individual particles of the system are *weak*, the N-body potential may be reduced to the simpler form of N one-body potentials, i.e. the problem of N-body interactions between all of the particles is reduced to the problem of N noninteracting and therefore independent single-particles. In this case we can write the potential as

$$\hat{V}\left(\mathbf{r}_1, \mathbf{r}_2, \ldots \mathbf{r}_N\right) = \sum_{i=1}^{N} \hat{V}_i\left(\mathbf{r}_i\right).$$

Such an approximation is known as a "mean-field" or "independent-particle" approach - we are assuming that the individual particles have no interactions with one another, or if they do, they are sufficiently weak and may be thus considered as negligible.

If the interactions between the individual particles are *strong* and there is no external potential, for instance if we were to consider our box packed with N neutrons subject to no external field, then it is not possible to simplify $\hat{V}\left(\mathbf{r}_1, \mathbf{r}_2, \ldots \mathbf{r}_N\right)$ in the form of one-body terms. In this case, the N-body potential must therefore describe the *complete* character of all the N-particle interactions which may occur. This is technically impossible to do and hence we must introduce some form of approximation to the N-body potential in order to make any progress at all.

In the case of *dilute* systems (where we qualify dilute as meaning the system has a relatively large mean interparticle spacing) we can approximate the N-body potential as the sum over all two-body interactions in the system - i.e. we assume that the interactions which are most dominant in the system happen between, at most, two different particles. Such an estimate as this works considerably well in describing simple properties of the nucleon-nucleon force for example [26], as well as a large number of other many-body systems. For the case of a dilute many-body system then, the potential can only depend on the relative difference between particle observables

(for example, position or momentum) among pairs of interacting particles, i.e. only two-body forces are important [2, 14]. By requiring that the two-body potential be translationally invariant [16] (it must be, since it is a quantum mechanical observable) and considering only position-dependent forces, we may thus approximate the N-body potential as

$$\hat{V}\left(\mathbf{r}_1, \mathbf{r}_2, \ldots \mathbf{r}_N\right) \mapsto \sum_{i<j}^{N} \hat{V}_{ij} = \frac{1}{2} \sum_{i \neq j}^{N} \hat{V}\left(\left|\mathbf{r}_i - \mathbf{r}_j\right|\right). \tag{1.3}$$

The additional factor of $\frac{1}{2}$ is added to avoid over counting of pairs.

If a many-body system is particularly dense, then it is possible that three-body interactions amongst the particles will become important - this is the case for the more modern studies and models of the nucleon-nucleon force (for example, see [27]). With these inclusions, the complexity of the problem is obviously increased a great deal. However, throughout the course of our investigations we will assume our systems can be accurately described by at most two-body forces and we will therefore *not* be concerned with the possibility of including any three-body interactions.

Returning to the discussion at hand, i.e. many-body systems which we consider to be modeled accurately by two-body forces, if we substitute an expression for our N-body Hamiltonian (describing interacting particles subject to no external force) into equation (1.1) we find

$$\left(-\sum_{i=1}^{N} \frac{\hbar^2}{2m_i} \nabla_i^2 + \frac{1}{2} \sum_{i \neq j}^{N} \hat{V}\left(\left|\mathbf{r}_i - \mathbf{r}_j\right|\right)\right) \Psi_0\left(\mathbf{r}_1, \mathbf{r}_2, \ldots \mathbf{r}_N\right) = E_0 \Psi_0\left(\mathbf{r}_1, \mathbf{r}_2, \ldots \mathbf{r}_N\right). \tag{1.4}$$

As it stands, we are charged with the task of attempting to solve a $3N$-dimensional partial differential equation in order to determine the ground-state energy of the N-body system - this is essentially impossible for all but the most trivial of cases, even when N may be relatively small. We have thus highlighted the great difficulty of the quantum many-body problem.

Even before we have considered important additional factors for a realistic physical problem - such as the symmetry (for bosons) or antisymmetry (for fermions) of the many-body wave function, spin-, isospin- or momentum-dependent forces, mixed species of particles and dependence on time or temperature - we have seen how extraordinarily complicated the general many-body problem is. This fact is inescapable even after we have already approximated our N-body force to a sum over two-body forces and neglected the case of any external potentials. To proceed any further with this problem we must formulate and develop approximation methods which, as best possible, are able cope with describing the interactions present in quantum many-body systems.

1.2 Quantum Many-Body Methods

Given the fundamental problem we face, we must equip ourselves with the tools that make evaluation of quantum many-body physics possible. Fortunately we are well placed to study these problems as there have been many fruitful advances made in the realm of quantum many-body theory in the past fifty years or so. It is not possible to document all of them here in great detail, suffice to say we will outline some of the more common and general approaches, as they are the most illuminating. Arguably two of the most important many-body approximation schemes that exist are perturbation theory and the variational method [16], both of which may start from the Schrödinger equation as given in equation (1.1) but differ quite considerably in their paths afterward. With that in mind, we dedicate the next two sections to discussing these general approaches. We then introduce the family of techniques known collectively as Independent Cluster (IC) methods, of which the CCM is a member.

Although first formulated in the marriage of special relativity and quantum mechanics to describe the creation and annihilation of particles and antiparticles, the language of second quantisation plays an extremely useful role in the realm of quantum many-body physics [28]. Although not expressly dealing with relativistic particle interactions, second quantisation is helpful in describing the features and interactions present in a nonrelativistic many-body system [28].

Important physical considerations such as particle statistics of either Bose or Fermi systems, or useful computational tools such as the counting of particles in a given state, are already accounted for in the language of second quantisation [28]. The overall notation is also much more physically transparent and compact, and much less cumbersome than standard coordinate representation, especially for complicated systems consisting of a large number of particles. Second quantisation also lends itself to an easier interpretation in terms of many-body diagrams [28].

With that in mind, the vast majority of work presented in this thesis is written using the language of second quantisation, bar a few exceptions (for example where we introduce a given model Hamiltonian for the first time or wish to explicitly discuss a single-particle problem). Although we will not utilise many of the techniques we are about to discuss in our work, they are presented here for sake of completeness, as well as to provide some sort of comparative basis as to where the CCM fits into the overall scheme of generally applicable quantum many-body methods.

1.2.1 Perturbation Theory

For many-body systems which may be described by a Hamiltonian similar to that given in equation (1.4), the underlying concept of perturbation theory is to calculate the energy eigenvalues and wave functions of a specific (relatively more complicated)

problem as small perturbations away from an exactly solvable and hence known (simple) problem. In this sense we must be able to express our many-body Hamiltonian $\hat{H}$ in the form

$$\hat{H} = \hat{H}_0 + \gamma \hat{H}_1, \tag{1.5}$$

where $\hat{H}_0$ is the Hamiltonian of some exactly solvable or "zeroth order" system, $\hat{H}_1$ is a small perturbation away from the exactly solvable system and γ is known as the "coupling constant", representing the strength of the perturbing interaction.

1.2.1.1 Time-Independent Perturbation Theory

In the case where $\hat{H}_0$ and $\hat{H}_1$ do not depend on time, we use the simpler form of *time-independent* perturbation theory. Provided the zeroth order system obeys the time-independent Schrödinger equation

$$\hat{H}_0 \big|\Phi_n^0\big\rangle = E_n^0 \big|\Phi_n^0\big\rangle, \tag{1.6}$$

and has states that are normalised as $\big\langle \Phi_n^0 | \Phi_n^0 \big\rangle = 1$, when the perturbation is "switched on" (by this we mean the zeroth order system becomes perturbed by the interaction), we assume that the energy eigenvalues and eigenfunctions are perturbed as

$$E_n^0 \mapsto E_n,$$

$$\big|\Phi_n^0\big\rangle \mapsto \big|\Phi_n\big\rangle, \tag{1.7}$$

provided there are no degeneracies in $\hat{H}_0$.

If $\hat{H}_0$ *is* degenerate, i.e. there are multiple possibilities for the state $\big|\Phi_n^0\big\rangle$ which give the same energy eigenvalue E_n^0, then we must find a way to somehow lift out these degeneracies. This is done by using the more complicated form of *degenerate* perturbation theory, where we relabel the degenerate states $\big|\Phi_n^{(i)}\big\rangle$ so they form an orthonormal set with respect to some other Hermitian operator which commutes with $\hat{H}_0$ [2]. Then, the perturbed states in equation (1.7) are expanded in terms of linear combinations of the degenerate (orthonormal) states $\big|\Phi_n^{(i)}\big\rangle$. Although it is an important method, we will not discuss degenerate perturbation theory here further, for the sake of simplicity.

In the nondegenerate case then, the perturbed energies and states of equation (1.7) obey the modified eigenvalue equation

$$\hat{H} \big|\Phi_n\big\rangle = E_n \big|\Phi_n\big\rangle, \tag{1.8}$$

where $\hat{H}$ is given by equation (1.5) and E_n and $\big|\Phi_n\big\rangle$ are given by

$$E_n = E_n^0 + \gamma E_n^1 + \gamma^2 E_n^2 + \ldots,$$

$$\big|\Phi_n\big\rangle = \big|\Phi_n^0\big\rangle + \gamma\big|\Phi_n^1\big\rangle + \gamma^2\big|\Phi_n^2\big\rangle + \ldots, \tag{1.9}$$

i.e. they are written as a power series expansion in terms of the coupling constant γ. Thus the goal of (nondegenerate) time-independent perturbation theory is to find the solutions of equation (1.8) as an expansion of the coupling constant γ, using the solutions from equation (1.6), i.e. the zeroth order system, as input.

By substituting the expressions for the perturbed energies and states of equation (1.9) into equation (1.8) and utilising the orthonormality of the states $\big|\Phi_n\big\rangle$, we may represent the expansion of the coupling constant in terms of matrix elements. Equating powers of γ in the expression

$$\big(\hat{H}_0 + \gamma\hat{H}_1\big)\big(\big|\Phi_n^0\big\rangle + \gamma\big|\Phi_n^1\big\rangle + \gamma^2\big|\Phi_n^2\big\rangle + \ldots\big) =$$

$$\big(E_n^0 + \gamma E_n^1 + \gamma^2 E_n^2 + \ldots\big)\big(\big|\Phi_n^0\big\rangle + \gamma\big|\Phi_n^1\big\rangle + \gamma^2\big|\Phi_n^2\big\rangle + \ldots\big), \tag{1.10}$$

we may thus calculate the perturbative corrections to first, second, third and higher order of γ. It may be shown using standard techniques [2, 14] that the first and second order corrections to the energy are given by

$$E_n^1 = \big\langle\Phi_n^0\big|\hat{H}_1\big|\Phi_n^0\big\rangle,$$

$$E_n^2 = \big\langle\Phi_n^0\big|\hat{H}_1\big|\Phi_n^1\big\rangle = \sum_{n\neq m}\frac{\big\langle\Phi_n^0\big|\hat{H}_1\big|\Phi_m^0\big\rangle\big\langle\Phi_m^0\big|\hat{H}_1\big|\Phi_n^0\big\rangle}{E_n^0 - E_m^0}, \tag{1.11}$$

where E_n^2 has been expanded using the first order correction to the wave function, given by

$$\big|\Phi_n^1\big\rangle = \sum_{n\neq m}\big|\Phi_m^0\big\rangle\frac{\big\langle\Phi_m^0\big|\hat{H}_1\big|\Phi_n^0\big\rangle}{E_n^0 - E_m^0}. \tag{1.12}$$

If the energy E_n^0 is defined as the ground-state energy of a many-body system, we may thus write the perturbation expansion of the ground-state energy shift as [28]

$$\Delta E = E_n - E_n^0 = E_n^1 + E_n^2 + \ldots,$$

$$= \big\langle\Phi_n^0\big|\hat{H}_1\big|\Phi_n^0\big\rangle + \sum_{n\neq m}\frac{\big\langle\Phi_n^0\big|\hat{H}_1\big|\Phi_m^0\big\rangle\big\langle\Phi_m^0\big|\hat{H}_1\big|\Phi_n^0\big\rangle}{E_n^0 - E_m^0} + \ldots, \tag{1.13}$$

where we only proceed as high as second order.

We thus observe that in principle, the perturbation expansion is of infinite order. In

general this algebraic approach becomes rather complicated for anything past the first few orders of γ, indeed, time-independent perturbation theory itself is only considered an optimal method if the convergence of the γ expansion is extremely fast [14] - which would generally be the case if the difference between the energy levels of the system was large compared to the extra energy which is added to the system due to the perturbation at each order [14]. If the series in γ diverges we may wish to consider using other many-body methods or perhaps a resummation of the perturbation series [29] in the hopes that the transformed series is numerically better behaved than the original series. However, for a typical many-body system we would usually wish to go up to very high order in γ, since low order calculations in general do not provide us with much physical insight [28].

Diagrammatic Representation

An efficient approach to time-independent perturbation theory is to employ a *diagrammatic* representation of the ground-state energy perturbation expansion. For the time-independent case of a many-fermion system (for example, nuclear matter) the matrix elements which make up the expansion as expressed in equation (1.13) may be represented by a class of many-body pictures known as *Goldstone diagrams* [28, 30, 31, 32]. For this particular problem - and after some considerable effort[4] - we may rewrite equation (1.13) as the matrix element sum

$$\Delta E = \left\langle \Phi_n^0 \right| \hat{H}_1 \sum_{l=0}^{+\infty} \left(\frac{1}{E_n^0 - \hat{H}_0} \hat{H}_1 \right)^l \left| \Phi_n^0 \right\rangle_{\text{connected}}, \tag{1.14}$$

where $\left|\Phi_n^0\right\rangle$ is the fermionic ket ground-state wave function (a filled Fermi sea or "Hartree-Fock" state of single-particle wave functions) and summation over the matrix elements is for connected Goldstone diagrams only [30].

We qualify diagrams as being disconnected when they are composed of two or more disjointed parts. For the case of a many-fermion system, we can specify this further as diagrams in which particle or hole lines do not communicate with the final interaction [28] - the terms "particle" and "hole" in this sense are defined relative to the filled Fermi sea (a more detailed discussion of the Fermi sea is given shortly in the section detailing the variational method). Equation (1.14) is a representation of the famous "Goldstone linked-cluster theorem" [30] (although the formula was originally derived from time-dependent perturbation theory [30], before being shown to be correct for the time-independent case as well [30]).

In order to show that ΔE in equation (1.14) is in fact the same expression as that

[4] for the details, see [28] for example.

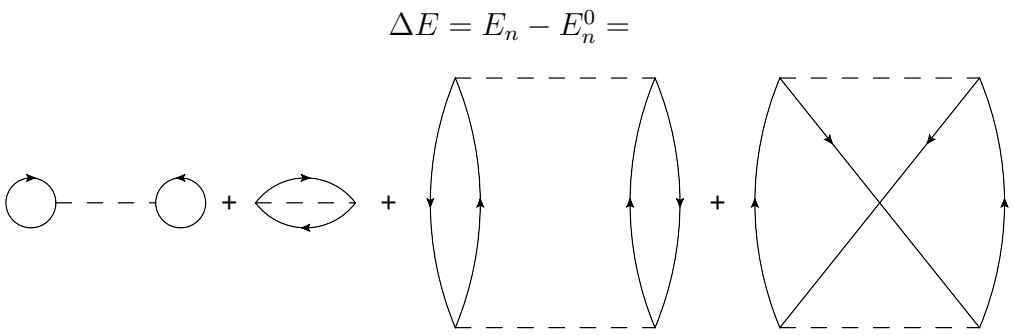

Figure 1.1: All first and second order Goldstone diagrams which contribute to ΔE in a uniform Fermi system.

in (1.13) we can expand (1.14) to second order. At first order we trivially have

$$E_n^1 = \langle \Phi_n^0 | \hat{H}_1 | \Phi_n^0 \rangle,$$

which does indeed match the previous first order result in equation (1.13). At second order we obtain

$$E_n^2 = \langle \Phi_n^0 | \hat{H}_1 \left(\frac{1}{E_n^0 - \hat{H}_0} \hat{H}_1 \right) | \Phi_n^0 \rangle.$$

If we insert a complete set of states $\sum_m |\Phi_m^0\rangle\langle\Phi_m^0|$ between successive $\hat{H}_1$ operators then we can replace the $\hat{H}_0$ operator in the denominator by the energy eigenvalue E_m^0. Hence we have

$$E_n^2 = \sum_{n \neq m} \frac{\langle \Phi_n^0 | \hat{H}_1 | \Phi_m^0 \rangle \langle \Phi_m^0 | \hat{H}_1 | \Phi_n^0 \rangle}{E_n^0 - E_m^0},$$

which again matches the previous second order energy correction of (1.13). Thus the Goldstone expansion of (1.14) is an exact reformulation of time-independent many-body perturbation theory to infinite order.

Figure (1.1) shows all of the connected Goldstone diagrams correct to second order that contribute to ΔE in a many-fermion system[5]. These diagrams represent the matrix elements of equation (1.14) and enumerate all the possible particle and hole interactions which may occur in the system due to the perturbation $\hat{H}_1$ under the proviso that we start with (and end at) the ground-state wave function $|\Phi_n^0\rangle$ [28]. In order to explain how we may construct the Goldstone diagrams of figure (1.1) using the algebraic form of ΔE from equation (1.14), we must write down an expression for $\hat{H}_1$. The most transparent way of doing this is in second quantised form, thus

$$\hat{H}_1 = \sum_{pqrs} \langle pq | \hat{V} | rs \rangle \hat{a}_p^\dagger \hat{a}_q^\dagger \hat{a}_s \hat{a}_r, \tag{1.15}$$

where $\hat{V}$ is the two-body potential of the many-fermion system, the operators $\hat{a}_{p,q}^\dagger$ and

[5]these diagrams have been drawn using the plotting tool JaxoDraw [33].

$\hat{a}_{s,r}$ are single-particle creation and annihilation operators respectively (obeying the usual fermionic anticommutation relations) and the states denoted by a letter, e.g. p, are shorthand for the single-particle states ϕ_p which make up $\left|\Phi_n^0\right\rangle$ (the explicit form of $\left|\Phi_n^0\right\rangle$ in terms of single-particle states is given in the following section on the variational method).

The summation in equation (1.15) is over states, thus $\hat{a}_p^\dagger$ creates a particle in state p above the Fermi sea and $\hat{a}_p$ annihilates a particle in state p within the Fermi sea. Since

$$\left\langle pq\middle|\hat{V}\middle|rs\right\rangle = \left\langle qp\middle|\hat{V}\middle|sr\right\rangle,$$

a distinction is made to sum the states only over one of these terms at each order. Assuming we are working with a uniform many-fermion system, we may write the first order correction to E_n as

$$E_n^1 = \left\langle\Phi_n^0\middle|\sum_{rs}\left\langle rs\middle|\hat{V}\middle|rs\right\rangle\hat{a}_r^\dagger\hat{a}_s^\dagger\hat{a}_s\hat{a}_r\middle|\Phi_n^0\right\rangle. \tag{1.16}$$

Here, $\hat{H}_1$ has removed particles in the states s and r from the Fermi sea, thus in order to return to the filled Fermi sea state, we must put particles in states s and r back into the Fermi sea immediately. The particle states *must* match the hole states at first order since there is only one interaction of $\hat{H}_1$ - if the particle states were different we would not be able to return to $\left|\Phi_n^0\right\rangle$ from a single application of $\hat{H}_1$. This term will thus give rise to so-called "closed loops", where a hole is made and filled immediately by a particle.

We are almost in a position to draw the Goldstone diagrams representing equation (1.16), however, we must first introduce a set of rules (which we will simply summarise from [31]) that allow us to represent matrix elements as pictures and *vice versa*. To begin with, time in Goldstone diagrams flows from bottom to top, thus interactions at the bottom of the diagram happen at earlier times than those at the top. The blank space below a diagram represents the particle vacuum state $\left|\Phi_n^0\right\rangle$ [31] (and similarly, a blank space at the top of the diagram symbolises we have returned the system to $\left|\Phi_n^0\right\rangle$ after all the interactions at each order have taken place).

A line that points upward represents an occupied state (particle) above the Fermi sea and a line that points downward represents an unoccupied state (hole) within the Fermi sea. The interaction matrix element $\left\langle pq\middle|\hat{V}\middle|rs\right\rangle$ is represented by a dashed line - at one end of this, r goes in and p comes out, and at the other end, s goes in and q comes out. In this way, the final state $\left\langle pq\right|$ is associated with the object $\hat{a}_p^\dagger\hat{a}_q^\dagger$ and all upward (particle) lines and the initial state $\left|rs\right\rangle$ is associated with the object $\hat{a}_s\hat{a}_r$ and all downward (hole) lines [31].

The denominator of the perturbative energy corrections is given by the sum of

particle energies minus the sum of hole energies. The overall sign (positive or negative) of a diagram's contribution to energy corrections is given by

$$(-1)^{h+l+e+u},$$

where h is the number of hole lines, l is the number of closed loops, e is the number of energy denominators and u is the number of external potential interactions. Utilising all of these rules, we may now draw a series of (connected) first order Goldstone diagrams to represent the matrix elements of equation (1.16). These are given by the first two diagrams in figure (1.1) and we explain their construction as follows.

The first diagram is the so-called "direct" term. The left hand loop represents the creation of a hole in state r before it is immediately filled by creation of a particle (or destruction of a hole) also in state r. The right hand loop represents the same process for the state s. The contribution to the first order energy shift from the direct term is thus given by

$$\frac{1}{2}\sum_{rs}\langle rs|\hat{V}|rs\rangle,$$

where the factor $\frac{1}{2}$ is to avoid over counting of the same matrix element (since $\langle rs|\hat{V}|rs\rangle = \langle sr|\hat{V}|sr\rangle$). The second diagram is the so-called "exchange" term, since it amounts to an exchange of hole states from the first (direct) term, and gives the contribution

$$-\frac{1}{2}\sum_{rs}\langle rs|\hat{V}|sr\rangle.$$

The minus sign arises from exchanging the position of the annihilation operators in equation (1.16).

We may carry out this process again for the second order energy corrections to obtain the third and fourth diagrams in figure (1.1), which represent second order direct and exchange Goldstone diagrams respectively. Each connected Goldstone diagram which contributes to the ground-state energy perturbation expansion scales linearly with particle number N [31] - they must do, since the ground-state energy is an extensive variable. Figures (1.2) and (1.3) show examples of disconnected Goldstone diagrams at second and third order respectively - it is important to note that these contributions are *products* of connected diagrams. Since each connected diagram scales like N, both these diagrams scale like N^2 - for cases where N is large this is a catastrophic result since it means many-body perturbation theory fails to produce an extensive ground-state energy and thus gives a potentially unphysical contribution to the energy spectrum of a many-body system.

Building upon Brueckner's initial work for nuclear matter [34], Goldstone managed to prove that all of these disconnected diagrams cancel out *exactly* at every order of the

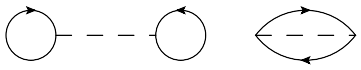

Figure 1.2: Example of a disconnected second order Goldstone diagram for a uniform Fermi system.

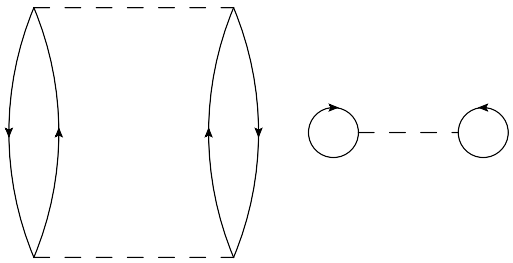

Figure 1.3: Example of a disconnected third order Goldstone diagram for a uniform Fermi system.

perturbation expansion however - it was this feat that has since become known as the Goldstone linked-cluster theorem. In words this simply states that the sum of energy corrections ΔE from time-independent many-body perturbation theory is given by the sum of connected Goldstone diagrams only. This relation is expressed mathematically in equation (1.14) as we have already stated.

The very nature of writing down a Goldstone expansion to n^{th} order can lead to some drawbacks - the main complication of using diagrammatic many-body perturbation theory is the vast number of diagrams the method produces. Past second order we have a sharp increase in the complexity and subtleties of the diagrams. Some of these will contribute almost nothing to the perturbation expansion and some may be simply too difficult to deal with. Thus a physical argument must be presented as to which diagrams should be included in the expansion and which should not - this of course introduces the possibility of more complications to compound the initial problem [17].

Although the use of Goldstone diagrams has (some) relevance to CCM techniques, in particular the origins of the method, we will not belabour the discussion of any diagrammatic techniques further, since the CCM formalism is presented throughout this thesis in a purely algebraic form. We do, however, present a somewhat more detailed discussion of the role Goldstone diagrams play in the CCM in the earlier part of chapter 2.

1.2.1.2 Time-Dependent Perturbation Theory

We have discussed the case of time-independent perturbation theory as a quantum many-body method and highlighted some of its shortcomings (both algebraic and diagrammatic). Ideally we would like to consider more general many-body problems using perturbation theory, in which case we will need to introduce time-dependence into the theory. This is usually done by assuming only the perturbative interaction is

time-dependent.

As with the time-independent case, we begin by supposing we know the energy eigenvalues and eigenstates of an idealised system, whose time-independent Hamiltonian $\hat{H}_0$ obeys the eigenvalue equation

$$\hat{H}_0\big|\Phi_n\big\rangle = E_n\big|\Phi_n\big\rangle.$$

We then wish to find the solutions of the time-dependent Schrödinger equation

$$\hat{H}\big|\Psi\left(t\right)\big\rangle = i\hbar\frac{\partial}{\partial t}\big|\Psi\left(t\right)\big\rangle, \tag{1.17}$$

where the Hamiltonian is given by $\hat{H}_0$ plus the now time-dependent perturbation $\hat{V}\left(t\right)$, i.e.

$$\hat{H} = \hat{H}_0 + \gamma\hat{V}\left(t\right). \tag{1.18}$$

The time-dependent wave functions $\big|\Psi\left(t\right)\big\rangle$ are expanded in terms of the time-independent (or stationary) states $\big|\Phi_n\big\rangle$

$$\big|\Psi\left(t\right)\big\rangle = \sum_n c_n\left(t\right) exp\Big(-i\frac{E_n}{\hbar}t\Big)\big|\Phi_n\big\rangle, \tag{1.19}$$

where the expansion coefficients $c_n\left(t\right)$ are also now time-dependent.

By substituting the states of equation (1.19) into equation (1.17), we can derive a differential equation for the amplitudes $c_n\left(t\right)$. The solutions of this equation are written as time integrations over matrix elements of the interaction $\hat{V}\left(t\right)$ [2]. By equating powers of γ in this expression, analogous to the time-independent case, we can thus form the time-dependent perturbation expansion of $c_n\left(t\right)$, and hence the states $\big|\Psi\left(t\right)\big\rangle$.

The reason why this approach works is that we are assuming that the time-dependent interaction is weak enough so that the perturbations it introduces to the system may be described in terms of the transitions between the stationary eigenstates $\big|\Phi_n\big\rangle$ [14]. Although this scheme may be used in the case of many-body Hamiltonians, it is not necessarily the most optimal method. Instead, it is often preferable to introduce the so-called "Green's functions" [28] (or "propagators"), as a means to perform calculations in time-dependent perturbation theory. Many-body Green's functions are preferable to evaluating the time-dependent perturbation expansion since they provide a simple and intuitive physical picture - they essentially describe the evolution of particles as they propagate through a many-body medium [26]. For the sake of brevity, we will not discuss many-body Green's functions here.

1.2.2 The Variational Method

Perturbation theory is a systematic approximation method - we may calculate increasingly higher orders shifts of energy in the form of a power series expansion in the coupling constant (interaction strength) [16, 28]. It is a reliable method for cases where the perturbative expansion converges rapidly (or if it is divergent, cases where the first few terms of small γ are able to accurately describe a given system [2] or cases where the series can be resummed to be convergent). The fundamental nature of the method means it is obviously only useful to us when we already know the complete set of solutions to an unperturbed system $\hat{H}_0$. Sometimes this is not possible however (for example, the BCS theory of superconductivity [16]). In problems where perturbation theory may not be best suited, we may consider using the variational method.

The variational method essentially exists because of the properties possessed by a set of orthonormal eigenstates, provided they obey the Schrödinger equation. Following the argument of [16], consider the Schrödinger equation of a many-body system, whose ground-state energy is E_0 and whose ket ground-state wave function is given by $\big|\Phi_0\big\rangle$

$$\hat{H}\big|\Phi_0\big\rangle = E_0\big|\Phi_0\big\rangle.$$

We may thus write the general energy eigenvalues and eigenstates of $\hat{H}$ as E_l and $\big|\Phi_l\big\rangle$, such that

$$\hat{H}\big|\Phi_l\big\rangle = E_l\big|\Phi_l\big\rangle;\ l = 0, 1, 2, 3, \ldots,$$

and we assume there is no degeneracy in the energies. Consider an arbitrary ket wave function $\big|\Psi\big\rangle$ which is normalised as $\big\langle\Psi|\Psi\big\rangle = 1$, and is expressible as a linear combination of the eigenstates $\big|\Phi_l\big\rangle$, thus

$$\big|\Psi\big\rangle = \sum_{l\geq 0} c_l\big|\Phi_l\big\rangle, \tag{1.20}$$

where c_l are complex number expansion coefficients.

If we calculate the energy this wave function corresponds to, i.e. we calculate the expectation value of the Hamiltonian, we find

$$\begin{aligned} E &= \big\langle\Psi\big|\hat{H}\big|\Psi\big\rangle \\ &= \sum_{m\geq 0}\sum_{l\geq 0} c_m^\star\big\langle\Phi_m\big|\hat{H}\big|\Phi_l\big\rangle c_l \\ &= \sum_{m\geq 0}\sum_{l\geq 0} c_m^\star c_l E_l\big\langle\Phi_m|\Phi_l\big\rangle \\ &= \sum_{l\geq 0}\big|c_l\big|^2 E_l \end{aligned}$$

$$\geq E_0 \sum_{l\geq 0} \left|c_l\right|^2.$$

However, since $\left|\Psi\right\rangle$ is normalised to unity, then

$$\sum_{l\geq 0} \left|c_l\right|^2 = 1,$$

and we thus have the important result

$$\left\langle \Psi \middle| \hat{H} \middle| \Psi \right\rangle \geq E_0, \tag{1.21}$$

for an *arbitrary* wave function $\left|\Psi\right\rangle$ which may be expanded in a basis of eigenstates $\left\{\left|\Phi_l\right\rangle\right\}$ [16], provided the system has no degenerate energies. If at any time the wave function $\left|\Psi\right\rangle$ is equal to the state $\left|\Phi_0\right\rangle$ then the inequality of equation (1.21) obviously becomes exact.

Thus in the variational method, we begin with the known Hamiltonian $\hat{H}$ of some many-body system and we attempt to guess a form, or write down a "trial ansatz" for the ground-state wave function $\left|\Psi\right\rangle$, written as a function of a number of "trial variables" $\left(\alpha_1, \alpha_2, \ldots, \alpha_n\right)$ [2, 16]. This *must* be a normalised quantity (else the relation of equation (1.21) will not hold). We then calculate the expectation value of the Hamiltonian $E = \left\langle \Psi \middle| \hat{H} \middle| \Psi \right\rangle$ and minimise the resulting expression with respect to the complete set of trial variables [2], i.e. we solve the set of equations

$$\begin{aligned}
\frac{\partial}{\partial \alpha_1} \left\langle \Psi \middle| \hat{H} \middle| \Psi \right\rangle &= 0, \\
\frac{\partial}{\partial \alpha_2} \left\langle \Psi \middle| \hat{H} \middle| \Psi \right\rangle &= 0, \\
&\vdots \\
\frac{\partial}{\partial \alpha_n} \left\langle \Psi \middle| \hat{H} \middle| \Psi \right\rangle &= 0,
\end{aligned} \tag{1.22}$$

in an attempt to tailor the wave function $\left|\Psi\right\rangle$ to being as close to the ground-state wave function $\left|\Phi_0\right\rangle$ as possible.

One of the great strengths of the variational method is that it guarantees an upper bound to the ground-state energy of a system, regardless of how poor the first guess may be (provided of course the trial ansatz is normalised) [26]. However, the success of the method is in part dependent on the ability to write down a "good" starting approximation to the ground-state wave function, which comes from a strong physical intuition of the systems behavior [14]. In general this is not particularly easy for the case of complicated many-body systems, although there exist classes of trial wave functions which prove useful in this regard (such as Jastrow or Jastrow-Feenberg types

[17]). There also exist techniques that seek to naturally improve upon these typical trial wave functions, for example the *correlated basis function* (or CBF) method, which attempts a systematic improvement on the initial variational ansatz [17]. Even if a trial wave function is able to approximate the ground-state energy accurately, there is no guarantee that it will work equally well for another observable however.

1.2.2.1 The Hartree-Fock Approximation

Arguably one of the most well-known uses of the variational method in quantum many-body theory is the so-called "Hartree-Fock approximation". This is an independent-particle or "mean-field" approach to the many-body problem of atomic physics and nuclear matter (specifically it is usually applied to models of the atom, the electron gas in a solid ("jellium" [16]) and the nucleus [16]). Although it is a rather simple scheme, it has had remarkable success in describing certain systems - indeed the idea of a mean-field or "self-consistent" approach to nuclear many-body theory is based on the successes of the nuclear shell model [26].

Following the derivation in [26], we make the assumption that it is possible to approximate a system of N identical fermions which interact via a two-body force in terms of an average single-particle potential

$$\hat{H}^{HF} = \sum_{i=1}^{N} \hat{h}\left(\mathbf{r}_i\right), \tag{1.23}$$

where $\mathbf{r}_i$ is the position vector of the i^{th} particle in the system and we neglect any other internal labels for convenience. Here, $\hat{h}$ is the average potential of the system, which accounts for the presence of the background $N-1$ fermions as any single fermion interacts with them - in other words, a single fermion interacts with an average field created by the other $N-1$ fermions [28]. Since the Hartree-Fock approximation is an independent-particle approach, interparticle correlations are completely ignored [28] (although strangely enough, this naive approximation can still provide good results).

We denote the lowest energy eigenvalue of the Hamiltonian in (1.23) as E_0^{HF}, which is an approximation to the true ground-state energy of the system E_0 known as the "Hartree-Fock energy" [26]. The state which corresponds to this eigenvalue is given by $\Psi^{\text{HF}}\left(\mathbf{r}_1, \mathbf{r}_2, \mathbf{r}_3, \ldots \mathbf{r}_N\right)$ (or $\left|\text{HF}\right\rangle$), which is the so-called "Hartree-Fock wave function/state". We now assume that $\Psi^{\text{HF}}\left(\mathbf{r}_1, \mathbf{r}_2, \ldots \mathbf{r}_N\right)$ can be written as a product of N individual (arbitrary) single-particle wave functions (which describe the N individual particles that make up the system) provided that they are orthonormal eigenstates of the single-particle Hamiltonian

$$\hat{h}\left(\mathbf{r}_i\right)\phi_i\left(\mathbf{r}_i\right) = \epsilon_i \phi_i\left(\mathbf{r}_i\right),\ i = 1, 2, 3, \ldots N. \tag{1.24}$$

We have thus approximated the N-body problem to the sum of N one-body problems.

In order to incorporate the Pauli exclusion principle for fermions, i.e. the anti-symmetrisation of the many-fermion wave function, we employ the use of a Slater determinant [2]. We therefore write the Hartree-Fock wave function as

$$\Psi^{\mathrm{HF}}\left(\mathbf{r}_1, \mathbf{r}_2, \mathbf{r}_3, \ldots \mathbf{r}_N\right) = \frac{1}{\sqrt{N!}} \begin{vmatrix} \phi_1\left(\mathbf{r}_1\right) & \phi_2\left(\mathbf{r}_1\right) & \cdots & \phi_N\left(\mathbf{r}_1\right) \\ \phi_1\left(\mathbf{r}_2\right) & \phi_2\left(\mathbf{r}_2\right) & \cdots & \phi_N\left(\mathbf{r}_2\right) \\ \vdots & \vdots & \ddots & \vdots \\ \phi_1\left(\mathbf{r}_N\right) & \phi_2\left(\mathbf{r}_N\right) & \cdots & \phi_N\left(\mathbf{r}_N\right) \end{vmatrix}, \tag{1.25}$$

where the single-particle wave functions $\phi_i\left(\mathbf{r}_i\right)$ are given by equation (1.24). As a side note, if we were to consider a *many-boson* system, this wave function would be given by the permanent

$$\Psi^{\mathrm{HF}}\left(\mathbf{r}_1, \mathbf{r}_2, \mathbf{r}_3, \ldots \mathbf{r}_N\right) = \frac{1}{\sqrt{N!}} \begin{vmatrix} \phi_1\left(\mathbf{r}_1\right) & \phi_2\left(\mathbf{r}_1\right) & \cdots & \phi_N\left(\mathbf{r}_1\right) \\ \phi_1\left(\mathbf{r}_2\right) & \phi_2\left(\mathbf{r}_2\right) & \cdots & \phi_N\left(\mathbf{r}_2\right) \\ \vdots & \vdots & \ddots & \vdots \\ \phi_1\left(\mathbf{r}_N\right) & \phi_2\left(\mathbf{r}_N\right) & \cdots & \phi_N\left(\mathbf{r}_N\right) \end{vmatrix}_{\mathcal{S}}, \tag{1.26}$$

where the label $\mathcal{S}$ denotes the bosonic Hartree-Fock wave function is symmetrised with respect to the single-particle wave functions $\phi_i\left(\mathbf{r}_i\right)$ (all the minus signs in a determinant become positive in a permanent). We can thus summarise the Hartree-Fock approximation as follows - we choose a set of N arbitrary single-particle wave functions $\phi_i\left(\mathbf{r}_i\right)$ which obey equation (1.24), in order to describe the N particles in the system. We substitute them into the Hartree-Fock wave function $\Psi^{\mathrm{HF}}\left(\mathbf{r}_1, \mathbf{r}_2, \mathbf{r}_3, \ldots \mathbf{r}_N\right)$ and then minimise the energy of the system with respect to this set to ensure that the lowest N states in $\Psi^{\mathrm{HF}}\left(\mathbf{r}_1, \mathbf{r}_2, \mathbf{r}_3, \ldots \mathbf{r}_N\right)$ are filled (and hence ensure the Hartree-Fock energy is given by E_0^{HF} and represents the closest approximation to E_0) [26].

To find the Hartree-Fock wave function we must first calculate the Hartree-Fock energy, as given by

$$E_0^{\mathrm{HF}} = \left\langle \mathrm{HF} \middle| \hat{H} \middle| \mathrm{HF} \right\rangle. \tag{1.27}$$

Here, $\hat{H}$ is the full many-body Hamiltonian, which we choose to write as [26]

$$\hat{H} = \sum_{n_1 n_2} \varepsilon_{n_1 n_2} \hat{c}_{n_1}^{\dagger} \hat{c}_{n_2} + \frac{1}{4} \sum_{n_1 n_2 n_3 n_4} V_{n_1 n_2 n_3 n_4} \hat{c}_{n_1}^{\dagger} \hat{c}_{n_2}^{\dagger} \hat{c}_{n_3} \hat{c}_{n_4}, \tag{1.28}$$

where the operators $\hat{c}_n^{\dagger}$ and $\hat{c}_n$ are single-particle fermionic creation and annihilation operators respectively (producing orthonormal states when they act on $\left|\mathrm{HF}\right\rangle$), $\varepsilon_{n_1 n_2}$ are single-particle kinetic energies and $V_{n_1 n_2 n_3 n_4}$ are the antisymmetrised matrix elements of the two-body potential energy operator [26]. We may write the Hartree-Fock energy

of equation (1.27) as a functional of the so-called single-particle density ρ, i.e.

$$E_0^{\mathrm{HF}}(\rho) = \sum_{n_1 n_2} \varepsilon_{n_1 n_2} \rho_{n_2,n_1} + \frac{1}{2} \sum_{n_1 n_2 n_3 n_4} \rho_{n_3,n_1} V_{n_1 n_2 n_3 n_4} \rho_{n_4,n_2}, \tag{1.29}$$

where ρ is defined by the general matrix element

$$\rho_{n_2,n_1} = \big\langle \mathrm{HF} \big| \hat{c}_{n_1}^{\dagger} \hat{c}_{n_2} \big| \mathrm{HF} \big\rangle, \tag{1.30}$$

and, in effect, represents all possible single-particle transitions between the levels n_1 and n_2 in the state $\big|\mathrm{HF}\big\rangle$ [26].

In the so-called "Hartree-Fock basis" $\big\{\phi_i(\mathbf{r}_i)\big\}$, the single-particle density matrix is diagonal and $\mathrm{Tr}\rho = N$. By enforcing ρ to be diagonal and minimising equation (1.29) with respect to ρ, we can find an expression for the Hartree-Fock potential given in equation (1.23). In doing this [26] we find that $\hat{h}$ contains the single-particle kinetic energies ε as well as a term Γ, given by

$$\Gamma_{k,k'} = \sum_{ll'} V_{kl'k'l} \rho_{l,l'}, \tag{1.31}$$

which represents the average potential or mean-field. The Hartree-Fock method is hence typically viewed as a first order approximation to a realistic system - it is possible to generalise the approach to include extra particle correlations however, but this will be discussed in more detail during chapter 2.

1.2.3 Independent Cluster Methods

Standing somewhere in between perturbative and variational approaches to the quantum many-body problem are the so-called Independent Cluster methods [35, 36, 37, 38]. We will outline the generic features that IC methods possess here, before briefly discussing the more specific forms of the Configuration Interaction and Coupled Cluster Methods. One particularly interesting principle of IC methods - that they may be shown to map a quantum many-body problem onto the problem of interacting classical fields [35, 36] - will not be discussed here however.

As usual, the starting point for our analysis is the (time-independent) many-body Schrödinger equation

$$\hat{H}\big|\Psi_0\big\rangle = E_0\big|\Psi_0\big\rangle.$$

When applying IC methods, we seek a solution for the ket ground-state wave function $\big|\Psi_0\big\rangle$, which we assume can be parametrised in the form

$$\big|\Psi_0\big\rangle = f\big(\hat{X}\big)\big|\Phi_0\big\rangle. \tag{1.32}$$

Here, $\left|\Phi_0\right\rangle$ is a normalised "starting" or "model state" wave function, usually chosen to be the exactly known solution $\left|\Phi_n^0\right\rangle$ of the zeroth order Hamiltonian from perturbation theory [39] (see equation (1.6)) but this may not always be the case. The object $f\big(\hat{X}\big)$ is some function of the so-called "cluster operator" $\hat{X}$ - this operator acts on the state $\left|\Phi_0\right\rangle$ to produce wave functions which describe correlated groups or "clusters" of particles in the many-body medium. Hence, $\hat{X}$ is a generalised creation operator of what we call "independent clusters", relative to the state $\left|\Phi_0\right\rangle$.

The bra ground-state wave function of IC methods is parametrised as

$$\left\langle\tilde{\Psi}_0\right| = \left\langle\Phi_0\right|\tilde{f}\big(\hat{\tilde{X}}\big). \tag{1.33}$$

Here, $\tilde{f}\big(\hat{\tilde{X}}\big)$ is typically the conjugate function to $f\big(\hat{X}\big)$ and the operator $\hat{\tilde{X}}$ is the Hermitian conjugate of $\hat{X}$ - i.e. it is the generalised annihilation operator of "independent clusters", relative to $\left\langle\Phi_0\right|$. Using these IC parametrisations we may hence write down the expectation value of the Hamiltonian $\hat{H}$ [35] as

$$\left\langle\hat{H}\right\rangle = \left\langle\Phi_0\right|\tilde{f}\big(\hat{\tilde{X}}\big)\hat{H}f\big(\hat{X}\big)\left|\Phi_0\right\rangle. \tag{1.34}$$

The IC operators $\hat{X}$ and $\hat{\tilde{X}}$ are usually expressed in the forms [35]

$$\hat{X} = \sum_I x_I \hat{C}_I^\dagger, \tag{1.35}$$

$$\hat{\tilde{X}} = \sum_I \tilde{x}_I \hat{C}_I, \tag{1.36}$$

where the coefficients x_I and $\tilde{x}_I$ are termed IC "amplitudes" and the operators $\hat{C}_I^\dagger$ and $\hat{C}_I$ are generalised *multiconfigurational* creation and annihilation operators respectively [35], defined relative to the starting wave function $\left|\Phi_0\right\rangle$ (the exact details of this important relationship are discussed in more detail at the start of chapter 2). For reasons that will become apparent later, it is crucial that these operators form a *mutually commutative* algebra. The summation variable I contains all of the information about a particular configuration (again, this is expanded upon in chapter 2). Using the definitions of (1.35) and (1.36), we thus deduce that the expression for $\left\langle\hat{H}\right\rangle$ in equation (1.34) is a *functional* of the IC amplitudes x_I and $\tilde{x}_I$ [35].

In order to find numerical values for the IC amplitudes and hence an expression for the ground-state wave functions of equations (1.32) and (1.33) and the ground-state energy E_0, we apply the variational method[6] and hence minimise $\left\langle\hat{H}\right\rangle$ with respect to

[6] or more correctly, the *bivariational* method.

the IC amplitudes, solving the resulting simultaneous equations

$$\frac{\partial}{\partial x_I}\big(\langle\Phi_0|\tilde{f}(\hat{\tilde{X}})\hat{H}f(\hat{X})|\Phi_0\rangle - \epsilon\big(\langle\tilde{\Psi}_0|\Psi_0\rangle - 1\big)\big) = 0,$$

$$\frac{\partial}{\partial \tilde{x}_I}\big(\langle\Phi_0|\tilde{f}(\hat{\tilde{X}})\hat{H}f(\hat{X})|\Phi_0\rangle - \epsilon\big(\langle\tilde{\Psi}_0|\Psi_0\rangle - 1\big)\big) = 0. \tag{1.37}$$

We have included the Lagrange multiplier ϵ here to ensure normalisation of the wave functions [35] (this is the standard way of formally ensuring the wave functions are normalised, however, normalisation within the CCM is not incorporated in this manner, as will be discussed shortly).

This general formalism outlines the most common features of IC methods. Strictly speaking, IC methods are neither wholly perturbative nor wholly variational (in that they produce an upper bound for the ground-state energy) yet they utilise elements from both of these approaches in order to calculate many-body wave functions and observables. There are still some distinct differences between the three different IC approaches however, some of which we shall now demonstrate.

1.2.3.1 The Configuration Interaction Method

The Configuration Interaction Method (CIM) [40] is in some ways the lowest level approximation within the hierarchy of IC methods [35, 36]. That is not to say the method is particularly *weak* - on the contrary, the CIM has found extensive use within the realm of quantum chemistry, where it is used predominantly to describe electron configurations of atoms. It provides a very simple approach to the many-body problem, which is arguably its greatest asset [36].

The ket and bra ground-state wave functions of the CIM are written as

$$|\Psi_0\rangle = \big(1 + \hat{F}\big)|\Phi_0\rangle = \Big(1 + \sum_I f_I \hat{C}_I^\dagger\Big)|\Phi_0\rangle, \tag{1.38}$$

$$\langle\tilde{\Psi}_0| = \langle\Phi_0|\big(1 + \hat{\tilde{F}}\big) = \langle\Phi_0|\Big(1 + \sum_I \tilde{f}_I \hat{C}_I\Big), \tag{1.39}$$

where summation in both terms begins from $I = 1$. The expectation value of the Hamiltonian is therefore given by

$$\langle\hat{H}\rangle = \frac{\langle\Phi_0|\big(1 + \hat{\tilde{F}}\big)\hat{H}\big(1 + \hat{F}\big)|\Phi_0\rangle}{\langle\Phi_0|\big(1 + \hat{\tilde{F}}\big)\big(1 + \hat{F}\big)|\Phi_0\rangle}. \tag{1.40}$$

In the realm of quantum chemistry, $|\Phi_0\rangle$ is usually chosen as a Hartree-Fock state, i.e. a Slater determinant of some zeroth order single-particle electron wave functions which make up some specified configuration. As $\hat{F}$ acts on $|\Phi_0\rangle$, we thus form a many-electron

wave function with single, double, triple etc excitations relative to $\left|\Phi_0\right\rangle$ [41].

In order to calculate the ground-state energy in the CIM, we truncate the operators $\hat{F}$ and $\hat{\hat{F}}$ (i.e. the number of excitations out of $\left|\Phi_0\right\rangle$ and $\left\langle\Phi_0\right|$) to some value N and then diagonalise the Hamiltonian in the form of an $N \times N$ matrix [17]. If we increase the value of N, we expect to observe convergence toward the *true* ground-state energy [17]. However, complete (i.e. untruncated) CIM calculations are impossible for anything but the most simplest of molecules in the smallest of finite spaces [41]. If we attempt to use the CIM to study a large number of particles in a large space, we uncover one of the biggest problems of the CIM - namely that it fails to obey the property of *size-extensivity* [17]. As such, macroscopic quantities such as the energy do not scale correctly with particle number N [39] and we find the presence of unphysical terms [34].

1.2.3.2 The Coupled Cluster Method

At the lowest level of the IC method hierarchy is the CIM. Although it provides a rudimentary approach to the general many-body problem, it is blighted by the fact it is not a size-extensive method. Following [17], we can define the concept of size-extensivity as follows.

Size-Extensivity

Suppose we have a completely general many-body system of N particles and the ket ground-state wave function of the system is given by $\left|\Psi_0\right\rangle$. If the system is then partitioned into two subsystems A and B - where we have N_A particles in subsystem A and N_B particles in subsystem B - as A and B become increasingly separated from one another (i.e. $\mathbf{r}_{AB} \mapsto \infty$) we assume that communication between A and B desists [17]. In the limit that the two subsystems are infinitely far apart we have

$$\hat{H} \mapsto \hat{H}^A + \hat{H}^B,$$

where

$$\left[\hat{H}^A, \hat{H}^B\right] = 0.$$

This implies that the ground-state energy becomes *additively separable* [17]

$$E_0 \mapsto E_0^A + E_0^B, \tag{1.41}$$

and the ket ground-state wave function becomes *multiplicatively separable* [17]

$$\left|\Psi_0\right\rangle \mapsto \left|\Psi_0^A\right\rangle \otimes \left|\Psi_0^B\right\rangle. \tag{1.42}$$

If a system obeys the relations of (1.41) and (1.42) then it is described as *size-extensive*. We can thus rectify the problems of the CIM, provided we use a wave function parametrisation which obeys equation (1.42).

Normal Coupled Cluster Method

The next step up from the CIM in the IC method hierarchy is the so-called Normal Coupled Cluster Method (hence forth abbreviated as NCCM) [35, 42]. This method was initially developed by Coester [43] and then Coester and Kümmel [44] in the realm of nuclear physics, before it was introduced into quantum chemistry by Čížek and Paldus [45, 46, 47] amongst others.

In the NCCM scheme, the ket and bra ground-state wave functions are parametrised as

$$\big|\Psi_0\big\rangle = e^{\hat{S}}\big|\Phi_0\big\rangle, \tag{1.43}$$

$$\big\langle\tilde{\Psi}_0\big| = \big\langle\Phi_0\big|\hat{\tilde{S}}e^{-\hat{S}}, \tag{1.44}$$

where

$$\hat{S} = \sum_{I\neq 0} s_I \hat{C}_I{}^{\dagger};\ \hat{\tilde{S}} = 1 + \sum_{I\neq 0} \tilde{s}_I \hat{C}_I. \tag{1.45}$$

The expectation value of the Hamiltonian is given by

$$\big\langle\hat{H}\big\rangle = \big\langle\Phi_0\big|\hat{\tilde{S}}e^{-\hat{S}}\hat{H}e^{\hat{S}}\big|\Phi_0\big\rangle. \tag{1.46}$$

Comparing (1.43) and (1.44) we observe immediately that Hermitian conjugacy between ket and bra states is broken in the NCCM. This is done for a particular reason, which we discuss in detail during the formalism of chapter 2 - suffice to say a parametrisation of this form ensures the NCCM is size-extensive, regardless of how the $\hat{S}$ and $\hat{\tilde{S}}$ operators are truncated.

The presence of the object $e^{-\hat{S}}\hat{H}e^{\hat{S}}$ ensures that the important Goldstone linked-cluster theorem [30] is naturally contained within the expectation value of an arbitrary many-body Hermitian operator [17]. In this sense, the amplitudes s_I are of linked-cluster nature but the amplitudes $\tilde{s}_I$ are not (the Goldstone diagrams which represent $\tilde{s}_I$ contain disconnected pieces). Nevertheless, a parametrisation such as this means that the amplitudes s_I and $\tilde{s}_I$ are canonically conjugate to one another [35].

Extended Coupled Cluster Method

The parametrisations (1.43) and (1.44) are not the most general we can make in the CCM, indeed the NCCM bra ground-state wave function does not actually obey the multiplicatively separable relation of equation (1.42) after truncation [36]. Standing at the pinnacle of IC methods therefore is the Extended Coupled Cluster Method

(hence forth abbreviated as ECCM) [35]. This is a powerful generalisation of the CCM approach, first proposed by Arponen [42] as a means to ensure that both amplitudes s_I and $\tilde{s}_I$ are linked-cluster quantities.

In the ECCM, ket and bra ground-state wave functions are parametrised as

$$\big|\Psi_0\big\rangle = e^{\hat{S}} e^{-\hat{\tilde{S}}} \big|\Phi_0\big\rangle, \tag{1.47}$$

$$\big\langle\tilde{\Psi}_0\big| = \big\langle\Phi_0\big| e^{\hat{\tilde{S}}} e^{-\hat{S}}, \tag{1.48}$$

where

$$\hat{S} = \sum_{I\neq 0} s_I \hat{C}_I{}^{\dagger};\ \hat{\tilde{S}} = \sum_{I\neq 0} \tilde{s}_I \hat{C}_I. \tag{1.49}$$

The expectation value of the Hamiltonian is given by

$$\big\langle\hat{H}\big\rangle = \big\langle\Phi_0\big| e^{\hat{\tilde{S}}} e^{-\hat{S}} \hat{H} e^{\hat{S}} e^{-\hat{\tilde{S}}} \big|\Phi_0\big\rangle. \tag{1.50}$$

The method is size-extensive - it still has the Goldstone linked-cluster theorem encoded within its structure. The object $e^{\hat{\tilde{S}}} e^{-\hat{S}} \hat{H} e^{\hat{S}} e^{-\hat{\tilde{S}}}$ also introduces a "double-linking" structure to the CCM, which can be said to take place in two ways. Firstly, both s_I and $\tilde{s}_I$ of equation (1.50) are linked-cluster amplitudes since they are both written in exponential form, thus there are two independent sets of linked-cluster amplitudes in the ECCM compared to one in the NCCM. Secondly, the Hamiltonian of (1.50) has undergone a double similarity transformation - meaning all of the operators in $\hat{S}$ are linked to $\hat{H}$, and the operators in $\hat{\tilde{S}}$ are either linked to $\hat{H}$ or multiple $\hat{S}$ operators. This specific linking structure is explained in more detail during chapter 2. Written in this form, although s_I and $\tilde{s}_I$ of equation (1.49) are linked-cluster amplitudes, they are not canonically conjugate to one another - this relationship can be enforced however, by means of a specific transformation [35].

IC methods are extremely useful in the study of many-body systems as they provide a systematic means to approach a given problem - by increasing the truncation of the IC operators, we are able to incorporate increasingly higher order particle correlations. In turn this usually leads to improved results for the observable we are calculating. They are more general than perturbative methods, since the starting wave function $\big|\Phi_0\big\rangle$ need not be known from an exactly solvable system - in which case we may choose or perhaps guess a specific form of $\big|\Phi_0\big\rangle$, similar in principle to writing down a trial ansatz in the variational method. We must stress that this stage that, although we have outlined many of the important features of CCM techniques very briefly here, the formalism presented in chapter 2 goes into much more detail concerning these attributes.

1.3 Outline of Thesis

We have covered some of the core elements of the quantum many-body problem and some of the general methods and techniques which may be used in an attempt to solve the problem approximately - namely perturbative, variational and IC methods. Each of these methods was explained in a rather general way and applications to admittedly simplified many-body problems were highlighted. Nevertheless, all of these methods are capable of explaining real physical systems to good accuracy, though some have more obvious merits over others. We will now become much more specific with our aims and focus predominantly on the use of CCM techniques, particularly in their applications to pairing problems.

The remainder of this chapter is dedicated to a literature review. The majority of this section details a concise (and not exhaustive) list of research and work that has been performed using the CCM, in both the NCCM and ECCM formalisms, since it was first devised. We focus on the core papers in the field - be they the foundations upon which the CCM was built, the formal developments of the method or the key, more modern applications of the CCM. We then succinctly survey the topic of pairing, specifically in the realm of atomic and nuclear many-body systems. This leads in turn to an overview of the BCS theory of superconductivity and Bose-Einstein condensation (BEC) in trapped gases - ultimately our interest lies in the BCS-BEC crossover, which we pay particular attention to.

Chapter 2 details much of the core formalism of the CCM and is broken down into three sections. The first discusses NCCM techniques and derivations of many key formulae are provided. Extensions to include time-dependence and hence calculations of excited-states are outlined. The second section details ECCM formalism. Since much of this formalism can be simply generalised from NCCM techniques, this section is rather brief. Finally, section three introduces a generic many-fermion model of s-wave pairing - we apply the ECCM to this system at the lowest possible order of approximation and gain some useful insight. This section provides us with a formulation of the ECCM which is geared towards studying pairing problems, via the use of quasi-particles.

As a means to demonstrate the formalism developed in chapter 2, chapter 3 presents studies of two different anharmonic oscillator models using various NCCM and ECCM techniques. We concentrate mainly on calculating the ground-state energies for each system, although we do provide excited-state results for one model. The chapter functions to explicitly show the output of a CCM calculation, as well as some of the intricacies of the method, which are perhaps not as easily observed from simply studying the mathematical structure of the CCM.

Chapters 4 and 5 detail work performed in collaboration with my Ph.D. supervisor, Prof. Niels Walet. In chapter 4, we apply the ECCM pairing formalism introduced

in the last section of chapter 2 to a completely generic but exactly solvable model of pairing. We perform several different types of CCM calculations and compare them with the exact solution. The results we obtain are somewhat surprising in certain cases, so we modify our approach slightly. Some of the methods show promise, but only at certain levels of approximation. We perform an RPA calculation to check the stability of the two most general CCM approaches used and determine which is the optimum method to use in general.

Chapter 5 presents a study of the most complicated system yet. We introduce a model to describe the pairing between fermionic atoms of an ultracold dilute gas confined within a harmonic trap. Our ultimate goal is to attempt an RPA calculation of the second order ECCM solutions - this will allow us to calculate the collective modes of a superfluid system which exhibits BCS-BEC crossover. We first wish to investigate the ground-state properties of such a system using the mean-field (or first order) ECCM. Unfortunately, the second order and RPA calculations for this model remain incomplete - due to time constraints we have been unable to determine any second order results for the ground-state energy E_0. In lieu of this fact, we outline our initial plans for the model and discuss the way in which the second order calculations may have been performed, given more time.

Chapter 6 acts as a conclusion to the thesis - we summarise our results and discuss their implications. We also outline the possibility of further work to be conducted on the models studied throughout this thesis.

1.4 Literature Review

It is not possible to completely categorise the vast physics and chemistry literature dedicated to the CCM since it was first conceived. We therefore attempt to present a succinct review of the technique, highlighting the most important papers in the field. We will also review the phenomenon of pairing in many-body systems as well as the historical background behind the realisation of the BCS-BEC crossover - these are the particular areas of physics we are most interested in applying the CCM to.

1.4.1 Origins of the CCM

The most elementary form of the CCM was established in 1958 by Coester [43], in an attempt to calculate the ground-state properties of closed-shell nuclei. In parametrising the many-fermion ground-state wave function $\left|\Psi_0\right\rangle$ in terms of an exponentially correlated operator acting on the zeroth order wave function $\left|\Phi_0\right\rangle$ (an idea first proposed by Hubbard [48]) Coester managed to prove the Goldstone linked-cluster theorem [30] of time-independent many-body perturbation theory in a very simple manner. The

previous work of Brueckner [34], Hubbard [48] and Hugenholtz [49, 50] was simplified in an almost trivial way through Coester's choice of the exponential form.

A collaboration between Coester and Kümmel in 1960 [44] would mark the very first steps towards expansion of the CCM (or the "expS" approach, as it was commonly called at the time). This work laid the foundations of what would become later classified as the "Normal" CCM by Arponen [42] - the similarity transformed Hamiltonian $e^{-\hat{S}}\hat{H}e^{\hat{S}}$ (which effectively reformulates the diagrammatic Goldstone linked-cluster theorem into an algebraic form) and the NCCM equations or "equations for s_n" (which when solved, provide input for the equation representing the ground-state energy) stem from both [43] and [44]. However, for several years after these papers were published, no further advances nor applications of the CCM (in the field of nuclear physics) were forthcoming [39]. This is in part due to the lack of computing power available at the time - it was believed to be simply too difficult for CCM calculations to be realised, either analytically or numerically [39].

Nevertheless, (and unbeknown to the physicists [39]) the CCM had attracted the attention of the quantum chemists of the time - perhaps this had happened because they were more computationally inclined than the physicists were [39]. Whatever the case may be, in 1966 Čížek[7] was to publish the first approximate CCM calculations from a quantum chemistry perspective [45]. This work was to effectively reintroduce the formalism of Coester and Kümmel to a much wider audience and as a result, the method was effectively revived - through the efforts of the quantum chemists such as Čížek and Paldus [46, 47], the physicists slowly became aware that CCM calculations were now a possibility.

1.4.2 Formal Developments of the CCM

Although the CCM was initially formulated to study the nuclear many-body problem, its greatest development and widest spread use has ultimately been observed in the realm of quantum chemistry (for example, see the recent review article [41] and references therein). Here it has displaced the CIM as the "method of choice" in dealing with many-electron configurations of atoms or molecules [41]. However, we will not discuss the development of CCM techniques in quantum chemistry here[8], unless they are of specific relevance to developments in the *overall* picture of CCM (for example, the introduction of time-dependence into the formalism).

[7] who was aided in the computations by Paldus [45].

[8] in some respects there are simply too many applications of the CCM in quantum chemistry alone to discuss succinctly.

The Nuclear Era

Within the realm of quantum many-body physics, it is the Bochum group, led by Kümmel, that have provided much of the driving force behind the application of CCM techniques, particularly in the field of nuclear many-body theory. A large majority of this work stems from the period of early to mid seventies[9], after Kümmel had been made aware of the quantum chemistry work carried out by Čížek and Paldus [39]. Over the short period of time between 1970 and 1972, the Bochum group would produce many papers detailing CCM techniques, as they gradually began to build up the technology of nuclear CCM calculations [52, 53, 54, 55].

A common theme amongst all of these works is the comparisons and parallels the authors draw between the CCM and other nuclear many-body methods prevalent at the time, such as Brueckner-Hartree-Fock - the limit of the Brueckner-Bethe-Goldstone theory of nuclear matter [31] dealing with hard-core or "strongly repulsive" potentials. Emphasis is also placed on the fact that it is not necessary to interpret the CCM in terms of many-body perturbation diagrams - it may be evaluated in a purely algebraic fashion [53] (although diagrams which represent the CCM amplitudes themselves may still be useful [54]).

This advancement of the method would eventually lead to the 1973 publication by Kümmel and Zabolitzky [56], in which the first CCM calculations for finite nuclei were presented [39]. Two different second order approximation schemes of the CCM were used to calculate the binding energies of the closed-shell, doubly magic nuclei ^{4}He and ^{16}O, for a variety of different nucleon-nucleon potentials. The results obtained offered no real improvement over other approximate Brueckner-Hartree-Fock results already obtained by others, however the CCM showed encouraging signs, especially since it had been truncated to relatively low order (although at the time, the computing time was to take several hours for ^{16}O calculations [56]).

An extension of the usual "single-reference" (i.e. single model state) CCM formalism was made by Offerman, Ey and Kümmel in 1976 by introducing the so-called "multi-reference" picture [57, 58, 59] (although Ey's work on a *linked* multi-reference formalism [59] came two years later in 1978). A scheme such as this naturally lends itself to the study of open-shell systems - where a single model state is not adequate enough to describe a system where nucleons occupy states above a closed-shell for example [39]. Not long after this, Lührmann [60] would apply a form of the CCM to the Lipkin, Meshkov and Glick or "LMG" model [61, 62, 63], representing the first application of CCM techniques to a finite dimensional model [39]. Outside of the Bochum group, time-dependence was added to the general CCM formalism in 1978 by Hoodbhoy and Negele [64] (although Monkhorst had introduced this independently in quantum chemistry

[9] or the "nuclear era" [51].

applications - see [65] and references therein).

Arguably the most seminal work produced by the Bochum group of this "nuclear era" was the 1978 report by Kümmel, Lührmann and Zabolitzky [66]. This was to lay down many of the fundamental techniques that all subsequent ground-state CCM calculations of closed-shell nuclei would use, as well as outline possible applications to nuclear matter, liquid ^{3}He and other problems - in essence it represents a culmination of the Bochum group's work throughout the seventies [51]. The actual presentation of the work is notoriously dense however, with some of the concepts expressed in a fashion that is rather complicated to understand.

Around the time of this report, Lührmann was to also collaborate with Bishop on a study of the electron gas ("jellium") [67, 68] (although the second paper [68] would not be published until 1982). Such applications were to highlight just how accurate the CCM results were and show how capable the CCM had become as a reliable *ab initio* many-body method - the CCM results for the correlation energy of this model over the full range of metallic densities would agree within 1% to the Green's function Monte Carlo results which are, essentially, exact for the model [68].

The Subnuclear Era

The work produced by the Bochum group in the eighties[10] was more general than that of the seventies, as applications to quantum field theories were made and properties such as temperature-dependence were incorporated to the formalism [39, 51]. A rather important breakthrough in the method came in 1981 - Emrich formulated an excited-state CCM formalism for closed-shell nuclei [69, 70, 71] (where the third paper in this series was a collaboration between Emrich and Zabolitzky). The excited-state CCM formalism was tested on the LMG model and the weakly interacting Bose gas [70], as well as the negative parity states of ^{16}O [71] - the results compare favorably to other approaches such as the CIM or diagrammatic perturbation theory.

The same year also saw the first application of the CCM to nuclear matter [39] in the form of Day and Zabolitzky's work [72]. Drawing on the work of [66] at many points, Day and Zabolitzky perform CCM calculations up to third order (and formulate an approximation scheme to calculate fourth order corrections) using the truncated Reid v_6 potential and the so-called "Bochum" or "χ_n" truncation scheme - a CCM approximation method formulated to cope with hard-core potentials. The CCM results converge relatively quickly (corrections at the approximate fourth order are minimal) and conform with the variational and Brueckner-Bethe hole-line results respectively.

Probably one of the single most important CCM papers to be written in the eighties came from outside of the Bochum group however - this was Arponen's 1983 work [42], in

[10] or the "subnuclear era" [51]

which he essentially reclassified all previous CCM calculations under the title "Normal" CCM (which he also showed was derivable from a bivariational principle) and proposed a novel development of the formalism he termed "Extended" CCM. By introducing a second exponential parametrisation into the bra ground-state wave function, he had managed to produce a theory composed solely of linked-cluster amplitudes and thus had rectified some of the deficiencies inherent to the NCCM. He was thus the first person to apply ECCM techniques to finite dimensional models [39] (namely the LMG model[11], although he also showed that the lowest order ECCM calculation could be classified as a generalised Hartree-Fock or mean-field method and thus showed that it could be written in a form identical to the BCS theory of superconductivity).

The ECCM was developed over a short period of time in the latter half of the decade together with Bishop, Pajanne and Robinson [74, 75, 76, 77] - many of the previous elements of the NCCM could be generalised in a straightforward manner to ECCM formalism. In 1985, the CCM formalism was first applied to the realm of quantum field theory [39] (namely φ^4 or quartic self-interacting scalar field theories) by Kaulfuss [78] and also by Hsue, Kümmel and Ueberholz [79].

During the early nineties, Arponen continued to collaborate with Bishop, most notably in a series of papers where the natural hierarchy of IC methods - the CIM, NCCM and ECCM respectively - was expressed and their formalisms further expanded [36, 37, 38]. Although an extension of the CCM formalism to temperature-dependent problems was first formulated by the Bochum group in 1986 (see [80] and references therein) in 1992 Mukherjee [81] proposed a more stable temperature-dependent extension [39].

Modern Applications

A little over ten years ago, the CCM enjoyed a resurgence of sorts in applications to nuclear physics, due in part to the work of Mihaila and Heisenberg [27, 82, 83, 84]. Although Mihaila and Heisenberg write their formalism slightly differently than the standard approach [17] the flavor of their work represents a natural evolution of that first produced by the Bochum group in the early seventies. Asides from performing a modern CCM calculation of the binding energy of ^{16}O [82, 84], they also extend CCM techniques to dealing with a realistic nucleon-nucleon interaction such as the Argonne $v18$ potential, as well as including a modern, phenomenological three-body force, namely the Urbana IX interaction [27, 83, 84].

A few years after the work of Mihaila and Heisenberg, even more advanced nuclear applications of the CCM were performed by Dean *et al.* [85, 86, 87, 88, 89, 90] which have continued up to the present day [91]. Much of their technology comes from

[11] see also [73].

techniques developed in quantum chemistry, thus their equations and language differ somewhat compared to that usually seen in physics papers. The main focus of their work is calculating ground- and excited-state properties of nuclei, using modern forms of the nucleon-nucleon potential and in some cases even including the effects of three-body forces.

A great deal more applications of CCM techniques than discussed here have been made since the method was first formulated in 1958. Topics such as lattice gauge theory, quantum optics and quantum fluid dynamics also deserve a mention [17] - it is simply not possible to detail all of the applications of the method within all the specific fields of physics and chemistry however.

1.4.3 Pairing in Atomic and Nuclear Many-Body Systems

The phenomenon of pairing between particles within a many-body medium (such as nuclei, infinite nuclear matter or metals) has been a topic of great theoretical interest for the past 60 years or so. It has found an especially renewed interest in three different areas of physics over the past decade or so. In the realm of atomic physics, experimental advances in studying ultracold atomic gases have allowed physicists to study the so-called BCS-BEC crossover [92, 93, 94, 95, 96, 97, 98] - this is the rather remarkable process whereby a trapped BCS-like fermionic superfluid composed of correlated atom pairs can crossover to form a BEC of tightly bound composite bosons (diatomic molecules) via the tuning of an external magnetic field [92].

In the realm of astrophysics, thermal readings from neutron stars have allowed a greater understanding of superfluidity in neutron star matter and nuclear matter to be reached [99]. Finally, in the realm of nuclear physics, studies have been performed on neutron-rich nuclei far from the valley of stability [99]. The effects of pairing are essential in describing all of these many-body systems accurately.

The BCS Theory of Superconductivity

Arguably one of the most well-known models of many-body pairing is the BCS theory of superconductivity [24, 25]. Although the phenomenon of superconductivity had been observed in metals since as early as 1911 by Kammerlingh-Onnes [16], it wasn't until 1957 that there was an adequate microscopic description of it. The crux of BCS theory rests on the concept that superconductivity arises due to a phase transition within a metal at sufficiently low temperature - at this point, the energy of the macroscopic system (as electrons form pairs near the Fermi surface) is rearranged so as to be *lower* than the normal ground-state energy of the system [16].

A crucial element of BCS theory[12] was to come from Cooper in 1956 [100]. In

[12] or in fact, general pairing theory.

considering a pair of electrons held slightly above a "frozen" filled Fermi sphere of other electrons, where one electron is in a time-reversed state relative to the other, he showed that the two free electrons would naturally form a pair, provided there was an attractive (negative) potential between the two. Importantly, he showed this to be true for any value of the attractive potential, no matter how small. This work held such importance that the description "Cooper pairs" has transcended Cooper's initial problem and is now used to describe any generic zero angular momentum (s-wave) particle pairing, where one particle is in the time-reversed state relative to the other.

When a superconducting metal is cooled below a certain critical temperature T_c therefore, the electrons in the metal undergo a phase transition and form correlated Cooper pairs - the attractive potential acting between pairs of electrons arises from the phonon vibrations of lattice ions. In essence, the wake of a moving electron within a metal during its superconducting phase produces a positive charge by displacing the ions around it. In turn, an electron is attracted to this wake and the two electrons form a correlated but *weakly* bound Cooper pair. The two electrons do *not* form a composite boson since the average distance between the two is rather large (i.e. greater than the mean interparticle spacing of the electrons in the metal [16]).

Shortly after BCS theory was first published, it was shown by Bogoliubov that the method could be reinterpreted in terms of noninteracting quasi-particles[13] with the starting BCS wave function playing the role of the quasi-particle vacuum [26]. Bogoliubov quasi-particles (or "Bogolons") thus allow us to describe pairing effects in terms of a mean-field (similar to the Hartree-Fock approach but where we treat *pairs* of interacting fermions as moving independently, subject to an averaged "pairing field"). Although the onset of superconducting properties was first believed to be only possible at extremely low temperatures (of the order $1-10K$ for example), it was subsequently shown that superconductivity may also be observed in cuprate oxides at temperatures as high as $100K$ [16] giving rise to further work in the field of so-called "high-T_c" or "unconventional" superconductors [101, 102].

Superconductivity in metals thus shares an unmistakable similarity with Bose-Einstein condensation of atoms [102, 103] - this is the phenomenon observed in gases of Bose particles where, at a low enough temperature, all of the particles will condense into the same quantum state and the system may ultimately be described in terms of a single "macroscopic" wave function [102]. The formation of correlated Cooper pairs within a many-body system is not just particular to superconductivity in metals however - a similar phenomenon may be observed in nonmetals which goes by the name of superfluidity [102]. Although superfluidity of Bose atoms such as ^{4}He may be described in terms of "normal" BEC, in the case of Fermi atoms such as ^{3}He, it may be described

[13] formed from the negatively charged electrons (particles) and positively charged vacancies (holes) in the metal.

in terms of a BCS-like transition into a fermionic condensate (or "pseudo-BEC") - where Fermi atoms have formed bound Cooper pairs in a BCS-like state at low temperature (the situation is actually a lot more complicated than this for ^{3}He but we will not go into further details here since we do not wish to study such complex dense systems). Superfluidity is also observed elsewhere in nature, particularly within neutron stars [99].

Superconductivity, therefore, is a phenomenon observed within metallic systems only and superfluidity a phenomenon observed within nonmetallic systems only. The two are essentially the same however, provided we make the distinction that for Bose systems, the resultant effects are due to BEC and for Fermi systems, the resultant effects are due to condensation of (BCS-like) Cooper pairs (sometimes called "pseudo-BEC") [102]. Thus we may draw the rather elegant analogy that BCS theory and BEC are really flip sides of the same coin - this gives rise to the concept of BCS-BEC crossover theory, which we shall discuss shortly.

Nuclei

Given the fact that BCS theory actually represents a seemingly widespread and rather generic mean-field theory of pairing, attempts have been made to apply BCS theory to other pairing phenomena within quantum many-body physics. In 1958, Bohr, Mottelson and Pines attempted to apply BCS theory to the realm of nuclear physics [104], namely to describe features of nuclei which had apparent similarities with superconducting metals - in particular, the structure of energy spectra for nuclei possessing even-even, even-odd or odd-odd numbers of protons and neutrons (the energy gap present between ground-state and excited-state energies of even-even nuclei due to pairing [26]). An understanding of nucleon pairing would also explain why even-even nuclei with strong pairing correlations tend to form a spherical shape [16] - it is energetically favorable for nucleons within a nucleus to form zero angular momentum pairs, which in turn produces spherically symmetric pair wave functions [26]. Ultimately, pairing correlations within nuclei are much less pronounced than those within superconductors or superfluids however, and do not produce such striking physical properties [16] - nonetheless, their effects must be taken into account to provide a realistic picture of nuclei [26].

Following the initial work of Bohr, Mottelson and Pines, other attempted applications of BCS theory to nuclei would follow [105, 106]. An immediate problem faced by such an application is the breaking of particle number. For the case of electrons within a superconducting metal, the particle number N is of the order 10^{23} [26] and thus the fact that BCS theory does not conserve particle number is not too much of a problem. However, for the case of finite nuclei, where N is a great deal smaller, the breaking of particle number can have huge repercussions. Nuclei are obviously much more massive

than electrons and are subject to the strong nuclear force as well [16]. In practice alternate methods (or extensions to nuclear BCS theory) have since been developed to account for these factors [99]. Nevertheless, BCS theory can provide a relatively good quantitative description of pairing in nuclei [16, 26], which is a testament to its generality.

The BCS-BEC Crossover

Although the first prediction of BEC dates all the way back to 1924 and the work performed by Bose and Einstein (see [103] and references therein), it wasn't until 1995 that the phenomenon could be realised experimentally - this was done by Anderson *et al.* for rubidium atoms [107] and Davis *et al.* for sodium atoms [108]. These revolutionary experiments were to essentially pave the way for experimentalists attempting to form condensates from different types of atomic gases at ultracold temperatures. In 1999, DeMarco and Jin [109] were to report the first results of quantum degeneracy in a dilute gas of (fermionic) ^{40}K atoms.

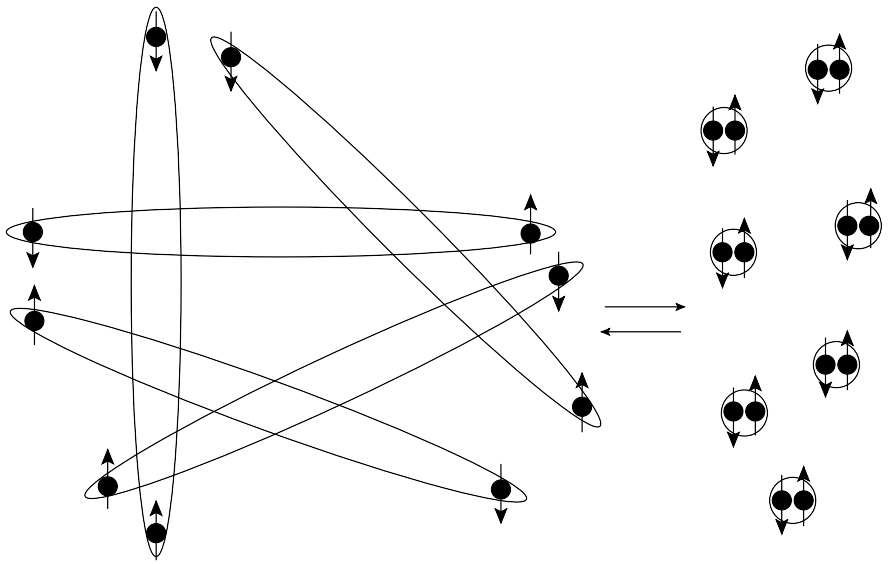

Figure 1.4: Pictorial representation of the BCS-BEC crossover in an ultracold dilute gas of fermionic atoms. The left hand side shows the BCS-like state, where atomic Cooper pairs are separated by distances much greater than the mean interparticle spacing of the atoms in the gas (thus many such pairs may overlap in this regime). The right hand side shows the BEC state of tightly bound diatomic molecules - in the so-called "deep BEC" limit it is practically impossible to resolve any internal structure of these molecules, thus they essentially behave as point-like bosons of spin 0. The directional arrows in between the two regimes represent the process is tunable, i.e. it is possible to tune the system back and forth between the two regimes. This picture has been adapted from the front cover of [102].

Such experiments were to provide hope for the observation of the long sought BCS-BEC crossover. Figure (1.4) shows an idealised picture of this phenomenon (it is

important to note that the pairing which takes place on the BCS side is in **k**-space, whereas the pairing which takes place on the BEC side is in **r**-space). The introduction of a magnetic Feshbach resonance [92] was to be the missing key of these experiments as it provided a means to enable tuning of the s-wave scattering length a_s of the many-body collisions within these Fermi gases. Over the short period of time between mid 2003 and early 2004, the fabled BCS-BEC crossover was finally produced experimentally by Greiner *et al.* [95], Zwierlein *et al.* [96] and others [92]. However, *irrefutable* evidence that both BCS and BEC regimes in these experiments were exhibiting superfluid behavior came slightly later in 2005 [98] with the observation of quantised vortices on both sides of the crossover (visible after the atomic gas had been stirred).

The concept of a transition between a BCS-like superfluid phase and a BEC has a rather long history, dating back as far as 1969 and to Eagles' hypothesis [110] that the general form of the variational BCS wave function could be used to describe states other than those in the weak coupling limit of BCS theory. This idea was also noted independently by Leggett in 1980 [111] who inferred that, provided certain scaling was performed to render the dynamics of a gas of Fermi atoms to be (essentially) solely dependent on the s-wave scattering length a_s, it would be possible to achieve a BCS superfluid system for a_s smaller than zero and a BEC of composite bosons for a_s greater than zero. An extension of Leggett's ground-state formalism to finite temperature was made in 1985 by Nozières and Schmitt-Rink [112] and further developed in 1993 by Sá de Melo *et al.* [113] in an attempt to calculate the critical temperature of crossover.

In one sense, the realisation of BCS-BEC crossover has led to a rather interesting meeting point between experimental and theoretical physics. Physicists working in the field of quantum many-body theory - mean-field techniques in particular - have essentially been provided with an enormous set of new data to digest. Of particular interest is the study of collective modes of ultracold fermionic gases, which govern dominant physical attributes at low temperature [114]. Recent experiments have shown that mean-field theories are incapable of describing these collective modes accurately however [115], thus methods which go beyond mean-field theory are being developed to study these excitations [116].

Although the CCM has been applied to some models of pairing (for example, the work of Emrich and Zabolitzky [19, 20]) and BCS-like systems (for example, the work of Bishop and Lahoz [21, 22]) some of these applications remain rather specific and have not necessarily been developed since their introduction. They also invariably use the Normal CCM, as opposed to the Extended CCM formalism, which is more general. With that in mind, we would like to develop a reliable ECCM approach to studying pairing problems and ultimately attempt a calculation for the collective modes of an ultracold fermionic atom gas - the second order approximation of ECCM is naturally a "beyond mean-field" approach and since the CCM is well-known for high precision

results, it is obviously a good candidate for this investigation. We don't have a clear idea of how to start though, so we will build up our pairing technology gradually.

Chapter 2

The Coupled Cluster Method Formalism

In this chapter we proceed to introduce the most important concepts of the ground-state, zero temperature, time-independent formalism of the Coupled Cluster Method. We focus on zero temperature calculations in order to work with pure states (i.e. to avoid having to deal with the complications of mixed states) and, essentially, because the physics we are ultimately interested in studying happens at very low temperature anyway [92]. Since the focal point of our CCM calculations is usually evaluating the ground-state energy E_0 and, to a lesser extent, the ground-state wave function $\left|\Psi_0\right\rangle$ of a given many-body system, we do not cover the Emrich scheme of excited-state formalism [69, 70] in any great detail.

Nonetheless, we do cover the formalism of time-dependent CCM and calculation of excited-state energies via the so-called Random Phase Approximation (RPA), since we wish to calculate some low order excitation energies for models presented in chapters 3, 4 and 5. As has already been established, there are two distinct branches of the CCM, the so-called Normal Coupled Cluster Method and the Extended Coupled Cluster Method. The vast majority of discussion will be concerned with NCCM techniques, although we do pay particular interest to the ECCM in the closing of the chapter.

Prior to any specific CCM discussion however, we introduce the important concept of a model state, which ultimately provides us with a groundwork on which to build our CCM description. The distinction is made of how this model state differs between bosonic and fermionic many-body systems. With this principle explained, we go on to build our NCCM ground-state description of ket and bra states and explain how we calculate the ground-state energy of a system using the NCCM. A bivariational principle is then introduced and shown to reproduce the NCCM equations in much more concise way. Time-dependence is introduced into the NCCM as a means to calculate excited-state energies using the RPA. A suitable approximation scheme is described in order to make the NCCM formalism tractable.

We then formally introduce the ECCM, detailing how ket and bra states are parametrised and explaining how the ground-state energy functional is constructed. The intrinsically complex structure of the method is highlighted. We also draw a comparison between the NCCM and ECCM.

The latter part of the chapter is concerned with the formalism of applying CCM techniques to study many-body pairing problems. To that end, we also introduce the Hartree-Fock-Bogoliubov (HFB) method, an approach which seeks to describe the nuclear many-body problem as a generalised mean-field theory, i.e. a generalised single-particle theory, wherein the "particles" of the theory are in fact "quasi-particles" - essentially clusters of low-lying excited nuclei [26]. We highlight the similarities the HFB method possesses with low order ECCM. Building upon all this formalism, we introduce the idea of using quasi-particles within the ECCM framework, with the hope of producing more accurate results for low order calculations, with respect to a standard (single-)particle approach.

2.1 The Normal Coupled Cluster Method

Suppose we are interested in studying a given quantum many-body problem in the many-body Hilbert space $\mathcal{H}$, and we wish to do so using CCM techniques. There are 2 distinct approaches we may adopt in order to derive the required formalism. Here, we choose to take the historical approach and formulate our equations in the style of Kümmel [39, 66, 117] and, in particular, Bishop [17, 118], amongst others. In keeping with this, we adapt much of our discussion using the overview [17] as a source. In this approach, we essentially derive our CCM formalism from the starting point of the Schrödinger equation. The more modern approach to the method is seen in the work of Arponen [42], where the starting point is to write down an action functional and then employ a bivariational principle to obtain the desired equations. Regardless of which approach is utilised, the crux of the CCM lies in the use of the so-called "model state" $\left|\Phi_0\right\rangle$ - a normalised, many-body wave function representing a "model" or "reference" noninteracting state in $\mathcal{H}$ [17].

2.1.1 The Model State

The model state's role is important because it acts as a zeroth order building block from which all other states may be constructed, as well as being the state with which all others may be compared or "referenced" to [17]. In general terms it may be regarded as the exact ground-state solution of a zeroth order Hamiltonian $\hat{H}_0$ [39] - an idealised starting wave function to build upon. In this way, it must also notably act as a generalised vacuum with respect to all given states in $\mathcal{H}$ [17]. Use of a single model

state $\left|\Phi_0\right\rangle$ corresponds to the so-called single-reference CCM [17] (and, naturally, using multiple model states $\left|\Phi_i\right\rangle$ where $i = 0, 1, 2\ldots$ would correspond to the so-called multi-reference CCM [17], the formalism of which we will not cover here). Hence, the CCM seeks to describe the true many-body ground-state wave function $\left|\Psi_0\right\rangle$ of a system in terms of a transformation of the model state $\left|\Phi_0\right\rangle$.

We are justified in using such an approach if we recall the Gell-Mann and Low theorem (see the appendix of [119], although it is expressed more conveniently in [28]). The Gell-Man and Low theorem tells us that the *interacting* ground-state wave function $\left|\Psi_0\right\rangle$ for a field theoretic or many-body system may be written as

$$\lim_{\epsilon\to 0}\frac{\hat{U}_\epsilon\left(0,-\infty\right)\left|\Phi_0\right\rangle}{\left\langle\Phi_0\right|\hat{U}_\epsilon\left(0,-\infty\right)\left|\Phi_0\right\rangle} \equiv \frac{\left|\Psi_0\right\rangle}{\left\langle\Phi_0|\Psi_0\right\rangle}, \tag{2.1}$$

and, provided this expressions holds true for all orders of time-dependent perturbation theory, it is a nondegenerate eigenstate of the given field theory or many-body Hamiltonian $\hat{H}$ [28], i.e.

$$\hat{H}\frac{\left|\Psi_0\right\rangle}{\left\langle\Phi_0|\Psi_0\right\rangle} = E_0\frac{\left|\Psi_0\right\rangle}{\left\langle\Phi_0|\Psi_0\right\rangle}. \tag{2.2}$$

Here, $\left|\Phi_0\right\rangle$ is the *noninteracting* ground-state wave function and $\hat{U}_\epsilon\left(0,-\infty\right)$ is the unitary time evolution operator written in the interaction representation [28, 42, 117]. The time-dependent Hamiltonian $\hat{H}$ is given by

$$\hat{H} = \hat{H}_0 + e^{-\epsilon|t|}\hat{H}_1,$$

where ϵ is a small positive variable, $\hat{H}_0$ is the zeroth order Hamiltonian and $\hat{H}_1$ is a perturbative interaction [28]. E_0 is simply the ground-state energy.

Thus, what we may take from this is that, provided equation (2.1) holds for all orders in time-dependent perturbation theory, we may describe a given eigenstate $\left|\Psi_0\right\rangle$ of $\hat{H}$ in terms of an operator (or string of operators) acting on a noninteracting model state $\left|\Phi_0\right\rangle$. Although the Gell-Mann and Low theorem is used in the description of time-dependent states and how they evolve from the model state, in principle the time-independent CCM formalism is built upon a completely analogous concept. Kümmel has even gone so far as to suggest that the Gell-Mann and Low theorem acts as a precursor to the CCM [39], especially since the time evolution operator $\hat{U}_\epsilon\left(0,-\infty\right)$ may be written in an exponential form, which is the cornerstone of CCM theory.

Having established the justification of our approach, we go on to postulate that all quantum many-body states that exist in $\mathcal{H}$ for a given many-body problem may be constructed via the action of a set of many-body *multiconfigurational* creation or annihilation operators on the generalised vacuum state $\left|\Phi_0\right\rangle$ [17]. We denote these sets

as $\{\hat{C}_I^\dagger\}$ and $\{\hat{C}_I\}$, referring to creation and annihilation operators respectively, with the summation variable I playing the role of a single-particle "umbrella" label - i.e. I contains all the single-particle labels necessary to describe a given state configuration relative to $|\Phi_0\rangle$ [17]. For example, if we were to study a system of infinite nuclear matter, I might be expected to contain information on the single-particle wave vector $\mathbf{k}$, spin component σ and isospin component τ of a given (single) fermion configuration. For this reason, it is often useful to define $I = 0$ as the null set [17], and hence enforce the relation

$$\hat{C}_0 \equiv 1 \equiv \hat{C}_0^\dagger. \tag{2.3}$$

The many-body multiconfigurational annihilation operators $\{\hat{C}_I\}$ are defined by their action on the generalised ket vacuum state

$$\hat{C}_I|\Phi_0\rangle = 0, \, \forall I \neq 0. \tag{2.4}$$

The Hermitian adjoints of the $\{\hat{C}_I\}$ operators, the multiconfigurational creation operators $\{\hat{C}_I^\dagger\}$ are defined by their action on the generalised bra vacuum state

$$\langle\Phi_0|\hat{C}_I^\dagger = 0, \, \forall I \neq 0. \tag{2.5}$$

Furthermore, these operators are assumed to obey the commutation relations

$$\left[\hat{C}_I, \hat{C}_J\right] = 0 = \left[\hat{C}_I^\dagger, \hat{C}_J^\dagger\right]. \tag{2.6}$$

As we shall see, it is usually convenient (but not essential) to have the operators obey orthonormality

$$\langle\Phi_0|\hat{C}_I\hat{C}_J^\dagger|\Phi_0\rangle = \delta_{IJ}. \tag{2.7}$$

In general, the operators of equations (2.4) and (2.5) are defined to be products (or sums of products) of single-particle operators, defined relative to the model state [17].

For a given many-body problem, the sets defined by $\{\hat{C}_I^\dagger\}$ and $\{\hat{C}_I\}$, as well as the choice of the model state $|\Phi_0\rangle$ will naturally vary, depending on the properties and nature of the system under discussion. The model state must be chosen to take account of the underlying symmetries of the system and the single-particle operators which make up the multiconfigurational operators must obey the correct particle statistics, with regards to whether the system is composed of bosons or fermions.

For the case of bosonic or field theoretic systems for example, $|\Phi_0\rangle$ may take the form of a bare vacuum $|0\rangle$ or a BEC ground-state $\frac{1}{\sqrt{N!}}\left(a_1^\dagger\right)^N|0\rangle$ for an N-body noninteracting Bose system [42] (where $a_1^\dagger$ is a single-particle creation operator obeying the usual bosonic commutation relations). In a many-fermion system, $|\Phi_0\rangle$ may take the form of an antisymmetrised single-particle Slater determinant or Hartree-

Fock state $\big|\mathrm{HF}\big\rangle$ (where the constituent orthonormal single-particle operators obey the usual fermionic anticommutation relations) or a modified Slater determinant $\big|\mathrm{BCS}\big\rangle$ composed of quasi-particle operators (as first proposed in the BCS theory of superconductivity [24, 25]). The model state may yet take other forms, but further discussion of these choices will be made in later chapters, in the context of studying particular systems. Thus, with these definitions for the model state $\big|\Phi_0\big\rangle$ and the set of operators $\big\{\hat{C}_I^\dagger\big\}$ and $\big\{\hat{C}_I\big\}$, we may now begin to address the underlying formalism of the CCM.

2.1.2 Ket Ground-State Wave Function

The heart of the CCM lies in the use of an exponentially correlated many-body (or field theoretic) ground-state wave function, as first suggested by Hubbard [48] and later applied by Coester [43] (and then by Coester and Kümmel [44]) to calculate the ground-state energy of closed-shell nuclei. We consider such a wave function to be expressed as

$$\big|\Psi_0\big\rangle = e^{\hat{S}}\big|\Phi_0\big\rangle, \tag{2.8}$$

where the so-called cluster correlation operator $\hat{S}$ is given by

$$\hat{S} = \sum_{I\neq 0} s_I \hat{C}_I{}^\dagger. \tag{2.9}$$

This operator is thus constructed from a sum of many-body multiconfigurational creation operators $\big\{\hat{C}_I^\dagger\big\}$, the coefficients of which, $\big\{s_I\big\}$, form a complete set of so-called "cluster amplitudes" or "cluster correlation coefficients".

Coester used an exponential parametrisation of this form, since previous work by Hubbard [48] and Hugenholtz [49, 50] had shown that the time-independent perturbation expansion of such an operator did not include any unlinked or disconnected Goldstone diagrams, and that the ground-state energy E_0 was comprised solely of linked diagrams (all unlinked diagrams cancel exactly, as a consequence of the exponential construction [39]). Brueckner had previously managed to derive this feature but only for the first few terms in the expansion [34]. In Coester's own words, *"The diagrams representing the matrix elements of $\hat{S}$ contain no unlinked parts"* [43], where as before we qualify unlinked or disconnected to mean diagrams in which particle or hole lines do not communicate with the final interaction [28] (in the language of Brueckner, linked diagrams are referred to as "irreducible clusters" and unlinked diagrams as "reducible clusters" [34]).

In this way, a parametrisation of this nature implicitly preserves the Goldstone linked-cluster theorem [30], which states that only linked or connected diagrams can contribute to the time-independent perturbation series of the ground-state energy of a many-body system. Such a property as this is important for a general many-body

method since it means the theory is *size-extensive*, i.e. that the ground-state energy E_0 of the system is proportional to (or scales correctly with) particle number N [39]. Unlinked diagrams do not scale correctly as $N \to \infty$ (they scale as powers of N [34]) and thus represent unphysical terms in the energy spectrum [34].

Coester's initial motivation for introducing the exponential form of equation (2.8) was in order to simplify the previous work of Brueckner, Goldstone, Hubbard and Hugenholtz [30, 34, 48, 49, 50] and hence show how the ground-state energy perturbation series could be shown to contain no unlinked many-body diagrams in a much simpler manner [43]. In this way, it is thus entirely possible to use the CCM formalism in a solely algebraic form, avoiding the need to deal with many-body perturbation theory diagrams completely [42, 66].

2.1.3 Ground-State Energy

With the CCM ket ground-state parametrisation explained, we proceed to find an expression for the ground-state energy of a given many-body system. We begin by writing down the time-independent Schrödinger equation for a general ket ground-state wave function

$$\hat{H}\big|\Psi_0\big\rangle = E_0\big|\Psi_0\big\rangle. \tag{2.10}$$

Once we insert the CCM parametrisation of $\big|\Psi_0\big\rangle$ given in equation (2.8) into equation (2.10) we obtain

$$\hat{H}e^{\hat{S}}\big|\Phi_0\big\rangle = E_0 e^{\hat{S}}\big|\Phi_0\big\rangle. \tag{2.11}$$

Taking the scalar product of equation (2.11) with the state $\big\langle\Phi_0\big|e^{-\hat{S}}$ therefore gives us

$$E_0 = \big\langle\Phi_0\big|e^{-\hat{S}}\hat{H}e^{\hat{S}}\big|\Phi_0\big\rangle, \tag{2.12}$$

which is an expression for the ground-state energy of the system as a function of the cluster amplitudes $\{s_I\}$ [17].

The Hamiltonian of equation (2.12) is now written in a similarity transformed manner, which is the signature characteristic of the CCM. This transformed Hamiltonian is described as being "fully linked" [17]. An explanation of this term is best illuminated by considering the so-called "linked-cluster" or "nested commutator" expansion, given by

$$e^{-\hat{S}}\hat{H}e^{\hat{S}} = \hat{H} + \Big[\hat{H},\hat{S}\Big] + \frac{1}{2!}\Big[\Big[\hat{H},\hat{S}\Big],\hat{S}\Big] + \frac{1}{3!}\Big[\Big[\Big[\hat{H},\hat{S}\Big],\hat{S}\Big],\hat{S}\Big] + \ldots. \tag{2.13}$$

In evaluating this sum of commutators, the only possible contractions that may occur do so between the operators in $\hat{H}$ and those in a given $\hat{S}$, summed over a particular state. In this way (the contractions coupled with the state summation) we say $\hat{H}$ and

$\hat{S}$ are "linked" [17, 66]. No such contractions may occur between $\hat{S}$ operators since they are all defined to commute with one another, therefore there are no links between successive $\hat{S}$ operators [17, 66].

This idea of links may be further exemplified by writing

$$e^{-\hat{S}}\hat{H}e^{\hat{S}} = \hat{H} + \left\{\hat{H}\hat{S}\right\}_{\mathcal{L}} + \frac{1}{2!}\left\{\hat{H}\hat{S}\hat{S}\right\}_{\mathcal{L}} + \frac{1}{3!}\left\{\hat{H}\hat{S}\hat{S}\hat{S}\right\}_{\mathcal{L}} + \ldots, \tag{2.14}$$

in the style of Kümmel *et al.* [66], where the expression $\left\{\hat{A}\hat{B}\hat{C}\hat{D}\ldots\right\}_{\mathcal{L}}$ means *"take the sum of all possible links (contractions) between the operators $\hat{A}\hat{B}\hat{C}\hat{D}\ldots$ such that there is at least one link between $\hat{A}$ and $\hat{B}$, one link between the product $\hat{A}\hat{B}$ and $\hat{C}$, at least one link between the product $\hat{A}\hat{B}\hat{C}$ and $\hat{D}$ and so on"* [66]. In this way, we can clearly see that the similarity transformed Hamiltonian $e^{-\hat{S}}\hat{H}e^{\hat{S}}$ is fully linked, in that every term in the $\hat{S}$ operator given in equation (2.9) is linked to the Hamiltonian [17]. Expressing the ground-state energy E_0 in terms of the similarity transformed Hamiltonian of equation (2.13) may thus be considered as an algebraic reformulation of the Goldstone linked-cluster theorem [17].

The ground-state energy given in equation (2.12) produces a finite-order polynomial in the amplitudes $\{s_I\}$ since the linked-cluster expansion of equation (2.13) is finite, provided there are a finite number of operators in $\hat{H}$ [17] (the $\hat{S}$ operators may only contract with the operators in $\hat{H}$ in a finite number of ways). In order to evaluate the ground-state energy E_0, we require a set of values for the cluster amplitudes $\{s_I\}$. By rearranging equation (2.11) and multiplying on the left by $e^{-\hat{S}}$ we obtain

$$\left(e^{-\hat{S}}\hat{H}e^{\hat{S}} - E_0\right)\left|\Phi_0\right\rangle = 0. \tag{2.15}$$

If we take the scalar product of equation (2.15) with the complete set of states

$$\{\hat{C}_I^\dagger\left|\Phi_0\right\rangle;\, \forall I \neq 0\},$$

we obtain

$$\left\langle\Phi_0\right|\hat{C}_I e^{-\hat{S}}\hat{H}e^{\hat{S}}\left|\Phi_0\right\rangle = 0,\, \forall I \neq 0, \tag{2.16}$$

which is an infinite hierarchy of coupled, nonlinear, polynomial equations for the cluster amplitudes $\{s_I\}$ [17]. The results of solving this set of simultaneous equations for all $\{s_I\}$ may be substituted into equation (2.12) in order to obtain a numerical solution for the ground-state energy E_0 [17]. We may combine both the equation for E_0, (2.12), and the equations for $\{s_I\}$, (2.16), into one succinct expression, given by

$$\left\langle\Phi_0\right|\hat{C}_I e^{-\hat{S}}\hat{H}e^{\hat{S}}\left|\Phi_0\right\rangle = E_0\delta_{I0}. \tag{2.17}$$

Importantly, the matrix elements of equation (2.17) remain size-extensive regardless of how we may approximate the $\hat{S}$ operator [17].

Since at no point in the derivation of the ground-state energy do we require a calculation of the norm of our ground-state, the normalisation condition $\langle\Psi_0|\Psi_0\rangle = 1$ is never imposed, and thus there is no guarantee that the parametrisation of $|\Psi_0\rangle$ given in equation (2.8) will produce a ground-state that is well behaved or even normalisable. In fact, as we shall see in the next section, the CCM parametrisation is not normalised in the usual sense and is manifestly nonHermitian [17] (since bra states are not parametrised as Hermitian adjoints of ket states in the CCM). Nevertheless, by imposing the *intermediate normalisation* condition

$$\langle\Phi_0|\Psi_0\rangle = \langle\Phi_0|e^{\hat{S}}|\Phi_0\rangle = \langle\Phi_0|\Phi_0\rangle = 1, \tag{2.18}$$

we do indeed find expressions for $|\Psi_0\rangle$ which are well behaved and act as good approximations to the true ground-state wave function.

One last point to note is that, in solving the simultaneous equations which arise from equation (2.16), there is also no guarantee that the ground-state energy E_0 of equation (2.12) will be uniquely determined by the solutions of $\{s_I\}$. In fact, when using CCM techniques we are often presented with several possible solutions for the ground-state energy. Only one of these can possibly be correct and the rest of the solutions correspond to unphysical energies, however, there are some subtleties involved in how we determine which solution is the correct one. Further discussion of this may be found in chapter 3, where it is explained first hand how we deal with multiple solution branches and determine the correct solution.

2.1.4 Bra Ground-State Wave Function

Although we can calculate the ground-state energy E_0 without strictly ever needing to write down an expression for the bra ground-state $\langle\tilde{\Psi}_0|$, in practice if we wish to calculate expectation values of general many-body operators, we *will* require some algebraic expression for it [17]. It is at this exact stage that the distinction between general CCM techniques (i.e. those used in solely evaluating a many-body ground-state energy) and the NCCM is made. This division was first made explicit by Arponen [42], who introduced the phrase "normal" into the language, in order to differentiate it from what he called the "extended" approach, an expansion on the basic CCM formalism he himself conceived. Before this distinction was made, workers in the field had simply referred to the method as the "expS" approach [66], a name obviously derived from the parametrisation of the ket ground-state wave function (2.8).

An intriguing difference that the NCCM formalism encompasses in comparison to other quantum mechanical theories, is that in general, bra and ket states are not Her-

mitian adjoints of one another. Instead, we define our bra ground-state wave function using the parametrisation

$$\big\langle\tilde{\Psi}_0\big| = \big\langle\Phi_0\big|\hat{\tilde{S}}e^{-\hat{S}}, \tag{2.19}$$

where the adjoint cluster correlation operator $\hat{\tilde{S}}$ is given by

$$\hat{\tilde{S}} = 1 + \sum_{I\neq 0}\tilde{s}_I\hat{C}_I. \tag{2.20}$$

Such a parametrisation thus now produces the typical normalisation condition

$$\big\langle\tilde{\Psi}_0|\Psi_0\big\rangle = \big\langle\Phi_0\big|\hat{\tilde{S}}e^{-\hat{S}}e^{\hat{S}}\big|\Phi_0\big\rangle = 1. \tag{2.21}$$

It may be shown [42] that if the multiconfigurational operators are orthonormal as in (2.7), the adjoint amplitudes $\tilde{s}_I$ are given by the ground-state expectation value of the operators $\hat{C}_I^\dagger$, i.e. $\tilde{s}_I = \big\langle\tilde{\Psi}_0\big|\hat{C}_I^\dagger\big|\Psi_0\big\rangle = \big\langle\hat{C}_I^\dagger\big\rangle$, which contain unlinked terms, and thus so does $\hat{\tilde{S}}$ [42].

One might naively assume that a bra parametrisation such as $\big\langle\Psi_0\big| = \big\langle\Phi_0\big|e^{\hat{S}^\dagger}$ would be more suitable, in that it retains the Hermitian adjoint relationship between bra and ket states. However, consider we were to calculate the ground-state energy using a variation principle with this definition [17], i.e.

$$E_0 = \frac{\big\langle\Psi_0\big|\hat{H}\big|\Psi_0\big\rangle}{\big\langle\Psi_0|\Psi_0\big\rangle} = \frac{\big\langle\Phi_0\big|e^{\hat{S}^\dagger}\hat{H}e^{\hat{S}}\big|\Phi_0\big\rangle}{\big\langle\Psi_0|\Psi_0\big\rangle}.$$

In this case, the expression for E_0 invariably contains an infinite number of terms, regardless of how the cluster operators are approximated [17, 42]. Furthermore, a parametrisation such as this for the bra state contradicts the Hellmann-Feynman theorem [17, 74]. Thus in the NCCM we must break the Hermitian adjoint relationship between bra and ket states in order to produce a sensible, i.e. *size-extensive* expression for the ground-state energy. This breaking is done by using the definitions given in equations (2.19) and (2.20), which may actually be derived from the Hellmann-Feynman theorem itself[1] [17]. We give up Hermiticity in the CCM to produce a size-extensive energy whereas in the CIM, we maintain Hermiticity but lose the important attribute of size-extensivity. It is not possible to satisfy both of these conditions simultaneously, thus given the choice, it is much more important to retain size-extensivity over Hermiticity, hence one of the reasons why the CCM is now commonly regarded as the method of choice over the CIM [41].

Such a parametrisation as equation (2.19) is chosen in order to ensure that the

[1] in this context, the fact that the NCCM obeys the Hellmann-Feynman theorem to all orders means that the expectation values of all Hermitian many-body operators (including the Hamiltonian) have the same algebraic structure.

expectation value of the Hamiltonian $\hat{H}$, i.e.

$$\langle \hat{H} \rangle = \langle \tilde{\Psi}_0 | \hat{H} | \Psi_0 \rangle = \langle \Phi_0 | \hat{\tilde{S}} e^{-\hat{S}} \hat{H} e^{\hat{S}} | \Phi_0 \rangle = \bar{\hat{H}}\big(\{s_I, \tilde{s}_I\}\big), \tag{2.22}$$

preserves the similarity transformed Hamiltonian of equation (2.12) [17]. In this way, the expression in equation (2.22) remains fully linked, regardless of the fact that the set $\{\tilde{s}_I\}$ contain unlinked terms [17, 42] and hence, the description of any given eigenstate of $\hat{H}$ in the Hilbert space $\mathcal{H}$, as a function of the independent cluster amplitudes $\{s_I, \tilde{s}_I\}$ is valid [17].

2.1.5 NCCM Equations

We now move onto expressing what are generally referred to as the "NCCM equations". We already have an expression for the ground-state energy E_0 as given in equation (2.12), which uses the results for $\{s_I\}$ obtained from equation (2.16) as input. However, we do not have a similar set of equations for the adjoint cluster amplitudes $\{\tilde{s}_I\}$.

Following a similar approach as above, we consider the time-independent Schrödinger equation for a general bra ground-state wave function

$$\langle \tilde{\Psi}_0 | \hat{H} = E_0 \langle \tilde{\Psi}_0 |, \tag{2.23}$$

and substitute the NCCM parametrisation for $\langle \tilde{\Psi}_0 |$ from equation (2.19) into (2.23) to obtain

$$\langle \Phi_0 | \hat{\tilde{S}} e^{-\hat{S}} \hat{H} = E_0 \langle \Phi_0 | \hat{\tilde{S}} e^{-\hat{S}}. \tag{2.24}$$

Multiplying equation (2.24) on the right with $e^{\hat{S}}$ and rearranging gives

$$\langle \Phi_0 | \hat{\tilde{S}} \left(e^{-\hat{S}} \hat{H} e^{\hat{S}} - E_0 \right) = 0. \tag{2.25}$$

If we take the scalar product of equation (2.25) with the complete set of states

$$\{\hat{C}_I^\dagger | \Phi_0 \rangle ; \, \forall I \neq 0\},$$

we have

$$\langle \Phi_0 | \hat{\tilde{S}} \left(e^{-\hat{S}} \hat{H} e^{\hat{S}} - E_0 \right) \hat{C}_I^\dagger | \Phi_0 \rangle = 0, \, \forall I \neq 0. \tag{2.26}$$

Employing equation (2.15) and multiplying it on the left with $\langle \Phi_0 | \hat{\tilde{S}} \hat{C}_I^\dagger$ gives

$$\langle \Phi_0 | \hat{\tilde{S}} \hat{C}_I^\dagger \left(e^{-\hat{S}} \hat{H} e^{\hat{S}} \right) | \Phi_0 \rangle = \langle \Phi_0 | \hat{\tilde{S}} \hat{C}_I^\dagger E_0 | \Phi_0 \rangle, \tag{2.27}$$

which means we can thus eliminates E_0 from equation (2.26) to get

$$\langle\Phi_0|\hat{\tilde{S}}e^{-\hat{S}}\left[\hat{H},\hat{C}_I^\dagger\right]e^{\hat{S}}|\Phi_0\rangle = \langle\tilde{\Psi}_0|\left[\hat{H},\hat{C}_I^\dagger\right]|\Psi_0\rangle = 0,\ \forall I \neq 0. \tag{2.28}$$

Equation (2.28) will thus produce a hierarchy of equations for the adjoint cluster amplitudes $\{\tilde{s}_I\}$ requiring the additional information of the cluster amplitudes $\{s_I\}$ from equation (2.16) for their solution [17].

We thus conclude that the complete NCCM equations are given by

$$\begin{aligned} E_0 &= \langle\Phi_0|e^{-\hat{S}}\hat{H}e^{\hat{S}}|\Phi_0\rangle, \\ \langle\Phi_0|\hat{C}_I e^{-\hat{S}}\hat{H}e^{\hat{S}}|\Phi_0\rangle &= 0,\ \forall I \neq 0, \\ \langle\Phi_0|\hat{\tilde{S}}e^{-\hat{S}}\left[\hat{H},\hat{C}_I^\dagger\right]e^{\hat{S}}|\Phi_0\rangle &= 0,\ \forall I \neq 0. \end{aligned} \tag{2.29}$$

Solving the entire set of equations given in equation (2.29) completely parametrises a ground-state many-body wave function in terms of the cluster amplitudes $\{s_I, \tilde{s}_I\}$ and is directly comparable to solving the time-independent Schrödinger equation of a given many-body problem [17].

2.1.6 Time-Independent Bivariational Principle

The derivation required in order to obtain an equation for the adjoint cluster amplitudes $\{\tilde{s}_I\}$ is somewhat tedious and makes use of a lot of different CCM relations and scalar products. Fortunately, thanks to the work of Arponen [42], there is a way in which we may derive the complete set of NCCM equations (2.29) in a much more straightforward way. Consider the following energy functional

$$\mathcal{F}\big(\{s_I,\tilde{s}_I\}\big) = \langle\Phi_0|\hat{\tilde{S}}e^{-\hat{S}}\hat{H}e^{\hat{S}}|\Phi_0\rangle, \tag{2.30}$$

as first proposed in [42]. We describe this as a "bivarational" functional, since it depends on both sets of the amplitudes $\{s_I, \tilde{s}_I\}$. If we enforce that $\mathcal{F}\big(\{s_I, \tilde{s}_I\}\big)$ is stationary with respect to all possible changes in the amplitudes $\{s_I, \tilde{s}_I\}$ (i.e. we minimise this functional with respect to either cluster amplitude) we obtain

$$\begin{aligned} \frac{\partial}{\partial s_I}\mathcal{F}\big(\{s_I,\tilde{s}_I\}\big) &= \langle\Phi_0|\hat{C}_I e^{-\hat{S}}\hat{H}e^{\hat{S}}|\Phi_0\rangle = 0,\ \forall I \neq 0, \\ \frac{\partial}{\partial \tilde{s}_I}\mathcal{F}\big(\{s_I,\tilde{s}_I\}\big) &= \langle\Phi_0|\hat{\tilde{S}}e^{-\hat{S}}\left[\hat{H},\hat{C}_I^\dagger\right]e^{\hat{S}}|\Phi_0\rangle = 0,\ \forall I \neq 0, \end{aligned} \tag{2.31}$$

which are precisely the NCCM equations of equation (2.29) [42]. At the actual stationary point we have the simple result

$$\mathcal{F}\big(\{s_I, \tilde{s}_I\}\big)\big|_{stat} = E_0, \tag{2.32}$$

since as equation (2.31) shows, the functional does not depend on $\hat{\tilde{S}}$ at the stationary point. There is no need to insert an undetermined Lagrange multiplier into these equations since the bra and ket ground-states are now normalised to 1 [35]. However, since $\langle\tilde{\Psi}_0|$ and $|\Psi_0\rangle$ are not Hermitian adjoints of one another, the variational energy of (2.32) determined after truncation of the $\hat{S}$ operator, does *not* represent an upper bound to the value of E_0 [17].

In showing how the NCCM equations can be derived from a static bivariational principle, Arponen had hence shown that the method that could be therefore extended to calculate expectation values of *arbitrary* quantum mechanical many-body operators [42]. Hence, for a some general Hermitian operator $\hat{O}$, if we define the expectation value $\langle\hat{O}\rangle$ as

$$\langle\hat{O}\rangle = \langle\tilde{\Psi}_0|\hat{O}|\Psi_0\rangle = \langle\Phi_0|\hat{\tilde{S}}e^{-\hat{S}}\hat{O}e^{\hat{S}}|\Phi_0\rangle = \bar{\hat{O}}\big(\{s_I, \tilde{s}_I\}\big), \tag{2.33}$$

then we may calculate the average value of $\hat{O}$ as a function of the independent cluster amplitudes $\{s_I, \tilde{s}_I\}$ using the ground-state, time-independent NCCM formalism.

2.1.7 Excited-States (Emrich Scheme)

Thus far in our discussion of NCCM formalism we have only concerned ourselves with the ground-state properties of a many-body system. Indeed, one of the great strengths of the CCM is that it can produce extremely accurate results for many-body ground-state energies [17]. However, an introduction of general CCM formalism would not be complete without addressing the way in which excited-state energies and wave functions may be calculated. Although we will not perform any calculations in the later chapters which require the explicit form of the CCM excited-state wave functions, we briefly describe the method here for the sake of completeness.

The general formalism for calculating excited-states using the CCM was introduced by Emrich [69, 70, 71], after previous attempts at an excited-state CCM approach proved to be unable to deal with infinite systems [69]. As such, the following parametrisation of excited-states is now commonly referred to as the "Emrich scheme" or "Emrich ansatz". We begin by considering the time-independent Schrödinger equation for some general ket excited-state

$$\hat{H}|\Psi_l\rangle = \varepsilon_l|\Psi_l\rangle = (E_0 + \omega_l)\,|\Psi_l\rangle;\; l \neq 0, \tag{2.34}$$

where ε_l are the excited-state energies and ω_l are the excitation energies with respect to the ground-state energy E_0, i.e.

$$\omega_l = \varepsilon_l - E_0. \tag{2.35}$$

Using the so-called Emrich ansatz, the CCM excited-state wave functions are written as

$$\big|\Psi_l\big\rangle = \hat{X}^{(l)}\big|\Psi_0\big\rangle = \hat{X}^{(l)}e^{\hat{S}}\big|\Phi_0\big\rangle, \tag{2.36}$$

where the objects

$$\hat{X}^{(l)} = \sum_{I\neq 0} x_I^{(l)}\hat{C}_I{}^{\dagger}, \tag{2.37}$$

form a set of "linear excitation operators" [17] which act on the exact ket ground-state $\big|\Psi_0\big\rangle$ to produce the ket excited-states $\big|\Psi_l\big\rangle$ [69].

Since the actual parametrisation of the ket ground-state $e^{\hat{S}}\big|\Phi_0\big\rangle$ can in principle also describe excited-state wave functions with the same symmetry as that of the ground-state [69], it is important to impose the condition

$$\big\langle\Phi_0|\Psi_l\big\rangle = 0.$$

Due to their construction, the excitation operators $\hat{X}^{(l)}$ commute with the cluster correlation operators $\hat{S}$ [69] and thus excluding the zeroth order term in equation (2.37) ensures that the excited-state wave functions are orthogonal to the ground-state [69].

By considering the ground-state Schrödinger equation of (2.11) and the excited-state Schrödinger equation of (2.34) [17, 69], we may derive the relation

$$e^{-\hat{S}}\left[\hat{H},\hat{X}^{(l)}\right]e^{\hat{S}}\big|\Phi_0\big\rangle = \omega_l\hat{X}^{(l)}\big|\Phi_0\big\rangle. \tag{2.38}$$

Multiplying equation (2.38) on the left by the complete set of states

$$\big\{\big\langle\Phi_0|\hat{C}_I;\,\forall I\neq 0\big\}\big\},$$

gives [17, 69]

$$\big\langle\Phi_0|\hat{C}_I e^{-\hat{S}}\left[\hat{H},\hat{X}^{(l)}\right]e^{\hat{S}}\big|\Phi_0\big\rangle = \omega_l x_I^{(l)},\ \forall I\neq 0, \tag{2.39}$$

which are the excited-state NCCM equations for $\big\{x_I^{(l)}\big\}$, comparable to the ground-state NCCM equations for $\big\{s_I\big\}$ as given in equation (2.16). They require the amplitudes $\big\{s_I\big\}$ as input in order for the excitation energies as given in equation (2.35) to be computed. This is not the only way in which excited-state energies may be calculated however, as will be shown shortly.

2.1.8 Time-Dependent Bivariational Principle

If we wish to apply NCCM techniques to dynamic many-body problems, it is inevitable that we will need to introduce time-dependence into our formalism. Thus we now propose a *time-dependent* bivariational principle [42] and define a quantum mechanical action functional

$$A = \int_{-\infty}^{+\infty} dt \langle \tilde{\Psi}(t) | \left(i\frac{\partial}{\partial t} - \hat{H} \right) | \Psi(t) \rangle. \tag{2.40}$$

If we require this functional to be stationary with respect to arbitrary changes in the ket or bra ground-state wave functions [17] we find

$$\frac{\delta A}{\delta \langle \tilde{\Psi}(t) |} = 0 \Rightarrow i\frac{\partial}{\partial t} | \Psi(t) \rangle = \hat{H} | \Psi(t) \rangle,$$

$$\frac{\delta A}{\delta | \Psi(t) \rangle} = 0 \Rightarrow -i\frac{\partial}{\partial t} \langle \tilde{\Psi}(t) | = \langle \tilde{\Psi}(t) | \hat{H}, \tag{2.41}$$

i.e. we obtain nothing more than the time-dependent Schrödinger equations for $|\Psi(t)\rangle$ and $\langle \tilde{\Psi}(t) |$ [17, 42]. We introduce time-dependence into our bra and ket states via the parametrisation given in [42], namely

$$| \Psi(t) \rangle = e^{\hat{S}(t)} | \Phi_0 \rangle,$$

$$\langle \tilde{\Psi}(t) | = \langle \Phi_0 | \hat{\tilde{S}}(t) \, e^{-\hat{S}(t)}, \tag{2.42}$$

where the time-dependence is placed strictly in the cluster amplitudes only [42], i.e.

$$\hat{S}(t) = \sum_{I \neq 0} s_I(t) \, \hat{C}_I^{\dagger},$$

$$\hat{\tilde{S}}(t) = 1 + \sum_{I \neq 0} \tilde{s}_I(t) \, \hat{C}_I. \tag{2.43}$$

If we substitute the expressions of equation (2.42) into equation (2.40) and enforce orthonormality of the multiconfigurational creation and annihilation operators as in (2.7), we have

$$A = \int_{-\infty}^{+\infty} dt \left(i \sum_{I \neq 0} \tilde{s}_I(t) \, \dot{s}_I(t) - \bar{\hat{H}}\left(\{ s_I, \tilde{s}_I \} \right) \right), \tag{2.44}$$

where $\bar{\hat{H}}\left(\{ s_I, \tilde{s}_I \} \right)$ is the NCCM ground-state expectation value of the Hamiltonian as given in equation (2.22) and $\dot{s}_I(t) = \frac{d}{dt} s_I(t)$. This expression for A is nothing more than a classical Hamiltonian action [120]. If we enforce that this functional be stationary with respect to the now time-dependent cluster amplitudes, we obtain the

NCCM equations of motion for $s_I(t)$ and $\tilde{s}_I(t)$

$$\frac{\partial A}{\partial \tilde{s}_I} = 0 \Rightarrow i\dot{s}_I = \frac{\partial \bar{\hat{H}}}{\partial \tilde{s}_I},$$

$$\frac{\partial A}{\partial s_I} = 0 \Rightarrow -i\dot{\tilde{s}}_I = \frac{\partial \bar{\hat{H}}}{\partial s_I}. \tag{2.45}$$

It is now seen that a fundamental link exists between the set of cluster amplitudes $\{s_I, \tilde{s}_I\}$, namely that the pair are *canonically conjugate* to one another, in the language of classical Hamiltonian dynamics [17, 120]. We can make this mapping formally exact [17] by introducing 2 new objects

$$\phi_I = \frac{1}{\sqrt{2}}(\tilde{s}_I + s_I),$$

$$\pi_I = \frac{i}{\sqrt{2}}(\tilde{s}_I - s_I), \tag{2.46}$$

where ϕ_I is the generalised multiconfigurational field [17] and π_I is the generalised multiconfigurational momenta [17]. We then have Hamilton's equations of motion [120] given by

$$\dot{\phi}_I = \frac{\partial \bar{\hat{H}}}{\partial \pi_I},$$

$$\dot{\pi}_I = -\frac{\partial \bar{\hat{H}}}{\partial \phi_I}, \tag{2.47}$$

where $\bar{\hat{H}} = \bar{\hat{H}}(\phi_I, \pi_I)$ [17].

The parametrisation of the NCCM bra ground-state as $\langle \tilde{\Psi}_0 | = \langle \Phi_0 | \hat{\tilde{S}} e^{-\hat{S}}$ has thus not only proceeded to encode the Goldstone linked-cluster theorem within the method but has also been shown to produce a canonically conjugate set of variables $\{s_I, \tilde{s}_I\}$, representative of a set of classical fields that have been mapped from a quantum many-body or field theoretic problem exactly [17]. A much more detailed set of discussions on this underlying principle may be found in [35, 121] and the series of papers [36, 37, 38] offers an extremely detailed overview of this mapping structure and related ideas.

2.1.9 Excited-State Energies (RPA Scheme)

We have already shown in principle how excited-state energies may be calculated in the NCCM using the Emrich scheme. Here, we introduce the so-called Random Phase Approximation (RPA) as a means to derive an easier way of calculating such energies. As we know from equation (2.31), by writing down the ground-state expectation value $\bar{\hat{H}} = \langle \tilde{\Psi}_0 | \hat{H} | \Psi_0 \rangle$ and making it stationary with respect to the set of cluster amplitudes

$\left\{s_I, \tilde{s}_I\right\}$,

$$\frac{\partial \bar{\hat{H}}}{\partial \tilde{s}_I} = 0 = \frac{\partial \bar{\hat{H}}}{\partial s_I},$$

we produce the complete time-independent NCCM equations for the ground-state. At the actual stationary point of $\bar{\hat{H}}$ we have the simple relation

$$\bar{\hat{H}}\Big|_{stat} = E_0 = \left\langle \Phi_0 \middle| e^{-\hat{S}} \hat{H} e^{\hat{S}} \middle| \Phi_0 \right\rangle,$$

where $\bar{\hat{G}}\Big|_{stat}$ means that the expectation value of the operator $\hat{G}$ is evaluated at the stationary point $\left\{s_I^{(0)}, \tilde{s}_I^{(0)}\right\}$ [17, 42].

In order to find an expression for the excited-state energies, we first consider a static variation to our Hamiltonian $\hat{H}$. Thus we introduce a small time-independent perturbation $\lambda\hat{A}$ [17, 42] and expand around the stationary point $\left\{s_I^{(0)}, \tilde{s}_I^{(0)}\right\}$ [17, 35]. Writing

$$s_I \mapsto s_I^{(0)} + \delta s_I;\ \tilde{s}_I \mapsto \tilde{s}_I^{(0)} + \delta \tilde{s}_I, \tag{2.48}$$

we Taylor expand $\bar{\hat{H}}$ to second order [17, 42] and observe that close to the stationary point we have

$$\bar{\hat{H}} = E_0 + J\left(x\right)\big|_{stat} \delta x + \frac{1}{2} \left(\delta x\right)^T H\left(x\right)\big|_{stat} \delta x + \ldots, \tag{2.49}$$

where the vector δx is given by

$$\delta x = \begin{pmatrix} \delta s_I \\ \delta \tilde{s}_I \end{pmatrix},$$

the Jacobian matrix $J\left(x\right)$ is given by

$$J\left(x\right) = \begin{pmatrix} \frac{\partial \bar{\hat{H}}}{\partial x_1} & \frac{\partial \bar{\hat{H}}}{\partial x_2} \end{pmatrix},$$

and the Hessian matrix $H\left(x\right)$ is given by

$$H\left(x\right) = \begin{pmatrix} \frac{\partial^2 \bar{\hat{H}}}{\partial x_1^2} & \frac{\partial^2 \bar{\hat{H}}}{\partial x_1 \partial x_2} \\ \frac{\partial^2 \bar{\hat{H}}}{\partial x_2 \partial x_1} & \frac{\partial^2 \bar{\hat{H}}}{\partial x_2^2} \end{pmatrix}.$$

Writing equation (2.49) more explicitly we have

$$\bar{\hat{H}} \simeq E_0 + \sum_{I \neq 0} \left(\frac{\partial \bar{\hat{H}}}{\partial s_I} \delta s_I + \frac{\partial \bar{\hat{H}}}{\partial \tilde{s}_I} \delta \tilde{s}_I \right) \Bigg|_{stat}$$

$$+\sum_{I\neq 0}\sum_{J\neq 0}\left(\delta\tilde{s}_I\frac{\partial^2\bar{\hat{H}}}{\partial\tilde{s}_I\partial s_J}\delta s_J+\frac{1}{2}\delta s_I\frac{\partial^2\bar{\hat{H}}}{\partial s_I\partial s_J}\delta s_J+\frac{1}{2}\delta\tilde{s}_I\frac{\partial^2\bar{\hat{H}}}{\partial\tilde{s}_I\partial\tilde{s}_J}\delta\tilde{s}_J\right)\Bigg|_{stat}, \tag{2.50}$$

but since we already know that

$$\frac{\partial\bar{\hat{H}}}{\partial s_I}=\frac{\partial\bar{\hat{H}}}{\partial\tilde{s}_I}=0,$$

at the stationary point, and that we can never have terms bi-linear in $\delta\tilde{s}_I$ due to the construction of our ground-state expectation value [17], this expression simplifies to

$$\bar{\hat{H}}\simeq E_0+\sum_{I\neq 0}\sum_{J\neq 0}\left(\delta\tilde{s}_I\frac{\partial^2\bar{\hat{H}}}{\partial\tilde{s}_I\partial s_J}\delta s_J+\frac{1}{2}\delta s_I\frac{\partial^2\bar{\hat{H}}}{\partial s_I\partial s_J}\delta s_J\right)\Bigg|_{stat}. \tag{2.51}$$

We choose to write this in the form

$$\bar{\hat{H}}\simeq E_0+\sum_{I\neq 0}\sum_{J\neq 0}\left(\delta\tilde{s}_I E_{IJ}\delta s_J+\frac{1}{2}\delta s_I F_{IJ}\delta s_J\right), \tag{2.52}$$

where the matrices E_{IJ} and F_{IJ} are given by

$$E_{IJ}=\left.\frac{\partial^2\bar{\hat{H}}}{\partial\tilde{s}_I\partial s_J}\right|_{stat}=\left(E^T\right)_{JI}, \tag{2.53}$$

and

$$F_{IJ}=\left.\frac{\partial^2\bar{\hat{H}}}{\partial s_I\partial s_J}\right|_{stat}=F_{JI}. \tag{2.54}$$

Finally, we may simplify this expression still further and write the expansion given in equation (2.52) in the succinct block matrix form [17]

$$\bar{\hat{H}}\simeq E_0+\frac{1}{2}\left(\delta x\right)^T\mathcal{H}\delta x, \tag{2.55}$$

where

$$\mathcal{H}=\begin{pmatrix}F_{IJ} & \left(E_{IJ}\right)^T\\ E_{IJ} & 0\end{pmatrix}=\mathcal{H}^T. \tag{2.56}$$

If we now use this information and consider a *time-dependent* expansion of $\bar{\hat{H}}$ close to the stationary point, i.e. the case where the perturbations of the cluster amplitudes are time-dependent

$$s_I\mapsto s_I^{(0)}+\delta s_I\left(t\right);\ \tilde{s}_I\mapsto\tilde{s}_I^{(0)}+\delta\tilde{s}_I\left(t\right), \tag{2.57}$$

then the equations of motion for the amplitudes $s_I(t)$ and $\tilde{s}_I(t)$ are given by

$$i\dot{s}_I(t) = \frac{\partial \bar{\hat{H}}}{\partial \tilde{s}_I};\ -i\dot{\tilde{s}}_I(t) = \frac{\partial \bar{\hat{H}}}{\partial s_I}.$$

We can combine these expressions together to show that small oscillations about the unperturbed ground-state stationary point of $\bar{\hat{H}}$ (given by $\left\{s_I^{(0)}, \tilde{s}_I^{(0)}\right\}$) are described by

$$i\frac{d}{dt}\delta x \simeq \hat{H}_D \delta x \tag{2.58}$$

where $\hat{H}_D$ is the *effective Hamiltonian* or *dynamic matrix* [17], given by

$$\hat{H}_D = \mathcal{O}\mathcal{H} = \begin{pmatrix} E_{IJ} & 0 \\ -F_{IJ} & -(E_{IJ})^T \end{pmatrix}, \tag{2.59}$$

and

$$\mathcal{O} = \begin{pmatrix} 0 & 1 \\ -1 & 0 \end{pmatrix}.$$

In order to solve equation (2.58) we separate the variables and make the *harmonic assumption* [17] (i.e. that our solutions behave as *normal modes* [17, 120]) thus we write

$$\delta x \to \gamma_n(\omega, t) = \gamma_n e^{-i\omega_n t}, \tag{2.60}$$

where γ_n and ω_n are calculated via the eigenvalue equation

$$\hat{H}_D \gamma_n = \omega_n \gamma_n, \tag{2.61}$$

which may be expressed as the matrix equation

$$\begin{pmatrix} E_{IJ} & 0 \\ -F_{IJ} & -(E_{IJ})^T \end{pmatrix} \begin{pmatrix} \delta s_J \\ \delta \tilde{s}_J \end{pmatrix} = \omega_n \begin{pmatrix} \delta s_I \\ \delta \tilde{s}_I \end{pmatrix}. \tag{2.62}$$

This is the essence of the RPA approach - we calculate the excited-state energies $\varepsilon_n = \omega_n + E_0$ via the time-dependent fluctuations about the stationary point of $\hat{H}_D$. We therefore we want to calculate the eigenvalues of the dynamic matrix $\hat{H}_D$.

Since $\hat{H}_D$ is a product of an antisymmetric and a symmetric matrix, the set of eigenvalues $\{\omega_n\}$ will appear in the pairs $\omega = \pm\omega_n$ - but since these eigenvalues represent excitation energies relative to the ground-state energy, i.e. $\omega_n = \varepsilon_n - E_0$ (as with equation (2.35) in the Emrich scheme), we only wish to calculate the positive values of

ω_n [17]. This means equation (2.62) is therefore reduced to the problem

$$E_{IJ}\delta s_J = \sum_{J\neq 0} \frac{\partial^2 \bar{\hat{H}}}{\partial \tilde{s}_I \partial s_J}\delta s_J = \omega_n \delta s_I. \tag{2.63}$$

which solely depends on the cluster amplitudes $\{s_I\}$. This feature is rather desirable since it these cluster amplitudes that contain no unlinked pieces in the NCCM [17].

The so-called *RPA matrix* E_{IJ} may be written explicitly as

$$E_{IJ} = \sum_{J\neq 0} \langle \Phi_0 | \hat{C}_I e^{-\hat{S}} \left[\hat{H}, \hat{C}_J^\dagger\right] e^{\hat{S}} | \Phi_0 \rangle \, , \forall I \neq 0, \tag{2.64}$$

or even more succinctly as

$$E_{IJ} = \partial_{s_J} E_I, \tag{2.65}$$

where $\partial_{s_J} = \frac{\partial}{\partial s_J}$, index summation is implied and E_I is the "I^{th} **N**CCM equation"

$$\langle \Phi_0 | \hat{C}_I e^{-\hat{S}} \hat{H} e^{\hat{S}} | \Phi_0 \rangle \, , \forall I \neq 0.$$

As a trivial example, if I and J ran from 1 to 3, the RPA matrix would be given by

$$E_{IJ} = \begin{pmatrix} \partial_{s_1} E_1 & \partial_{s_2} E_1 & \partial_{s_3} E_1 \\ \partial_{s_1} E_2 & \partial_{s_2} E_2 & \partial_{s_3} E_2 \\ \partial_{s_1} E_3 & \partial_{s_2} E_3 & \partial_{s_3} E_3 \end{pmatrix}.$$

Thus, we have established the RPA approach to calculating excited-state energies using the NCCM formalism - we calculate the NCCM equations for $\{s_I\}$ as given in (2.16), construct the RPA matrix E_{IJ} of (2.64) by differentiating the equations for $\{s_I\}$, then calculate the positive eigenvalues ω_n of the RPA matrix before utilising the relation $\varepsilon_n = \omega_n + E_0$ in order to calculate the excited-state energies ε_n. Although the approach may at first seem quite arduous, since it is essential that any ground-state NCCM calculation will require the equations of (2.16) to be evaluated, constructing the RPA matrix is rather trivial, and allows excited-state energies to be calculated very easily.

2.1.10 Truncation and Approximation

Having covered much of the mathematical foundations of the ground-state NCCM formalism, we now focus on the idea of actually evaluating the complete NCCM equations as they are given in equation (2.29). If we take the problem at face value, we are looking at an infinitely large hierarchy of equations to solve. Inevitably, these equations must somehow be approximated at some stage of calculation, in order to be solved

numerically.

When using the NCCM to study the ground-state properties of a many-body system, the most basic and general truncation scheme we can use is known as the "SUB(n) approximation". This is a scheme which neglects specific higher order terms of the cluster correlation operator $\hat{S}$ (or the adjoint operator $\hat{\tilde{S}}$). Importantly, this truncation in turn makes the equations for the set $\{s_I\}$ (or $\{\tilde{s}_I\}$) as given in equation (2.16) (or (2.28)) finite [17]. If we have our cluster operator given by $\hat{S} = \hat{S}_1 + \hat{S}_2 + \ldots + \hat{S}_i$, then the SUB($n$) scheme neglects terms of order $i > n$ and only includes terms with $i \leq n$ [17]. Hence, to SUB(n), the cluster operator would be given by $\hat{S} = \hat{S}_1 + \hat{S}_2 + \ldots + \hat{S}_n$. Essentially we are setting $\hat{S}_i = 0$ for $i > n$ [17]. If we are actually required to solve the complete NCCM equations (2.29), i.e. we wish to find the expectation value of some general many-body operator using the NCCM, the operators $\hat{S}$ and $\hat{\tilde{S}}$ are truncated to the same order.

Importantly, once the cluster correlation operator has been truncated, no more approximation schemes need to be applied as the similarity transformed structure of the Hamiltonian (or any other Hermitian many-body operator) will produce finite order equations [17] - thus the equations are exact and there is no need to approximate them in order to solve for the ground-state energy. Due to the exponential parametrisation of the ground-state wave function, the NCCM continues to be size-extensive, i.e. scale properly with particle number N, regardless of how the cluster correlation operator is approximated [17]. The SUB(n) scheme may be described as a "hierarchical approximation scheme" [17], in that increasingly higher order SUB(n) approximations include increasingly more many-body interactions [17].

Other such truncation schemes exist, the most common of which is probably the "SUB(m,n) approximation", applied in the time-independent Emrich approach of excited-states [17, 69, 70]. In the SUB(m,n) approximation scheme, the linear excitation operator $\hat{X}^{(l)}$ and cluster operator $\hat{S}$ are truncated at m^{th} or n^{th} order respectively (in precisely the same manner as how terms in $\hat{S}$ of order greater than n are set equal to zero in the SUB(n) scheme). The numbers m and n do not necessarily have to be the same [17].

There are no specific rules of how a series in the set of cluster amplitudes $\{s_I, \tilde{s}_I\}$ is best truncated, indeed it is usually dependent on the problem at hand. Thus it is common to find authors defining their own approximation schemes in relation to their work, usually with some significant initials prefixing the "SUB(n)" name [17] (for instance, during chapter 4 we will make use of the so-called "QPSUB(n) approximation", where the initials QP relate to the fact our Hamiltonian is written in terms of quasi-particle operators).

2.2 The Extended Coupled Cluster Method

Having established the details of the NCCM formalism, we now introduce the most important concepts of the ECCM formalism in as concise a manner as possible, focusing only on the features that will be most useful to us in the work discussed in chapters 3, 4 and 5. As we shall see, the ECCM approach is fundamentally more complicated than the NCCM and thus has not been as widely applied to problems as the NCCM has. Nevertheless, it is an extremely powerful many-body tool and one that has been shown to be able to describe such global system properties as spontaneous symmetry breaking and phase transitions extremely well [77].

The idea of the ECCM essentially grew from the desire to have a more general form of the CCM, one in which both sets of cluster correlation amplitudes would contain no unlinked terms [42]. It was first introduced by Arponen [42], alongside his development of the "normal expS" method, as he called it at the time. It has since been refined a great deal, particularly in the series of papers [74, 75] where much of the established NCCM formalism is generalised to the ECCM framework. This in turn leads up to an ECCM description of Bose fluids given in [76] and an in-depth study of the LMG model in [77]. Here, we begin from Arponen's initial approach [42], and thus formulate the ECCM from a time-independent bivariational principle

2.2.1 Ground-State Energy Functional

Following on from exactly the same idea expressed in equation (2.30) for the NCCM, we write down a similar functional for the ECCM [42], namely

$$E\big(\{s_I, \tilde{s}_I\}\big) = \big\langle \Phi_0 \big| e^{\hat{\tilde{S}}} e^{-\hat{S}} \hat{H} e^{\hat{S}} \big| \Phi_0 \big\rangle, \tag{2.66}$$

where again we have $E\big(\{s_I, \tilde{s}_I\}\big)\big|_{stat} = E_0$ at the stationary point of the functional. Note that this differs from the NCCM expression by the term $\hat{\tilde{S}}$, which is now replaced by $e^{\hat{\tilde{S}}}$, often labeled $e^{\hat{S}''}$ in older literature (for example, [42]). The adjoint cluster correlation operator $\hat{\tilde{S}}$ is now defined by

$$\hat{\tilde{S}} = \sum_{I \neq 0} \tilde{s}_I \hat{C}_I,$$

where the now fully linked adjoint cluster amplitudes $\tilde{s}_I$ are given by the ground-state expectation value $\big\langle \hat{C}_I{}^{\dagger} \big\rangle_{\text{linked}}$ [42]. We therefore now have a ground-state energy functional $E\big(\{s_I, \tilde{s}_I\}\big)$ which is defined solely in terms of the set of *linked-cluster* amplitudes $\{s_I, \tilde{s}_I\}$ [17, 42].

We may further write this functional as

$$E\big(\{s_I, \tilde{s}_I\}\big) = \big\langle \Phi_0 \big| e^{\hat{\tilde{S}}} e^{-\hat{S}} \hat{H} e^{\hat{S}} e^{-\hat{\tilde{S}}} \big| \Phi_0 \big\rangle, \tag{2.67}$$

since by definition $e^{-\hat{\tilde{S}}}\big|\Phi_0\big\rangle = \big|\Phi_0\big\rangle$, and we hence observe that the Hamiltonian of equation (2.67) has undergone a *double* similarity transformation [17]. This transformation is not unitary [17] (i.e. it doesn't preserve length) and therefore the ECCM remains manifestly nonHermitian, as was the case for the NCCM. As one would expect, this functional may also be derived directly from the Schrödinger equation for the ket ground-state wave function $\big|\Psi_0\big\rangle = e^{\hat{S}} e^{-\hat{\tilde{S}}}\big|\Phi_0\big\rangle$, thus

$$\hat{H}\big|\Psi_0\big\rangle = E_0\big|\Psi_0\big\rangle \Rightarrow \hat{H} e^{\hat{S}} e^{-\hat{\tilde{S}}}\big|\Phi_0\big\rangle = E_0 e^{\hat{S}} e^{-\hat{\tilde{S}}}\big|\Phi_0\big\rangle$$

$$\Rightarrow \big\langle \Phi_0 \big| e^{\hat{\tilde{S}}} e^{-\hat{S}} \hat{H} e^{\hat{S}} e^{-\hat{\tilde{S}}} \big| \Phi_0 \big\rangle = E_0. \tag{2.68}$$

The corresponding bra ground-state wave function is parametrised as $\big\langle \tilde{\Psi}_0 \big| = \big\langle \Phi_0 \big| e^{\hat{\tilde{S}}} e^{-\hat{S}}$ [42] and we therefore maintain the intermediate normalisation condition given by

$$\big\langle \tilde{\Psi}_0 | \Psi_0 \big\rangle = 1, \tag{2.69}$$

as with the NCCM.

Furthermore, utilising the fact that the first term in the expansion of $e^{\hat{\tilde{S}}}$ is 1, we observe that to first order in $\hat{\tilde{S}}$, the ECCM functional (2.67) is given by

$$E = \big\langle \Phi_0 \big| \big(1 + \hat{\tilde{S}}\big) e^{-\hat{S}} \hat{H} e^{\hat{S}} \big| \Phi_0 \big\rangle,$$

which is precisely the NCCM expression for the ground-state energy functional, as given in equation (2.30) (note the actual definition of $\hat{\tilde{S}}$ in each case differs slightly but the functional remains the same). Consequently, the ECCM naturally incorporates the entire ground-state NCCM formalism to first order in the adjoint cluster operator $\hat{\tilde{S}}$ - thus the NCCM formalism acts in some respects as a first order starting point for the ECCM.

2.2.2 ECCM Equations

Continuing in the same manner as the bivariational formulation of the NCCM given in equation (2.31), we minimise the ECCM functional (2.66) or (2.67) with respect to the set of linked-cluster amplitudes $\big\{s_I, \tilde{s}_I\big\}$ to obtain the so-called ECCM equations

$$\frac{\partial}{\partial s_I} E\big(\{s_I, \tilde{s}_I\}\big) = \big\langle \Phi_0 \big| e^{\hat{\tilde{S}}} e^{-\hat{S}} \left[\hat{H}, \hat{C}_I^{\dagger}\right] e^{\hat{S}} e^{-\hat{\tilde{S}}} \big| \Phi_0 \big\rangle = 0, \; \forall I \neq 0,$$

$$\frac{\partial}{\partial \tilde{s}_I} E\big(\{s_I, \tilde{s}_I\}\big) = \big\langle \Phi_0 \big| \left[\hat{C}_I, \hat{H}'\right] \big| \Phi_0 \big\rangle = 0, \, \forall I \neq 0, \tag{2.70}$$

where $\hat{H}'$ is the double similarity transformed Hamiltonian $e^{\hat{\tilde{S}}} e^{-\hat{S}} \hat{H} e^{\hat{S}} e^{-\hat{\tilde{S}}}$. In practice we never evaluate these equations using direct commutator algebra, we simply differentiate the ground-state energy functional $E\big(\{s_I, \tilde{s}_I\}\big)$ with respect to either cluster amplitude and solve the resulting coupled, nonlinear equations simultaneously for s_I and $\tilde{s}_I$.

This is one of the added complexities of the ECCM however - both of the ECCM equations given in (2.70) are functions of both cluster amplitudes. For the NCCM case we would solve equation (2.16) solely for s_I, then solve equation (2.28) for $\tilde{s}_I$ using the values of s_I as input. For the ECCM case however, we must solve *simultaneously* for both cluster amplitudes. For low order approximations such as SUB(1) or SUB(2) this may not prove too difficult, however, for SUB(3) or higher the ECCM equations for a given system can become extremely complicated, resulting in a huge amount of solutions for the ground-state energy.

We therefore conclude that the complete ECCM equations are given explicitly by

$$\begin{aligned} E_0 &= \big\langle \Phi_0 \big| e^{\hat{\tilde{S}}} e^{-\hat{S}} \hat{H} e^{\hat{S}} \big| \Phi_0 \big\rangle, \\ \big\langle \Phi_0 \big| e^{\hat{\tilde{S}}} e^{-\hat{S}} \left[\hat{H}, \hat{C}_I^{\dagger}\right] e^{\hat{S}} e^{-\hat{\tilde{S}}} \big| \Phi_0 \big\rangle &= 0, \, \forall I \neq 0, \\ \big\langle \Phi_0 \big| \left[\hat{C}_I, e^{\hat{\tilde{S}}} e^{-\hat{S}} \hat{H} e^{\hat{S}} e^{-\hat{\tilde{S}}}\right] \big| \Phi_0 \big\rangle &= 0, \, \forall I \neq 0, \end{aligned} \tag{2.71}$$

in analogy with equation (2.29). At a given level of SUB(n) approximation, both $\hat{S}$ and $\hat{\tilde{S}}$ are truncated to the same order. As before, this truncation means the second and third equations in (2.71) become finite polynomials in both s_I and $\tilde{s}_I$, the solutions of which form the input for the first equation, which determines the ground-state energy of the many-body system under consideration.

2.2.3 Equations of Motion

Utilising the action functional of equation (2.40), we may derive the ECCM equations of motion analogous to those of the NCCM given in equation (2.45). For the ECCM case we obviously write this functional as

$$A = \int_{-\infty}^{+\infty} dt \big\langle \Phi_0 \big| e^{\hat{\tilde{S}}(t)} e^{-\hat{S}(t)} \left(i \frac{\partial}{\partial t} - \hat{H} \right) e^{\hat{S}(t)} \big| \Phi_0 \big\rangle, \tag{2.72}$$

where again the cluster amplitudes now carry all of the time-dependence, i.e.

$$\hat{S}(t) = \sum_{I \neq 0} s_I(t) \, \hat{C}_I{}^{\dagger}; \; \hat{\tilde{S}}(t) = \sum_{I \neq 0} \tilde{s}_I(t) \, \hat{C}_I, \tag{2.73}$$

and the normalisation of equation (2.69) is implied [42]. If we insert the amplitudes of (2.73) into (2.72) we obtain

$$A = \int_{-\infty}^{+\infty} dt \Bigg(-i \big\langle \Phi_0 \big| \dot{\hat{\tilde{S}}}(t)\, e^{\hat{\tilde{S}}(t)} \hat{S}(t) \big| \Phi_0 \big\rangle - \bar{\hat{H}}\big(\{ s_I, \tilde{s}_I \} \big) \Bigg), \tag{2.74}$$

where the first term of (2.74) has come from the integration by parts of $e^{\hat{\tilde{S}}(t)} \dot{\hat{S}}(t)$ [17, 42] and $\bar{\hat{H}}\big(\{ s_I, \tilde{s}_I \} \big)$ is the usual ECCM ground-state expectation value of the Hamiltonian.

Unfortunately this expression does not appear in the same form as that of the classical action [120] nor that of the NCCM action, as given in equation (2.44). Thankfully, this can be rectified by introducing a new set of linked-cluster amplitudes [42]

$$\hat{\Sigma} = \sum_{I \neq 0} \sigma_I \hat{C_I}^{\dagger},$$

$$\hat{\tilde{\Sigma}} = \sum_{I \neq 0} \tilde{\sigma}_I \hat{C}_I, \tag{2.75}$$

where

$$\sigma_I = \big\langle \Phi_0 \big| \hat{C}_I e^{\hat{\tilde{S}}(t)} \hat{S}(t) \big| \Phi_0 \big\rangle, \tag{2.76}$$

$$\tilde{\sigma}_I = \tilde{s}_I, \tag{2.77}$$

and s_I can be written in terms of $\hat{\Sigma}$ and $\hat{\tilde{\Sigma}}$ [17] by the expression

$$s_I = \big\langle \Phi_0 \big| \hat{C}_I e^{-\hat{\tilde{\Sigma}}} \hat{\Sigma} \big| \Phi_0 \big\rangle. \tag{2.78}$$

If we now use the relations of (2.75), (2.76) and (2.77) in equation (2.74) we have

$$A = \int_{-\infty}^{+\infty} dt \Bigg(i \sum_{I \neq 0} \tilde{\sigma}_I(t)\, \dot{\sigma}_I(t) - \bar{\hat{H}}\big(\{ \sigma_I, \tilde{\sigma}_I \} \big) \Bigg). \tag{2.79}$$

Again, by requiring this functional to be stationary with respect to variations in the new cluster amplitudes $\sigma_I(t)$ and $\tilde{\sigma}_I(t)$, we have the ECCM equations of motion given by

$$\frac{\partial A}{\partial \tilde{\sigma}_I} = 0 \Rightarrow i \dot{\sigma}_I = \frac{\partial \bar{\hat{H}}}{\partial \tilde{\sigma}_I},$$

$$\frac{\partial A}{\partial \sigma_I} = 0 \Rightarrow -i \dot{\tilde{\sigma}}_I = \frac{\partial \bar{\hat{H}}}{\partial \sigma_I}. \tag{2.80}$$

Thus, we recognise that the new ground-state ECCM amplitudes $\{ \sigma_I, \tilde{\sigma}_I \} = \{ \sigma_I, \tilde{s}_I \}$ are a canonically conjugate set [17], analogous to the NCCM canonically conjugate set $\{ s_I, \tilde{s}_I \}$ as seen in equation (2.44). We have therefore shown that the ground-

state properties of a many-body system may be completely parametrised by the set of linked-cluster amplitudes $\{s_I, \tilde{s}_I\}$ or $\{\sigma_I, \tilde{\sigma}_I\}$ in the ECCM formalism. Similarly we also have the exact mapping discussed earlier, where the amplitudes $\{\sigma_I, \tilde{\sigma}_I\}$ behave as a pair of canonically conjugate fields, subject to classical Hamiltonian dynamics [17]. In practice we tend not to work with the canonically conjugate amplitudes since their evaluation proves difficult, hence in all of the work presented later we parametrise states according to the set $\{s_I, \tilde{s}_I\}$.

It may be shown that a vast amount of the properties and features of the NCCM formalism, for example the Emrich ansatz for excited-states, can be generalised by the ECCM [74, 75]. Indeed, the ECCM is much more rich in technical depth than the NCCM, as already pointed out in Arponen's original formulation of it [42] as well as by the later series of papers [36, 37, 38]. We will not cover these augmentations here however, as they are generally related to the underlying mathematical structure of the theory and its roots in diagrammatic many-body perturbation theory [42, 74] and as such, have no bearing on the work we wish to present.

2.3 Applications to Many-Fermion Systems with Pairing

We are now almost in a position to begin analysing some specific many-body systems using either the NCCM or ECCM. However, there are still some useful techniques that we have not yet covered, particularly for many-body systems with pairing. In the final section of this chapter, we introduce a generic many-fermion model which includes pairing and perform a SUB(1) ECCM calculation for the system. As we shall see, this will prove to be extremely valuable in approaching pairing problems using the ECCM to higher SUB(n). The additional formalism we will cover here is important for the work we will discuss in chapters 4 and 5.

2.3.1 Hamiltonian for s-wave Pairing

We will consider a system of N identical fermions of spin $\frac{1}{2}$, held at zero temperature and interacting via an attractive two-body force (where we do not specify any particular one-body external potential). This attractive interaction drives the fermion pairing mechanism which leads to the presence of Cooper pairs [100] - where we use the term here to describe bound pairs composed of one fermion in a given state and one in the time-reversed state, for example, one fermion with momentum $\mathbf{k}$ and spin $\uparrow$ $(+\frac{1}{2})$ and one fermion with momentum $-\mathbf{k}$ and spin $\downarrow$ $(-\frac{1}{2})$.

This system may be described by the Hamiltonian

$$\hat{H} = \sum_{k,\sigma} \epsilon_k \hat{a}^\dagger_{\mathbf{k}\sigma} \hat{a}_{\mathbf{k}\sigma} + \sum_{k_1 k_2 k_3 k_4 > 0} V_{k_1 k_2 k_3 k_4} \hat{a}^\dagger_{\mathbf{k}_1\uparrow} \hat{a}^\dagger_{-\mathbf{k}_2\downarrow} \hat{a}_{-\mathbf{k}_4\downarrow} \hat{a}_{\mathbf{k}_3\uparrow} \delta_{\mathbf{k}_1-\mathbf{k}_2+\mathbf{k}_3-\mathbf{k}_4,\mathbf{0}}. \tag{2.81}$$

Here, the single-particle operators $\hat{a}^\dagger_{\mathbf{k}\sigma}$ and $\hat{a}_{\mathbf{k}\sigma}$ are fermion creation and annihilation operators respectively, creating and annihilating fermions in states of momentum $\mathbf{k}$ and spin σ. They obey the usual canonical anticommutation relations

$$\left\{\hat{a}_{\mathbf{k}\sigma}, \hat{a}^\dagger_{\mathbf{q}\sigma'}\right\} = \delta_{\mathbf{kq}}\delta_{\sigma\sigma'},$$

$$\left\{\hat{a}_{\mathbf{k}\sigma}, \hat{a}_{\mathbf{q}\sigma'}\right\} = 0 = \left\{\hat{a}^\dagger_{\mathbf{k}\sigma}, \hat{a}^\dagger_{\mathbf{q}\sigma'}\right\}, \tag{2.82}$$

and are defined relative to the bare vacuum $\big|0\big\rangle$, i.e. $\hat{a}_{\mathbf{k}\sigma}\big|0\big\rangle = 0$. The labels $\uparrow$ and $\downarrow$ denote spin alignments - if we were to specify our model to atomic Bose-Einstein condensates or neutron matter for example, we may wish to include isospin labels as well. The Kronecker delta $\delta_{\mathbf{k}_1-\mathbf{k}_2+\mathbf{k}_3-\mathbf{k}_4,\mathbf{0}}$ is to ensure momentum is conserved. This is *not* a separable pairing Hamiltonian and thus the two-body potential is summed over four different state labels instead of only two.

The single-particle energies are given by ϵ_k - in the absence of any external one-body potentials $\epsilon_k = \frac{\hbar^2 k^2}{2m}$. The coefficients $V_{k_1 k_2 k_3 k_4}$ are the matrix elements

$$\big\langle \mathbf{k}_1\uparrow, -\mathbf{k}_2\downarrow \big| \hat{V} \big| \mathbf{k}_3\uparrow, -\mathbf{k}_4\downarrow \big\rangle, \tag{2.83}$$

where $\hat{V}$ is the two-body interaction [28]. We have chosen s-wave, i.e. spin-singlet pairing, hence there is no additional factor of $\frac{1}{4}$ in front of the potential term (due to the specific ordering of our potential operators, the matrix element in equation (2.83) can be written in four equivalent forms dependent on the ordering of our spins, thus we factor out these possible combinations). For pairing of this type we would most likely choose $\hat{V}$ as a delta or Gaussian function of the position vector $\mathbf{x}$, independent of spin [16].

2.3.2 SUB(1) ECCM Calculation

Using the Hamiltonian of equation (2.81), we wish to formulate the ECCM ground-state energy functional

$$E\big(\{s_I, \tilde{s}_I\}\big) = \big\langle \Phi_0 \big| e^{\hat{\tilde{S}}} e^{-\hat{S}} \hat{H} e^{\hat{S}} \big| \Phi_0 \big\rangle,$$

to SUB(1) approximation. Before we can do this however, we will need to define our model state $\big|\Phi_0\big\rangle$ and the cluster correlation operators $\hat{S}$ and $\hat{\tilde{S}}$ for a pairing problem.

2.3.2.1 Hartree-Fock Model State

The typical model state used for fermionic CCM calculations is the Hartree-Fock or "filled Fermi sea" state, which is just a Slater determinant constructed of single-particle wave functions [66]. We may write this model state as

$$\left|\Phi_0\right\rangle = \prod_{k\leq k_F;\sigma=\uparrow,\downarrow} \hat{a}^\dagger_{\mathbf{k}\sigma}|0\rangle, \tag{2.84}$$

in the style of [20], where k_F is the wave number at the Fermi surface. In the language of [66] we describe the states below and up to the Fermi surface as *occupied* and those above the Fermi surface (i.e. excited-states relative to $\left|\Phi_0\right\rangle$) as *unoccupied*.

2.3.2.2 Pairing Cluster Correlation Operators

We now wish to find an expression for $\hat{S}$ to SUB(1) approximation, which can describe the formation of Cooper pairs arising from our Hamiltonian of equation (2.81). Consider the object

$$\sum_{\mathbf{k},k>k_F} s_k \hat{a}^\dagger_{\mathbf{k}\uparrow}\hat{a}^\dagger_{-\mathbf{k}\downarrow}. \tag{2.85}$$

When acting on the Hartree-Fock model state of (2.84), this expression creates groups of two paired fermions above the Fermi sea, one with momentum $\mathbf{k}$ and spin $\uparrow$ and the other with momentum $-\mathbf{k}$ and spin $\downarrow$. Similarly, the object

$$\sum_{\mathbf{k},k<k_F} s_k \hat{a}_{\mathbf{k}\downarrow}\hat{a}_{-\mathbf{k}\uparrow}, \tag{2.86}$$

annihilates groups of paired fermions in the Fermi sea, again conserving momentum and spin.

Thus, combining equations (2.85) and (2.86) we may write our *pairing* cluster correlation operator as

$$\hat{S} = \sum_{\mathbf{k},k>k_F} s_k \hat{a}^\dagger_{\mathbf{k}\uparrow}\hat{a}^\dagger_{-\mathbf{k}\downarrow} + \sum_{\mathbf{k},k<k_F} s_k \hat{a}_{\mathbf{k}\downarrow}\hat{a}_{-\mathbf{k}\uparrow}, \tag{2.87}$$

where we neglect to explicitly denote these operators and amplitudes as SUB(1) terms for convenience. It is physically transparent that this expression for $\hat{S}$ annihilates groups of paired fermions from the Fermi sea and creates groups of paired fermions above the Fermi sea, conserving both momentum and spin in the process. It therefore acts as a generalised creation operator of Cooper pairs with respect to the Hartree-Fock model state. In analogy with $\hat{S}$, we may write the adjoint pairing cluster correlation

operator as

$$\hat{\tilde{S}} = \sum_{\mathbf{k},k>k_F} \tilde{s}_k \hat{a}_{\mathbf{k}\downarrow} \hat{a}_{-\mathbf{k}\uparrow} + \sum_{\mathbf{k},k<k_F} \tilde{s}_k \hat{a}^\dagger_{\mathbf{k}\uparrow} \hat{a}^\dagger_{-\mathbf{k}\downarrow}. \tag{2.88}$$

Again it is obvious at a glance that this expression acts as a generalised annihilation operator of Cooper pairs with respect to the Hartree-Fock model state - it is not possible to annihilate Cooper pairs above the Fermi sea (none exist there) nor create Cooper pairs below the Fermi sea (it is already filled), hence $\hat{\tilde{S}}\big|\Phi_0\big\rangle = 0$.

Although the expressions (2.87) and (2.88) have physically transparent meanings, our current notation is somewhat cumbersome. Instead of explicitly labeling states of given momentum which are either below or above the Fermi sea, we may talk in terms of "holes" or "particles", relative to the filled Fermi sea state. Thus a term denoting an excitation out of the Fermi sea would be represented by a label $\mathbf{p}$, standing for particle, and a term denoting the appearance of a gap in the Fermi sea would be represented by a label $\mathbf{h}$, standing for hole. In this sense we have the following relations

$$\begin{aligned} &\forall k > k_F,\ \hat{a}^\dagger_{\mathbf{k}} \to \hat{a}^\dagger_{\mathbf{p}}; \hat{a}_{\mathbf{k}} \to \hat{a}_{\mathbf{p}}, \\ &\forall k < k_F,\ \hat{a}_{\mathbf{k}} \to \hat{a}_{\mathbf{h}}; \hat{a}^\dagger_{\mathbf{k}} \to \hat{a}^\dagger_{\mathbf{h}}. \end{aligned} \tag{2.89}$$

Following this, we may therefore rewrite our Hartree-Fock model state (2.84) as

$$\big|\Phi_0\big\rangle = \prod_{\mathbf{h},\sigma=\uparrow,\downarrow} \hat{a}^\dagger_{\mathbf{h}\sigma} \big|0\big\rangle, \tag{2.90}$$

and our pairing cluster correlation operators as

$$\begin{aligned} \hat{S} &= \sum_{\mathbf{p}} s_p \hat{a}^\dagger_{\mathbf{p}\uparrow} \hat{a}^\dagger_{-\mathbf{p}\downarrow} + \sum_{\mathbf{h}} s_h \hat{a}_{\mathbf{h}\downarrow} \hat{a}_{-\mathbf{h}\uparrow} = \hat{S}_p + \hat{S}_h, \\ \hat{\tilde{S}} &= \sum_{\mathbf{p}} \tilde{s}_p \hat{a}_{\mathbf{p}\downarrow} \hat{a}_{-\mathbf{p}\uparrow} + \sum_{\mathbf{h}} \tilde{s}_h \hat{a}^\dagger_{\mathbf{h}\uparrow} \hat{a}^\dagger_{-\mathbf{h}\downarrow} = \hat{\tilde{S}}_p + \hat{\tilde{S}}_h. \end{aligned} \tag{2.91}$$

2.3.2.3 Ground-State Energy Functional

We now return to the problem of actually calculating the ground-state energy functional. In order to evaluate the required matrix elements, the first step is to write down the linked-cluster expansion for the similarity transformed Hamiltonian $e^{-\hat{S}} \hat{H} e^{\hat{S}}$,

$$e^{-\hat{S}} \hat{H} e^{\hat{S}} = \hat{H} + \Big[\hat{H},\hat{S}\Big] + \frac{1}{2!}\Big[\Big[\hat{H},\hat{S}\Big],\hat{S}\Big] + \frac{1}{3!}\Big[\Big[\Big[\hat{H},\hat{S}\Big],\hat{S}\Big],\hat{S}\Big] + \ldots,$$

and break this down into one- and two-body terms. For the Hamiltonian of equation (2.81), the linked-cluster expansion of one-body terms $e^{-\hat{S}}\hat{T}e^{\hat{S}}$ truncates as

$$e^{-\hat{S}}\hat{T}e^{\hat{S}} = \hat{T} + \left[\hat{T},\hat{S}\right] + \frac{1}{2!}\left[\left[\hat{T},\hat{S}\right],\hat{S}\right], \tag{2.92}$$

and similarly the expansion of the two-body terms $e^{-\hat{S}}\hat{V}e^{\hat{S}}$ truncates as

$$e^{-\hat{S}}\hat{V}e^{\hat{S}} = \hat{V} + \left[\hat{V},\hat{S}\right] + \frac{1}{2!}\left[\left[\hat{V},\hat{S}\right],\hat{S}\right] + \frac{1}{3!}\left[\left[\left[\hat{V},\hat{S}\right],\hat{S}\right],\hat{S}\right] + \frac{1}{4!}\left[\left[\left[\left[\hat{V},\hat{S}\right],\hat{S}\right],\hat{S}\right],\hat{S}\right], \tag{2.93}$$

due to the specific construction of $\hat{S}$ [66] (namely the individual operators which make up $\hat{S}$ can only contract with $\hat{T}$ as many as two times and with $\hat{V}$ as many as four times).

After calculating the commutators of equations (2.92) and (2.93) we then multiply on the left by $e^{\hat{\tilde{S}}}$ and evaluate all the possible matrix elements

$$E\big(\{s_p,\tilde{s}_p,s_h,\tilde{s}_h\}\big) = \big\langle\Phi_0\big|e^{\hat{\tilde{S}}}e^{-\hat{S}}\hat{T}e^{\hat{S}}\big|\Phi_0\big\rangle + \big\langle\Phi_0\big|e^{\hat{\tilde{S}}}e^{-\hat{S}}\hat{V}e^{\hat{S}}\big|\Phi_0\big\rangle. \tag{2.94}$$

In practice this is an extremely tedious and involved calculation, requiring an extremely large amount of commutators to be evaluated and lots of algebraic manipulation. However, if we focus on the specific forms of $\hat{H}$, $\hat{S}$ and $\hat{\tilde{S}}$ we notice something extremely useful.

In the commutators between $\hat{H}$ and $\hat{S} = \hat{S}_p + \hat{S}_h$, we observe that either one of the single-particle operators in $\hat{S}_p$ or $\hat{S}_h$ will contract with $\hat{H}$ or both will. If only one single-particle operator contracts with $\hat{H}$ then the operator $\hat{H}\hat{S}$ may be further contracted with subsequent $\hat{S}$ operators (i.e. at the next order of the linked-cluster expansion). If both of the single-particle operators contract with $\hat{H}$ then the series terminates as it is not possible for the operator $\hat{H}\hat{S}$ to contract with any more $\hat{S}$ operators. Thus the object $e^{-\hat{S}}\hat{H}e^{\hat{S}}$ may be expressed as a series of contractions between $\hat{H}$ and multiple $\hat{S}$ operators.

Now we consider the $\hat{\tilde{S}}$ terms. In contracting the operator $e^{\hat{\tilde{S}}}$ with $e^{-\hat{S}}\hat{H}e^{\hat{S}}$ we have 3 possible outcomes - the single-particle operators in $\hat{\tilde{S}}_p$ or $\hat{\tilde{S}}_h$ may contract with two different $\hat{S}$ operators, one may contract with an $\hat{S}$ operator and one with $\hat{H}$, or finally both may contract with $\hat{H}$. The result of this complete set of contractions leads to a factorisation of $\big\langle\Phi_0\big|e^{\hat{\tilde{S}}}e^{-\hat{S}}\hat{H}e^{\hat{S}}\big|\Phi_0\big\rangle$ into general two-body terms. Such a generalisation as this already exists in the form of the Hartree-Fock-Bogoliubov method [26]. Consequently, we may associate the series of linked s_p, s_h, $\tilde{s}_p$ and $\tilde{s}_h$ terms arising from the complete set of contractions from $\big\langle\Phi_0\big|e^{\hat{\tilde{S}}}e^{-\hat{S}}\hat{H}e^{\hat{S}}\big|\Phi_0\big\rangle$ in terms of the so-called normal and abnormal densities of the HFB method [26]. We now proceed with a rudimentary discussion of such an approach.

2.3.2.4 The Hartree-Fock-Bogoliubov Method

As has already been alluded to, the HFB method is a generalised independent-particle or mean-field approach to the nuclear many-body problem. Its formalism seeks to unify the mean-field approach of the Hartree-Fock method and the Bogoliubov quasi-particle description of fermion pairing correlations from BCS theory [24, 25] into a single variational theory [26]. In the Hartree-Fock method, a many-body system is approximated to the problem of single particles moving independently throughout the system, subject to an "average potential" or mean-field Γ created by the background interactions of the other $N-1$ particles [26]. In BCS theory, a superconducting system may be described in terms of quasi-particles of interacting fermion pairs, where we treat each given quasi-particle as interacting independently subject to a background "pairing field" Δ, due to the rest of the quasi-particles (or fermion pairs) [26]. The mean-field Γ details the long range particle-hole effects and the pairing field Δ details short range particle-particle or hole-hole effects of the interactions [26].

In the HFB method, the overall average potential is given by the combination $\Gamma + \Delta$, thus covering all possible particle-hole, particle-particle and hole-hole effects which may be present in a given nuclear many-body system [26]. Presently, we will not be concerned too much with an in-depth discussion of HFB formalism, we simply introduce it here in order to calculate our SUB(1) ECCM problem in an easier fashion.

According to the HFB method, for a many-body Hamiltonian describing fermions interacting via at most a two-body force,

$$\hat{H} = \sum_{n_1 n_2} \varepsilon_{n_1 n_2} \hat{c}^{\dagger}_{n_1} \hat{c}_{n_2} + \frac{1}{4} \sum_{n_1 n_2 n_3 n_4} V_{n_1 n_2 n_3 n_4} \hat{c}^{\dagger}_{n_1} \hat{c}^{\dagger}_{n_2} \hat{c}_{n_3} \hat{c}_{n_4}, \tag{2.95}$$

(where $\hat{c}^{\dagger}_{n}$ and $\hat{c}_{n}$ are single-particle fermionic creation and annihilation operators respectively, $\varepsilon_{n_1 n_2}$ are the single-particle energies and $V_{n_1 n_2 n_3 n_4}$ are the antisymmetrised potential energy matrix elements) the ground-state expectation value of the Hamiltonian, i.e. the variational ground-state energy

$$E_0 = \frac{\langle \phi | \hat{H} | \phi \rangle}{\langle \phi | \phi \rangle},$$

may be expressed as a functional of two quantities, ρ and κ

$$E\big(\{\rho, \kappa\}\big) = \sum_{n_1 n_2} \varepsilon_{n_1 n_2} \rho_{n_2, n_1} + \frac{1}{4} \sum_{n_1 n_2 n_3 n_4} V_{n_1 n_2 n_3 n_4} \big(\rho_{n_4 n_1} \rho_{n_3 n_2} - \rho_{n_3 n_1} \rho_{n_4 n_2}\big)$$

$$- \frac{1}{4} \sum_{n_1 n_2 n_3 n_4} V_{n_1 n_2 n_3 n_4} \kappa^{\star}_{n_2, n_1} \kappa_{n_4, n_3}. \tag{2.96}$$

Note that the factor of $\frac{1}{4}$ is present in equation (2.95) since we are describing the

general case where spins have not been fixed.

The quantities ρ and κ are known as the normal and abnormal densities respectively [26]. The normal density (or density matrix) is defined by the matrix elements

$$\rho_{n,n'} = \big\langle \phi \big| \hat{c}^{\dagger}_{n'} \hat{c}_{n} \big| \phi \big\rangle, \tag{2.97}$$

and contains the complete description of (number conserving) many-particle states in $\big|\phi\big\rangle$ [26]. The abnormal densities (or pairing-tensors) are defined by the matrix elements

$$\kappa_{n,n'} = \big\langle \phi \big| \hat{c}_{n'} \hat{c}_{n} \big| \phi \big\rangle, \tag{2.98}$$

$$-\kappa^{\star}_{n,n'} = \big\langle \phi \big| \hat{c}^{\dagger}_{n'} \hat{c}^{\dagger}_{n} \big| \phi \big\rangle, \tag{2.99}$$

and contain the complete description of (number nonconserving) many-particle states in $\big|\phi\big\rangle$, provided any state transitions are expressed in pairs [26]. The expression for $E\big(\{\rho, \kappa\}\big)$ in equation (2.96) holds as a consequence of Wick's theorem [26] and the Gaussian factorisation of $\big\langle \phi \big| \hat{H} \big| \phi \big\rangle$ due to $\big|\phi\big\rangle$ being a Slater determinant. Minimising the energy functional $E\big(\{\rho, \kappa\}\big)$ with respect to ρ and κ will lead to the so-called HFB equations [26], in the same manner as the Hartree-Fock method. The so-called generalised density matrix $\mathcal{R}$ is given by

$$\mathcal{R} = \begin{pmatrix} \rho & \kappa \\ -\kappa^{\star} & I - \rho \end{pmatrix}, \tag{2.100}$$

where I is the unit matrix. When the normal and abnormal densities are written in canonical form, $\mathcal{R}$ is idempotent, i.e. $\mathcal{R}^2 = \mathcal{R}$. Thus we can make use of this relation in order to verify that any canonical normal and abnormal densities we calculate produce an idempotent generalised density matrix.

Although the single-particle operators $\hat{c}^{\dagger}_{n}$ and $\hat{c}_{n}$ are defined relative to a filled Fermi sea state (for example, that of equation (2.84)), in order to describe pairing correlations in the HFB method, we use the quasi-particle operators

$$\begin{aligned} \alpha_{k} &= \sum_{n} \Big(\mathcal{U}^{\star}_{nk} \hat{c}_{n} + \mathcal{V}^{\star}_{nk} \hat{c}^{\dagger}_{n} \Big), \\ \alpha^{\dagger}_{k} &= \sum_{n} \Big(\mathcal{V}_{nk} \hat{c}_{n} + \mathcal{U}_{nk} \hat{c}^{\dagger}_{n} \Big), \end{aligned} \tag{2.101}$$

which are constructed from a linear Bogoliubov transformation of $\hat{c}^{\dagger}_{n}$ and $\hat{c}_{n}$ [26]. The factors $\mathcal{U}$ and $\mathcal{V}$ are variationally determined parameters. Equation (2.101) is also

expressible as the matrix relation

$$\begin{pmatrix} \alpha_k \\ \alpha_k^\dagger \end{pmatrix} = \begin{pmatrix} \mathcal{U}^\dagger & \mathcal{V}^\dagger \\ \mathcal{V}^T & \mathcal{U}^T \end{pmatrix} \begin{pmatrix} \hat{c}_n \\ \hat{c}_n^\dagger \end{pmatrix},$$

and in order for α_k and $\alpha_k^\dagger$ to maintain the standard fermionic anticommutation relations, the matrices U and V must satisfy the relations [26]

$$\mathcal{U}^\dagger\mathcal{U} + \mathcal{V}^\dagger\mathcal{V} = 1 = \mathcal{U}\mathcal{U}^\dagger + \mathcal{V}^\star\mathcal{V}^\dagger,$$

$$\mathcal{U}^\dagger\mathcal{V} + \mathcal{V}^T U = 0 = \mathcal{U}\mathcal{V}^\dagger + \mathcal{V}^\star\mathcal{U}^T,$$

in order to provide a unitary transformation. The new operators α_k and $\alpha_k^\dagger$ are defined relative to the quasi-particle vacuum $\big|\phi\big\rangle$ [26], i.e. $\alpha_k\big|\phi\big\rangle = 0$, and the matrix elements of equations (2.97), (2.98) and (2.99) are therefore evaluated with respect to this vacuum. From our discussion previously we can thus conclude that the SUB(1) ECCM calculation for our pairing Hamiltonian of (2.81) is identical to calculating the normal and abnormal densities of HFB theory with the quasi-particle vacuum states

$$\big|\varphi_0\big\rangle = e^{\hat{S}}\big|\Phi_0\big\rangle, \tag{2.102}$$

$$\big\langle\tilde{\varphi}_0\big| = \big\langle\Phi_0\big|e^{\hat{\tilde{S}}}e^{-\hat{S}}. \tag{2.103}$$

2.3.2.5 Ground-State Energy Functional Revisited

Having now identified that the series of linked contractions that make up the ground-state energy functional $E\big(\{s_p, \tilde{s}_p, s_h, \tilde{s}_h\}\big)$ to SUB(1) ECCM approximation are actually just the normal and abnormal densities of the HFB method, we therefore now wish to evaluate the matrix elements

$$\begin{aligned} \rho_{\mathbf{i}\sigma,\mathbf{j}\sigma'}\big(s_p, \tilde{s}_p, s_h, \tilde{s}_h\big) &= \big\langle\tilde{\varphi}_0\big|\hat{a}^\dagger_{\mathbf{j},\sigma'}\hat{a}_{\mathbf{i},\sigma}\big|\varphi_0\big\rangle, \\ \kappa_{\mathbf{i}\sigma,\mathbf{j}\sigma'}\big(s_p, \tilde{s}_p, s_h, \tilde{s}_h\big) &= \big\langle\tilde{\varphi}_0\big|\hat{a}_{\mathbf{j},\sigma'}\hat{a}_{\mathbf{i},\sigma}\big|\varphi_0\big\rangle, \\ -\kappa^\star_{\mathbf{i}\sigma,\mathbf{j}\sigma'}\big(s_p, \tilde{s}_p, s_h, \tilde{s}_h\big) &= \big\langle\tilde{\varphi}_0\big|\hat{a}^\dagger_{\mathbf{j},\sigma'}\hat{a}^\dagger_{\mathbf{i},\sigma}\big|\varphi_0\big\rangle, \end{aligned} \tag{2.104}$$

where $\big|\varphi_0\big\rangle$ and $\big\langle\tilde{\varphi}_0\big|$ are given by (2.102) and (2.103). By carefully calculating only the contributing terms of these matrix elements, we save ourselves the arduous task of attempting to evaluate the commutators of equation (2.94). We may do this by explicitly writing down, in series, all the operators of $e^{\hat{\tilde{S}}}e^{-\hat{S}}\hat{H}e^{\hat{S}}$ which will contribute in the densities of equation (2.104), and performing all *allowed* contractions within the matrix element - we essentially seek only those terms which will contribute from $e^{\hat{\tilde{S}}}e^{-\hat{S}}\hat{H}e^{\hat{S}}$.

Normal Density

The contributions to the normal density may be written as

$$\rho_{\mathbf{i}\sigma,\mathbf{j}\sigma'} = \left\langle \Phi_0 \middle| \hat{a}^\dagger_{\mathbf{j},\sigma'} \hat{a}_{\mathbf{i},\sigma} \middle| \Phi_0 \right\rangle + \left\langle \Phi_0 \middle| e^{\hat{\tilde{S}}} \left[\hat{a}^\dagger_{\mathbf{j},\sigma'} \hat{a}_{\mathbf{i},\sigma}, \hat{S} \right] \middle| \Phi_0 \right\rangle,$$

and evaluating these gives

$$\rho_{\mathbf{i}\sigma,\mathbf{j}\sigma'} = \delta_{\sigma,\sigma'} \left(\sum_{\mathbf{h}} \left(1 - \tilde{s}_h s_h\right) \delta^h_{\mathbf{i},\mathbf{j}} + \sum_{\mathbf{p}} \tilde{s}_p s_p \delta^p_{\mathbf{i},\mathbf{j}} \right). \tag{2.105}$$

We thus observe that ρ is diagonal in particle-particle and hole-hole space and zero in particle-hole or hole-particle space.

Abnormal Densities

The contributions to the abnormal density are more involved compared to that of the normal density. We have

$$\kappa_{\mathbf{i}\sigma,\mathbf{j}\sigma'} = \left\langle \Phi_0 \middle| \hat{\tilde{S}}_h \hat{a}_{\mathbf{j},\sigma'} \hat{a}_{\mathbf{i},\sigma} \middle| \Phi_0 \right\rangle + \left\langle \Phi_0 \middle| \hat{a}_{\mathbf{j},\sigma'} \hat{a}_{\mathbf{i},\sigma} \hat{S}_p \middle| \Phi_0 \right\rangle$$

$$+ \frac{1}{2} \left\langle \Phi_0 \middle| \hat{\tilde{S}}_p \left[\left[\hat{a}_{\mathbf{j},\sigma'} \hat{a}_{\mathbf{i},\sigma}, \hat{S}_p \right], \hat{S}_p \right] \middle| \Phi_0 \right\rangle,$$

which gives

$$\kappa_{\mathbf{i}\sigma,\mathbf{j}\sigma'} = \left[\delta_{\sigma,\uparrow} \delta_{\sigma',\downarrow} - \delta_{\sigma,\downarrow} \delta_{\sigma',\uparrow} \right] \left(\sum_{\mathbf{h}} \tilde{s}_h \delta^h_{\mathbf{i},-\mathbf{j}} + \sum_{\mathbf{p}} s_p \left(1 - \tilde{s}_p s_p\right) \delta^p_{\mathbf{i},-\mathbf{j}} \right). \tag{2.106}$$

For the conjugate abnormal density we have

$$-\kappa^\star_{\mathbf{i}\sigma,\mathbf{j}\sigma'} = \left\langle \Phi_0 \middle| \hat{\tilde{S}}_p \hat{a}^\dagger_{\mathbf{j},\sigma'} \hat{a}^\dagger_{\mathbf{i},\sigma} \middle| \Phi_0 \right\rangle + \left\langle \Phi_0 \middle| \hat{a}^\dagger_{\mathbf{j},\sigma'} \hat{a}^\dagger_{\mathbf{i},\sigma} \hat{S}_h \middle| \Phi_0 \right\rangle$$

$$+ \frac{1}{2} \left\langle \Phi_0 \middle| \hat{\tilde{S}}_h \left[\left[\hat{a}^\dagger_{\mathbf{j},\sigma'} \hat{a}^\dagger_{\mathbf{i},\sigma}, \hat{S}_h \right], \hat{S}_h \right] \middle| \Phi_0 \right\rangle,$$

which gives

$$-\kappa^\star_{\mathbf{i}\sigma,\mathbf{j}\sigma'} = -\left[\delta_{\sigma,\uparrow} \delta_{\sigma',\downarrow} - \delta_{\sigma,\downarrow} \delta_{\sigma',\uparrow} \right] \left(\sum_{\mathbf{p}} \tilde{s}_p \delta^p_{\mathbf{i},-\mathbf{j}} + \sum_{\mathbf{h}} s_h \left(1 - \tilde{s}_h s_h\right) \delta^h_{\mathbf{i},-\mathbf{j}} \right), \tag{2.107}$$

2.3.2.6 SUB(1) ECCM Result

Utilising equation (2.96) it is thus possible to evaluate the SUB(1) ECCM ground-state energy functional given in equation (2.94) in a very simple manner. Before doing that however, we make some important observations. According to [26], the canonical form

of the normal and abnormal densities may be written as

$$\rho = v_p^2 \delta_{\mathbf{p},\mathbf{p}'} + u_h^2 \delta_{\mathbf{h},\mathbf{h}'},$$

$$\kappa = -\kappa^\star = u_k v_k \delta_{\mathbf{k},\bar{\mathbf{k}}'}, \tag{2.108}$$

but since we have already assumed that $\hat{S}$ is diagonal (i.e. diagonal in particle-particle and hole-hole terms and contains no particle-hole nor hole-particle terms) then our densities are already in canonical form. From equation (2.105) we therefore have

$$v_p^2 = \tilde{s}_p s_p,$$

$$u_h^2 = (1 - \tilde{s}_h s_h),$$

but according to BCS theory,

$$v_k^2 + u_k^2 = 1,$$

which implies

$$\tilde{s}_p s_p = \tilde{s}_h s_h.$$

Furthermore, we now note that all the calculations we have performed for ρ, κ and $-\kappa^\star$ are still also true if we use the bare particle vacuum $\big|0\big\rangle$ instead of the Hartree-Fock wave function as the model state. If we substitute the bare particle vacuum into the normal and abnormal densities (hence all hole terms now become zero) we produce the starting wave function of BCS theory - thus the quasi-particle vacuum is given by

$$\big|\varphi_0\big\rangle = e^{\hat{S}}\big|0\big\rangle, \tag{2.109}$$

where $\hat{S}$ is now

$$\hat{S} = \sum_{\mathbf{k},k>0} s_k \hat{a}_{\mathbf{k}}^\dagger \hat{a}_{\bar{\mathbf{k}}}^\dagger,$$

and we use the shorthand notation

$$\mathbf{k} = \mathbf{k}\uparrow, \bar{\mathbf{k}} = -\mathbf{k}\downarrow.$$

Comparing equation (2.109) with a standard form of the BCS ground-state wave function [26]

$$\begin{aligned}\big|\mathrm{BCS}\big\rangle &= \prod_{k>0}\left(1 + \frac{v_k}{u_k}\hat{a}_k^\dagger \hat{a}_{\bar{k}}^\dagger\right)\big|0\big\rangle, \\ &= \exp\left(\sum_{k>0}\frac{v_k}{u_k}\hat{a}_k^\dagger \hat{a}_{\bar{k}}^\dagger\right)\big|0\big\rangle,\end{aligned} \tag{2.110}$$

we see the two are formally identical provided $s_k = \frac{v_k}{u_k}$ (note, equation (2.110) sums

only over half the total number of states). Our canonical SUB(1) ECCM normal and abnormal densities thus become

$$\rho_{\mathbf{i}\sigma,\mathbf{j}\sigma'} = \delta_{\sigma,\sigma'} \sum_{\mathbf{k}} \tilde{s}_k s_k \delta^k_{\mathbf{i},\mathbf{j}},$$

$$\kappa_{\mathbf{i}\sigma,\mathbf{j}\sigma'} = \left[\delta_{\sigma,\uparrow}\delta_{\sigma',\downarrow} - \delta_{\sigma,\downarrow}\delta_{\sigma',\uparrow}\right] \sum_{\mathbf{k}} s_k \left(1 - \tilde{s}_k s_k\right) \delta^k_{\mathbf{i},-\mathbf{j}},$$

$$-\kappa^\star_{\mathbf{i}\sigma,\mathbf{j}\sigma'} = -\left[\delta_{\sigma,\uparrow}\delta_{\sigma',\downarrow} - \delta_{\sigma,\downarrow}\delta_{\sigma',\uparrow}\right] \sum_{\mathbf{k}} \tilde{s}_k \delta^k_{\mathbf{i},-\mathbf{j}}, \tag{2.111}$$

and using equation (2.96) we may therefore write our bivariational SUB(1) ECCM ground-state energy functional as

$$E\big(\{s_k, \tilde{s}_k\}\big) = 2\sum_{k>0} \epsilon_k s_k \tilde{s}_k + \sum_{k_1 k_2 > 0} V_{k_1 k_2 k_1 k_2} s_{k_1} \tilde{s}_{k_1} s_{k_2} \tilde{s}_{k_2} + \sum_{k_1 k_2 > 0} V_{k_1 k_1 k_2 k_2} \tilde{s}_{k_1} s_{k_2} \big(1 - s_{k_2}\tilde{s}_{k_2}\big). \tag{2.112}$$

In their canonical form, the BCS normal and abnormal densities become

$$\rho = v_k^2 \big(\delta_{\mathbf{k},\mathbf{k}'} + \delta_{\bar{\mathbf{k}},\bar{\mathbf{k}}'}\big),$$

$$\kappa = -\kappa^\star = u_k v_k \delta_{\mathbf{k},\bar{\mathbf{k}}'}.$$

We can easily check this statement using the expression for the generalised density matrix given in equation (2.100). Writing down $\mathcal{R}_k$ we thus have

$$\mathcal{R}_k = \begin{pmatrix} v_k^2 & u_k v_k \\ u_k v_k & u_k^2 \end{pmatrix},$$

and hence

$$\begin{aligned} \mathcal{R}_k^2 &= \begin{pmatrix} v_k^2 & u_k v_k \\ u_k v_k & u_k^2 \end{pmatrix} \begin{pmatrix} v_k^2 & u_k v_k \\ u_k v_k & u_k^2 \end{pmatrix} \\ &= \begin{pmatrix} v_k^2\big(v_k^2 + u_k^2\big) & u_k v_k \big(v_k^2 + u_k^2\big) \\ u_k v_k \big(v_k^2 + u_k^2\big) & u_k^2 \big(v_k^2 + u_k^2\big) \end{pmatrix} \\ &= \mathcal{R}_k. \end{aligned}$$

Explicitly, the complete expression for the generalised density matrix actually takes the block diagonal form

$$\mathcal{R} = \begin{pmatrix} \mathcal{R}_{k_1} & 0 & 0 & \dots \\ 0 & \mathcal{R}_{k_2} & 0 & \dots \\ 0 & 0 & \mathcal{R}_{k_3} & \dots \\ \vdots & \vdots & \vdots & \ddots \end{pmatrix},$$

where

$$\mathcal{R}_{k_i} = \begin{pmatrix} v_{k_i}^2 & u_{k_i}v_{k_i} \\ u_{k_i}v_{k_i} & u_{k_i}^2 \end{pmatrix}.$$

Using these expressions for the canonical BCS normal and abnormal densities we can therefore make the connection between our SUB(1) ECCM ground-state energy functional (2.112) and the unconstrained, zero temperature BCS ground-state energy [26]

$$E_{\mathrm{BCS}}\big(\{u_k, v_k\}\big) = 2\sum_{k>0}\epsilon_k v_k^2 + \sum_{k_1k_2>0} V_{k_1k_2k_1k_2}v_{k_1}^2 v_{k_2}^2 + \sum_{k_1k_2>0} V_{k_1k_1k_2k_2}u_{k_1}v_{k_1}u_{k_2}v_{k_2}, \tag{2.113}$$

by enforcing the relations

$$\begin{aligned} v_k^2 &= s_k\tilde{s}_k, \\ u_kv_k &= s_k\left(1 - s_k\tilde{s}_k\right) = \tilde{s}_k. \end{aligned} \tag{2.114}$$

These imply that

$$\tilde{s}_k = v_ku_k;\ s_k = \frac{v_k}{u_k}. \tag{2.115}$$

We thus observe that for a fermionic many-body system with s-wave pairing, a SUB(1) ECCM calculation relative to the bare particle vacuum $\big|0\big\rangle$ is equivalent to calculating the BCS ground-state energy as given in equation (2.113). This equivalence may be made exact by using the relations given in equation (2.115). Hence, during the discussion presented in later chapters, the terms "SUB(1) ECCM" (when defined relative to the bare particle vacuum) and "BCS" may be used interchangeably, since they both describe the same calculation of the ground-state energy. As a final check, we write down the diagonal element of the generalised density matrix in terms of our SUB(1) ECCM terms. Thus

$$\mathcal{R}_k = \begin{pmatrix} s_k\tilde{s}_k & s_k\left(1 - \tilde{s}_ks_k\right) \\ \tilde{s}_k & 1 - s_k\tilde{s}_k \end{pmatrix},$$

and therefore

$$\begin{aligned} \mathcal{R}_k^2 &= \begin{pmatrix} s_k\tilde{s}_k & s_k\left(1 - \tilde{s}_ks_k\right) \\ \tilde{s}_k & 1 - s_k\tilde{s}_k \end{pmatrix}\begin{pmatrix} s_k\tilde{s}_k & s_k\left(1 - \tilde{s}_ks_k\right) \\ \tilde{s}_k & 1 - s_k\tilde{s}_k \end{pmatrix} \\ &= \begin{pmatrix} s_k\tilde{s}_k\big(s_k\tilde{s}_k + 1 - s_k\tilde{s}_k\big) & s_k\left(1 - \tilde{s}_ks_k\right)\big(s_k\tilde{s}_k + 1 - s_k\tilde{s}_k\big) \\ \tilde{s}_k\big(s_k\tilde{s}_k + 1 - s_k\tilde{s}_k\big) & s_k\tilde{s}_k\big(s_k\tilde{s}_k + 1 - s_k\tilde{s}_k\big) \end{pmatrix} \\ &= \mathcal{R}_k, \end{aligned}$$

hence we have proved our SUB(1) ECCM normal and abnormal densities are also written in canonical form (note, this relation holds *without* the extra requirement $v_k^2 + u_k^2 = 1$ that needs to be imposed in the BCS case).

2.3.2.7 BCS Solutions and the Gap Equation

Before we leave discussion of the BCS and SUB(1) ECCM ground-state energies, it is an interesting exercise to attempt a solution for s_k and $\tilde{s}_k$ in the ECCM case. At first sight this may appear straightforward, nevertheless, upon investigation of this problem we uncover some hidden subtleties. We begin by calculating the standard solution for the BCS parameters u_k and v_k, which we can derive from equation (2.113). Since the BCS wave function does not correspond to a fixed number of particles, we must first constrain the ground-state energy expectation value in order to fix particle number [26] (or equivalently use the *grand potential* $\hat{K}$ [28]). Hence we must evaluate

$$\langle \hat{H} \rangle - \lambda \langle \hat{N} \rangle,$$

where λ is the chemical potential. Since the BCS particle number operator is given by

$$\hat{N} = \sum_{k>0} \hat{a}^{\dagger}_{\mathbf{k}\uparrow} \hat{a}_{\mathbf{k}\uparrow} + \sum_{k>0} \hat{a}^{\dagger}_{-\mathbf{k}\downarrow} \hat{a}_{-\mathbf{k}\downarrow}, \tag{2.116}$$

the expectation value of the number operator is given by

$$\langle \hat{N} \rangle = \langle \mathrm{BCS} | \hat{N} | \mathrm{BCS} \rangle = 2 \sum_{k>0} v_k^2, \tag{2.117}$$

where we assume there are equally filled numbers of spin $\uparrow$ and spin $\downarrow$ states. Thus we may rewrite the constrained form of equation (2.113) as

$$E_{\mathrm{BCS}}\big(\{u_k, v_k\}\big) = 2 \sum_{k>0} (\epsilon_k - \lambda) v_k^2 + \sum_{k_1 k_2 > 0} V_{k_1 k_2 k_1 k_2} v_{k_1}^2 v_{k_2}^2 + \sum_{k_1 k_2 > 0} V_{k_1 k_1 k_2 k_2} u_{k_1} v_{k_1} u_{k_2} v_{k_2}. \tag{2.118}$$

In order to find a solution for the BCS parameters we must minimise equation (2.118). We impose the relation $v_k^2 + u_k^2 = 1$ and use the total derivative

$$\begin{aligned} \frac{d}{dv_k} &= \frac{\partial}{\partial v_k}\bigg|_{u_k} + \frac{du_k}{dv_k} \frac{\partial}{\partial u_k}\bigg|_{v_k} \\ &= \frac{\partial}{\partial v_k}\bigg|_{u_k} - \frac{v_k}{u_k} \frac{\partial}{\partial u_k}\bigg|_{v_k}, \end{aligned}$$

i.e. we therefore want to solve the equation

$$\frac{d}{dv_k} E_{\mathrm{BCS}}\big(\{u_k, v_k\}\big) = 0. \tag{2.119}$$

After evaluating the derivative in equation (2.119), multiplying the result by $\frac{u_k}{2}$ gives

us the standard equation

$$2\tilde{\epsilon}_k u_k v_k + \Delta_k\big(v_k^2 - u_k^2\big) = 0, \tag{2.120}$$

where we have defined

$$\tilde{\epsilon}_k = \big(\epsilon_k - \lambda\big) + \sum_{k'>0} V_{kk'kk'} v_{k'}^2, \tag{2.121}$$

the so-called BCS *gap parameter* Δ_k is given by

$$\Delta_k = -\sum_{k>0} V_{kkk'k'} u_{k'} v_{k'}, \tag{2.122}$$

and we have relabeled our summation variables from $\big(k_1, k_2\big)$ to $\big(k, k'\big)$ for convenience. The quantity 2Δ represents the amount of energy required to reach the first excited-state in a superconductor of even particle number N and thus the energy required to break up an electron Cooper pair (which results in a reordering of all other electron Cooper pairs at the Fermi surface).

Using the relation $v_k^2 + u_k^2 = 1$, we can show that the solutions to equation (2.120) for the BCS parameters are given by

$$\begin{aligned} u_k^2 &= \frac{1}{2}\left(1 + \frac{\tilde{\epsilon}_k}{\sqrt{\tilde{\epsilon}_k^2 + \Delta_k^2}}\right), \\ v_k^2 &= \frac{1}{2}\left(1 - \frac{\tilde{\epsilon}_k}{\sqrt{\tilde{\epsilon}_k^2 + \Delta_k^2}}\right), \end{aligned} \tag{2.123}$$

where we have resolved the sign ambiguities of these solutions in the limit $\Delta_k \to 0$. These expressions for u_k and v_k can be substituted into equation (2.122) to yield the so-called *gap equation*

$$\Delta_k = -\frac{1}{2}\sum_{k>0} V_{kkk'k'} \frac{\Delta_k}{\sqrt{\tilde{\epsilon}_k^2 + \Delta_k^2}}, \tag{2.124}$$

which must be solved self-consistently (along with the energies $\tilde{\epsilon}_k$) by iteration [26].

2.3.2.8 SUB(1) ECCM Solutions

Having derived the standard set of solutions for the BCS problem, we now derive solutions for the SUB(1) cluster amplitudes s_k and $\tilde{s}_k$ in a similar manner. Although it is not usually the case, for this problem we expect to find a general analytic form for both s_k and $\tilde{s}_k$ since we already know it is possible to write them in terms of u_k and v_k in the pure BCS limit (i.e. the richer and more complicated SUB(1) ECCM problem reduces to pure BCS when enforcing the relations of equation (2.115)). We begin in the same way as before and rewrite the SUB(1) ECCM ground-state energy functional

from equation (2.112) in the constrained form

$$E\big(\{s_k,\tilde{s}_k\}\big) = 2\sum_{k>0}\big(\epsilon_k-\lambda\big)s_k\tilde{s}_k + \sum_{kk'>0} V_{kk'kk'}s_k\tilde{s}_k s_{k'}\tilde{s}_{k'} + \sum_{kk'>0} V_{kkk'k'}\tilde{s}_k s_{k'}\big(1-s_{k'}\tilde{s}_{k'}\big), \tag{2.125}$$

where λ is the chemical potential and we now use summation labels $\big(k,k'\big)$. At face value this expression is rather more complicated than the equivalent BCS form (2.118) since we are now dealing with two independent variables - u_k and v_k are not independent in BCS theory[2] and the square of their values can only take values between 0 and 1. There is no such constraint on s_k and $\tilde{s}_k$ however, and as such, unphysical solutions for the ground-state energy are possible.

Minimising equation (2.125) with respect to either cluster amplitude we obtain the coupled set of equations

$$\begin{aligned} 2\tilde{\epsilon}_k s_k - \alpha_k + \beta_k s_k^2 &= 0, \\ 2\tilde{\epsilon}_k\tilde{s}_k + \beta_k\big(2s_k\tilde{s}_k - 1\big) &= 0, \end{aligned} \tag{2.126}$$

where we have used the following definitions

$$\begin{aligned} \tilde{\epsilon}_k &= \big(\epsilon_k-\lambda\big) + \sum_{k'>0} V_{kk'kk'}s_{k'}\tilde{s}_{k'}, \\ \alpha_k &= -\sum_{k'>0} V_{kkk'k'}s_{k'}\big(1-s_{k'}\tilde{s}_{k'}\big), \\ \beta_k &= -\sum_{k'>0} V_{kkk'k'}\tilde{s}_k. \end{aligned} \tag{2.127}$$

Before solving these equations for the general case, we substitute the known BCS solutions from equations (2.115) and (2.123) into the equations in (2.126) as a check. In which case we find that

$$\alpha_k = \beta_k = \Delta_k,$$

and the SUB(1) ECCM cluster amplitudes which form the solutions of (2.126) are given by

$$\begin{aligned} s_k &= \frac{-\tilde{\epsilon}_k - \sqrt{\Delta_k^2+\tilde{\epsilon}_k^2}}{\Delta_k}, \\ \tilde{s}_k &= -\frac{\Delta_k}{2\sqrt{\Delta_k^2+\tilde{\epsilon}_k^2}}. \end{aligned} \tag{2.128}$$

Thus we have proved that embedding the BCS solutions into the SUB(1) ECCM calculation constitutes a correct physical solution to the ECCM equations. If we do not enforce the BCS relations in the SUB(1) ECCM problem then the general solutions to

[2]indeed, we can in fact write BCS theory in terms of a single parameter ψ_k, the angle formed between u_k and v_k in the 2-dimensional Cartesian plane.

equation (2.126) are given by

$$s_k = \frac{-\tilde{\epsilon}_k - \sqrt{\alpha_k \beta_k + \tilde{\epsilon}_k^2}}{\beta_k},$$

$$\tilde{s}_k = -\frac{\beta_k}{2\sqrt{\alpha_k \beta_k + \tilde{\epsilon}_k^2}}, \tag{2.129}$$

which may be solved by iteration, in a similar manner to equation (2.124).

Physical Subspace Condition

In our arguments thus far, we have failed to impose a condition that will ensure the Pauli exclusion principle is not violated - there is a chance that our SUB(1) ECCM solutions will put more than one fermion into the same state (produce an occupation number larger than 1). In order to rectify this problem we can introduce the "physical subspace" condition - namely that the abnormal density must be Hermitian. This in turn means we must enforce the relation

$$\tilde{s}_k = s_k\big(1 - s_k \tilde{s}_k\big),$$

or written another way

$$\tilde{s}_k = \frac{s_k}{1 + s_k^2}. \tag{2.130}$$

We are now back to the pure BCS problem but we have managed to reduce the number of SUB(1) variables (cluster amplitudes) by half. The constrained ground-state energy now takes the form

$$E\big(s_k\big) = 2\sum_{k>0}\big(\epsilon_k - \lambda\big)\frac{s_k^2}{1+s_k^2} + \sum_{kk'>0} V_{kk'kk'}\frac{s_k^2}{1+s_k^2}\frac{s_{k'}^2}{1+s_{k'}^2} + \sum_{kk'>0} V_{kkk'k'}\frac{s_k}{1+s_k^2}\frac{s_{k'}}{1+s_{k'}^2}. \tag{2.131}$$

Minimising this with respect to s_k gives

$$2\tilde{\epsilon}_k s_k + \Delta_k\big(s_k^2 - 1\big) = 0, \tag{2.132}$$

where we have made the usual definitions

$$\tilde{\epsilon}_k = \sum_{k>0}\big(\epsilon_k - \lambda\big) + \sum_{kk'>0} V_{kk'kk'}\frac{s_{k'}^2}{1+s_{k'}^2},$$

$$\Delta_k = -\sum_{kk'>0} V_{kkk'k'}\frac{s_{k'}}{1+s_{k'}^2}.$$

The solutions to equation (2.132) are given by

$$s_k = \frac{-\tilde{\epsilon}_k \pm \sqrt{\Delta_k^2 + \tilde{\epsilon}_k^2}}{\Delta_k}. \tag{2.133}$$

When faced with more complicated forms of the SUB(1) ECCM equations for pairing problems, it is possible that imposing the physical subspace condition will make solving the equations easier, since we are able to reduce the number of variables by half. We will see why this may become important in chapter 5.

2.3.3 Quasi-Particle Basis

We have seen in detail that the ECCM to SUB(1) approximation is identical to the HFB method for a generic pairing problem, indeed it can be made exactly equivalent to a BCS calculation through a specific choice of the model state and cluster amplitudes. Such a property implies that the SUB(1) ECCM may in fact be considered as a generalised independent-particle variational theory [42], expressed in terms of quasi-particles. Therefore, for higher order calculations in the ECCM it may be useful to define some distinct basis of quasi-particle operators in terms of the SUB(1) cluster amplitudes.

Proceeding in the same manner as the HFB method, we consider our quasi-particle vacuum to be a collection of low-lying excited-states of the bare particle vacuum $|0\rangle$ and thus define

$$\big|\varphi_0\big\rangle = e^{\widehat{S}_1}\big|0\big\rangle, \tag{2.134}$$

$$\big\langle\tilde{\varphi}_0\big| = \big\langle\Phi_0\big|e^{\hat{\tilde{S}}_1}e^{-\hat{S}_1}, \tag{2.135}$$

where $\big|\varphi_0\big\rangle$ and $\big\langle\tilde{\varphi}_0\big|$ will henceforth denote the ket and bra quasi-particle vacuum states and the cluster correlation operators are constructed from a set of single-particle operators $\hat{a}_k^\dagger$ and $\hat{a}_k$. If we act on $\big|\varphi_0\big\rangle$ with a particle annihilation operator we obtain

$$\hat{a}_k\big|\varphi_0\big\rangle = \hat{a}_k e^{\widehat{S}_1}\big|0\big\rangle = s_k\hat{a}_{\bar{k}}^\dagger\big|\varphi_0\big\rangle,$$

(where again we neglect explicit labeling of s_k as a SUB(1) term for simplicity). Therefore we have the relation that

$$\Big(\hat{a}_k - s_k\hat{a}_{\bar{k}}^\dagger\Big)\big|\varphi_0\big\rangle = 0,$$

i.e. the object $\Big(\hat{a}_k - s_k\hat{a}_{\bar{k}}^\dagger\Big)$ acts as a quasi-particle annihilation operator with respect to the quasi-particle vacuum $\big|\varphi_0\big\rangle$.

If we repeat this process for all subsequent bra and ket quasi-particle vacuum states with the corresponding particle creation and annihilation operators, we form a bi-

canonical quasi-particle basis. This may be defined by the following relations

$$\hat{c}_k = \hat{a}_k + \left[\hat{S}, \hat{a}_k\right] = \hat{a}_k - s_k \hat{a}^\dagger_{\bar{k}},$$

$$\hat{c}_{\bar{k}} = \hat{a}_{\bar{k}} + \left[\hat{S}, \hat{a}_{\bar{k}}\right] = \hat{a}_{\bar{k}} - s_k \hat{a}^\dagger_{k},$$

$$\hat{d}^\dagger_k = \hat{a}^\dagger_k + \left[\hat{\tilde{S}}, \hat{a}^\dagger_k\right] + \left[\hat{S}, \left[\hat{\tilde{S}}, \hat{a}^\dagger_k\right]\right] = (1 - \tilde{s}_k s_k)\, \hat{a}^\dagger_k - \tilde{s}_k \hat{a}_{\bar{k}},$$

$$\hat{d}^\dagger_{\bar{k}} = \hat{a}^\dagger_{\bar{k}} + \left[\hat{\tilde{S}}, \hat{a}^\dagger_{\bar{k}}\right] + \left[\hat{S}, \left[\hat{\tilde{S}}, \hat{a}^\dagger_{\bar{k}}\right]\right] = (1 - \tilde{s}_k s_k)\, \hat{a}^\dagger_{\bar{k}} - \tilde{s}_k \hat{a}_{k}. \tag{2.136}$$

Inverting these operators gives us expressions for our standard particle operators in terms of quasi-particle operators

$$\hat{a}_k = (1 - \tilde{s}_k s_k)\, \hat{c}_k + s \hat{d}^\dagger_{\bar{k}},$$

$$\hat{a}_{\bar{k}} = (1 - \tilde{s}_k s_k)\, \hat{c}_{\bar{k}} - s \hat{d}^\dagger_{k},$$

$$\hat{a}^\dagger_k = \tilde{s}_k \hat{c}_{\bar{k}} + \hat{d}^\dagger_k,$$

$$\hat{a}^\dagger_{\bar{k}} = -\tilde{s}_k \hat{c}_k + \hat{d}^\dagger_{\bar{k}}. \tag{2.137}$$

Using a quasi-particle basis of this form for an ECCM calculation means we will automatically include all SUB(1) terms without having to evaluate them explicitly. Therefore, higher order calculations of the ground-state energy functional will exclude any SUB(1) terms, provided the Hamiltonian is written in terms of quasi-particle operators. For example, to SUB(2) we would have

$$E\big(\{s, \tilde{s}, s_2, \tilde{s}_2\}\big) = \big\langle \tilde{\varphi}_0 \big| e^{\hat{\tilde{S}}_2} e^{-\hat{S}_2} \hat{H}_{qp} e^{\hat{S}_2} \big| \varphi_0 \big\rangle, \tag{2.138}$$

where the Hamiltonian $\hat{H}_{qp}$ is written in terms of the quasi-particle operators defined in equation (2.136). Such an approach as this uses the so-called "Brueckner orbitals" $\big|\varphi_0\big\rangle$ and $\big\langle\tilde{\varphi}_0\big|$ [42, 74, 75, 76, 77] (where the term is used predominantly in quantum chemistry literature).

Rewriting the pairing Hamiltonian of (2.81) in terms of quasi-particle operators is a long winded exercise, due in part to the specific form of the Hamiltonian. A much simpler pairing Hamiltonian is introduced in chapter 4 and we find it can be written in terms of quasi-particle operators relatively easily, indeed the quasi-particle ECCM formalism we have derived here has been introduced as a precursor to the discussion of chapter 4. Having covered all of the necessary NCCM and ECCM formalisms which we will require, we thus proceed to apply these techniques to various problems.

Chapter 3

Illustrative Applications of the Coupled Cluster Method to Simple Models

In order to illustrate exactly how the CCM works in practice, it is probably best to first apply it to some simple and well understood physical models as demonstration. This chapter will thus concentrate on two such models with a view to illustrate how the NCCM and ECCM function at different levels of approximation. We begin with a purely quartic anharmonic oscillator and apply the NCCM, calculating the ground-state energy E_0 as a function of the coupling constant λ up to SUB(5). Implementing a better method of solution, we then increase our truncation scheme up to SUB(10). We also calculate some of the low level excited-state energies of the model. Some of the drawbacks of the method are explained and discussed. We then calculate E_0 using the ECCM up to SUB(2), as a means to further validate our work and to more clearly demonstrate how the ECCM works. Finally, we turn our attention to a different problem and address the double-well quartic anharmonic oscillator. We calculate the ground-state energy E_0 as a function of the mass coefficient k using the NCCM up to SUB(5). Some alternate NCCM approaches to the model are discussed. We conclude the chapter by calculating E_0 using the ECCM to SUB(2).

3.1 The Quartic Anharmonic Oscillator

The first model we wish to discuss is the quartic anharmonic oscillator, which is the standard quantum simple harmonic oscillator with an extra quartic term in the potential. We weight this term with a real, nonnegative parameter λ, which we call the coupling constant - this governs the strength of the anharmonic interaction. The model Hamiltonian is thus given by

$$\hat{H} = \frac{\hat{p}^2}{2m} + \frac{1}{2}m\omega^2\hat{x}^2 + \lambda\hat{x}^4, \tag{3.1}$$

where $\hat{x}$ and $\hat{p}$ are the usual single-particle position and momentum operators respectively, m is the mass of the oscillating particle and ω the angular frequency.

A great many studies have been performed on various anharmonic oscillator models within the last thirty years or so, using a variety of different approaches (most notable of which using perturbative [122], variational [123, 124] and CCM techniques [80, 125, 126, 127]). The particular case of the quartic anharmonic oscillator is an intriguing system to study. One especially interesting viewpoint is that it may be considered a (0+1)-dimensional analogue of a basic scalar field theory which includes quartic self-interactions, i.e. a (0+1)-dimensional φ^4 field theory model [122]. This analogy exists because of the duality of the quantum simple harmonic oscillator, which may be seen as both a quantum mechanical model of oscillation and a quantum field theoretic model of a (0+1)-dimensional scalar field. As such, studies of these toy models can provide useful insight towards constructing more complicated and realistic field theories in (d+1)-dimensional space-time (d being the number of spatial dimensions) [122, 128] as well as facilitating a basis from which field theory calculations may begin from. On a much simpler level, the Hamiltonian as given in equation (3.1) could also be used to describe nonlinear vibrations of a particular atom or molecule (the anharmonicity describing fluctuations away from the usual harmonic motion).

The perturbation expansion for the ground-state energy of the quartic anharmonic oscillator about the unperturbed simple harmonic oscillator (i.e. the trivial case of $\lambda = 0$) although well-defined, is known to diverge for all real values of λ, no matter how small λ is [122]. By continuing their investigation and allowing λ to become complex, viewing what happens to the energy levels in the complex λ plane, Bender and Wu concluded that the perturbation series for the ground-state energy $E_0(\lambda)$ is actually divergent for *all* values of $\lambda \neq 0$ [122]. Although the first few orders of perturbation theory can systematically produce increasingly better results for the ground-state energy, beyond a certain limit (around 10^{th} order) all perturbative corrections then begin to produce increasingly worse results. An outcome such as this inevitably led people to explore using alternate, nonperturbative approaches to the anharmonic oscillator, such as the variational method.

The Bender and Wu result is in some ways analogous to the ground-state energy perturbation expansion of quantum electrodynamics being divergent in the coupling constant α [129]. However, in the case of the anharmonic oscillator, calculating the diagonal Padé approximants for the perturbation series may be shown to converge for any given energy eigenvalue, in which the limit of the convergence is the eigenvalue itself [130]. Such an approach has been improved upon by the application of Borel

summability [131]. In [131], the authors begin by calculating the Borel transform of the perturbation series and proceed to find the diagonal Padé approximants of this function, as opposed to that of the initial perturbation series (this scheme has since become known as Padé-Borel summation). They conclude that this method converges to the eigenvalues faster than using a pure Padé approximant.

A particularly elegant and innovative approach to anharmonic oscillator models was proposed in [132] where the so-called "two-step" method was introduced. In the first step, a generalised coherent state $\left|\phi\right\rangle$ is assumed as a trial ansatz for the ket ground-state wave function. Upon introduction of a Bogoliubov transformation of the standard simple harmonic creation and annihilation operators, $\hat{a}^{\dagger}$ and $\hat{a}$ respectively, this ansatz then plays the role of a quasi-particle vacuum with respect to the newly formulated quasi-particle operators $\hat{b}^{\dagger}$ and $\hat{b}$. The original Hamiltonian is then rewritten using these new operators and the ground-state energy E_0 is calculated via the variational method. This step may be considered identical to the Hartree approximation.

The second step is then to calculate the matrix elements of the Hamiltonian written in this form, using the quasi-particle operators in the construction of the basis vectors $\left|n\right\rangle$. If the resultant matrix has a size $N \times N$, by enforcing that n is small in comparison to N, all the energy eigenvalues may be calculated in a single diagonalisation of the matrix, by means of a numerical Jacobi eigenvalue algorithm. Using this method, the eigenvalues show fast convergence and stability with respect to N, for all λ [132]. Hsue and Chern were thus able to calculate the *exact* ground-state energy eigenvalues over a large range of λ (0.1 to 1000.0). It is these results which will provide the benchmark for our own CCM calculations to be compared to.

There have been much more complex studies of the quartic anharmonic oscillator produced than will be presented here. Indeed, studies utilising a Bogoliubov quasi-particle CCM approach [125] (as inspired by [132]), excited-state CCM formalism [125] and temperature-dependent CCM formalism [80] all exist, with [80] and [127] essentially regarding the anharmonic oscillator solely as a testing ground for the applicability of the CCM, rather than an attempt to improve upon the accuracy of previous results for the model [132]. In any case, for our needs the anharmonic oscillator simply acts as a demonstrative tool. We are not concerned with reproducing complicated CCM formulations of the anharmonic oscillator to extremely high accuracy, we simply want to show how the CCM works and discuss how closely it matches known results to relatively low order. With that in mind, we begin our discussion with the simplest CCM approximation we can make and develop our analysis onward from there.

3.1.1 Normal Coupled Cluster Method

Since the CCM is normally expressed in the language of second quantisation, we do not want to work with the Hamiltonian as written in equation (3.1) and so introduce the standard simple harmonic oscillator creation and annihilation operators given by

$$\hat{a}^\dagger = \frac{1}{\sqrt{2}}\left(\sqrt{\frac{m\omega}{\hbar}}\hat{x} - \frac{i}{\sqrt{m\omega\hbar}}\hat{p}\right),$$

$$\hat{a} = \frac{1}{\sqrt{2}}\left(\sqrt{\frac{m\omega}{\hbar}}\hat{x} + \frac{i}{\sqrt{m\omega\hbar}}\hat{p}\right). \tag{3.2}$$

For simplicity's sake, we choose to work in the natural units $m = \omega = \hbar = 1$, to avoid carrying the excess baggage of m, ω and $\hbar$ terms throughout our calculations. Thus we may now write our model Hamiltonian given in equation (3.1) as

$$\hat{H} = \frac{1}{2}\left(\hat{p}^2 + \hat{x}^2\right) + \lambda\hat{x}^4, \tag{3.3}$$

and our creation and annihilation operators as given in equation (3.2) as

$$\hat{a}^\dagger = \frac{1}{\sqrt{2}}\left(\hat{x} - i\hat{p}\right),$$

$$\hat{a} = \frac{1}{\sqrt{2}}\left(\hat{x} + i\hat{p}\right). \tag{3.4}$$

It is a triviality to show that these operators obey the commutation relations

$$\left[\hat{a}, \hat{a}^\dagger\right] = 1,$$

$$[\hat{a}, \hat{a}] = 0 = \left[\hat{a}^\dagger, \hat{a}^\dagger\right]. \tag{3.5}$$

Rearranging these operators in terms of $\hat{x}$ and $\hat{p}$ we thus have

$$\hat{x} = \frac{1}{\sqrt{2}}\left(\hat{a} + \hat{a}^\dagger\right),$$

$$\hat{p} = -\frac{i}{\sqrt{2}}\left(\hat{a} - \hat{a}^\dagger\right). \tag{3.6}$$

The action of the annihilation operator on the ket vacuum state wave function, and similarly the action of the creation operator on the bra vacuum state wave function are both defined by the equation

$$\hat{a}\big|0\big\rangle = 0 = \big\langle 0\big|\hat{a}^\dagger, \tag{3.7}$$

and it is important to note that the vacuum state itself is normalised

$$\langle 0|0\rangle = 1. \tag{3.8}$$

The action of the creation operator on a general state $|n\rangle$ is given by

$$\hat{a}^\dagger|n\rangle = \sqrt{(n+1)}|n+1\rangle, \tag{3.9}$$

and the action of the annihilation operator on a general state $|n\rangle$ is given by

$$\hat{a}|n\rangle = \sqrt{n}|n-1\rangle. \tag{3.10}$$

In this way, the creation and annihilation operators move up or down the harmonic oscillator energy ladder $\varepsilon_n = \left(n + \frac{1}{2}\right)$ respectively, creating and annihilating quanta of energy. By convention, normalised states (Hilbert space vectors) are written as

$$|0\rangle, |1\rangle, |2\rangle ... |n\rangle, \tag{3.11}$$

where

$$|n\rangle = \frac{(\hat{a}^\dagger)^n}{\sqrt{n!}}|0\rangle. \tag{3.12}$$

With our operator formalism now defined, we return to the Hamiltonian of equation (3.3). Utilising our expressions for $\hat{x}$ and $\hat{p}$ written in terms of $\hat{a}^\dagger$ and $\hat{a}$, as given in equation (3.6), we may rewrite the Hamiltonian as

$$\hat{H} = \hat{a}^\dagger\hat{a} + \frac{1}{2} + \frac{\lambda}{4}\left(\hat{a} + \hat{a}^\dagger\right)^4. \tag{3.13}$$

Expanding the anharmonic term and subsequently normal ordering the resultant expression, we obtain the Hamiltonian written in the form most useful to us,

$$\hat{H} = \hat{a}^\dagger\hat{a} + \frac{1}{2} + \frac{\lambda}{4}\left(3 + \hat{a}^4 + 6\hat{a}^2 + 4\hat{a}^\dagger\hat{a}^3 + 6\hat{a}^{\dagger 2}\hat{a}^2 + 12\hat{a}^\dagger\hat{a} + 4\hat{a}^{\dagger 3}\hat{a} + 6\hat{a}^{\dagger 2} + \hat{a}^{\dagger 4}\right). \tag{3.14}$$

Written in this way, we have a much more physically transparent model - the Hamiltonian clearly enforces a specific set of selection rules where only transitions of 0, 2 or 4 steps of energy quanta are allowed, i.e. n may only remain unchanged or go up or down by 2 or 4 steps in this model. An insight such as this would not be as forthcoming from our expression in equation (3.1).

3.1.1.1 SUB(1) Calculation

For a given Hamiltonian, the starting point of any CCM calculation lies in the choice of both the model state $|\Phi_0\rangle$ and the cluster correlation operator $\hat{S}$, which are used to

parametrise the ket ground-state wave function $\big|\Psi_0\big\rangle$ as given by

$$\big|\Psi_0\big\rangle = e^{\hat{S}}\big|\Phi_0\big\rangle. \tag{3.15}$$

More correctly, since we have the general cluster correlation operators defined as

$$\hat{S} = \sum_{I\neq 0} s_I \hat{C}_I{}^{\dagger},$$

$$\hat{\tilde{S}} = 1 + \sum_{I\neq 0} \tilde{s}_I \hat{C}_I, \tag{3.16}$$

in the NCCM scheme, we must choose the multiconfigurational operators $\hat{C}_I{}^{\dagger}$ and $\hat{C}_I$ carefully, in order to accurately and appropriately model excitations relative to the noninteracting model state $\big|\Phi_0\big\rangle$.

For the case of the quartic anharmonic oscillator, the choice is fairly trivial and simply amounts to using the harmonic oscillator creation and annihilation operators

$$\hat{C}_n^{\dagger} = \hat{a}^{\dagger n},\ \hat{C}_n = \hat{a}^n, \tag{3.17}$$

and the bare bosonic vacuum $\big|0\big\rangle$ as the model state. Note that the general configuration label I is just denoted n in this case, since this is all the state information we require (once we know n, we know the energy of the state and hence the level of excitation above the ground-state). Using the operators given in equation (3.17) we thus have our cluster correlation operators given by

$$\hat{S} = \sum_{n\neq 0} s_n \hat{a}^{\dagger n},$$

$$\hat{\tilde{S}} = 1 + \sum_{n\neq 0} \tilde{s}_n \hat{a}^n, \tag{3.18}$$

where n runs over even numbers only (as a consequence of our selection rules). Note that we do not need to explicitly normalise our $\hat{S}$ and $\hat{\tilde{S}}$ operators, we simply require that intermediate normalisation

$$\big\langle\Phi_0|\Psi_0\big\rangle = \big\langle 0\big|e^{\hat{S}}\big|0\big\rangle = \big\langle 0\big|\sum_{\gamma=0}^{+\infty}\frac{1}{\gamma!}\left(\sum_{n\neq 0} s_n\hat{a}^{\dagger n}\right)^{\gamma}\big|0\big\rangle = 1. \tag{3.19}$$

is not violated. In a manner of speaking, we may deem the normalisation constants as being absorbed into the cluster correlation amplitudes $\big\{s_n\big\}$ and $\big\{\tilde{s}_n\big\}$, so we do not need to worry about them in general (this also avoids the necessity of carrying terms proportional to $\frac{1}{\sqrt{n!}}$ throughout the entire calculation, which becomes especially

cumbersome for higher n).

The ground-state energy E_0 of a system according to the NCCM may be formally written as

$$E_0 = \left\langle \Phi_0 \right| e^{-\hat{S}} \hat{H} e^{\hat{S}} \left| \Phi_0 \right\rangle. \tag{3.20}$$

Evaluation of the so-called NCCM equations

$$\left\langle \Phi_0 \right| \hat{C}_I e^{-\hat{S}} \hat{H} e^{\hat{S}} \left| \Phi_0 \right\rangle = 0, \, \forall I \neq 0, \tag{3.21}$$

produces an infinite set of coupled, nonlinear polynomial equations for the amplitudes $\left\{ s_I \right\}$, the solutions of which may be then substituted into equation (3.20) in order to determine E_0. This hierarchy of equations is made finite once we impose a truncation on $\hat{S}$, thus in general we expect the SUB(n) approximation scheme to produce more accurate results the higher n becomes (since increasingly more correlations in $\hat{S}$ are taken into account).

For simplicity we proceed by making a SUB(1) approximation to our operator $\hat{S}$. Since there are no contributions to the matrix element given by $\left\langle \Phi_0 \right| e^{-\hat{S}} \hat{H} e^{\hat{S}} \left| \Phi_0 \right\rangle$ if $\hat{S}$ contains terms of odd power, due to the formation of the Hamiltonian as expressed in equation (3.14), our SUB(1) or "first order" approximation of $\hat{S}$ is actually given by

$$\hat{S} = s_2 \hat{a}^{\dagger 2}, \tag{3.22}$$

which means the complete NCCM equations we wish to solve are given by

$$E_0 = \left\langle 0 \right| e^{-s_2 \hat{a}^{\dagger 2}} \hat{H} e^{s_2 \hat{a}^{\dagger 2}} \left| 0 \right\rangle, \tag{3.23}$$

$$\left\langle 0 \right| \hat{a}^2 e^{-s_2 \hat{a}^{\dagger 2}} \hat{H} e^{s_2 \hat{a}^{\dagger 2}} \left| 0 \right\rangle = 0. \tag{3.24}$$

Considering our Hamiltonian consists of terms up to fourth order in both $\hat{a}^\dagger$ and $\hat{a}$, the linked-cluster expansion will terminate at fourth order

$$e^{-s_2 \hat{a}^{\dagger 2}} \hat{H} e^{s_2 \hat{a}^{\dagger 2}} = \hat{H} + s_2 \left[\hat{H}, \hat{a}^{\dagger 2} \right] + \frac{1}{2!} s_2^2 \left[\left[\hat{H}, \hat{a}^{\dagger 2} \right], \hat{a}^{\dagger 2} \right]$$

$$+ \frac{1}{3!} s_2^3 \left[\left[\left[\hat{H}, \hat{a}^{\dagger 2} \right], \hat{a}^{\dagger 2} \right], \hat{a}^{\dagger 2} \right] + \frac{1}{4!} s_2^4 \left[\left[\left[\left[\hat{H}, \hat{a}^{\dagger 2} \right], \hat{a}^{\dagger 2} \right], \hat{a}^{\dagger 2} \right], \hat{a}^{\dagger 2} \right].$$

Analytical evaluation of these commutators is aided by the commutator relation

$$\left[\hat{a}^n, \hat{a}^{\dagger 2} \right] = 2n \hat{a}^\dagger \hat{a}^{n-1} + n(n-1) \hat{a}^{n-2},$$

which is used repeatedly at each step of the calculation. We thus obtain the expression

$$e^{-s_2 \hat{a}^{\dagger 2}} \hat{H} e^{s_2 \hat{a}^{\dagger 2}} = \frac{1}{2} + \lambda \left(\frac{3}{4} + 3 s_2 + 3 s_2^2 \right)$$

$$+\lambda\left(\frac{1}{\lambda}+3+12s_2+12s_2^2\right)\hat{a}^\dagger\hat{a}+\lambda\left(\frac{3}{2}+6s_2+6s_2^2\right)\hat{a}^{\dagger 2}\hat{a}^2$$
$$+\lambda\left(1+6s_2+12s_2^2+8s_2^3\right)\hat{a}^{\dagger 3}\hat{a}+\lambda\left(\frac{3}{2}+\left(\frac{2}{\lambda}+9\right)s_2+18s_2^2+12s_2^3\right)\hat{a}^{\dagger 2}$$
$$+\lambda\left(1+2s_2\right)\hat{a}^\dagger\hat{a}^3+\lambda\left(\frac{3}{2}+3s_2\right)\hat{a}^2$$
$$+\lambda\left(\frac{1}{4}+2s_2+6s_2^2+8s_2^3+4s_2^4\right)\hat{a}^{\dagger 4}+\frac{\lambda}{4}\hat{a}^4. \tag{3.25}$$

Calculating the ground-state energy matrix element $\langle 0|e^{-s_2\hat{a}^{\dagger 2}}\hat{H}e^{s_2\hat{a}^{\dagger 2}}|0\rangle$ therefore gives us

$$E_0=\frac{1}{2}+\lambda\left(\frac{3}{4}+3s_2+3s_2^2\right). \tag{3.26}$$

As a trivial check, substituting $\lambda=0$ into this expression does indeed give us the simple harmonic oscillator ground-state energy as $\frac{1}{2}$, as we would expect.

In order to calculate the matrix element $\langle 0|\hat{a}^2e^{-s_2\hat{a}^{\dagger 2}}\hat{H}e^{s_2\hat{a}^{\dagger 2}}|0\rangle$ we must pick out only the terms in equation (3.25) which will contribute, i.e. we need to evaluate

$$\langle 0|\hat{a}^2\left(\lambda\left(1+6s_2+12s_2^2+8s_2^3\right)\hat{a}^{\dagger 3}\hat{a}+\lambda\left(\frac{3}{2}+\left(\frac{2}{\lambda}+9\right)s_2+18s_2^2+12s_2^3\right)\hat{a}^{\dagger 2}\right)|0\rangle. \tag{3.27}$$

Writing both strings of operators $\hat{a}^2\hat{a}^{\dagger 3}\hat{a}$ and $\hat{a}^2\hat{a}^{\dagger 2}$ in normal order it may be shown that

$$\hat{a}^2\hat{a}^{\dagger 3}\hat{a}=6\hat{a}^\dagger\hat{a}+6\hat{a}^{\dagger 2}\hat{a}^2+\hat{a}^{\dagger 3}\hat{a}^3,$$
$$\hat{a}^2\hat{a}^{\dagger 2}=2+4\hat{a}^\dagger\hat{a}+\hat{a}^{\dagger 2}\hat{a}^2,$$

hence the first term in equation (3.27) is zero and the second term gives

$$\langle 0|\left(\lambda\left(\frac{3}{2}+\left(\frac{2}{\lambda}+9\right)s_2+18s_2^2+12s_2^3\right)\right)\left(2+4\hat{a}^\dagger\hat{a}+\hat{a}^{\dagger 2}\hat{a}^2\right)|0\rangle,$$

and so we have our NCCM equation for s_2 given by

$$\lambda\left(3+\left(\frac{4}{\lambda}+18\right)s_2+36s_2^2+24s_2^3\right)=0. \tag{3.28}$$

We now wish to find the roots of equation (3.28) in order to determine the ground-state energy E_0 as a function of λ. Making the stipulation that s_2 is real (since if s_2 were complex, the ground-state energy would be unphysical) we use Mathematica and find that the only possible real solution of equation (3.28) is given by

$$s_2\left(\lambda\right)=-\frac{1}{2}-\frac{1}{3\left(9\lambda^2+\sqrt{8\lambda^3+81\lambda^4}\right)^{\frac{1}{3}}}+\frac{\left(9\lambda^2+\sqrt{8\lambda^3+81\lambda^4}\right)^{\frac{1}{3}}}{6\lambda}, \tag{3.29}$$

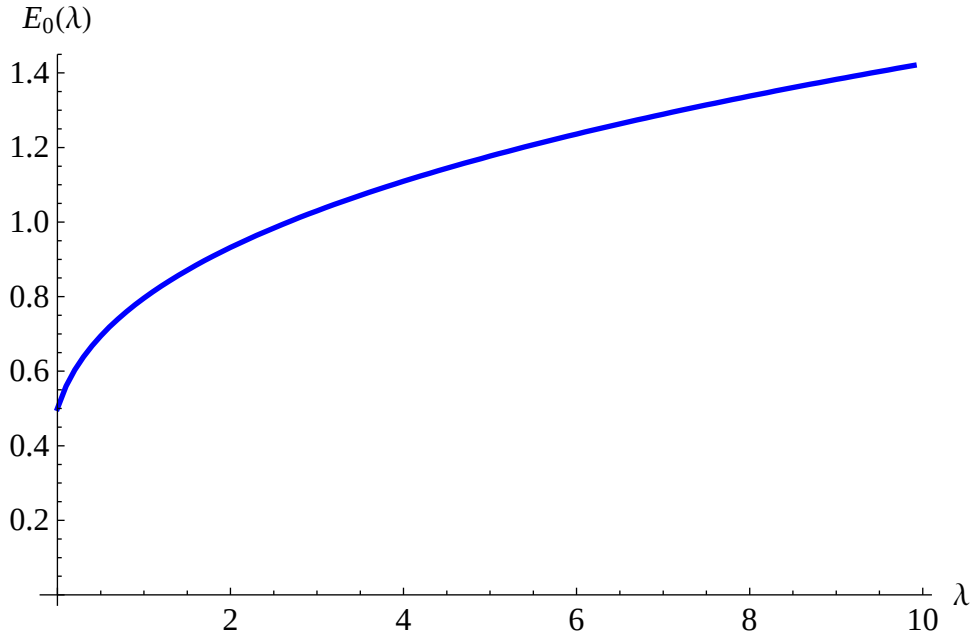

Figure 3.1: Plot of $E_0(\lambda)$ vs λ using the SUB(1) NCCM approximation.

λ	$E_0(\lambda)$ (SUB(1) NCCM)	$E_0(\lambda)$ (Exact)	% Error
0.1	0.559 827	0.559 146	0.12
0.5	0.694 416	0.696 176	0.36
1.0	0.795 954	0.803 771	0.97
10.0	1.424 286	1.504 972	5.36
100.0	2.834 205	3.131 384	9.49

Table 3.1: SUB(1) NCCM ground-state energy $E_0(\lambda)$ for various values of λ.

i.e. we have managed to find the amplitude s_2 as a function of λ for this case (however it would be naive to assume that this is always possible, as we shall see in the SUB(2) calculation). Upon substituting equation (3.29) into equation (3.26) we can determine the ground-state energy purely as a function of λ, i.e. $E_0(\lambda)$.

A plot of $E_0(\lambda)$ is shown in figure (3.1). Results for five nontrivial values of λ and $E_0(\lambda)$ can be found in table (3.1) and may be compared with the exact values of $E_0(\lambda)$ [132] which are also tabulated, correct to 6 decimal places. Percentage errors correct to 2 decimal places are also tabulated. It is evident that for even such a basic approximation as SUB(1), the NCCM performs relatively well for small λ (for example, a percentage error of 0.12 for $\lambda = 0.1$). As λ increases however, we see begin to see a deterioration in the accuracy of $E_0(\lambda)$ (for example, a percentage error of 5.36 for $\lambda = 10.0$). The value we obtain for $E_0(\lambda)$ for $\lambda = 10$ to SUB(1) is already enough information to see how poor the NCCM does for large λ, however, we also tabulate data for $\lambda = 100.0$ as this will provide a useful comparison tool between the NCCM and ECCM results for very large λ.

3.1.1.2 SUB(2) Mathematica Code

As a means of improving the accuracy of calculating the ground-state energy of the quartic anharmonic oscillator, we now consider truncating our $\hat{S}$ operator at second-order and hence calculate E_0 to SUB(2) approximation. We therefore now define our cluster correlation operator as

$$\hat{S} = s_2\hat{a}^{\dagger 2} + s_4\hat{a}^{\dagger 4}, \tag{3.30}$$

since as before, odd powers of $\hat{S}$ will not contribute in our equations. The matrix elements we thus wish to calculate are given by

$$E_0 = \left\langle 0\right| e^{-\left(s_2\hat{a}^{\dagger 2}+s_4\hat{a}^{\dagger 4}\right)}\hat{H}e^{\left(s_2\hat{a}^{\dagger 2}+s_4\hat{a}^{\dagger 4}\right)}\left|0\right\rangle,$$

$$\left\langle 0\right|\hat{a}^2 e^{-\left(s_2\hat{a}^{\dagger 2}+s_4\hat{a}^{\dagger 4}\right)}\hat{H}e^{\left(s_2\hat{a}^{\dagger 2}+s_4\hat{a}^{\dagger 4}\right)}\left|0\right\rangle = 0,$$

$$\left\langle 0\right|\hat{a}^4 e^{-\left(s_2\hat{a}^{\dagger 2}+s_4\hat{a}^{\dagger 4}\right)}\hat{H}e^{\left(s_2\hat{a}^{\dagger 2}+s_4\hat{a}^{\dagger 4}\right)}\left|0\right\rangle = 0,$$

which we may recast more succinctly as

$$\left\langle 0\right|\hat{a}^n e^{-\left(s_2\hat{a}^{\dagger 2}+s_4\hat{a}^{\dagger 4}\right)}\hat{H}e^{\left(s_2\hat{a}^{\dagger 2}+s_4\hat{a}^{\dagger 4}\right)}\left|0\right\rangle = E_0\delta_{n0},\ n = 0, 2, 4. \tag{3.31}$$

The linked-cluster expansion still terminates at fourth order for SUB(2), but the number of commutators we are required to evaluate has now been increased by a huge number. We can now also expect to find terms bi-linear in s_2 and s_4 in our NCCM equations, arising from the fact that we can have contractions between linked-cluster terms like $s_2 s_4\hat{H}\hat{a}^{\dagger 2}\hat{a}^{\dagger 4}$ which produce a nonzero contribution in matrix elements such as $s_2 s_4\left\langle 0\right|\hat{a}^4\hat{H}\hat{a}^{\dagger 2}\hat{a}^{\dagger 4}\left|0\right\rangle$. The most logical approach to calculating so many commutators is to program a piece of computer code capable of evaluating equation (3.31).

Using Mathematica, we define a noncommutative algebra in order to solve these commutators and evaluate the matrix elements given in (3.31). Our SUB(2) NCCM ground-state energy is then given by

$$E_0 = \frac{1}{2} + \lambda\left(\frac{3}{4} + 3s_2 + 3s_2^2 + 6s_4\right), \tag{3.32}$$

and our SUB(2) NCCM equations are given by

$$\lambda\left(3 + \left(\frac{4}{\lambda} + 18\right)s_2 + 36s_2^2 + 24s_2^3 + 84s_4 + 168s_2 s_4\right) = 0, \tag{3.33}$$

$$\lambda\left(1 + 8s_2 + 24s_2^2 + 32s_2^3 + 16s_2^4 + \left(\frac{16}{\lambda} + 120\right)s_4 + 816s_4^2 + 480s_2^2 s_4 + 480s_2 s_4\right) = 0. \tag{3.34}$$

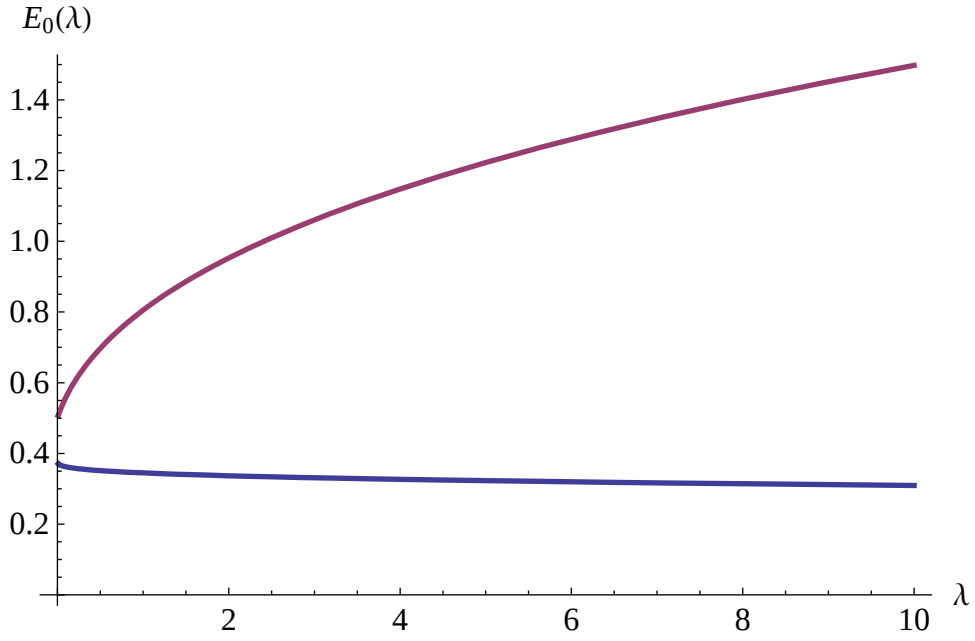

Figure 3.2: Plot of $E_0(\lambda)$ vs λ using the SUB(2) NCCM approximation.

As a simple check, if we set all s_4 terms equal to zero in equations (3.33) and (3.34), we do indeed recover our SUB(1) NCCM equations as given by equations (3.26) and (3.28). We thus see how higher order SUB(n) calculations systematically improve upon the lower order estimates produced by the method (lower order approximations are naturally encoded within all higher order calculations).

In this case it is not possible to solve equations (3.33) and (3.34) simultaneously for s_2 and s_4 in terms of general λ, as it was for the SUB(1) case where we found an expression for $s_2(\lambda)$. Thus, in order to calculate the ground-state energy as given in equation (3.32), we introduce the following procedure in our Mathematica code:

1. Assign a small value to λ (e.g. $\lambda = 0.001$) and solve equations (3.33) and (3.34) simultaneously for s_2 and s_4. Increase λ by a small amount and solve the NCCM equations again for this new value of λ. Repeat for further small increments up to $\lambda = 10$.

2. Use the Select statement to pick out only the real values of the cluster amplitudes with respect to the specified value of λ, storing the results of λ, s_2 and s_4 in a table.

3. Calculate the ground-state energy E_0 from the solution table of λ, s_2 and s_4 using equation (3.32) and plot the result.

Figure (3.2) displays the SUB(2) NCCM solutions for $E_0(\lambda)$, plotted over the same values of λ as in figure (3.1).

Solution Branch Analysis

A somewhat surprising feature of figure (3.2) is that we have two branches of solutions. The lower branch on the plot is clearly an unphysical solution since it does not give the energy as $\frac{1}{2}$ at $\lambda = 0$ (we know this must obviously be the case since it is the unperturbed ground-state energy of the harmonic oscillator). This is quite worrying when we consider equations (3.32), (3.33) and (3.34) which at first glance seem to suggest that the only possible solution for $\lambda = 0$ has an energy of $\frac{1}{2}$ with both cluster amplitudes s_2 and s_4 equal to zero.

As it happens, the situation is rather more subtle than can be reflected in the plot of figure (3.2). The only solution Mathematica can *resolve* for the energy at $\lambda = 0$ is the correct value of $\frac{1}{2}$, with both cluster amplitudes equal to zero. We can verify this simple fact in an arbitrarily high order SUB(n) calculation, wherein every single cluster amplitude is zero - this actually gives us a test for determining the correct solution branch when faced with multiple possibilities, namely that all the cluster amplitudes tend to zero as λ goes to zero. At $\lambda = 0$, the ground-state energy must equal $\frac{1}{2}$. The blue solution branch in figure (3.2) never intercepts the y-axis in this plot, at least, Mathematica cannot *resolve* this solution branch at $\lambda = 0$. For extremely small values of λ we actually find additional real solutions - these converge in pairs and go off into the complex plane however, thus it is simply not possible to represent them on the same scale as figure (3.2).

The fact that the blue solution branch shows an energy below $\frac{1}{2}$ for very small λ is intriguing - looking more closely at the NCCM equations seems to imply that either one of the cluster amplitudes s_2 or s_4 becomes extremely large and negative as one remains small and finite or that both amplitudes become extremely large and negative as λ tends to zero. It is possible that either of these cases could produce a finite value for E_0 which is less than $\frac{1}{2}$. By following the blue solution branch to extremely small λ we can uncover the reason for this rather interesting behaviour. Table (3.2) lists the results for s_2, s_4 and the ground-state energy $E_0(\lambda)$ for various values of small λ along the unphysical (blue) solution branch.

It is clear that the s_2 amplitude remains essentially fixed at a small and finite value (i.e. $s_2 = \frac{7}{3}$) whereas the s_4 amplitude seems to vary as approximately $\bar{s}_4/\lambda$, where $\bar{s}_4$ is some fixed, negative number. For $\lambda > 10^{-5}$ this correspondence breaks down and there is no longer a simple relationship between the cluster amplitudes and λ. Since we are interested in the behaviour of the NCCM equations near $\lambda = 0$, we can make use of the results from table (3.2) and thus substitute

$$s_4 = \frac{\bar{s}_4}{\lambda},$$

into equations (3.32), (3.33) and (3.34). Setting $\lambda = 0$ and bearing in mind that s_2 is

λ	s_2	s_4	$E_0(\lambda)$
10^{-50}	2.333 333	-1.960 784$\times 10^{48}$	0.382 353
10^{-40}	2.333 333	-1.960 784$\times 10^{38}$	0.382 353
10^{-30}	2.333 333	-1.960 784$\times 10^{28}$	0.382 353
10^{-20}	2.333 333	-1.960 784$\times 10^{18}$	0.382 353
10^{-10}	2.333 334	-1.960 784$\times 10^{8}$	0.382 353
10^{-5}	2.358 076	-1.965 598$\times 10^{3}$	0.382 310
10^{-4}	2.670 377	-2.019 811$\times 10^{2}$	0.381 827
10^{-3}	-4.554 123	-29.093 970	0.374 744
10^{-2}	-2.133 797	-3.490 936	0.370 623
10^{-1}	-1.204 566	-0.477 977	0.362 138

Table 3.2: Ground-state energy $E_0(\lambda)$ and cluster amplitudes s_2 and s_4 for various values of small λ along the unphysical SUB(2) solution branch.

a finite number, we obtain the expressions

$$E_0(\lambda = 0) = \frac{1}{2} + 6\bar{s}_4,$$

$$4s_2 + 84\bar{s}_4 + 168 s_2 \bar{s}_4 = 0,$$

$$16\bar{s}_4 + 816\bar{s}_4^2 = 0. \tag{3.35}$$

The last line of equation (3.35) gives us the following value for $\bar{s}_4$

$$\bar{s}_4 = -\frac{1}{51} = 0.019607843\ldots,$$

which agrees with the results in table (3.2). Substituting this value for $\bar{s}_4$ into the second line of equation (3.35) gives us $s_2 = \frac{7}{3}$ which again matches with what we have already found. Finally, substituting the value of $\bar{s}_4$ into the expression for the ground-state energy we find

$$E_0(\lambda = 0) = \frac{13}{34} = 0.382352941\ldots,$$

which is the same value in table (3.2), i.e. the cluster amplitudes s_2 and s_4 as well as the ground-state energy E_0 all become fixed (and exact) quantities in the limit that (very) small λ becomes zero.

Even though Mathematica is unable to resolve any solution at the point $\lambda = 0$ other than the correct physical branch, we have been able to prove analytically that there *do* exist solutions for the NCCM equations at $\lambda = 0$ that do *not* give the ground-state energy as $\frac{1}{2}$ (in this case the branch gives the ground-state energy as less than $\frac{1}{2}$). This fact alone allows us to determine that these branches are unphysical and hence we may discard them. Further evidence for this unphysical behaviour comes from consideration

λ	s_2	s_4	$E_0(\lambda)$
10^{-50}	-7.500 000$\times10^{-51}$	-6.250 000$\times10^{-52}$	0.500 000
10^{-40}	-7.500 000$\times10^{-41}$	-6.250 000$\times10^{-42}$	0.500 000
10^{-30}	-7.500 000$\times10^{-31}$	-6.250 000$\times10^{-32}$	0.500 000
10^{-20}	-7.500 000$\times10^{-21}$	-6.250 000$\times10^{-22}$	0.500 000
10^{-10}	-7.500 000$\times10^{-11}$	-6.250 000$\times10^{-12}$	0.500 000
10^{-5}	-7.499 531$\times10^{-6}$	-6.249 156$\times10^{-7}$	0.500 007
10^{-4}	-7.495 317$\times10^{-5}$	-6.241 574$\times10^{-6}$	0.500 075
10^{-3}	-7.453 578$\times10^{-4}$	-6.166 722$\times10^{-5}$	0.500 747
10^{-2}	-7.072 276$\times10^{-3}$	-5.504 148$\times10^{-4}$	0.507 256
10^{-1}	-4.985 899$\times10^{-2}$	-2.574 551$\times10^{-4}$	0.559 243

Table 3.3: Ground-state energy $E_0(\lambda)$ and cluster amplitudes s_2 and s_4 for various values of small λ along the physical SUB(2) solution branch.

of the CCM wave function - in this case, since s_4 is divergent at small λ then clearly the wave function

$$\big|\Psi_0\big\rangle = \exp\big(s_2\hat{a}^{\dagger 2} + s_4\hat{a}^{\dagger 4}\big)\big|\Phi_0\big\rangle,$$

is divergent as well. This categorically rules out any chance that the blue solution branch in figure (3.2) constitutes a physical SUB(2) solution.

It is interesting to observe the behaviour of the cluster amplitudes in the physical solution branch over roughly the same limits of λ used for our unphysical solution branch analysis. Table (3.3) lists the results for s_2, s_4 and the ground-state energy $E_0(\lambda)$ for various values of small λ along the physical (purple) solution branch. Here, as λ tends to zero we observe that the cluster amplitudes behave like

$$s_2 \sim \bar{s}_2\lambda,$$

$$s_4 \sim \bar{s}_4\lambda,$$

where both $\bar{s}_2$ and $\bar{s}_4$ represent fixed, negative numbers. This correspondence between the cluster amplitudes and λ is not surprising since we already know that the amplitudes must become zero at the point $\lambda = 0$. For $\lambda \geq 10^{-3}$ we see these relationships break down, in a similar manner to that seen for s_4 in the unphysical branch. Importantly, what table (3.3) tells us is that the cluster amplitudes tend to zero at approximately the same speed as λ. Coupled with the fact that this branch gives the ground-state energy as $\frac{1}{2}$ at $\lambda = 0$, we have enough conclusive evidence to deduce that this *must* be the correct, physical solution branch (as we have already assumed from a comparison of the SUB(1) solution).

Ultimately, the SUB(2) calculation for this model has exposed one of the shortcomings of the CCM, namely that solving the CCM equations in general will produce multiple possible solutions for the ground-state energy. It is only ever one of these

results that is the true, physical energy however, so in practice we must find a way to discredit all the unphysical solutions we get (or equivalently, rigorously prove which of the solutions is the true ground-state). In this case, the unphysical solution is obvious but it will not always be this simple (indeed for higher order SUB(n) calculations we may in fact find a large number of solutions that all look similar).

In general, whenever we are faced with multiple solution branches we must make the stipulation that the physical CCM solution is smoothly and continuously connected to the exact (unperturbed) ground-state. This information alone will be almost enough for us to determine the physical CCM solutions of the anharmonic oscillator to arbitrary SUB(n) approximation, however, additional subtleties in determining the physical solution are discussed below.

For problems that have nontrivial solution branches, i.e. several possible solutions are connected to the unperturbed ground-state, there are several techniques we may employ in order to determine which branch is the correct one. One such method is to look at the values of the cluster amplitudes along all branches - the physical branch typically has very small values for the cluster amplitudes whereas unphysical branches do not typically follow this trend. This is a rather fundamental property of the CCM itself - the better the starting approximation for $\left|\Phi_0\right\rangle$, the smaller the correlations of s_n need to be [21]. Unfortunately this approach is of little help when multiple branches all have cluster amplitudes of the same order. A more reliable method of isolating the true ground-state energy in this case is to use time-dependent CCM formalism and perform dynamical stability analysis about each possible solution branch. Thus the (dynamically stable) true ground-state solution will have a dynamic matrix of only real eigenvalues [42, 127] (this will be discussed in more detail later).

A more innovative way of determining which solution is the true ground-state is proposed in [80] where the quartic anharmonic oscillator is immersed in a heat bath and only states which are stable against thermal fluctuations to SUB(n) truncation are considered reliable candidates for the ground-state. This technique obviously requires the introduction of temperature-dependent CCM formalism however. A much more basic approach is to simply compare solutions with ground-state figures already known, however, the unmistakable drawback to this approach is that we require that the system has already been solved independently, to sufficient accuracy. Further discussion on the nonuniqueness of solutions in the CCM scheme when applied to anharmonic oscillators and how the situation may be dealt with can be found in [127].

SUB(5) Solutions

Using the Mathematica code initially written for the SUB(2) calculation, we may now choose to increase our level of truncation, in order to see how accurate the NCCM approach becomes to higher order. It is important to note however, even though we

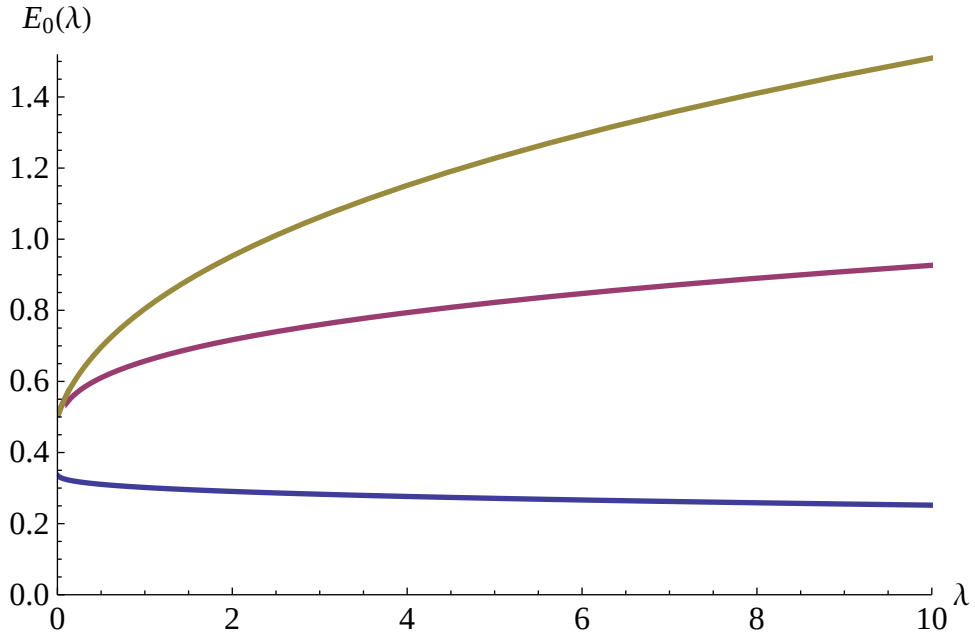

Figure 3.3: Plot of $E_0(\lambda)$ vs λ using the SUB(4) NCCM approximation.

are increasing the number of terms in our $\hat{S}$ operator, the result for the ground-state energy as given in equation (3.32) will not include any additional terms. This is because there are no more contributions to the matrix element $\langle 0|e^{-\hat{S}}\hat{H}e^{\hat{S}}|0\rangle$ as the truncation of $\hat{S}$ increases past SUB(2). Since $\hat{H}$ only contains terms to fourth order of either $\hat{a}^\dagger$ or $\hat{a}$ operators, it is not possible to have contractions with $\hat{S}$ when $\hat{S}$ contains terms higher than fourth order (e.g. the SUB(3) element $s_6\hat{a}^{\dagger 6}$). So the ground-state energy is purely a function of λ, s_2 and s_4 for all calculations of SUB(2) and higher, but the energy will differ between these higher order calculations since the amplitudes will be different for each calculation (the NCCM equations for the set $\{s_n\}$ will produce different results in each different calculation).

To complicate matters further, if we make a plot of the ground-state energy to SUB(4) (see figure (3.3)) we see a third (unphysical) branch in the solutions. We may discard this solution branch for the same reasons as the SUB(2) unphysical branch, namely that it does not produce a ground-state energy of $\frac{1}{2}$ at $\lambda = 0$ and its cluster amplitudes do not all tend to zero at this point - indeed, for small λ, s_2 is equal to zero, s_4 and s_6 behave like $-\frac{1}{\lambda}$, s_8 behaves like $\frac{1}{\lambda^2}$ and the ground-state energy at $\lambda = 0$ is given by 0.481899 correct to 6 decimal places. By comparison, for small λ in the physical solution branch, s_2 and s_4 behave like $-\lambda$, s_6 behaves like λ^2 and s_8 behaves like $-\lambda^2$, thus they all tend to zero as λ goes to zero (either at the same speed as λ or for the s_6 and s_8 amplitudes, twice as fast).

Table (3.4) lists all the values of the ground-state energy $E_0(\lambda)$ calculated up to SUB(5) using the Mathematica code (note that for percentage errors that give 0 to 2 decimal places, an additional 2 decimal places are presented in parenthesis). For

small λ we thus see a much more rapid convergence for increasingly higher SUB(n) approximations, compared to that for large λ (at SUB(5) we have a 0.33 percentage error for $\lambda = 100.0$, compared to finding the exact result at SUB(4) for $\lambda = 0.1$, correct to 6 decimal places).

λ	n	$E_0(\lambda)$	% Error
0.1	2	0.559 243	0.02
	3	0.559 153	0.00(13)
	4	0.559 146	0
	5	0.559 146	0
	Exact	**0.559 146**	
0.5	2	0.697 220	0.15
	3	0.696 600	0.06
	4	0.696 300	0.02
	5	0.696 196	0.00(29)
	Exact	**0.696 176**	
1.0	2	0.805 252	0.18
	3	0.804 844	0.13
	4	0.804 279	0.06
	5	0.803 971	0.02
	Exact	**0.803 771**	
10.0	2	1.497 330	0.51
	3	1.507 865	0.19
	4	1.509 246	0.28
	5	1.508 950	0.26
	Exact	**1.504 972**	
100.0	2	3.075 496	1.78
	3	3.124 441	0.22
	4	3.137 725	0.20
	5	3.141 706	0.33
	Exact	**3.131 384**	

Table 3.4: SUB(2)-SUB(5) NCCM ground-state energy $E_0(\lambda)$ for various values of λ.

The solution method of which the code itself uses is extremely expensive however, especially for high order SUB(n). Calculations at the SUB(1) or SUB(2) level may only take a minute or so but to SUB(4) or SUB(5), with such a proliferation of terms in the cluster operator $\hat{S}$ and so many commutators to explicitly evaluate, computing time can become as slow as 15 or 20 minutes, especially since we are in fact calculating *all* possible solution branches and not just the "correct" one. If we wish to push our NCCM calculations yet further we would require a much more elegant method to evaluate our equations.

3.1.1.3 Binomial Routine

As a means to reduce the computing time of our Mathematica code and to sensibly reach results for higher SUB(n) approximations, we introduce an alternative method to evaluating the linked-cluster expansion and its matrix elements through direct commutators and noncommutative algebra. Instead of calculating all such commutators that arise in $e^{-\hat{S}}\hat{H}e^{\hat{S}}$ term by term, we utilise the relation

$$\left[\hat{a}^n, \hat{a}^{\dagger m}\right] = \sum_k \begin{pmatrix} n \\ k \end{pmatrix} \begin{pmatrix} m \\ k \end{pmatrix} k! \hat{a}^{\dagger m-k} \hat{a}^{n-k}, \tag{3.36}$$

where the standard binomial coefficient is given by

$$\begin{pmatrix} n \\ k \end{pmatrix} = \frac{n!}{(n-k)!k!},$$

and the summation over k runs from 0 to the lower of the two values of n or m. In this way, we may quickly and readily evaluate commutators in the form of a series expansion (which is also automatically written in normal order) as opposed evaluating each part separately and repeatedly applying the relations given in equation (3.5) over and over. As a simple example, setting both n and m equal to 4 we have

$$\left[\hat{a}^4, \hat{a}^{\dagger 4}\right] = \sum_{k=0}^{4} \begin{pmatrix} 4 \\ k \end{pmatrix} \begin{pmatrix} 4 \\ k \end{pmatrix} k! \hat{a}^{\dagger 4-k} \hat{a}^{4-k}$$

$$= \frac{4!4!}{4!4!0!}\hat{a}^{\dagger 4}\hat{a}^4 + \frac{4!4!}{3!3!1!}\hat{a}^{\dagger 3}\hat{a}^3 + \frac{4!4!}{2!2!2!}\hat{a}^{\dagger 2}\hat{a}^2 + \frac{4!4!}{1!1!3!}\hat{a}^{\dagger}\hat{a} + \frac{4!4!}{0!0!4!}$$

$$= \hat{a}^{\dagger 4}\hat{a}^4 + 16\hat{a}^{\dagger 3}\hat{a}^3 + 72\hat{a}^{\dagger 2}\hat{a}^2 + 96\hat{a}^{\dagger}\hat{a} + 24,$$

and we reach this answer far more quickly than we would if we had evaluated $\left[\hat{a}^4, \hat{a}^{\dagger 4}\right]$ directly with commutators. Using the binomial relation given in equation (3.36) now makes our Mathematica code much more economical and means we can push towards much higher SUB(n) approximations far more easily.

Figure (3.4) shows a plot of the SUB(7) ground-state energy solutions as an example of where we have four different branches. The lower two branches (blue and purple) are the persistent unphysical solutions first observed at SUB(2) and SUB(4) order respectively. The other two branches lie extremely close to one another at small λ and both give the ground-state energy as $\frac{1}{2}$ at $\lambda = 0$. However, we conclude that the green branch is the physical solution in this case since all of its cluster amplitudes are proportional to λ or λ^2 in the small λ limit, whereas the yellow branch has cluster amplitudes that are either zero (s_2, s_4, s_6) or proportional to $\pm\frac{1}{\lambda}$ (s_8, s_{10}) or $\pm\frac{1}{\lambda^2}$ (s_{12}, s_{14}). As a further check, dynamic stability analysis of the yellow, purple and

red branches reveals (large) positive *and* negative excitation energies over the range $0 < \lambda \leq 10$ but the green branch has only positive excitation energies.

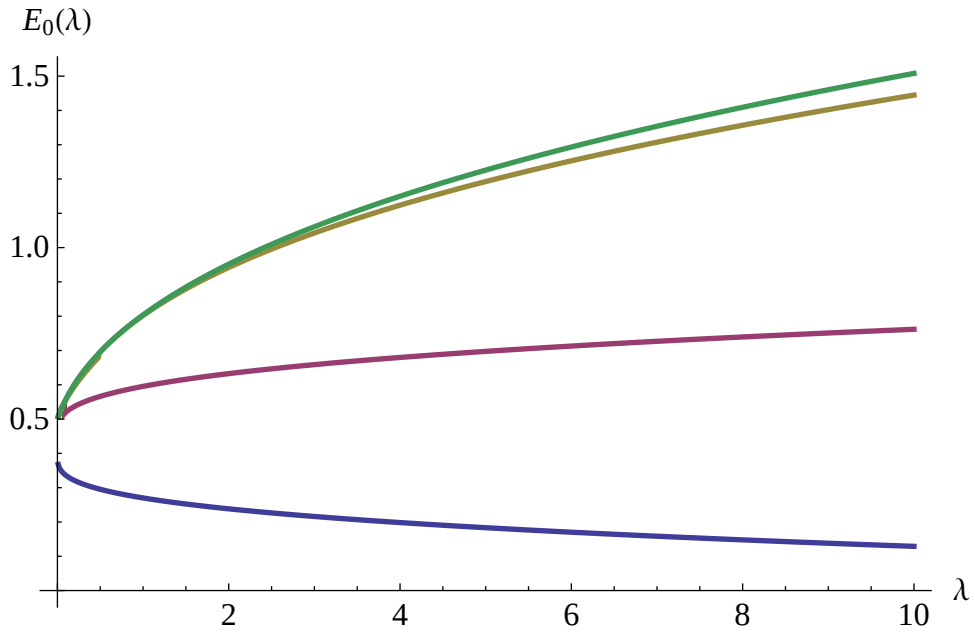

Figure 3.4: Plot of $E_0(\lambda)$ vs λ using the SUB(7) NCCM approximation.

Table (3.5) lists the ground-state energy results $E_0(\lambda)$ for SUB(n) approximation using the binomial approach, where n runs from 6 to 10 (the percentage errors for $\lambda = 100.0$ are given to 4 decimal places since they almost all give the same value when rounded to 2 decimal places). As we have already seen, we have managed to reproduce the exact ground-state energy for $\lambda = 0.1$, although for higher λ we unfortunately fail to see such a convergence (at $\lambda = 10.0$ we see a genuine but slow convergence with a percentage error of 0.16 to SUB(10), which is not much of an improvement over the SUB(5) calculation which has a percentage error of 0.26).

λ	n	$E_0(\lambda)$	% Error
0.1	6	0.559 146	0
	7	0.559 146	0
	8	0.559 146	0
	9	0.559 146	0
	10	0.559 146	0
	Exact	**0.559 146**	
0.5	6	0.696 163	0.00(19)
	7	0.696 157	0.00(27)
	8	0.696 159	0.00(24)
	9	0.696 163	0.00(19)
	10	0.696 169	0.00(10)
	Exact	**0.696 176**	
1.0	6	0.803 818	0.00(58)
	7	0.803 741	0.00(37)
	8	0.803 703	0.00(85)
	9	0.803 686	0.01
	10	0.803 684	0.01
	Exact	**0.803 771**	
10.0	6	1.508 438	0.23
	7	1.508 033	0.20
	8	1.507 773	0.19
	9	1.507 593	0.17
	10	1.507 433	0.16
	Exact	**1.504 972**	
100.0	6	3.142 839	0.3658
	7	3.143 067	0.3731
	8	3.143 025	0.3718
	9	3.142 900	0.3678
	10	3.142 744	0.3628
	Exact	**3.131 384**	

Table 3.5: SUB(6)-SUB(10) NCCM ground-state energy $E_0(\lambda)$ for various values of λ.

Upon increasing the order of SUB(n) approximation we observe an extremely slow convergence, followed by a somewhat oscillatory convergence of the results to the exact values for large λ, as has been noted elsewhere [80, 125]. We should not find the nature of this convergence too disconcerting however, the results in [125], which make use of a more complicated CCM formalism to begin with, only observe genuine convergence for $\lambda \leq 1.0$ (for the case of $\lambda = 1$, the exact result is reproduced at SUB(18) in [125] and at SUB(12) in [80]). For $\lambda > 1$ there is no convergence to exact values seen up to as high as SUB(20) in [125], and the strange behavior of the $\lambda = 100.0$ solutions is similarly observed in [80] - so our results for $\lambda = 10.0$ and $\lambda = 100.0$ should not worry us too much. As is noted in [126], by utilising a Bogoliubov transformation on the harmonic oscillator operators $\hat{a}^\dagger$ and $\hat{a}$, working with the transformed operators $\hat{b}^\dagger$ and $\hat{b}$ actually

produces a much faster convergence, thus if we were solely interested in obtaining high precision results using the NCCM, we would incorporate such a transformation into our calculations.

3.1.1.4 Excited-State Energies

Having shown how we can calculate the ground-state energy of the quartic anharmonic oscillator using the NCCM to different levels of approximation, we now proceed to calculate the first two (even) excited-state energies of the model. As was established in the formalism of chapter 2, in order to find the excited-state energies using the RPA approach, we need to calculate the positive energy eigenvalues ω_n from the eigenvalue equation

$$E_{IJ}\delta s_J = \omega_n \delta s_I, \tag{3.37}$$

where the RPA matrix E_{IJ} is given by

$$E_{IJ} = \sum_{J\neq 0} \langle \Phi_0 | \hat{C}_I e^{-\hat{S}} \left[\hat{H}, \hat{C}_J^\dagger \right] e^{\hat{S}} | \Phi_0 \rangle = \partial_{s_J} E_I, \; \forall I \neq 0. \tag{3.38}$$

Since the eigenvalues give the excitation energy relative to the ground-state, excited-state energies are thus given by $\varepsilon_n = \omega_n + E_0$.

This method will only find excited-states with the same symmetry as the ground-state however, hence we will only be able to calculate the excited-state energies ε_2, ε_4, ε_6 and so on, since our generalised vacuum was chosen to be the (even parity) state $|0\rangle$. In practice, the full set of excited-state energies may be found by use of either the Emrich approach [69, 70] or by repeating the RPA calculations with respect to the (odd parity) state $|1\rangle$, where all odd indexed terms in the cluster correlation operator $\hat{S}$ are not set equal to zero. Since this discussion is designed to be a pedagogical introduction to how the general CCM formalism is applied, we are not concerned with replicating the entire excited-state energy spectrum. Thus, comparison of the exact results found in [132] with the values of ε_2 and ε_4 found via the RPA approach at different levels of SUB(n) approximation will serve the demonstrative purposes we require.

Evaluating the RPA matrix to SUB(n) will find the n excited-state energies above the ground-state, having the same parity as the ground-state. As an example, working to SUB(2) approximation means E_{IJ} is given by a simple 2×2 matrix

$$E_{IJ} = \begin{pmatrix} e_{11} & e_{12} \\ e_{21} & e_{22} \end{pmatrix} = \begin{pmatrix} \partial_{s_2} E_2 & \partial_{s_4} E_2 \\ \partial_{s_2} E_4 & \partial_{s_4} E_4 \end{pmatrix}, \tag{3.39}$$

where E_2 and E_4 are given by

$$E_2 = \lambda\left(\frac{3}{2} + \left(\frac{2}{\lambda} + 9\right)s_2 + 18s_2^2 + 12s_2^3 + 42s_4 + 84s_2s_4\right) \tag{3.40}$$

$$E_4 = \lambda\left(\frac{1}{4} + 2s_2 + 6s_2^2 + 8s_2^3 + 4s_2^4 + \left(\frac{4}{\lambda} + 30\right)s_4 + 204s_4^2 + 120s_2^2s_4 + 120s_2s_4\right), \tag{3.41}$$

i.e. they are simply the NCCM equations

$$E_2 = \left\langle 2\middle|e^{-\hat{S}}\hat{H}e^{\hat{S}}\middle|0\right\rangle,$$

$$E_4 = \left\langle 4\middle|e^{-\hat{S}}\hat{H}e^{\hat{S}}\middle|0\right\rangle,$$

and we will only be able to calculate the energies ε_2 and ε_4. Note that equations (3.40) and (3.41) have been obtained by using normalised states, as stipulated in the excited-state formalism in chapter 2.

Calculating each term of the RPA matrix we obtain

$$\partial_{s_2}E_2 = 2 + \lambda\left(9 + 36s_2 + 36s_2^2 + 84s_4\right),$$

$$\partial_{s_4}E_2 = \lambda\left(42 + 84s_4\right),$$

$$\partial_{s_2}E_4 = \lambda\left(2 + 12s_2 + 24s_2^2 + 240s_2s_4 + 120s_4 + 16s_2^3\right),$$

$$\partial_{s_4}E_4 = 4 + \lambda\left(30 + 480s_4 + 120s_2^2 + 120s_2\right). \tag{3.42}$$

In generalised notation, we now evaluate the determinant

$$\begin{vmatrix} e_{11} - \omega_n & e_{12} \\ e_{21} & e_{22} - \omega_n \end{vmatrix} = 0,$$

i.e. we solve the quadratic equation

$$\omega_n^2 - (e_{11} + e_{22})\,\omega_n + (e_{11}e_{22} - e_{12}e_{21}) = 0, \tag{3.43}$$

to find the eigenvalues ω_n, which appear as functions of λ, s_2 and s_4 i.e. $\omega_n = \omega_n(\lambda, s_2, s_4)$. As a brief check, if we set $\lambda = 0$ the RPA matrix becomes

$$E_{IJ} = \begin{pmatrix} 2 & 0 \\ 0 & 4 \end{pmatrix},$$

which trivially has the eigenvalues $\omega_1 = 2$ and $\omega_2 = 4$, meaning that the second and fourth excited-state energies of the simple harmonic oscillator are given by $\varepsilon_2 = \frac{5}{2}$ and $\varepsilon_4 = \frac{9}{2}$ respectively, exactly what we already know from the simple harmonic energy spectrum $\varepsilon_n = \left(n + \frac{1}{2}\right)$.

In practice, we calculate the excited-state energies using the RPA approach as follows:

1. Evaluate the matrix elements $\langle\Phi_0|\hat{C}_I e^{-\hat{S}}\hat{H}e^{\hat{S}}|\Phi_0\rangle$, $\forall I \neq 0$ and solve the NCCM equations $\langle\Phi_0|\hat{C}_I e^{-\hat{S}}\hat{H}e^{\hat{S}}|\Phi_0\rangle = 0$, $\forall I \neq 0$ for a given value of λ.

2. Formulate the RPA matrix E_{IJ} according to equation (3.38).

3. Substitute the solutions of the NCCM equations and the value of λ from step 1 into the RPA matrix.

4. Calculate the eigenvalues ω_n of the RPA matrix for values of λ and the amplitude solutions as found in step 1.

5. Discounting negative or complex values for ω_n, deduce the excited-state energies from the relation $\varepsilon_n = \omega_n + E_0$.

For a given physical solution to the ground-state energy E_0, the corresponding RPA matrix must have real, nonnegative eigenvalues for the entire length of the solution branch. Table (3.6) lists values for the excited-state energies ε_2 and ε_4 calculated up to SUB(5), as well as the exact results from [132] to 4 decimal places. In all cases, the (multiple) unphysical solution branches had negative and/or complex eigenvalues, therefore each one of them may be discounted from being the true solution to the ground-state (as they result in either complex values for the excitation energies or they produce an excited-state energy which is lower than that of the ground-state).

λ	n	ε_2	ε_2 % Error	ε_4	ε_4 % Error
0.1	2	3.1476	0.29	7.0052	12.62
	3	3.1373	0.04	6.3734	2.46
	4	3.1379	0.02	6.2340	0.22
	5	3.1384	0.00(64)	6.2119	0.14
	Exact	**3.1386**		**6.2203**	
0.5	2	4.5102	4.22	12.8539	42.37
	3	4.3698	0.98	10.7765	19.36
	4	4.3275	0	9.8844	9.48
	5	4.3164	0.27	9.4194	4.33
	Exact	**4.3275**		**9.0288**	
1.0	2	5.5787	7.71	17.3957	58.67
	3	5.3239	2.79	14.4887	32.15
	4	5.2210	0.87	13.1468	19.91
	5	5.1760	0.06	12.3854	12.97
	Exact	**5.1792**		**10.9636**	
10.0	2	12.4886	20.70	46.3165	
	3	11.6558	12.65	40.1473	
	4	11.2288	8.52	37.6473	
	5	10.9903	6.22	36.5081	
	Exact	**10.3471**		**22.4088**	

Table 3.6: SUB(2)-SUB(5) NCCM excited-state energies ε_2 and ε_4 for various values of λ.

For small λ we see a close match for the lower of the two excited-states, ε_2 (a percentage error of 0.0064 at SUB(5) for $\lambda = 0.1$) although this gap increases for large λ at the same level of approximation (a percentage error of 6.22 for $\lambda = 10.0$). For the higher excited-state ε_4, we don't see as rapid a convergence for small λ as ε_2 (a percentage error of 0.14 at SUB(5) for $\lambda = 0.1$) and for large λ we see a catastrophic failure of the method. This failure is not surprising in some ways, since it is an artifact of the method we have employed. Our RPA matrix is only a second-order approximation to begin with, hence we should not expect to see it reproduce accurate higher order energies for large values of the coupling constant. For $\lambda = 100.0$ there were no real and positive eigenvalues ω_n, thus the approximation genuinely breaks down in the large λ limit using this approach.

3.1.2 Extended Coupled Cluster Method

To conclude our study of the quartic anharmonic oscillator, we introduce the ECCM and calculate the ground-state energy functional $E\left(\left\{s_I, \tilde{s}_I\right\}\right)$, with a view to comparing the results with those of the previous sections. As we shall see, the ECCM is much more complicated in its structure when compared to the NCCM, even to relatively low order SUB(n). With that in mind, we begin with a straightforward SUB(1) ECCM

calculation and proceed only up to SUB(2).

Although the fundamental formalism of the ECCM begins with a double similarity-transformed Hamiltonian,

$$e^{\hat{\tilde{S}}}e^{-\hat{S}}\hat{H}e^{\hat{S}}e^{-\hat{\tilde{S}}}$$

in practice we begin by evaluating the functional

$$E\left(\left\{s_I,\tilde{s}_I\right\}\right)=\left\langle\Phi_0\right|e^{\hat{\tilde{S}}}e^{-\hat{S}}\hat{H}e^{\hat{S}}\left|\Phi_0\right\rangle, \tag{3.44}$$

since we know by definition that

$$e^{-\hat{\tilde{S}}}\left|\Phi_0\right\rangle=\left|\Phi_0\right\rangle,$$

as $\hat{\tilde{S}}$ is constructed of generalised annihilation operators with respect to $\left|\Phi_0\right\rangle$. Therefore, in order to calculate the ground-state energy functional in general, we expand the left hand operator as

$$e^{\hat{\tilde{S}}}=\sum_{\gamma=0}^{+\infty}\frac{1}{\gamma!}\left(\sum_{I\neq 0}\tilde{s}_I\hat{C}_I\right)^{\gamma}, \tag{3.45}$$

and seek all the contributing contractions of the matrix element given in equation (3.44).

3.1.2.1 SUB(1) Calculation

To SUB(1), we already know that the linked-cluster expansion $e^{-\hat{S}}\hat{H}e^{\hat{S}}$ is given by equation (3.25) and therefore our $\hat{\tilde{S}}$ operator is given by

$$e^{\hat{\tilde{S}}_{\mathrm{SUB(1)}}}=1+\tilde{s}_2\hat{a}^2+\frac{1}{2}\tilde{s}_2^2\hat{a}^4, \tag{3.46}$$

since $e^{-\hat{S}}\hat{H}e^{\hat{S}}$ only contains terms up to fourth order in $\hat{a}^\dagger$. Hence we want to evaluate

$$E_0=\left\langle 0\right|\left(1+\tilde{s}_2\hat{a}^2+\frac{1}{2}\tilde{s}_2^2\hat{a}^4\right)e^{-s_2\hat{a}^2}\hat{H}e^{s_2\hat{a}^2}\left|0\right\rangle, \tag{3.47}$$

which, as it turns out, is very simple to calculate as it is essentially a sum of linear combinations of the NCCM equations $\left\langle 2\right|e^{-s_2\hat{a}^2}\hat{H}e^{s_2\hat{a}^2}\left|0\right\rangle$ and $\left\langle 4\right|e^{-s_2\hat{a}^2}\hat{H}e^{s_2\hat{a}^2}\left|0\right\rangle$, which we have already evaluated. We therefore derive that the ground-state energy is given by

$$E_0=\frac{1}{2}+\lambda\left(\frac{3}{4}+3s_2+3s_2^2+3\tilde{s}_2+3\tilde{s}_2^2\right)$$
$$+\lambda\left(\left(\frac{4}{\lambda}+18\right)s_2\tilde{s}_2+36s_2^2\tilde{s}_2+24s_2^3\tilde{s}_2+24s_2\tilde{s}_2^2+72s_2^2\tilde{s}_2^2+96s_2^3\tilde{s}_2^2+48s_2^4\tilde{s}_2^2\right). \tag{3.48}$$

If we substitute $\tilde{s}_2 = 0$ into equation (3.48) we recover the NCCM result for the ground-state energy given in equation (3.26), and we thus observe first hand how the NCCM is automatically encoded within the structure of the ECCM formalism.

In order to numerically calculate the ground-state energy, we minimise E_0 with respect to either cluster amplitude and solve the resulting simultaneous equations for s_2 and $\tilde{s}_2$, i.e. we wish to solve the ECCM equations

$$\frac{\partial E_0}{\partial s_2} = \frac{1}{2} + \lambda\left(3 + 6s_2 + \left(\frac{4}{\lambda} + 18\right)\tilde{s}_2 + 24\tilde{s}_2^2\right)$$

$$+\lambda\left(72s_2\tilde{s}_2 + 72s_2^2\tilde{s}_2 + 144s_2\tilde{s}_2^2 + 288s_2^2\tilde{s}_2^2 + 192s_2^3\tilde{s}_2^2\right) = 0, \tag{3.49}$$

$$\frac{\partial E_0}{\partial \tilde{s}_2} = \lambda\left(3 + \left(\frac{4}{\lambda} + 18\right)\tilde{s}_2 + 36s_2^2 + 24s_2^3 + 6\tilde{s}_2\right)$$

$$+\lambda\left(48s_2\tilde{s}_2 + 144s_2^2\tilde{s}_2 + 192s_2^3\tilde{s}_2 + 96s_2^4\tilde{s}_2\right) = 0. \tag{3.50}$$

The method of solution we program in Mathematica is very similar to the NCCM case. We assign a value to λ, solve equations (3.49) and (3.50) simultaneously for real values of s_2 and $\tilde{s}_2$ and tabulate the results. Varying λ over the range 0 to 10, we then substitute all these results into equation (3.48) and evaluate the ground-state energy E_0.

Table (3.7) shows the values of the SUB(1) ECCM ground-state energy for the five values of λ we used previously. If we compare these results to those given in table (3.1) then we observe that the NCCM actually outperforms the ECCM for all values of the coupling constant below 10. For $\lambda = 10.0$ and $\lambda = 100.0$ however, the ECCM produces values with a much smaller percentage error. This is still an extremely low order calculation though and we should perhaps not expect to see such a marked increase in accuracy when using the ECCM as opposed to the NCCM.

λ	$E_0(\lambda)$ (SUB(1) ECCM)	$E_0(\lambda)$ (Exact)	% Error
0.1	0.560 307	0.559 146	0.21
0.5	0.701 668	0.696 176	0.79
1.0	0.812 500	0.803 771	1.09
10.0	1.531 250	1.504 972	1.75
100.0	3.192 444	3.131 384	1.95

Table 3.7: SUB(1) ECCM ground-state energy $E_0(\lambda)$ for various values of λ.

3.1.2.2 SUB(2) Calculation

If we now increase the truncation on the cluster correlation operators so we are working to SUB(2), the situation rapidly becomes a lot more difficult. The general expression

for the linked-cluster expansion $e^{-\hat{S}}\hat{H}e^{\hat{S}}$ to SUB(2) is already given in equation (3.32) but since this object contains terms up to twelfth order of $\hat{a}^{\dagger}$, our expression for $e^{\hat{\tilde{S}}}$ becomes considerably more complicated than the SUB(1) case

$$e^{\hat{\tilde{S}}_{\mathrm{SUB}(2)}} = 1 + \tilde{s}_2\hat{a}^2 + \left(\frac{1}{2}\tilde{s}_2^2 + \tilde{s}_4\right)\hat{a}^4$$

$$+ \left(\frac{1}{6}\tilde{s}_2^3 + \tilde{s}_2\tilde{s}_4\right)\hat{a}^6 + \left(\frac{1}{24}\tilde{s}_2^4 + \frac{1}{2}\tilde{s}_2^2\tilde{s}_4 + \frac{1}{2}\tilde{s}_4^2\right)\hat{a}^8$$

$$+ \left(\frac{1}{120}\tilde{s}_2^5 + \frac{1}{6}\tilde{s}_2^3\tilde{s}_4 + \frac{1}{2}\tilde{s}_2\tilde{s}_4^2\right)\hat{a}^{10} + \left(\frac{1}{720}\tilde{s}_2^6 + \frac{1}{24}\tilde{s}_2^4\tilde{s}_4 + \frac{1}{4}\tilde{s}_2^2\tilde{s}_4^2 + \frac{1}{6}\tilde{s}_4^3\right)\hat{a}^{12}, \qquad (3.51)$$

as we need to include all possible terms in $e^{\hat{\tilde{S}}}$ to SUB(2) which contract with $e^{-\hat{S}}\hat{H}e^{\hat{S}}$ in the vacuum expectation value, i.e. we require all possible terms in $e^{\hat{\tilde{S}}}$ up to twelfth order in $\hat{a}$. Such a growth in the number of terms and the power of the operators involved implies that our ground-state energy functional

$$E\left(\left\{s_2, \tilde{s}_2, s_4, \tilde{s}_4\right\}\right) = \left\langle 0\middle|e^{\hat{\tilde{S}}_{\mathrm{SUB}(2)}}e^{-\hat{S}_{\mathrm{SUB}(2)}}\hat{H}e^{\hat{S}_{\mathrm{SUB}(2)}}\middle|0\right\rangle \qquad (3.52)$$

will include many more terms than that seen in the SUB(2) NCCM case, given in equation (3.32).

If we deal with this ground-state energy functional at face value, we obtain an expression where several numerical coefficients of cluster amplitude terms take on huge order. Attempting to minimise this for each of the 4 cluster amplitudes independently will prove extremely expensive computationally and coupled with this, it is likely to produce an extremely large amount of solutions regardless, further compounding our computing problems. In order to make the functional more compliant, we choose to scale our cluster amplitudes as follows

$$s_2 \rightarrow \frac{1}{2!}s_2,\ \tilde{s}_2 \rightarrow \frac{1}{2!}\tilde{s}_2,$$

$$s_4 \rightarrow \frac{1}{4!}s_4,\ \tilde{s}_4 \rightarrow \frac{1}{4!}\tilde{s}_4. \qquad (3.53)$$

Such a scaling is perfectly legal (again, we may view it purely as our redefined cluster amplitudes absorbing large valued coefficients in equation (3.52), as a means to expedite computation) and will mean $E\left(\left\{s_2, \tilde{s}_2, s_4, \tilde{s}_4\right\}\right)$ and our ECCM equations are much more tractable to work with.

There are six solution different solution branches for the ECCM ground-state energy to SUB(2), i.e. many more than the simple SUB(2) NCCM case which gave two branches. Table (3.8) lists the values of the SUB(2) ground-state energy for the usual values of λ. Comparing this with the analogous NCCM results given in table (3.4)

λ	$E_0(\lambda)$ (SUB(2) ECCM)	$E_0(\lambda)$ (Exact)	% Error
0.1	0.559 188	0.559 146	0.01
0.5	0.696 767	0.696 176	0.08
1.0	0.804 973	0.803 771	0.15
10.0	1.509 274	1.504 972	0.29
100.0	3.134 552	3.131 384	0.10

Table 3.8: SUB(2) ECCM ground-state energy $E_0(\lambda)$ for various values of λ.

we can clearly see that the ECCM now outperforms the NCCM for all values of the coupling constant. The percentage errors in the ECCM do still increase the larger λ becomes, but the range in which they vary (from 0.01 to 0.29) is smaller than that of the NCCM case (0.02 to 0.51).

Although this increase in accuracy initially seems positive, it comes at the cost of an extensive and laborious computational scheme. With the NCCM producing such decent results with such a simple approach and in a fraction of the computing time, the benefit of using the ECCM in this case is questionable. For the study of the quartic anharmonic oscillator, the NCCM proves admirable in the respect that it is so simple and quick and yet still produces excellent result for low values of the coupling constant, to low order SUB(n) approximation. The improvements of the ECCM scheme over the NCCM probably aren't necessarily justified in the case of this model. At the same time, we must emphasise that finding *all* of the real CCM solutions is not optimal, but we do so in order to establish in detail the typical outcome of a CCM calculation. Our intent was to give a demonstrative example of how the ECCM is applied, and give a comparison with the equivalent NCCM results. With that done, we conclude the study of this model and proceed to address a slightly different anharmonic oscillator.

3.2 The Double-Well Quartic Anharmonic Oscillator

Having completed our discussion on the application of CCM techniques to the quartic anharmonic oscillator, an interesting extension to the work we have thus far covered would be a study of the *double-well* quartic anharmonic oscillator. Since we have already developed our computational toolbox throughout the investigation of the previous model, analysis of the double-well model can be performed in a fairly concise manner. Continuing with the use of our natural units, we therefore describe this model by the Hamiltonian

$$\hat{H} = \frac{1}{2}\left(\hat{p}^2 - k\hat{x}^2 + \hat{x}^4\right) \tag{3.54}$$

where the mass term k is real and positive (note that this is sometimes labeled Z^2 in certain literature [123, 125]). This Hamiltonian evidently has the 1-dimensional

potential

$$V(x) = \frac{1}{2}\left(-kx^2 + x^4\right), \tag{3.55}$$

which, $\forall k > 0$ corresponds to a symmetric double-well, centered at the origin with minima situated at the points $x = \pm\sqrt{\frac{k}{2}}$. Figure (3.5) shows a plot of the potential $V(x)$ for 4 values of k.

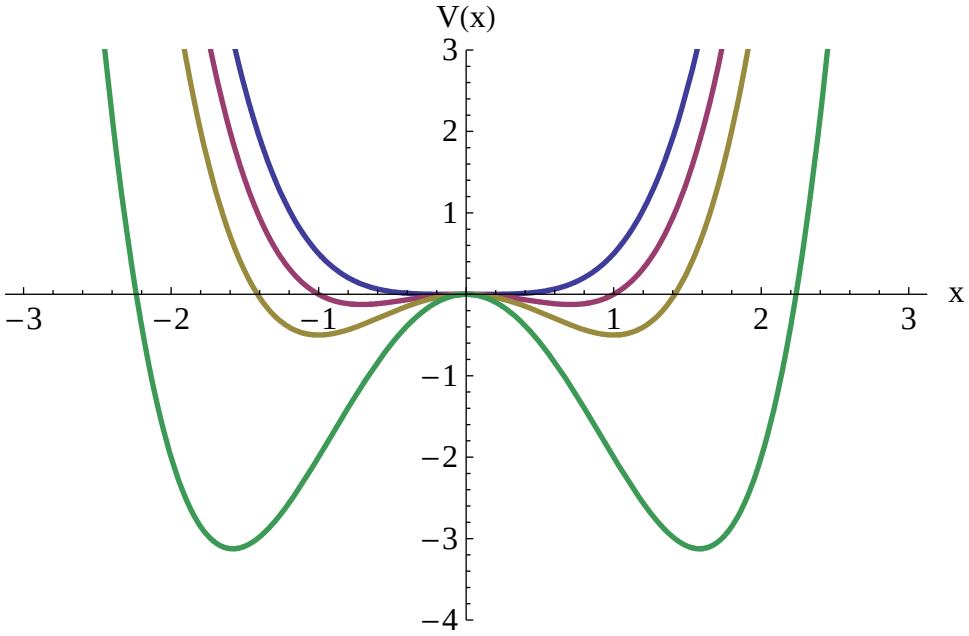

Figure 3.5: Plot of the double-well potential $V(x) = \frac{1}{2}\left(-kx^2 + x^4\right)$ for $k = 0$ (blue), $k = 1$ (red), $k = 2$ (yellow) and $k = 5$ (green).

If we make the observation that the Hamiltonian of equation (3.54) may be written as

$$\hat{H} = \frac{1}{2}\hat{p}^2 + \frac{1}{2}\left(\hat{x}^2 - \frac{1}{2}k\right)^2 - \frac{k^2}{8}, \tag{3.56}$$

then we remark that by adding the depth of the well $\frac{k^2}{8}$ to our results for the ground-state energy, i.e. shifting the double-well potential upwards by $\frac{k^2}{8}$, we ensure that the Hamiltonian given in equation (3.54) is positive definite for all k [125, 133]. Thus for this model, we will use the exact, rescaled values of $E_0(k)$ as given in [125] as our benchmark figures for comparison (the rescaling may be performed on the exact results given in [123] and tabulated but since it has already been done in [125] we use their values). Figure (3.6) shows a plot of the shifted double-well potential

$$V_s(x) = \frac{1}{2}\left(x^2 - \frac{1}{2}k\right)^2, \tag{3.57}$$

plotted for the same values of k as in figure (3.5).

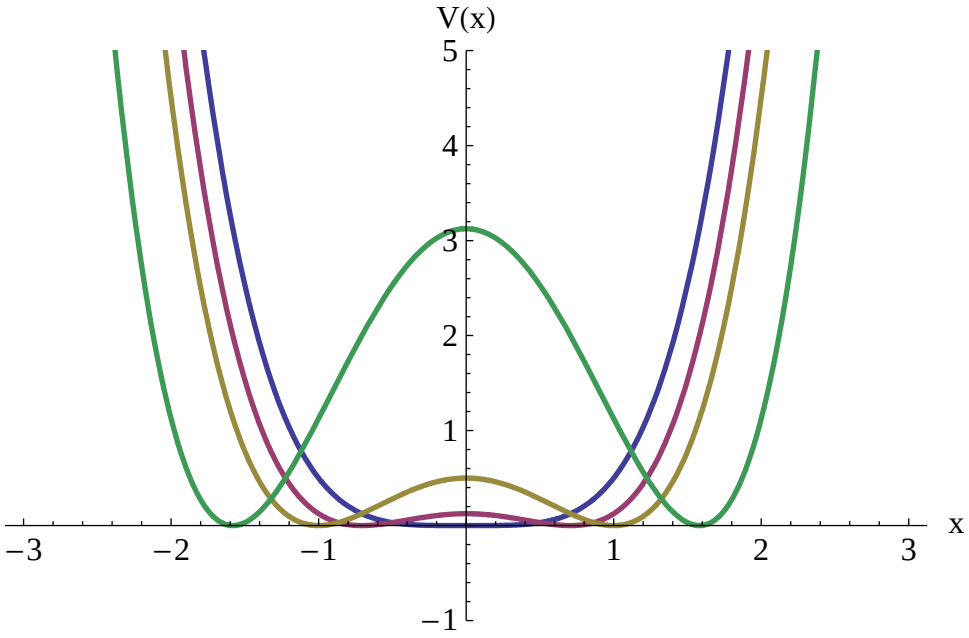

Figure 3.6: Plot of the shifted double-well potential $V_s(x) = \frac{1}{2}\left(x^2 - \frac{1}{2}k\right)^2$ for $k = 0$ (blue), $k = 1$ (red), $k = 2$ (yellow) and $k = 5$ (green).

For the case $k = 0$, the potential shown in figure (3.6) is clearly a single-well (that of a purely quartic oscillator) and we would perhaps naively assume that the states of this well may be fairly accurately described using an initial model state centered at $x = 0$, i.e. using the standard harmonic oscillator vacuum $|0\rangle$, as used to study the quartic anharmonic oscillator. Indeed, this assumption proves to be correct as we can see in the results of [124, 125, 134] with the so-called case-1 solutions of [125] providing excellent results for the $k = 0$ single-well potential.

In fact, as further shown in [125], using a Gaussian function centered at the origin as the model state does still work for values of k greater than 0. For small k (generally values up to $k \approx 2$) the states in the system essentially behave as if they were in a single-well and do not particularly "perceive" the presence of the double-well minima, since the ground-state energy is greater than the mid-well potential barrier [125]. However, above this value of k the height of the mid-well potential barrier becomes important, since as k increases, the height of the barrier increases and no longer can the low-lying states of the system be accurately described by a model state centered at the origin [141]. We can easily observe this by comparing the plot of $V(x)$ in figure (3.6) for cases $k = 2$ and $k = 5$ (the $k = 2$ case is not too strongly deformed away from the $k = 0$ case, however, the $k = 5$ case is radically different).

In the quantum field theory analog of this problem, changing the sign in front of the mass term k in the Hamiltonian of equation (3.54) from positive to negative for a real scalar field results in spontaneous symmetry breaking of the vacuum (the discrete Z_2 symmetry, $\phi \to -\phi$ of the system is broken), and hence the vacuum state changes

from being singular to doubly degenerate. For the case of a complex scalar field, this symmetry breaking leads to an infinitely degenerate family of vacuum solutions, the so-called "Mexican Hat" potential.

In principle, the quantum mechanical case has a doubly degenerate vacuum, since either the left or the right well could support a particle in a stable ground-state, provided the other well wasn't there [135, 136] (the double-well potential itself is essentially 2 standard harmonic single-wells squeezed together). However, this degeneracy is lifted due to the phenomenon of quantum mechanical tunneling, wherein a particle may in fact tunnel underneath the mid-well potential barrier to produce a nondegenerate ground-state, which is a superposition of either "vacuum" state [135]. To illustrate this, if we consider $\big|0\big\rangle_L$ to be the left hand side "vacuum" state and $\big|0\big\rangle_R$ the right hand side "vacuum" state, it turns out that the true ket ground-state wave function is given by the symmetric superposition of the two states [135, 137], i.e.

$$\big|\Phi_0\big\rangle = \frac{1}{\sqrt{2}}\Big(\big|0\big\rangle_L + \big|0\big\rangle_R\Big),$$

and the first excited-state wave function is given by the antisymmetric superposition of the two states

$$\big|\Phi_1\big\rangle = \frac{1}{\sqrt{2}}\Big(\big|0\big\rangle_L - \big|0\big\rangle_R\Big).$$

In this way, when the well of equation (3.55) is suitably deep (i.e. k is suitably large) the low-lying eigenstates of the double-well potential are observed as "parity pairs" which have an almost degenerate energy [133, 136, 138, 139]. Since the potential is symmetric under the change $x \to -x$ (as with our previous quartic anharmonic oscillator model), the states of the double-well model have definite parity. For suitably deep wells then, the (even) state $\big|\Phi_0\big\rangle$ has almost the same energy as the (odd) state $\big|\Phi_1\big\rangle$, i.e. E_0 has almost exactly the same value as E_1. Likewise, E_2 is paired with E_3, E_4 is paired with E_5 and so on. The classical problem of studying a double-well potential is thus usually to calculate the energy splittings [125, 132, 133, 138, 139], for example $\Delta E = E_1 - E_0$, that arise from tunneling.

As k becomes increasingly larger and the mid-well potential barrier becomes increasingly higher, tunneling effects become negligible (since the barrier is so high and so wide). At the point where the mid-well potential barrier becomes infinitely high, the level splitting becomes 0 since the problem has evolved into 2 standard harmonic oscillator wells between which communication is impossible - i.e. either well can support identical states and energies since tunneling between the 2 wells is impossible. Tunneling is thus much less important for very deep wells, e.g. $k \sim 50$ (where, for all intents and purposes, the double-well in effect acts as 2 single wells separated by an infinitely high barrier) but it is most notable in the region $3 \leq k \leq 4$ [125] where the

ground-state energy is just below the height of the mid-well potential barrier.

Due to this presence of tunneling, the general double-well model may be used as the starting point in describing certain molecules in chemistry [135], for example the ammonia molecule NH_3, and specifically the vibrational spectra of the Nitrogen atom as it tunnels either side of the plane formed by the 3 Hydrogen atoms [14, 140].

As has been remarked elsewhere [125], the single-reference CCM lacks any intrinsic system to model quantum mechanical tunneling. As such, the single-reference CCM cannot accurately reproduce the energy level splittings that, for example, a variational calculation may [125, 141]. It may be possible to calculate splittings using a double-reference formalism where either model state is localised at the center of either well (such an approach is outlined later). However, time constraints have meant we are unable to explore this problem further. With this in mind, we simply wish to evaluate the ground-state energy as a function of the mass term k and do not attempt to calculate any energy level splittings. We do, however, briefly discuss 2 alternative approaches that can be made using the NCCM, as way of improving on using the standard harmonic basis centered at $x = 0$.

3.2.1 Normal Coupled Cluster Method

We begin the study of the double-well problem in much the same manner as the previous model. We thus use the state $|0\rangle$ as our generalised vacuum and the cluster correlation operators as given formerly in equation (3.18). As we have already iterated, utilising $|0\rangle$ as the model state gives a poor starting approximation for wave functions in a double-well, especially when $k > 2$. Regardless of this, we proceed in using this state in order to show exactly how the CCM can cope when starting from a poor initial approximation.

Rewriting the Hamiltonian of equation (3.54) using the standard harmonic operators (as given in equation (3.4)) and normal ordering all resultant strings of operators gives

$$\hat{H} = \frac{(5-2k+k^2)}{8} + \frac{(4-k)}{2}\hat{a}^\dagger\hat{a} + \frac{(2-k)}{4}\left(\hat{a}^2 + \hat{a}^{\dagger 2}\right) + \frac{3}{4}\hat{a}^{\dagger 2}\hat{a}^2 + \frac{1}{2}\left(\hat{a}^{\dagger 3}\hat{a} + \hat{a}^\dagger\hat{a}^3\right) + \frac{1}{8}\left(\hat{a}^4 + \hat{a}^{\dagger 4}\right), \tag{3.58}$$

(where we also add the depth of the well $\frac{k^2}{8}$ to this expression, as stated earlier). As a check, substituting $k = -1$ into the Hamiltonian of equation (3.58) and neglecting the depth term gives us

$$\hat{H} = \frac{3}{8} + \frac{5}{2}\hat{a}^\dagger\hat{a} + \frac{3}{4}\left(\hat{a}^2 + \hat{a}^{\dagger 2}\right) + \frac{3}{4}\hat{a}^{\dagger 2}\hat{a}^2 + \frac{1}{2}\left(\hat{a}^{\dagger 3}\hat{a} + \hat{a}^\dagger\hat{a}^3\right) + \frac{1}{8}\left(\hat{a}^4 + \hat{a}^{\dagger 4}\right),$$

which does indeed match the Hamiltonian of equation (3.14) with $\lambda = \frac{1}{2}$. We observe

that this system retains exactly the same selection rules as the quartic anharmonic oscillator, namely that $n = 0, \pm 2, \pm 4$ are the only transitions allowed between energy levels.

3.2.1.1 SUB(n) Calculations

In evaluating the matrix element $E_0 = \langle 0 | e^{-\hat{S}} \hat{H} e^{\hat{S}} | 0 \rangle$ to SUB(2), it may be shown that the exact NCCM ground-state energy to all SUB(n) approximations is given by

$$E_0 = \frac{1}{8}\left(k^2 - 2k + 5\right) + \Big(1 - 4k\Big)s_2 + \frac{3}{2}s_2^2 + 3s_4. \tag{3.59}$$

This expression is exact for the same reason that the ground-state energy in equation (3.32) is exact, namely that there are no additional contributions to the matrix element $\langle 0 | e^{-\hat{S}} \hat{H} e^{\hat{S}} | 0 \rangle$ for approximations higher than SUB(2). We employ precisely the same piece of Mathematica code as used previously in order to evaluate the double-well NCCM equations for $\{s_n\}$, as given by

$$\langle 0 | \hat{a}^n e^{-\hat{S}} \hat{H} e^{\hat{S}} | 0 \rangle = 0, \text{ for } n = 2, 4, 6, 8, 10, \tag{3.60}$$

where we proceed only to order SUB(5) for the sake of brevity.

The results for $E_0\,(k)$ to SUB(1), SUB(3) and SUB(5) are plotted in the figures (3.7), (3.8) and (3.9) respectively, showing the typical multiple solution branches arising from the solutions of equation (3.60). Table (3.9) lists the values of $E_0\,(k)$ for a large range of k values up to SUB(5) approximation, including the height of the mid-well potential barrier $\frac{k^2}{8}$ in order to ascertain whether the ground-state energy lies above or below the barrier.

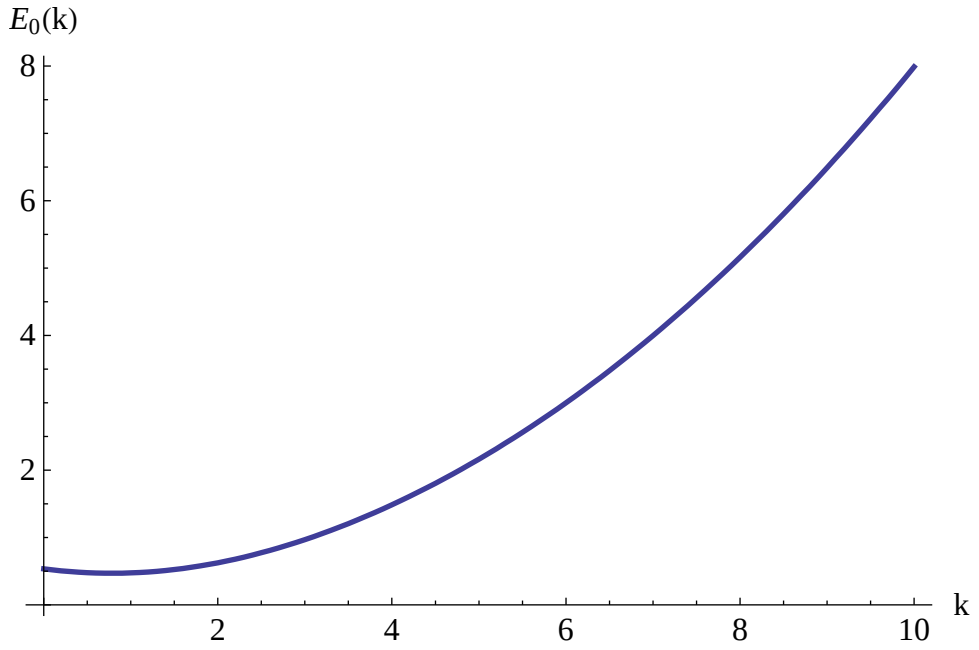

Figure 3.7: Plot of $E_0(k)$ vs k using the SUB(1) NCCM approximation.

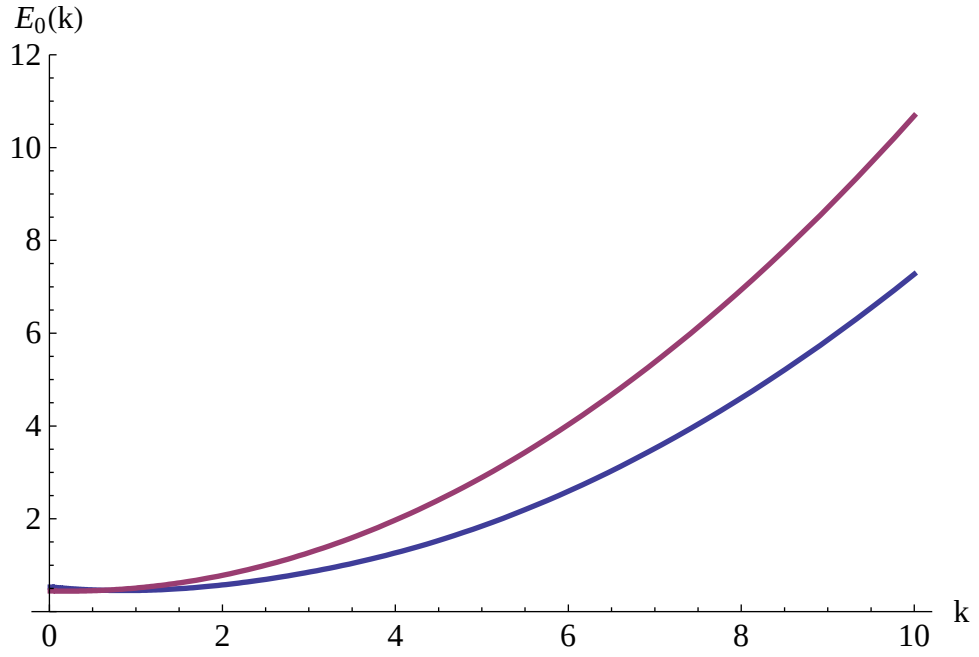

Figure 3.8: Plot of $E_0(k)$ vs k using the SUB(3) NCCM approximation.

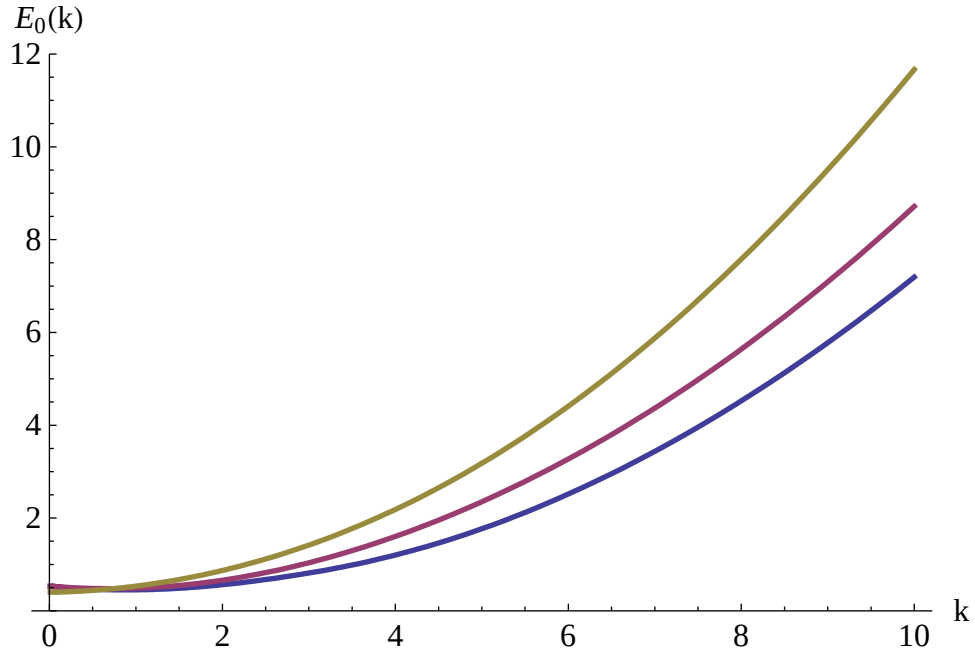

Figure 3.9: Plot of $E_0(k)$ vs k using the SUB(5) NCCM approximation.

k	$\frac{k^2}{8}$	n	$E_0(k)$	% Error
0	0	1	0.535 898	1.08
		2	0.533 291	0.59
		3	0.531 211	0.19
		4	0.530 405	0.04
		5	0.530 120	0.01
		Exact	**0.530 181**	
0.5	0.03125	1	0.478 273	2.58
		2	0.471 301	1.08
		3	0.467 838	0.37
		4	0.466 488	0.05
		5	0.465 986	0.06
		Exact	**0.466 259**	
1	0.125	1	0.475 066	4.70
		2	0.461 919	1.78
		3	0.456 225	0.53
		4	0.453 890	0.01
		5	0.452 934	0.20
		Exact	**0.453 827**	
2	0.5	1	0.625 000	9.86
		2	0.590 199	3.75
		3	0.574 591	1.00
		4	0.566 848	0.17
		5	0.563 112	1.02
		Exact	**0.568 893**	
5	3.125	1	2.163 673	52.38
		2	1.937 062	36.42
		3	1.842 827	29.78
		4	1.795 978	26.48
		5	1.768 914	24.58
		Exact	**1.419 929**	
10	12.5	1	7.897 174	
		2	7.413 721	
		3	7.269 979	
		4	7.217 231	
		5	7.192 346	
		Exact	**2.183 212**	
50	312.5	1	204. 627 060	
		2	196. 251 813	
		3	195. 106 834	
		4	195. 008 269	
		5	195. 081 459	
		Exact	**4.989 955**	

Table 3.9: SUB(1)-SUB(5) NCCM ground-state energy $E_0(k)$ for various values of k.

As expected, for small k (i.e. $k < 2$) the NCCM performs fairly admirably. We see a genuine convergence for the $k = 0$ energy (which should not be surprising since the

true ground-state wave function is actually centered at $x = 0$, thus our model state $|0\rangle$ acts as a good starting approximation in this case) although the SUB(5) expression for $E_0(k)$ implies an oscillatory convergence is likely to be observed if we were to go to higher SUB(n) approximation. A similar pattern is seen in the results for $k = 0.5$, $k = 1$ and $k = 2$, where an initial convergence between SUB(1) and SUB(4) (or SUB(1) and SUB(3) for the $k = 2$ case) is followed by some form of oscillation. Nevertheless, even with a small mid-well potential barrier and poor starting approximation, the NCCM provides decent results at these low level approximations (this is in part, likely to be due to the ground-state energy lying above the mid-well potential barrier, thus any complications arising from tunneling are avoided).

It is somewhat intriguing to see that the $k = 2$ case has an exact solution at SUB(1) approximation, so we will slightly labor our discussion on this specific case. Considering the exact NCCM ground-state energy given in equation (3.59), if we substitute $k = 2$ into this expression and neglect any terms higher than s_2 we have

$$E_0 = \frac{5}{8} - 7s_2 + \frac{3}{2}s_2^2, \tag{3.61}$$

and we find our equation for s_2 is given by

$$7s_2 + 12s_2^2 + 12s_2^3 = s_2\big(7 + 12s_2 + 12s_2^2\big) = 0. \tag{3.62}$$

The only noncomplex solution for equation (3.62) is given by $s_2 = 0$. Substituting this into equation (3.61) gives us a ground-state energy of $E_0 = \frac{5}{8} = 0.625$ and thus we can now understand where the exact SUB(1) answer comes from for the $k = 2$ case.

Unfortunately, for the case $k = 5$ the method clearly begins to breakdown. Despite the fact that a convergence is seen in the results, the percentage errors are extremely large, even up to SUB(5). By the time we reach the $k = 10$ and $k = 50$ cases we are clearly many orders of magnitude away from the exact answer and it seems unlikely we will ever be able to reconcile the NCCM results and the exact answer in double-well systems with extremely high barriers.

Such a catastrophic failing of the method is also seen in the case-1 solutions of [125], so we should not be too disheartened with such poor results. The inadequate starting approximation, coupled with the ground-state energy lying below the mid-well potential barrier and the fact that the single-reference NCCM is incapable of describing quantum mechanical tunneling have conspired against us. Although this pattern of poor results is easily observed from values of k in the range $0 \leq k \leq 10$, we include the value at $k = 50$ in keeping with [125] as well as to provide some large order k value which can serve some comparative use when we study the model using the ECCM.

3.2.1.2 Alternative Approaches

As a means to improve the accuracy of the NCCM results for $E_0(k)$, there are several possible approaches that could be taken. Invariably these methods will stem from either utilising a different form for the starting model state $\left|\Phi_0\right\rangle$ or taking into account the translational positions of the double-well minima. We describe two such alternative approaches here in brief detail.

Variationally Determined Vacuum $\left|0_\alpha\right\rangle$

The first approach we shall discuss is to introduce a (real) variable α into the description of the standard harmonic operators. This variable α will be used in an attempt to variationally tailor the model state into providing a better starting approximation for the NCCM to build upon. We thus introduce the scaled harmonic oscillator operators

$$\hat{a}_\alpha^\dagger = \frac{1}{\sqrt{2}}\left(\sqrt{\alpha}\hat{x} - \frac{i}{\sqrt{\alpha}}\hat{p}\right),$$

$$\hat{a}_\alpha = \frac{1}{\sqrt{2}}\left(\sqrt{\alpha}\hat{x} + \frac{i}{\sqrt{\alpha}}\hat{p}\right), \tag{3.63}$$

noting that these operators still obey the commutation relations as given previously in equation (3.5). The new vacuum state $\left|0_\alpha\right\rangle$ of these operators is defined by the relation

$$\hat{a}_\alpha\left|0_\alpha\right\rangle = 0, \tag{3.64}$$

and may be written in terms of the initial bare vacuum state $\left|0\right\rangle$ as a generalised coherent state [126, 132], i.e.

$$\left|0_\alpha\right\rangle \sim \exp\left(\frac{\alpha}{2}\hat{a}^{\dagger 2}\right)\left|0\right\rangle. \tag{3.65}$$

If the expression $\left\langle x|0\right\rangle$ in coordinate representation is a Gaussian function centered at the origin, then the expression $\left\langle x|0_\alpha\right\rangle$ represents a distorted or "squeezed" Gaussian function also centered at the origin, with respect to $\left\langle x|0\right\rangle$ [125, 126]. Hence, the operators of the form given in equation (3.63) are commonly referred to as "squeezed" operators. We may rearrange the squeezed operators of equation (3.63) for $\hat{x}$ and $\hat{p}$ to give

$$\hat{x} = \frac{1}{\sqrt{2\alpha}}\left(\hat{a}_\alpha + \hat{a}_\alpha^\dagger\right),$$

$$\hat{p} = -i\sqrt{\frac{\alpha}{2}}\left(\hat{a}_\alpha - \hat{a}_\alpha^\dagger\right), \tag{3.66}$$

which may be compared with the "nonsqueezed" normal position and momentum operators given in equation (3.6). Substituting these expressions for $\hat{x}$ and $\hat{p}$ into the

double-well Hamiltonian of equation (3.54) (again adding the depth of the double-well to shift the potential upwards by $\frac{k^2}{8}$) we have

$$\hat{H}_\alpha = E_0(\alpha) + \Big(\frac{\alpha}{2} - \frac{k}{2\alpha} + \frac{3}{2\alpha^2}\Big)\hat{a}_\alpha^\dagger \hat{a}_\alpha - \Big(\frac{\alpha}{4} + \frac{k}{4\alpha} + \frac{3}{4\alpha^2}\Big)\left(\hat{a}_\alpha^{\dagger 2} + \hat{a}_\alpha^2\right)$$

$$+\frac{3}{4\alpha^2}\Big(\hat{a}_\alpha^{\dagger 2}\hat{a}_\alpha^2\Big) + \frac{1}{2\alpha^2}\Big(\hat{a}_\alpha^\dagger \hat{a}_\alpha^3 + \hat{a}_\alpha^{\dagger 3}\hat{a}_\alpha\Big) + \frac{1}{8\alpha^2}\left(\hat{a}_\alpha^4 + \hat{a}_\alpha^{\dagger 4}\right), \tag{3.67}$$

where $E_0(\alpha)$ is the vacuum expectation value of $\hat{H}_\alpha$, i.e.

$$E_0(\alpha) = \langle 0_\alpha | \hat{H}_\alpha | 0_\alpha \rangle = \frac{k^2}{8} + \frac{\alpha}{4} - \frac{k}{4\alpha} + \frac{3}{8\alpha^2}, \tag{3.68}$$

In order to optimise the variable α for the squeezed vacuum $|0_\alpha\rangle$, we wish to minimise $E_0(\alpha)$ with respect to α, i.e. we wish to solve

$$\frac{\partial E_0(\alpha)}{\partial \alpha} = \frac{1}{4} + \frac{k}{4\alpha^2} - \frac{3}{4\alpha^3} = 0,$$

or, equivalently, the equation

$$\alpha^3 + k\alpha - 3 = 0,$$

for α as a function of k. Using Mathematica, we can determine that the only real root of this equation for all k is given by

$$\alpha(k) = \frac{-3^{\frac{1}{3}}(2k) + 2^{\frac{1}{3}}\left(27 + \sqrt{729 + 12k^3}\right)^{\frac{2}{3}}}{6^{\frac{1}{3}}\left(27 + \sqrt{729 + 12k^3}\right)^{\frac{2}{3}}}. \tag{3.69}$$

This expression for α is then substituted into the Hamiltonian of equation (3.67) and the usual NCCM equations are evaluated.

Table (3.10) lists the results of using the squeezed vacuum state $|0_\alpha\rangle$ in a set of NCCM calculations up to SUB(5) for small k (we only proceed as far as $k = 2$ since $|0_\alpha\rangle$ will still prove a poor starting approximation for cases where the ground-state energy lies below the mid-well potential barrier). The first thing we note in these results is that the squeezed SUB(1) approximation produces a worse estimate for $E_0(k)$ than the unsqueezed SUB(1) approximation for all values of k except $k = 2$, where the squeezed and unsqueezed approaches match identically (which appears to be a special by-product of the calculation for this specific value of k).

k	$\frac{k^2}{8}$	n	$E_0(k)$	% Error
0	0	1	0.540 844	2.01
		2	0.531 516	0.25
		3	0.530 125	0.01
		4	0.530 029	0.03
		5	0.530 101	0.02
		Exact	**0.530 181**	
0.5	0.03125	1	0.481 758	3.32
		2	0.468 824	0.55
		3	0.466 229	0.01
		4	0.465 873	0.08
		5	0.465 974	0.06
		Exact	**0.466 259**	
1	0.125	1	0.477 014	5.11
		2	0.458 916	1.12
		3	0.454 029	0.04
		4	0.452 868	0.21
		5	0.452 803	0.23
		Exact	**0.453 827**	
2	0.5	1	0.625 000	9.86
		2	0.590 199	3.75
		3	0.574 591	1.00
		4	0.566 848	0.17
		5	0.563 112	1.02
		Exact	**0.568 893**	

Table 3.10: SUB(1)-SUB(5) NCCM ground-state energy $E_0(k)$ for various values of k using squeezed vacuum state $|0_\alpha\rangle$.

However, with regards to results of approximations higher than SUB(1) we tend to observe a much faster convergence to the correct answer, indeed some results in the squeezed approach oscillate around the exact result quicker than those in the unsqueezed approach. Such a pattern as this should be expected when considering the discussion in [126]. An approach such as this, i.e. a variational optimisation of the vacuum prior to any calculations, may be seen throughout the work of [80, 123, 127, 132] and is commonly referred to as the Hartree or Gaussian variational approximation. It is generally applied in order to increase the speed of convergence, as has been demonstrated here.

Translationally Shifted Vacuum $|0\rangle_{x=\pm\beta}$

Having shown how we are able to obtain better results than those already given for shallow double-wells, the second approach, which we simply outline here, is aimed at producing better results for cases where the mid-well potential barrier will be substantial, and thus the ground-state energy will lie beneath the barrier. A model state

centered at the origin gives an extremely poor approximation to the true ground-state wave function in this case. Therefore in this approach, we would consider using two individual harmonic bases, each translationally (and symmetrically) shifted either side of the origin by a length β, where β is the position of either double-well minima (in this case, $\pm\sqrt{\frac{k}{2}}$).

Whilst utilising a double-reference approach such as this would seemingly produce NCCM wave functions that look very much like the true wave functions of the double-well problem, we are, however, still faced with the quandary of including tunneling within the NCCM formalism. It is not known whether using these translationally shifted vacuums would lead to the presence of level splitting or not. Added to this are the intricate matters concerning satisfying size-extensivity within a multi-reference NCCM formalism [125]. It appears nothing less than an extension to the NCCM formalism itself would be able to rectify the problems concerning the inability to model quantum mechanical tunneling [125]. A similar set of concerns is raised in the ECCM study of the LMG model [77].

3.2.2 Extended Coupled Cluster Method

We have discussed some of the shortcomings of the NCCM in relation to the double-well quartic anharmonic oscillator and some possible ways in which we may achieve better results. To conclude this chapter, we raise the more interesting idea of using the ECCM to study our double-well model. Since the potential given in equations (3.55) or (3.6) can in some ways be viewed as having a phase transition about the point $k = 0$, i.e. the point at which the potential changes from being a single-well to a double-well, the ECCM should hopefully prove more successful for this model at large k than the NCCM, since it is well known the ECCM can adequately deal with phase transitions [77]. We are also concerned with how the ECCM can deal with such a poor starting approximation, relative to deep double-wells.

3.2.2.1 SUB(1) and SUB(2) Calculations

As established earlier, the starting point of an ECCM calculation is evaluating the ground-state energy functional

$$E\left(\left\{s_n, \tilde{s}_n\right\}\right) = \left\langle \Phi_0 \middle| e^{\hat{\tilde{S}}} e^{-\hat{S}} \hat{H} e^{\hat{S}} \middle| \Phi_0 \right\rangle,$$

which is then minimised with respect to either cluster amplitude and the resultant equations are solved simultaneously for the set $\left\{s_n, \tilde{s}_n\right\}$. These values then provide the input for $E\left(\left\{s_n, \tilde{s}_n\right\}\right)$ in order to provide numerical values. Using precisely the same cluster correlation operators as previously defined (equation (3.46)) and the double-

well Hamiltonian given by equation (3.58) we find the SUB(1) ground-state energy functional is given by

$$E_0 = \frac{1}{8}\left(k^2 - 2k + 5\right) + \frac{1}{2}\left(2-k\right)s_2 + \frac{1}{2}\left(2-k\right)\tilde{s}_2 + \frac{3}{2}\left(s_2^2 + \tilde{s}_2^2\right)$$
$$+\left(11-2k\right)s_2\tilde{s}_2 + \left(16-2k\right)s_2^2\tilde{s}_2 + 12\left(s_2^3\tilde{s}_2 + s_2\tilde{s}_2^2\right)$$
$$+36s_2^2\tilde{s}_2^2 + 48s_2^3\tilde{s}_2^2 + 24s_2^4\tilde{s}_2^2. \tag{3.70}$$

Table (3.11) includes the numerical results for the SUB(1) ECCM ground-state energy using the usual values of k.

k	n	$E_0\,(k)$	% Error
0	1	0.540 844	2.01
	2	0.532 115	0.36
	Exact	**0.530 181**	
0.5	1	0.481 758	3.32
	2	0.469 872	0.77
	Exact	**0.466 259**	
1	1	0.477 014	5.11
	2	0.460 674	1.51
	Exact	**0.453 827**	
2	1	0.625 000	9.86
	2	0.593 786	4.38
	Exact	**0.568 893**	
5	1	2.228 577	56.95
	2	2.058 582	44.98
	Exact	**1.419 929**	
10	1	8.408 002	
	2	7.521 265	
	Exact	**2.183 212**	
50	1	208.348 333	
	2	194.393 581	
	Exact	**4.989 955**	

Table 3.11: SUB(1) and SUB(2) ECCM ground-state energy $E_0\,(k)$ for various values of k.

As before, we observe the NCCM out performs the ECCM at SUB(1) level, except for the case $k = 2$, where again we see the same exact solution as the NCCM case (for exactly the same reasons). Table (3.11) also includes the results of the SUB(2) calculation however, and here we see the ECCM is closer to the exact values than the SUB(2) NCCM results. There are also six different solution branches for the SUB(2) ECCM case, similar to the six different solutions for the quartic anharmonic oscillator model using the ECCM to SUB(2). It is perhaps disappointing to see the ECCM also breaks down at the same point as the NCCM, namely around the $k = 5$ mark, where

again we see results which are many orders of magnitude away from the correct values. We must assume that the reasons for such a breakdown are exactly the same as for the NCCM case.

Ideally we would like to push these calculations to much higher order to gain some further insight into how the ECCM deals with the double-well oscillator, especially since SUB(2) is regarded as very low order for a problem like this. In order to do this however, we would need to introduce a solution following routine into our Mathematica code and calculate only the correct solution branch from the ECCM equations - the plethora of solutions the ECCM produces, coupled with the great complexity of the ECCM ground-state energy functional past SUB(2) means our current code is simply not able to evaluate the SUB(3) solutions at all. Unfortunately, due to time constraints it has not been possible to implement this approach for the double-well model and thus we only present results up to SUB(2).

3.3 Discussion

This chapter has served as an introductory discussion on the application of NCCM and ECCM techniques to two well known model systems, where exact values are known and a comparison may be drawn between them and the CCM results. For the quartic anharmonic oscillator we see that the NCCM performs relatively well for low values of the coupling constant λ, to relatively low accuracy - we see the exact ground-state energy $E_0(\lambda)$ reproduced exactly for $\lambda = 0.1$ at SUB(4) to 6 decimal places for example. For large values of the λ however, the simple NCCM approach fails to produce any noticeable convergence to exact values. The ECCM proved somewhat better over the whole range of λ, even when only proceeding as far as SUB(2).

For the double-well quartic anharmonic oscillator we again see the NCCM performs relatively well, even when the starting model state is a poor approximation to the true ground-state wave function. The shortcomings of a single-reference NCCM or ECCM approach to double-well oscillators are all too noticeable however. We see very poor accuracy for relatively deep double-well potentials, even though we show a possible candidate for improved accuracy of shallow double-well calculations - the use of squeezed operators. Nevertheless, throughout this chapter we have shown explicitly how CCM techniques are applied in practice, albeit using some very simple models. This work will prove useful to us as we address the more complicated physics of many-body pairing over the course of the next two chapters.

Chapter 4

Single-Shell Pairing

The aim of the previous chapter was to demonstrate the practical application of CCM techniques to some simple models which are already well understood [125, 132]. In this chapter we present a case study which is much more physically interesting to us - we wish to apply the ECCM, namely a quasi-particle form of the ECCM, to a model of pure pairing [26]. We begin by introducing the model and explain its relevance. We detail the underlying SU(2) algebra that is inherent to the model and derive the exact ground-state energy E_0 of the system. We then calculate an expression for E_0 utilising the standard *particle* ECCM to SUB(1), drawing a comparison to the exact answer. Increasing the order of our approximation, we continue calculations with the particle ECCM up to SUB(4). We augment our approach by introducing a quasi-particle description of the system as detailed in chapter 2 and proceed to calculate E_0 using the *quasi-particle* ECCM to QPSUB(2). Again, we compare our results to the exact answer for the model before proceeding up to QPSUB(5) approximation. We also include results of using the NCCM with quasi-particle operators up to QPSUB(5). Some of the initial quasi-particle results for the model are somewhat confusing - we therefore perform an RPA calculation of the particle and quasi-particle ECCM solutions in order to see how stable the excitation energies of the model are. We end the chapter with a discussion of the results and surmise which method is the optimum CCM approach to studying pairing problems.

4.1 The Model

We wish to implement the pairing formalism presented at the end of chapter 2, particularly the use of quasi-particle operators and Brueckner orbitals, in the study of a many-fermion system. Ideally we must utilise a model which remains fairly simple to understand, in order to avoid any unnecessary complications in using the different ECCM approaches. We thus choose to study a simple, pure pairing force [26, 28], acting between a finite number of fermions in a finite space. This model has its origins

in describing the pairing between nucleons within a given j-shell of a nucleus, which arises from the short-ranged attractive part of the nucleon-nucleon potential [26]. We describe this model as "single-shell pairing", which is really just an artifact of the original nuclear problem - although our model is a completely generic pairing problem in a finite space, we make use of some of the language associated with the nuclear case. Thus the "shell" in our terminology is simply the total space to which the particles are confined.

The model consists of N_0 identical fermions, held at zero temperature with pairs comprising one fermion in a "normal" state (momentum k and spin $\uparrow$) and the other in a time-reversed state (momentum $-k$ and spin $\downarrow$) - hence we have generic s-wave Cooper pairs with a total angular momentum and total spin of zero ($L = 0$, $S = 0$). The Hamiltonian for our model is thus defined as

$$\hat{H} = -G\Big(\hat{\Delta}^\dagger\hat{\Delta} - \frac{1}{2}\hat{N}\Big), \tag{4.1}$$

where the pairing creation and annihilation operators are given by

$$\hat{\Delta}^\dagger = \sum_{k=1}^{\Omega}\hat{a}_k^\dagger\hat{a}_{\bar{k}}^\dagger, \tag{4.2}$$

$$\hat{\Delta} = \sum_{k=1}^{\Omega}\hat{a}_{\bar{k}}\hat{a}_k, \tag{4.3}$$

and the number operator $\hat{N}$ is given by

$$\hat{N} = \sum_{k=1}^{\Omega}\hat{a}_k^\dagger\hat{a}_k + \sum_{k=1}^{\Omega}\hat{a}_{\bar{k}}^\dagger\hat{a}_{\bar{k}}. \tag{4.4}$$

In this manner, we have a total of 2Ω states with spin $\uparrow$ or $\downarrow$ and we use the shorthand notation introduced in chapter 2

$$k = k\uparrow;\ \bar{k} = -k\downarrow,$$

i.e. k represents the normal state and $\bar{k}$ represents the time-reversed state [99]. The factor G is a scale constant for the model.

The single-particle operators $\hat{a}_k^\dagger$ and $\hat{a}_k$ which make up equations (4.2), (4.3) and (4.4) obey the standard fermionic anticommutation relations

$$\Big\{\hat{a}_k, \hat{a}_{k'}^\dagger\Big\} = \delta_{k,k'},$$

$$\Big\{\hat{a}_k, \hat{a}_{k'}\Big\} = 0 = \Big\{\hat{a}_k^\dagger, \hat{a}_{k'}^\dagger\Big\}.$$

Substituting the expressions for the pairing creation operator $\hat{\Delta}^{\dagger}$ (4.2), the pairing annihilation operator $\hat{\Delta}$ (4.3) and the number operator $\hat{N}$ (4.4) into the Hamiltonian of equation (4.1) means our single-shell pairing Hamiltonian is explicitly given by

$$\hat{H} = \frac{G}{2}\Big(\sum_{k=1}^{\Omega} \hat{a}_k^{\dagger}\hat{a}_k + \sum_{k=1}^{\Omega} \hat{a}_{\bar{k}}^{\dagger}\hat{a}_{\bar{k}}\Big) - G\sum_{k=1}^{\Omega}\sum_{q=1}^{\Omega} \hat{a}_k^{\dagger}\hat{a}_{\bar{k}}^{\dagger}\hat{a}_{\bar{q}}\hat{a}_q. \tag{4.5}$$

A pairing Hamiltonian similar to this was studied extensively by Richardson (see [142] and [143] for example) who was able to show that the model had an exactly solvable form. It also has many similarities with the later, so-called LMG model [61, 62, 63] which may also be shown to have an exactly solvable form, albeit using a different approach to that of Richardson. The fundamental reason why the class of pairing Hamiltonians similar to the LMG model can be solved exactly stems from the underlying SU(2) group algebra inherent in the models [144]. This is an important feature which we shall now discuss in some detail.

4.1.1 SU(2) Quasi-Spin Algebra

For many-fermion systems with pairing, where the particles which make up the pairs can only exist in two different states (e.g. k or $\bar{k}$), the idea of using a "fictitious" angular momentum [26] or quasi-spin representation [61, 144] is often very useful. The object which describes a particle being in either the state k or the state $\bar{k}$ may be considered a Pauli spinor [61] and likewise, the operators which govern a transition between either of these states may be considered the set of Pauli spin matrices [61]. Hence, these operators must obey the standard SU(2) group algebra of angular momentum [145]. We may therefore consider our single-shell pairing model in terms of a specific SU(2) "quasi-spin" algebra, which permeates the Hamiltonian of equation (4.1) (the LMG model was formulated with this very idea in mind [61], as was our own - an exactly solvable model is of great use to us, since it means we have exact values with which to compare our various ECCM results to, in a similar manner to the anharmonic oscillator models of chapter 3).

In order to make this algebra transparent, we evaluate some specific commutators of $\hat{\Delta}^{\dagger}$, $\hat{\Delta}$, and $\hat{N}$. Consider the following commutator between the pairing creation and annihilation operators

$$\Big[\hat{\Delta}, \hat{\Delta}^{\dagger}\Big] = \sum_{k=1}^{\Omega}\sum_{k'=1}^{\Omega}\Big[\hat{a}_{\bar{k}'}\hat{a}_{k'}, \hat{a}_k^{\dagger}\hat{a}_{\bar{k}}^{\dagger}\Big]$$

$$= \sum_{k=1}^{\Omega}\sum_{k'=1}^{\Omega}\Big(-\hat{a}_k^{\dagger}\Big\{\hat{a}_{\bar{k}'}, \hat{a}_{\bar{k}}^{\dagger}\Big\}\hat{a}_{k'} + \hat{a}_{\bar{k}'}\Big\{\hat{a}_{k'}, \hat{a}_k^{\dagger}\Big\}\hat{a}_{\bar{k}}^{\dagger}\Big)$$

$$= \sum_{k=1}^{\Omega}\sum_{k'=1}^{\Omega}\Big(-\delta_{\bar{k},\bar{k}'}\hat{a}_k^\dagger\hat{a}_{k'} + \delta_{k,k'}\Big(1 - \hat{a}_{\bar{k}}^\dagger\hat{a}_{\bar{k}'}\Big)\Big)$$

$$= \Omega - \Big(\sum_{k=1}^{\Omega}\hat{a}_k^\dagger\hat{a}_k + \sum_{k=1}^{\Omega}\hat{a}_{\bar{k}}^\dagger\hat{a}_{\bar{k}}\Big)$$

$$= \big(\Omega - \hat{N}\big)$$

$$= 2\hat{J}_0.$$

We write the result of this commutator as a quasi-spin operator $\hat{J}_0$, analogous to the standard $\hat{J}_z$ angular momentum operator [145]. If we take the commutator of this quasi-spin operator with the pairing creation operator $\hat{\Delta}^\dagger$ we have

$$\Big[\hat{J}_0, \hat{\Delta}^\dagger\Big] = \Big[\frac{1}{2}\Big(\Omega - \Big(\sum_{k=1}^{\Omega}\hat{a}_k^\dagger\hat{a}_k + \sum_{k=1}^{\Omega}\hat{a}_{\bar{k}}^\dagger\hat{a}_{\bar{k}}\Big)\Big), \sum_{k'=1}^{\Omega}\hat{a}_{k'}^\dagger\hat{a}_{\bar{k}'}^\dagger\Big]$$

$$= -\frac{1}{2}\Big[\sum_{k=1}^{\Omega}\hat{a}_k^\dagger\hat{a}_k, \sum_{k'=1}^{\Omega}\hat{a}_{k'}^\dagger\hat{a}_{\bar{k}'}^\dagger\Big] - \frac{1}{2}\Big[\sum_{k=1}^{\Omega}\hat{a}_{\bar{k}}^\dagger\hat{a}_{\bar{k}}, \sum_{k'=1}^{\Omega}\hat{a}_{k'}^\dagger\hat{a}_{\bar{k}'}^\dagger\Big]$$

$$= -\frac{1}{2}\sum_{k=1}^{\Omega}\sum_{k'=1}^{\Omega}\delta_{k,k'}\hat{a}_k^\dagger\hat{a}_{\bar{k}'}^\dagger - \frac{1}{2}\sum_{k=1}^{\Omega}\sum_{k'=1}^{\Omega}\delta_{\bar{k},\bar{k}'}\hat{a}_{k'}^\dagger\hat{a}_{\bar{k}}^\dagger$$

$$= -\sum_{k=1}^{\Omega}\sum_{k'=1}^{\Omega}\delta_{k,k'}\hat{a}_k^\dagger\hat{a}_{\bar{k}'}^\dagger$$

$$= -\hat{\Delta}^\dagger,$$

and in precisely the same manner we may show that

$$\Big[\hat{J}_0, \hat{\Delta}\Big] = \hat{\Delta}.$$

Combining all these results together we thus have an SU(2) quasi-spin algebra defined by

$$\Big[\hat{\Delta}, \hat{\Delta}^\dagger\Big] = \big(\Omega - \hat{N}\big) = 2\hat{J}_0,$$

$$\Big[\hat{J}_0, \hat{\Delta}^\dagger\Big] = -\hat{\Delta}^\dagger,$$

$$\Big[\hat{J}_0, \hat{\Delta}\Big] = \hat{\Delta}. \tag{4.6}$$

To further exemplify this analogy, we write the following mappings from our quasi-spin operators to those of "true" angular momentum

$$\hat{\Delta}^\dagger \mapsto \hat{J}_x + i\hat{J}_y = \hat{J}_+,$$

$$\hat{\Delta} \mapsto \hat{J}_x - i\hat{J}_y = \hat{J}_-,$$
$$\hat{J}_0 \mapsto \hat{J}_z, \tag{4.7}$$

where $\hat{J}_i$ $(i = x, y, z)$ are the standard angular momentum operators in 3-dimensions and $\hat{J}_\pm$ the angular momentum raising and lowering operators respectively [145].

This intrinsic SU(2) quasi-spin algebra will prove extremely useful to us when we begin our ECCM calculations since it will make analysis of the linked-cluster expansion $e^{-\hat{S}}\hat{H}e^{\hat{S}}$ very straightforward. Note that, although the single-particle operators $\hat{a}_k^\dagger$ and $\hat{a}_k$ obey fermionic anticommutation relations, the pairing operators $\hat{\Delta}^\dagger = \hat{a}_k^\dagger \hat{a}_{\bar{k}}^\dagger$ and $\hat{\Delta} = \hat{a}_{\bar{k}}\hat{a}_k$ obey boson-like commutation relations. This is because they are describing the bound-states of two-fermion pairs, i.e. they are describing composite boson-like objects. Thus in the calculations to come, as opposed to using anticommutation relations and dealing with the single-particle operators $\hat{a}_k^\dagger$ and $\hat{a}_k$, we instead use the pairing operators $\hat{\Delta}^\dagger$ and $\hat{\Delta}$ and choose to work with the commutation relations of equation (4.6) - we will essentially neglect the fact that the pairing operators are constructed from single-particle operators themselves (we are suppressing information in order for our ECCM calculations to be easier to deal with at face value).

4.1.2 Exact Ground-State Solution

Using the SU(2) quasi-spin algebra of equation (4.6) it is relatively simple to derive the exact ground-state energy E_0 for the Hamiltonian defined in equation (4.1). In order to see this, we rewrite equation (4.1) in terms of angular momentum operators

$$\hat{H} = -G\Big(\hat{J}_+\hat{J}_- + \hat{J}_z - \frac{\Omega}{2}\Big)$$
$$= -G\Big(\hat{J}^2 - \hat{J}_z^2 - \frac{\Omega}{2}\Big), \tag{4.8}$$

where we have made use of the angular momentum commutation relation

$$\hat{J}_z = i\Big[\hat{J}_x, \hat{J}_y\Big],$$

written in natural units of $\hbar = 1$. We may write the energy eigenvalues of equation (4.8) as

$$E\left(J, J_z\right) = -G\Big(J\big(J+1\big) - J_z^2 - \frac{\Omega}{2}\Big), \tag{4.9}$$

where $J\big(J+1\big)$ is the eigenvalue of the total angular momentum operator squared $(\hat{J}^2)$ and J_z is the eigenvalue of the z-component angular momentum operator $(\hat{J}_z)$ [26].

Since $\hat{J}_z = \frac{1}{2}\big(\Omega - \hat{N}\big)$, the eigenvalues of $\hat{J}_z$ are given by

$$J_z = \frac{1}{2}\big(\Omega - N_0\big),$$

where N_0 is the total number of particles in the shell. Following [144], due to angular momentum considerations we have that

$$J^{max} \geq \big|J_z^{max}\big|,$$

but since $J_z^{max} = \frac{\Omega}{2}$ when $N_0 = 0$, then $J^{max} = \frac{\Omega}{2}$ in the vacuum [26], i.e. we may write the single-shell pairing vacuum state as $\big|\frac{\Omega}{2}, \frac{\Omega}{2}\big\rangle$. Thus the ground-states for different (even) N_0 all have $J = \frac{\Omega}{2}$ [144]. Substituting the eigenvalues of J and J_z into equation (4.9) we can thus conclude that the *exact* ground-state energy for the Hamiltonian of equation (4.1) is given by

$$E_0\left(N_0\right) = -G\frac{N_0}{2}\left(\Omega - \frac{N_0}{2}\right). \tag{4.10}$$

4.2 Extended Coupled Cluster Method

Having found the exact ground-state energy for our single-shell pairing model, we now proceed to apply the ECCM in an effort to see how closely we can match the exact result.

4.2.1 Particle SUB(1) Calculation

We begin with an explicit calculation of the particle SUB(1) (or BCS) approximation as a starting point, in order to see how the lowest possible order calculation holds. For even N, the exact ket ground-state wave function is proportional to the state $\hat{\Delta}^{\dagger\frac{N}{2}}\big|0\big\rangle$, thus we will use the bare particle vacuum $\big|0\big\rangle$ as our model state. For simplicity, we make the assumption our cluster amplitudes don't depend on k and write our simplified SUB(1) pairing cluster correlation operators as

$$\hat{S} = s\hat{\Delta}^{\dagger}, \tag{4.11}$$

$$\hat{\tilde{S}} = \tilde{s}\hat{\Delta}, \tag{4.12}$$

where, in keeping with the notation defined in chapter 2, we don't specifically label these operators and amplitudes as SUB(1) terms.

Our goal is to evaluate the ground-state energy functional

$$E\big(\{s, \tilde{s}\}\big) = \big\langle 0\big|e^{\hat{\tilde{S}}}e^{-\hat{S}}\big(\hat{H} - \lambda\big(\hat{N} - N_0\big)\big)e^{\hat{S}}\big|0\big\rangle, \tag{4.13}$$

where the Lagrange multiplier λ is actually the chemical potential [26] and N_0 is the average number of particles in the ground-state. Since particle number is ill-defined in BCS theory (i.e. the ground-state wave function is *not* an eigenstate of the particle number operator $\hat{N}$ [26]) we must now constrain the energy in order to conserve particle number, i.e. to ensure the expectation value of the number operator has the correct value of N_0 [26].

The first task we must complete is evaluation of the linked-cluster expansion

$$\hat{h}_{LC} = e^{-\hat{S}}\big(\hat{H} - \lambda\big(\hat{N} - N_0\big)\big)e^{\hat{S}},$$

which is straightforward to evaluate in this case because we can make extensive use of the SU(2) quasi-spin algebra from equation (4.6). Since the object $\hat{H} - \lambda\big(\hat{N} - N_0\big)$ only contains terms of "one-body" pairing operators, the linked-cluster expansion terminates as

$$\hat{h}_{LC} = \hat{H} - \lambda\left(\hat{N} - N_0\right) + \left[\hat{H}, \hat{S}\right] - \lambda\left[\hat{N}, \hat{S}\right] + \frac{1}{2!}\left[\left[\hat{H}, \hat{S}\right], \hat{S}\right] - \lambda\frac{1}{2!}\left[\left[\hat{N}, \hat{S}\right], \hat{S}\right].$$

Evaluating all these commutators we find

$$\hat{h}_{LC} = -G\Big(\hat{\Delta}^\dagger\hat{\Delta} - \frac{1}{2}\hat{N}\Big) - \lambda\big(\hat{N} - N_0\big) + Gs\hat{\Delta}^\dagger\big(1 - \big(\Omega - \hat{N}\big)\big) - 2\lambda s\hat{\Delta}^\dagger + Gs^2\hat{\Delta}^{\dagger 2}. \quad (4.14)$$

We now want to evaluate the contributing contractions in the matrix element $\big\langle 0\big|e^{\hat{\tilde{S}}}\hat{h}_{LC}\big|0\big\rangle$ using the expression for $\hat{h}_{LC}$ given in equation (4.14). Since $\hat{h}_{LC}$ only contains terms up to second order in the pairing creation operator, the adjoint cluster operator is given by

$$e^{\hat{\tilde{S}}} = 1 + \tilde{s}\hat{\Delta} + \frac{\tilde{s}^2}{2}\hat{\Delta}^2. \quad (4.15)$$

In evaluating equation (4.13), we find our ground-state energy functional is given by

$$E_0 = \lambda N_0 - 2\lambda s\tilde{s}\Omega - G\tilde{s}s\Omega^2 + Gs\tilde{s}\Omega + G\tilde{s}^2s^2\Omega\left(\Omega - 1\right), \quad (4.16)$$

and so we have the ECCM equations given by

$$\frac{\partial E_0}{\partial \tilde{s}} = -2\lambda s\Omega - G\Omega\left(\Omega - 1\right)\left(s - 2s^2\tilde{s}\right) = 0,$$

$$\frac{\partial E_0}{\partial s} = -2\lambda\tilde{s}\Omega - G\Omega\left(\Omega - 1\right)\left(\tilde{s} - 2\tilde{s}^2s\right) = 0. \quad (4.17)$$

We must also minimise E_0 with respect to λ

$$\frac{\partial E_0}{\partial \lambda} = N_0 - 2s\tilde{s}\Omega = 0, \quad (4.18)$$

in order to constrain the chemical potential and thus ensure the average particle number is given by N_0.

The problem we now observe is that there exists no unique solution to these equations for both s and $\tilde{s}$ *independently* to SUB(1) approximation. In fact, the ground-state energy functional of equation (4.16) is actually a *function* of the variable $s' = s\tilde{s}$, i.e.

$$E_0 = \lambda N_0 - 2\lambda s'\Omega - G\Omega\left(\Omega - 1\right)s'\left(1 - s'\right). \tag{4.19}$$

The reason for this is that we are trying to describe a variational problem as a bi-variational problem (i.e. we are actually introducing redundant information into the problem).

Usually when faced with this problem, we would set the expectation values of the pairing operators equal to one another, thus

$$\langle\hat{\Delta}\rangle = \langle\hat{\Delta}^{\dagger}\rangle, \tag{4.20}$$

where we recall that in the ECCM scheme, the expectation value of a generic Hermitian operator $\hat{O}$ is written as

$$\langle\hat{O}\rangle = \langle\Phi_0|e^{\hat{\tilde{S}}}e^{-\hat{S}}\hat{O}e^{\hat{S}}|\Phi_0\rangle.$$

The condition in equation (4.20) thus gives

$$s = \sqrt{\frac{N_0}{2\Omega - N_0}},$$

$$\tilde{s} = \sqrt{\frac{N_0\left(2\Omega - N_0\right)}{\left(2\Omega\right)^2}}. \tag{4.21}$$

However, this step is not necessary for this case since we only need an expression for $s\tilde{s}$, which we already have due to the minimisation of E_0 with respect to λ, i.e. equation (4.18). Therefore

$$s\tilde{s} = \frac{N_0}{2\Omega}, \tag{4.22}$$

and our SUB(1) ground-state energy is thus given by

$$E_0\big(N_0\big) = -G\frac{N_0}{2}\left(1 - \frac{1}{\Omega}\right)\left(\Omega - \frac{N_0}{2}\right), \tag{4.23}$$

which is the same as the exact ground-state energy of equation (4.10) up to a factor of $\frac{1}{\Omega}$.

Figure (4.1) shows a comparison between the exact result for the ground-state energy and the BCS/SUB(1) ECCM result, plotted for $\Omega = 10$ and $G = 1$. It is immediately obvious that the only time the BCS/SUB(1) solution matches the exact

answer is either in a completely empty or a completely filled shell. Furthermore, the greater the state degeneracy Ω, the nearer the BCS/SUB(1) result lies to the exact answer. Although N_0 is plotted as if it were a continuous variable in this picture (as it will be throughout of all our results) we must remind ourselves it is fundamentally a discrete variable (the average number of particles) - thus only values of the ground-state energy E_0 for (even) *integer* values of N_0 constitute a physical result.

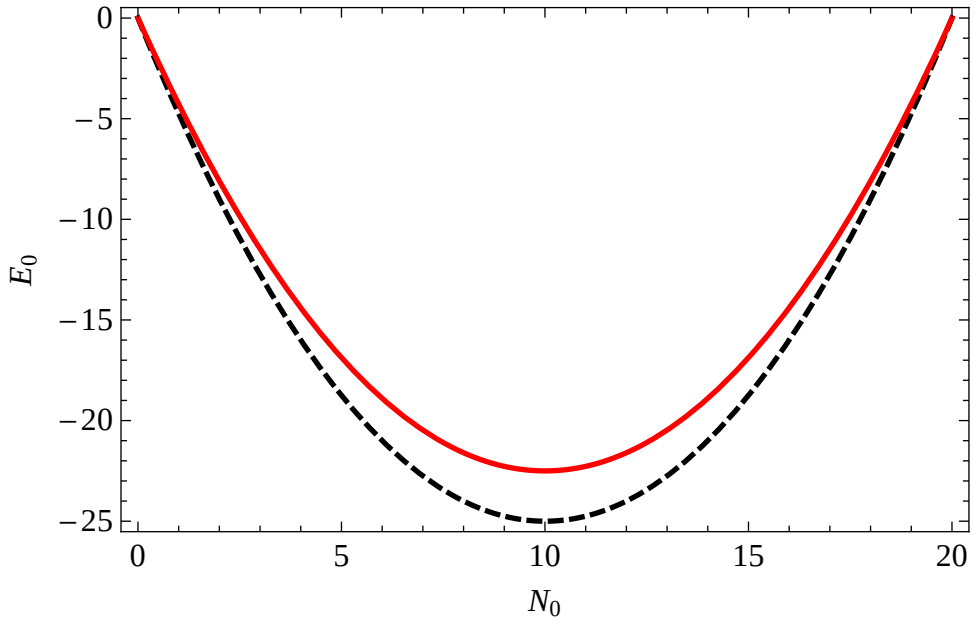

Figure 4.1: Plot of E_0 vs N_0 for the exact (dashed) and BCS/SUB(1) ECCM (red) solutions using $\Omega = 10$ and $G = 1$.

4.2.2 Particle SUB(n) Calculation

Using Mathematica we can go to higher order SUB(n) calculations relatively easily, again due to the inherent SU(2) quasi-spin algebra of the model as defined in equation (4.6). For higher order calculations our ket and bra ground-state wave functions are therefore given by

$$\left|\Phi_0\right\rangle = e^{\hat{S}}\left|0\right\rangle;\ \left\langle\Phi_0\right| = \left\langle 0\right|e^{\hat{\tilde{S}}}e^{-\hat{S}}, \tag{4.24}$$

where we continue to use the simplified cluster correlation operators defined as

$$\hat{S} = \sum_{n=1}^{m} s_n \hat{\Delta}^{\dagger n};\ \hat{\tilde{S}} = \sum_{n=1}^{m} \tilde{s}_n \hat{\Delta}^{n}. \tag{4.25}$$

We write a piece of Mathematica code to evaluate the ECCM ground-state energy functional of equation (4.13), using the cluster operators given in equation (4.25) and proceeding as far as $m = 4$. As with our study of anharmonic oscillators in chapter 3, we again seek all possible *real* solutions for the cluster amplitudes $\left\{s_n, \tilde{s}_n\right\}$ in order to

produce real solutions for the ground-state energy E_0. Before we discuss our results, we make note of a particularly useful relation regarding the particle number fluctuation.

Particle Number Fluctuation

In general, for unitary G it may be shown that

$$\langle \hat{H} \rangle = \frac{1}{4}\langle \hat{N}^2 \rangle - \frac{\Omega}{2}\langle \hat{N} \rangle. \tag{4.26}$$

However, since the exact ground-state energy may be written as

$$E_0\left(N_0\right) = \frac{1}{4}N_0^2 - \frac{\Omega}{2}N_0$$

$$= \frac{1}{4}\langle \hat{N} \rangle^2 - \frac{\Omega}{2}\langle \hat{N} \rangle,$$

it thus follows that a state where $\langle \hat{H} \rangle$ is the exact ground-state energy must also be a state where $\langle \hat{N}^2 \rangle = \langle \hat{N} \rangle^2$. Hence the fluctuation of particle number [42]

$$\Delta\hat{N} = \sqrt{\langle \hat{N}^2 \rangle - \langle \hat{N} \rangle^2}, \tag{4.27}$$

i.e. the object $\Delta\hat{N}^2$, must therefore be zero for the ground-state. We can therefore use this relation to determine how closely our ECCM approach varies in comparison to the exact answer and to see if our solutions become unphysical at any point.

SUB(4) Solutions

Figure (4.2) displays the results of the particle ECCM calculations from order SUB(1) to SUB(4), with $\Omega = 4$ and $G = 1$ - black circles denote a point where the ECCM solutions match the exact solution, excluding the cases of completely empty or completely filled shell. Also shown is the fluctuation of particle number at each order of approximation. The first picture is nothing more than our earlier BCS/SUB(1) result as shown in figure (4.1), albeit for a different value of Ω.

At the SUB(2) level we see additional solution branches emerge. The recurring BCS/SUB(1) branch gives a much worse estimate at this order, although it does still remain physical, i.e. $\Delta\hat{N}^2 > 0$. One branch is clearly unphysical since it starts with nonzero energy in the empty shell and has a particle number fluctuation $\Delta\hat{N}^2$ which goes negative. However, it *does* match the exact result at mid-shell ($N_0 = 4$). Some branches only exist for a short while near the empty shell. The remaining branch gives a promising result up to mid-shell before dropping off and giving a nonzero energy in the case of a completely filled shell. The particle number fluctuation never becomes negative for this solution however - we deem this branch as the physical

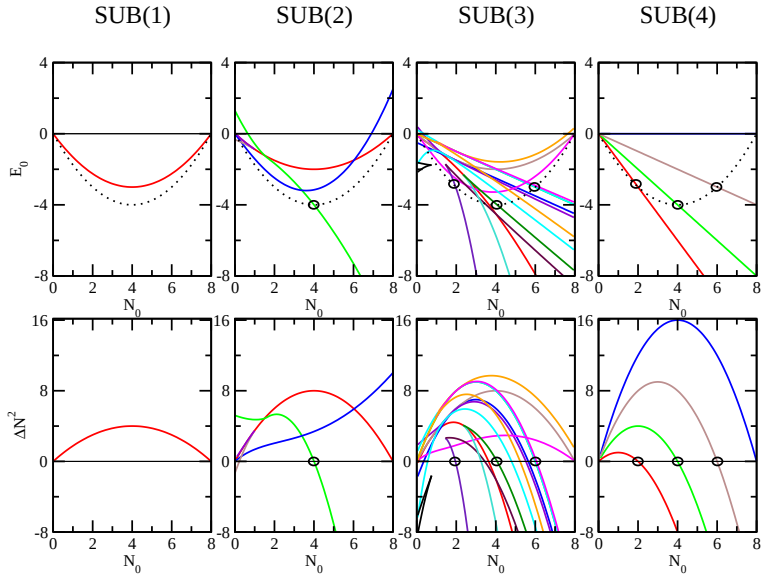

Figure 4.2: Plot of E_0 vs N_0 (upper panels) and particle number fluctuation ΔN^2 vs N_0 (lower panels) for the exact (dotted) and particle SUB(1)-SUB(4) ECCM solutions using $\Omega = 4$ and $G = 1$.

SUB(2) solution.

In the SUB(3) picture we now see a multitude of solutions - although we do observe that many of these different solution branches match the exact answer at some point (notably we see this occur for $N_0 = 0, 2, 4, 6, 8$). In the SUB(4) scheme, where the NCCM and ECCM actually become the same for this model, we only have four solution branches and each branch matches the exact ground-state energy twice, first at the trivial point of $N_0 = 0$ and then at the points $N_0 = 2, 4, 6, 8$ respectively. Each of these branches is infinitely degenerate and all bar one (the solution which trivially stays zero throughout particle number variation) become unphysical after hitting the exact answer.

It is somewhat disturbing to see that the most important feature we would like to assume from our CCM solutions - namely that any match with the exact answer would lie on *one* solution branch which is smoothly and continuously connected to the model state - is not seen for this model. This is possibly evidence to support not using a particle picture but instead applying a quasi-particle formulation of the ECCM. Before we can conclude this is the case however, we must investigate the particle ECCM further - for a large number of particles it is possible low order calculations may prove adequate for a system.

As we demonstrate in figure (4.3), the physical particle SUB(2) result seems to become increasingly stable and reliable as we increase Ω, especially in comparison to the BCS/SUB(1) result below the half-filled shell. This suggests an alternate scheme we might employ - working with a bare particle vacuum $|0\rangle$ and particle operators relative to $|0\rangle$ *below* the middle of the shell and working with a filled Hartree-Fock

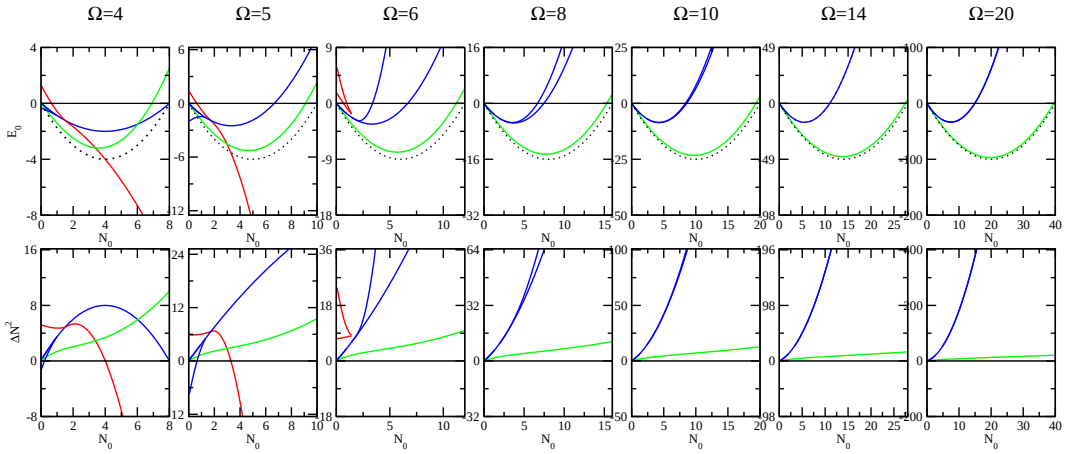

Figure 4.3: Plot of E_0 vs N_0 (upper panels) and particle number fluctuation ΔN^2 vs N_0 (lower panels) for the exact (dotted) and particle SUB(2) ECCM solutions using various values of Ω and $G = 1$.

state $\left|\mathrm{HF}\right\rangle$ and hole operators relative to the filled state *above* the middle of the shell. We thus split our ECCM calculations in two - working upward from $\left|0\right\rangle$ and working downward from $\left|\mathrm{HF}\right\rangle$ with either branch expected to meet in the middle of the shell.

Using solution following techniques we may focus on the physical ECCM solution branch, i.e. the branch smoothly connected to the model state, and look at higher order corrections to this result. Figure (4.4) displays our findings, where we have plotted the difference between the ECCM ground-state energy and the exact result for $\Omega = 10$ and $G = 1$. Unfortunately, the rate of convergence seen in these results is disappointing - we do see a marked improvement over the mean-field result, however, this improvement becomes increasingly smaller the higher we truncate our operators. Proceeding to higher order SUB(n) in this case will only get us *slightly* closer to the exact result each time - ultimately it is not worth the effort.

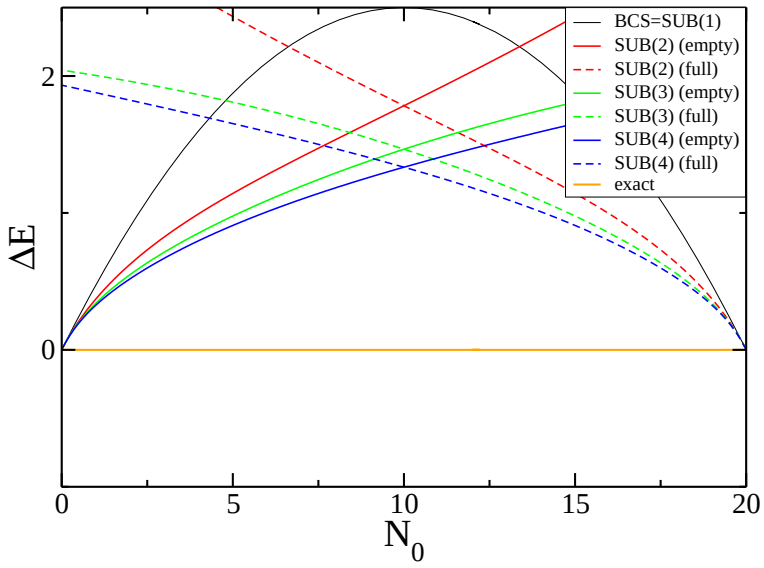

Figure 4.4: Plot of $\Delta E = E_0 - E_0^{exact}$ vs N_0 for particle SUB(1)-SUB(4) ECCM solutions using $\Omega = 10$ and $G = 1$. We compare different orders of approximation using either empty ($\big|0\big\rangle$) or full ($\big|\mathrm{HF}\big\rangle$) model states.

4.2.3 Quasi-Particle QPSUB(2) Calculation

The particle ECCM approach for our single-shell pairing model appears to have a few deficiencies and hints towards a relatively slow convergence past SUB(2). We now proceed to apply the quasi-particle formalism developed in the latter part of chapter 2 to our model, in order to see if there is any overwhelming improvement in our ECCM results. In order to explicitly show how this works, we will again demonstrate the quasi-particle calculation at the lowest possible order of approximation, i.e. the QPSUB(2) level (where we now prefix our approximation scheme description with the initials QP, to represent the fact the calculation is performed with respect to quasi-particle states). Thus our goal now is to evaluate the functional

$$E\big(\{s,\tilde{s},s_2,\tilde{s}_2\}\big) = \big\langle\tilde{\varphi}_0\big|e^{\hat{\tilde{S}}_2}e^{-\hat{S}_2}\big(\hat{H}_{qp} - \lambda\big(\hat{N}_{qp} - N_0\big)\big)e^{\hat{S}_2}\big|\varphi_0\big\rangle \tag{4.28}$$

where the Hamiltonian $\hat{H}_{qp}$, the number operator $\hat{N}_{qp}$ and the pairing cluster correlation operators $\hat{S}_2$ and $\hat{\tilde{S}}_2$ are written in terms of quasi-particle operators, as previously defined in equation (2.136). The usual quasi-particle ket and bra vacuum state wave functions are given by, respectively

$$\big|\varphi_0\big\rangle = e^{\hat{S}_1}\big|0\big\rangle,$$

$$\big\langle\tilde{\varphi}_0\big| = \big\langle\Phi_0\big|e^{\hat{\tilde{S}}_1}e^{-\hat{S}_1}, \tag{4.29}$$

where the SUB(1) terms are now specifically labeled as such and remain written in (simplified) terms of particle operators

$$\hat{S}_1 = s\hat{\Delta}^\dagger;\ \hat{\tilde{S}}_1 = \tilde{s}\hat{\Delta},$$

since the initial quasi-particle basis of equation (2.136) was defined relative to these states.

Since the quasi-particle basis is more general than that of the particle basis, and it naturally includes more information about pairing correlations within the model than when using a pure particle picture, our hope is that the quasi-particle ECCM will prove to be more accurate than the standard particle ECCM, especially to higher order QPSUB(n). Since the model is relatively simple to begin with, using the quasi-particle formalism in this case is not too complicated. In order to evaluate equation (4.28) however, we will need to derive quasi-particle expressions for all of our particle operators given in equations (4.2), (4.3) and (4.4).

We start by looking at each operator in turn, beginning with the pairing creation operator $\hat{\Delta}^\dagger$. In terms of quasi-particle operators we have

$$\begin{aligned}
\hat{\Delta}^\dagger &= \hat{a}_k^\dagger \hat{a}_{\bar{k}}^\dagger \\
&= \big(\tilde{s}\hat{c}_{\bar{k}} + \hat{d}_k^\dagger\big)\big(-\tilde{s}\hat{c}_k + \hat{d}_{\bar{k}}^\dagger\big) \\
&= -\tilde{s}^2\hat{c}_{\bar{k}}\hat{c}_k + \tilde{s}\hat{c}_{\bar{k}}\hat{d}_{\bar{k}}^\dagger - \tilde{s}\hat{d}_k^\dagger\hat{c}_k + \hat{d}_k^\dagger\hat{d}_{\bar{k}}^\dagger \\
&= -\tilde{s}^2\hat{c}_{\bar{k}}\hat{c}_k + \hat{d}_k^\dagger\hat{d}_{\bar{k}}^\dagger + \tilde{s}\big(-\hat{d}_k^\dagger\hat{c}_k + \hat{c}_{\bar{k}}\hat{d}_{\bar{k}}^\dagger\big) \\
&= -\tilde{s}^2\hat{\delta} + \hat{\delta}^\dagger + \tilde{s}\big(-\hat{d}_k^\dagger\hat{c}_k - \hat{d}_{\bar{k}}^\dagger\hat{c}_{\bar{k}} + \Omega\big) \\
&= -\tilde{s}^2\hat{\delta} + \hat{\delta}^\dagger + \tilde{s}\big(\Omega - \hat{n}\big),
\end{aligned}$$

where the quasi-particle pairing creation and annihilation operators, $\hat{\delta}^\dagger$ and $\hat{\delta}$ respectively, are given by

$$\hat{\delta}^\dagger = \hat{d}_k^\dagger\hat{d}_{\bar{k}}^\dagger;\ \hat{\delta} = \hat{c}_{\bar{k}}\hat{c}_k, \tag{4.30}$$

the quasi-particle number operator is given by

$$\hat{n} = \hat{d}_k^\dagger\hat{c}_k + \hat{d}_{\bar{k}}^\dagger\hat{c}_{\bar{k}}, \tag{4.31}$$

and Einstein summation convention has been used throughout for convenience. In precisely the same manner we may derive quasi-particle expressions for $\hat{\Delta}$ and $\hat{N}$, thus we have

$$\begin{aligned}
\hat{\Delta}_{qp}^\dagger &= \tilde{s}\big(\Omega - \hat{n}\big) - \tilde{s}^2\hat{\delta} + \hat{\delta}^\dagger, \\
\hat{\Delta}_{qp} &= s\big(1 - \tilde{s}s\big)\big(\Omega - \hat{n}\big) + \big(1 - \tilde{s}s\big)^2\hat{\delta} - s^2\hat{\delta}^\dagger,
\end{aligned}$$

$$\hat{N}_{qp} = \Omega - \big(1 - 2\tilde{s}s\big)\big(\Omega - \hat{n}\big) + 2\tilde{s}\big(1 - \tilde{s}s\big)\hat{\delta} + 2s\hat{\delta}^{\dagger}. \tag{4.32}$$

We are now in a position to rewrite equation (4.1) in terms of quasi-particle operators. Substituting the expressions of equation (4.32) into equation (4.1) therefore gives

$$\begin{aligned}\frac{\hat{H}_{qp}}{G} = \frac{\Omega}{2} - s\tilde{s}\big(1 - s\tilde{s}\big)\big(\Omega - \hat{n}\big)^2 \\ -\Big(\big(1 - s\tilde{s}\big)^2 + s^2\tilde{s}^2\Big)\left(\hat{\delta}^{\dagger}\hat{\delta} + \frac{\big(\Omega - \hat{n}\big)}{2}\right) \\ +s^2\hat{\delta}^{\dagger 2} + \tilde{s}^2\big(1 - s\tilde{s}\big)^2\hat{\delta}^2 \\ -s\big(1 - 2s\tilde{s}\big)\hat{\delta}^{\dagger}\big(\Omega - \hat{n} - 1\big) - \tilde{s}\big(1 - 2s\tilde{s}\big)\big(1 - s\tilde{s}\big)\big(\Omega - \hat{n} - 1\big)\hat{\delta}.\end{aligned} \tag{4.33}$$

In order to calculate the fluctuation of particle number $\Delta\hat{N}^2$, we will also require an expression for $\hat{N}^2$ written in terms of quasi-particle operators. We find this is given by

$$\begin{aligned}\hat{N}_{qp}^2 = \Omega^2 + 4\Omega s\hat{\delta}^{\dagger} + 4\Omega\tilde{s}\big(1 - s\tilde{s}\big)\hat{\delta} + 8s\tilde{s}\big(1 - s\tilde{s}\big)\hat{\delta}^{\dagger}\hat{\delta} \\ +\big(1 - 2s\tilde{s}\big)^2\big(\Omega - \hat{n}\big)^2 + 2\big(2s\tilde{s}\big(1 - s\tilde{s}\big) - \big(1 - 2s\tilde{s}\big)\Omega\big)\big(\Omega - \hat{n}\big) \\ +4s^2\hat{\delta}^{\dagger 2} + 4\tilde{s}^2\big(1 - s\tilde{s}\big)^2\hat{\delta}^2 \\ -4s\big(1 - 2s\tilde{s}\big)\hat{\delta}^{\dagger}\big(\Omega - \hat{n} - 1\big) - 4\tilde{s}\big(1 - s\tilde{s}\big)\big(1 - 2s\tilde{s}\big)\big(\Omega - \hat{n} - 1\big)\hat{\delta}.\end{aligned} \tag{4.34}$$

Pairing Cluster Correlation Operators

Having rewritten all of our previous operators using the quasi-particle formalism, we now wish to write down an expression for our pairing cluster correlation operators to QPSUB(2). We choose to write our second order cluster operators in the simplified form

$$\hat{S}_2 = \frac{1}{2}s_2\hat{\delta}^{\dagger 2};\ \hat{\tilde{S}}_2 = \frac{1}{2}\tilde{s}_2\hat{\delta}^2. \tag{4.35}$$

where Einstein summation convention is again assumed. Due to the construction of our quasi-particle basis, the operators in equation (4.35) are specifically given by

$$\hat{S}_2 = \frac{1}{2}\sum_{k+l=k'+l'} s_2\hat{d}_k^{\dagger}\hat{d}_{\bar{k}'}^{\dagger}\hat{d}_l^{\dagger}\hat{d}_{\bar{l}'}^{\dagger},$$

$$\hat{\tilde{S}}_2 = \frac{1}{2}\sum_{k+l=k'+l'} \tilde{s}_2\hat{c}_{\bar{k}'}\hat{c}_k\hat{c}_{\bar{l}'}\hat{c}_l,$$

i.e. we must remain aware that an object like $\hat{\delta}^{\dagger 2}$ does in fact have two different summation labels attached to it. We are almost at the stage where we can evaluate equation (4.28), however, this calculation can once again be aided by the model's

convenient SU(2) quasi-spin algebra, now written in terms of quasi-particles.

SU(2) Quasi-Spin Algebra

Although we can define a quasi-particle SU(2) algebra directly analogous to the particle scheme of equation (4.6), the most useful commutators we will require are given by

$$\Big[\hat{n},\hat{\delta}^{\dagger m}\Big] = m\hat{\delta}^{\dagger m},$$

$$\Big[\hat{\delta},\hat{\delta}^{\dagger m}\Big] = \hat{\delta}^{\dagger m-1}\big(\Omega-\hat{n}-m-1\big),$$

$$\Big[\hat{\delta}\hat{n},\hat{\delta}^{\dagger m}\Big] = m\hat{\delta}^{\dagger m-1}\big(\Omega-\hat{n}-m-1\big)\big(\hat{n}+2m\big)+2m\hat{\delta}^{\dagger m}\hat{\delta},$$

$$\Big[\hat{\delta}^2,\hat{\delta}^{\dagger m}\Big] = m\big(m-1\big)\hat{\delta}^{\dagger m-2}\big(\Omega-\hat{n}-m+2\big)\big(\Omega-\hat{n}-m+1\big)+2m\hat{\delta}^{\dagger m-1}\hat{\delta}\big(\Omega-\hat{n}-m+2\big). \tag{4.36}$$

These relations will naturally prove to be very useful in higher order QPSUB(n) calculations as well. The following relation is also particularly helpful for the QPSUB(2) calculation

$$\big\langle\tilde{\varphi}_0\big|e^{\hat{\tilde{S}}_2}\hat{\delta}^{\dagger l}\big|\varphi_0\big\rangle = \frac{\tilde{s}_2^{\frac{l}{2}}}{\big(\frac{l}{2}\big)!}\frac{l!\Omega!}{\big(\Omega-l!\big)};\ \text{for even } l.$$

Linked-Cluster Expansion

To QPSUB(2) truncation, we find the linked-cluster expansion terminates at second order in the number operator $\hat{N}_{qp}$ and fourth order in the Hamiltonian $\frac{\hat{H}_{qp}}{G}$ i.e.

$$e^{-\hat{S}_2}\bigg(\frac{\hat{H}_{qp}}{G}-\lambda\big(\hat{N}_{qp}-N_0\big)\bigg)e^{\hat{S}_2} = \frac{\hat{H}_{qp}}{G}-\lambda\big(\hat{N}_{qp}-N_0\big)$$

$$+\Big[\frac{\hat{H}_{qp}}{G},\hat{S}_2\Big]-\Big[\lambda\hat{N}_{qp},\hat{S}_2\Big]+\frac{1}{2!}\Big[\Big[\frac{\hat{H}_{qp}}{G},\hat{S}_2\Big],\hat{S}_2\Big]-\frac{1}{2!}\Big[\Big[\lambda\hat{N}_{qp},\hat{S}_2\Big],\hat{S}_2\Big]$$

$$+\frac{1}{3!}\Big[\Big[\Big[\frac{\hat{H}_{qp}}{G},\hat{S}_2\Big],\hat{S}_2\Big],\hat{S}_2\Big]+\frac{1}{4!}\Big[\Big[\Big[\Big[\frac{\hat{H}_{qp}}{G},\hat{S}_2\Big],\hat{S}_2\Big],\hat{S}_2\Big],\hat{S}_2\Big]. \tag{4.37}$$

Although long-winded, the evaluation of all these commutators is made considerably easier thanks to the relations given in equation (4.36).

Ground-State Energy and ECCM Equations

After evaluating all the commutators of equation (4.37) and then calculating all the contractions in the matrix element

$$E\big(\{s,\tilde{s},s_2,\tilde{s}_2\}\big) = \big\langle\tilde{\varphi}_0\big|e^{\hat{\tilde{S}}_2}e^{-\hat{S}_2}\bigg(\frac{\hat{H}_{qp}}{G}-\lambda\big(\hat{N}_{qp}-N_0\big)\bigg)e^{\hat{S}_2}\big|\varphi_0\big\rangle,$$

we finally arrive at an expression for the QPSUB(2) ground-state energy

$$
\begin{aligned}
E_0 = {} & s\Omega\big(\Omega-1\big)\big(\tilde{s}\big(s\tilde{s}-1\big)+s\tilde{s}_2\big)-2\lambda\Omega s\tilde{s}+\lambda N_0 \\
& +s_2\Omega\big(\Omega-1\big)\Big[\tilde{s}^2-2s\tilde{s}^3+s^2\tilde{s}^4-\Omega\tilde{s}_2+6\Omega s\tilde{s}\tilde{s}_2 \\
& -6\Omega s^2\tilde{s}^2\tilde{s}_2+2\tilde{s}_2-12s\tilde{s}\tilde{s}_2+12s^2\tilde{s}^2\tilde{s}_2-2\lambda\big(1-2s\tilde{s}\big)\tilde{s}_2\Big] \\
& +s_2^2\tilde{s}_2\Omega\big(\Omega-1\big)\Big[3\Omega^2\tilde{s}_2-15\Omega\tilde{s}_2+18\tilde{s}_2-18\Omega^2 s\tilde{s}\tilde{s}_2+90\Omega s\tilde{s}\tilde{s}_2 \\
& -108s\tilde{s}\tilde{s}_2+18\Omega^2 s^2\tilde{s}^2\tilde{s}_2-90\Omega s^2\tilde{s}^2\tilde{s}_2+108s^2\tilde{s}^2\tilde{s}_2 \\
& +9\tilde{s}^2-7\Omega\tilde{s}^2+\Omega^2\tilde{s}^2-18s\tilde{s}^3+14\Omega s\tilde{s}^3-2\Omega^2 s\tilde{s}^3+9s^2\tilde{s}^4-7\Omega s^2\tilde{s}^4+\Omega^2 s^2\tilde{s}^4\Big] \\
& -6\Omega\big(\Omega-1\big)\big(\Omega-2\big)\big(\Omega-3\big)\big(\Omega-4\big)\tilde{s}^2\big(1-s\tilde{s}\big)^2 s_2^3\tilde{s}_2^2 \\
& +15\Omega\big(\Omega-1\big)\big(\Omega-2\big)\big(\Omega-3\big)\big(\Omega-4\big)\big(\Omega-5\big)\tilde{s}^2\big(1-s\tilde{s}\big)^2 s_2^4\tilde{s}_2^3. \qquad (4.38)
\end{aligned}
$$

Even for such a comparatively simple but nonetheless physically "realistic" model we see how complicated the structure of the ECCM ground-state energy functional is, even to relatively low order approximation. A comparison with the particle SUB(1) result of equation (4.16) shows an enormous growth in the number of terms present for the QPSUB(2) case. In fact as a quick check, setting all s_2 and $\tilde{s}_2$ terms equal to zero in equation (4.38) means to SUB(1) we have

$$E_0 = \Omega\big(\Omega-1\big)s\tilde{s}\big(s\tilde{s}-1\big)-2\lambda\Omega s\tilde{s}+\lambda N_0,$$

which is precisely the result we obtained earlier in (4.16), thus we see again how the particle SUB(1) result is automatically retained in the QPSUB(2) result (or in general terms, how each lower order approximation is automatically included within higher order approximations of the CCM).

As it stands, this form of the ground-state energy functional is not much use to us. If we calculate the ECCM equations from this and try to solve the resulting simultaneous equations for all 4 cluster amplitudes, we are presented with a string of degenerate solutions. One of these amplitudes is a redundant variable and not required at all. Again, this is an artifact of attempting to solve a variational problem in a bivariational manner. Since the functional in equation (4.38) is scale invariant (for example, see the discussion of the BCS solution in [42]), in order to obtain some further insight we chose to rescale our variables as

$$s_2 = s^2 t_2;\ \tilde{s} = \frac{\tilde{t}}{s};\ \tilde{s}_2 = \frac{\tilde{t}_2}{s^2}, \qquad (4.39)$$

thereby eliminating s and hence rewriting the expression for the ground-state energy

functional in equation (4.38) in terms of t_2, $\tilde{t}$ and $\tilde{t}_2$. Evidently, using this substitution means we will lose the solutions of $s = 0$, therefore we must thus consider this specific case separately when we solve the ECCM equations.

Making the required substitutions we find

$$
\begin{aligned}
E_0\big(\{t_2,\tilde{t},\tilde{t}_2\}\big) &= \Omega\big(\Omega-1\big)\big(\tilde{t}^2-\tilde{t}+\tilde{t}_2\big)-2\lambda\Omega\tilde{t}+\lambda N_0\\
+t_2\Omega\big(\Omega-1\big)\big(\tilde{t}^2-2\tilde{t}^3+\tilde{t}^4-\Omega\tilde{t}_2+6\Omega\tilde{t}\tilde{t}_2-6\Omega\tilde{t}^2\tilde{t}_2+2\tilde{t}_2-12\tilde{t}\tilde{t}_2+12\tilde{t}^2\tilde{t}_2-2\lambda\big(1-2\tilde{t}\big)\tilde{t}_2\big)\\
+t_2^2\tilde{t}_2\Omega\big(\Omega-1\big)\Big(3\Omega^2\tilde{t}_2-15\Omega\tilde{t}_2+18\tilde{t}_2-18\Omega^2\tilde{t}\tilde{t}_2+90\Omega\tilde{t}\tilde{t}_2\\
-108\tilde{t}\tilde{t}_2+18\Omega^2\tilde{t}^2\tilde{t}_2-90\Omega\tilde{t}^2\tilde{t}_2+108\tilde{t}^2\tilde{t}_2\\
+9\tilde{t}^2-7\Omega\tilde{t}^2+\Omega^2\tilde{t}^2-18\tilde{t}^3+14\Omega\tilde{t}^3-2\Omega^2\tilde{t}^3+9\tilde{t}^4-7\Omega\tilde{t}^4+\Omega^2\tilde{t}^4\Big)\\
-6\Omega\big(\Omega-1\big)\big(\Omega-2\big)\big(\Omega-3\big)\big(\Omega-4\big)\big(\tilde{t}^2-2\tilde{t}^3+\tilde{t}^4\big)\tilde{t}_2^2t_2^3\\
+15\Omega\big(\Omega-1\big)\big(\Omega-2\big)\big(\Omega-3\big)\big(\Omega-4\big)\big(\Omega-5\big)\big(\tilde{t}^2-2\tilde{t}^3+\tilde{t}^4\big)\tilde{t}_2^3t_2^4. \qquad (4.40)
\end{aligned}
$$

We now minimise this functional with respect to our newly defined variables and the chemical potential (the Lagrange constraint condition), i.e. we solve the set of simultaneous equations

$$
\begin{aligned}
\frac{\partial}{\partial t_2}E_0\big(\{t_2,\tilde{t},\tilde{t}_2\}\big)&=0,\\
\frac{\partial}{\partial \tilde{t}}E_0\big(\{t_2,\tilde{t},\tilde{t}_2\}\big)&=0,\\
\frac{\partial}{\partial \tilde{t}_2}E_0\big(\{t_2,\tilde{t},\tilde{t}_2\}\big)&=0,\\
\frac{\partial}{\partial \lambda}E_0\big(\{t_2,\tilde{t},\tilde{t}_2\}\big)&=0,
\end{aligned}
$$

for t_2, $\tilde{t}$, $\tilde{t}_2$ and λ. This is most easily done within a piece of Mathematica code, where we set up a routine to calculate only real solutions for t_2, $\tilde{t}$, and $\tilde{t}_2$, in order to find the real, physical values of the ground-state energy.

QPSUB(2) Solutions

Figure (4.5) shows a plot of the QPSUB(2) ground-state energy E_0 against the average particle number N_0 for the case of $\Omega = 10$ and $G = 1$. The exact solution and the BCS/SUB(1) ECCM solution are also plotted for comparative purposes. We observe some strange behavior in the solutions. The QPSUB(2) solution branch which gives nonzero energy at $N_0 = 0$ is clearly unphysical and hence we may discard it. We have another solution branch which clearly lies below the exact answer throughout the entire shell (apart from when it is either empty or full) and thus we may discard that also. Most worryingly, the solution branch which we deem the true physical energy actually

collapses at mid-shell ($N_0 = 10$ in this case) to give an unphysical result in this region.

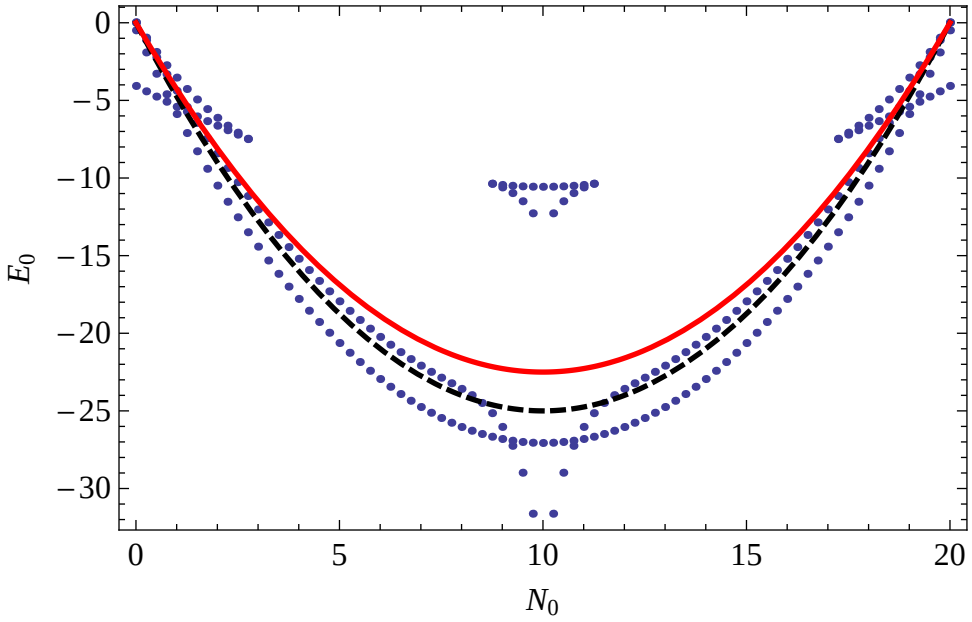

Figure 4.5: Plot of E_0 vs N_0 for the exact (dashed), BCS/SUB(1) ECCM (red) and quasi-particle QPSUB(2) ECCM (blue) solutions using $\Omega = 10$ and $G = 1$.

Analogous to the particle case, figure (4.6) shows all of the QPSUB(2) solutions for various values of Ω and $G = 1$. Whereas the particle SUB(2) results showed a vast improvement with increasing Ω, it is alarming to find that the quasi-particle QPSUB(2) result becomes worse the greater Ω becomes - the collapse at mid-shell of the physical solution branch becomes even more apparent.

Taking a step back, we consider using the NCCM with quasi-particle operators. Figure (4.7) shows the QPSUB(2) NCCM results, plotted for the same values of Ω as the ECCM case. Somewhat surprisingly we find the quasi-particle NCCM outperforms the quasi-particle ECCM - we observe no mid-shell collapse and see a slow convergence of the physical solution branch toward the exact result for increasing Ω. A more thorough investigation of the quasi-particle picture is required, preferably to higher order QPSUB(n).

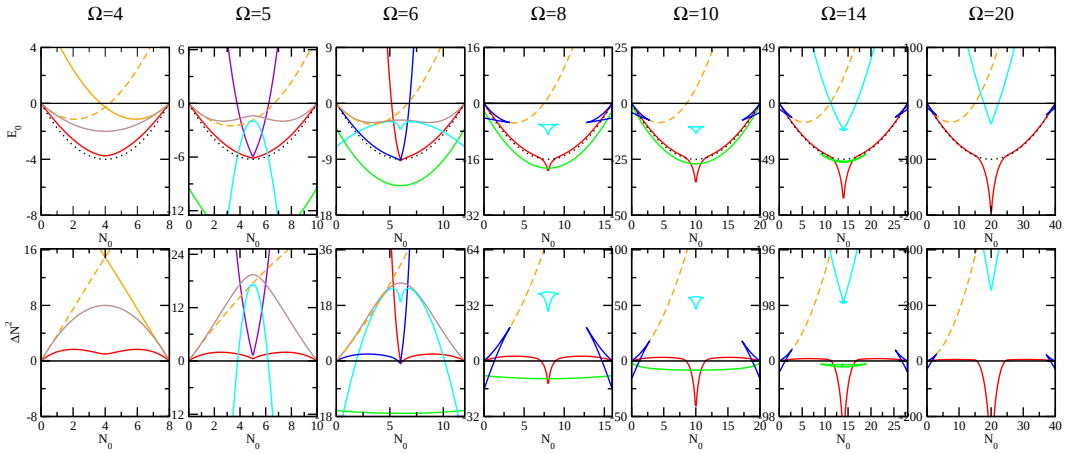

Figure 4.6: Plot of E_0 vs N_0 (upper panels) and particle number fluctuation ΔN^2 vs N_0 (lower panels) for the exact (dotted) and quasi-particle QPSUB(2) ECCM solutions using various values of Ω and $G = 1$.

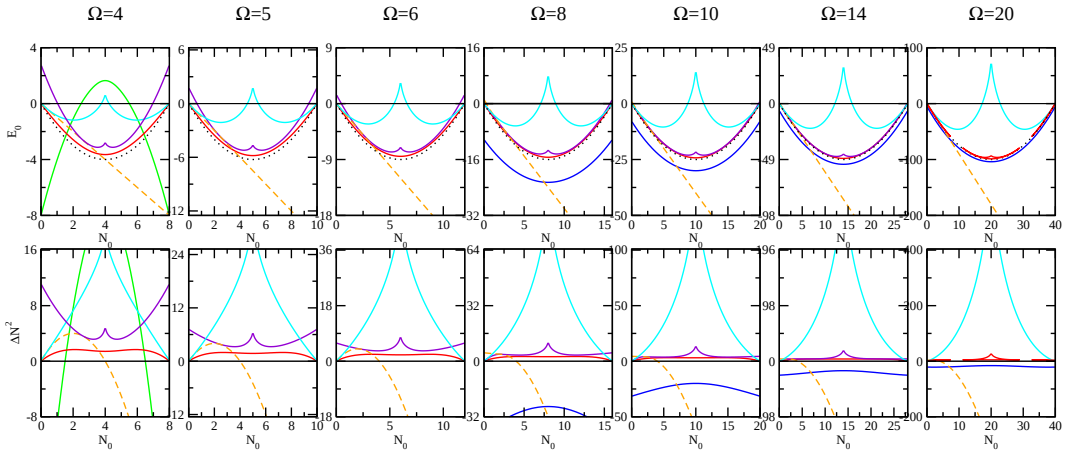

Figure 4.7: Plot of E_0 vs N_0 (upper panels) and particle number fluctuation ΔN^2 vs N_0 (lower panels) for the exact (dotted) and quasi-particle QPSUB(2) NCCM solutions using various values of Ω and $G = 1$.

4.2.4 Quasi-Particle QPSUB(n) Calculation

It is relatively straightforward to extend our quasi-particle ECCM investigation to higher order approximation as it was with the particle case. By adapting our original particle ECCM Mathematica code and making extensive use of the quasi-particle SU(2) quasi-spin relations given in equation (4.36), we may increase the truncation of the (simplified) cluster operators to QPSUB(n). Our model state remains as the quasi-particle vacuum $\left|\varphi_0\right\rangle$ but our higher order cluster correlation operators are given by

$$\hat{S} = \sum_{n=2}^{m} \frac{1}{n!} s_n \hat{\delta}^{\dagger n}; \; \hat{\tilde{S}} = \sum_{n=2}^{m} \frac{1}{n!} \tilde{s}_n \hat{\delta}^{n}, \tag{4.41}$$

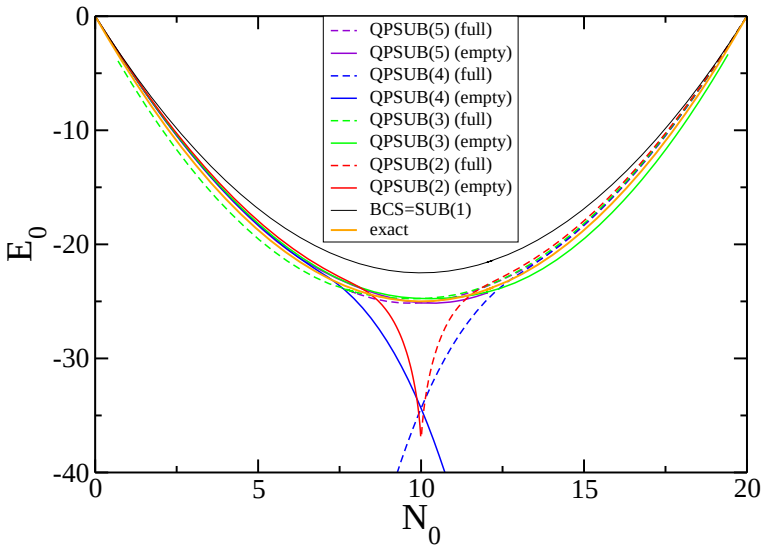

Figure 4.8: Plot of E_0 vs N_0 for quasi-particle QPSUB(2)-QPSUB(5) ECCM solutions using $\Omega = 10$ and $G = 1$. We compare different orders of approximation using either empty ($\big|0\big\rangle$) or full ($\big|\mathrm{HF}\big\rangle$) model states.

where we use normalised operators for convenience (similar to the quartic anharmonic oscillator ECCM calculation in chapter 3). We now perform calculations up to $m = 5$.

QPSUB(5) Solutions

Figure (4.8) displays the physical quasi-particle solutions for QPSUB(2) to QPSUB(5) approximation, plotted for $\Omega = 10$ and $G = 1$ (the quasi-particle equations were simply too complex to solve for all solution branches as plotted previously for the particle ECCM in figure (4.2), even for relatively small Ω). Again we plot results from using both empty (bare particle vacuum) and full (Hartree-Fock) model states.

For even orders of QPSUB(n) approximation we observe mid-shell collapse and unphysical energies - again this problem seems to become more pronounced as we go to higher order. At odd orders we see some convergence to the exact result. We can make an analogous picture to that of figure (4.4) and plot the energy difference between the exact result and the quasi-particle ECCM value, shown in figure (4.9). The energy difference of successive odd orders of truncation tends toward the exact result but does so in a somewhat erratic fashion.

Dropping down to the NCCM again, figure (4.10) shows a plot analogous to (4.8). The strange kinks in the QPSUB(4) result are correct - our solution following technique traces these out exactly. Overall we can conclude that the odd order quasi-particle ECCM solutions give the "best" results for this model - although we must also strongly emphasise that the particle SUB(2) ECCM and QPSUB(2) NCCM solutions for the case of large degeneracy Ω perform rather admirably.

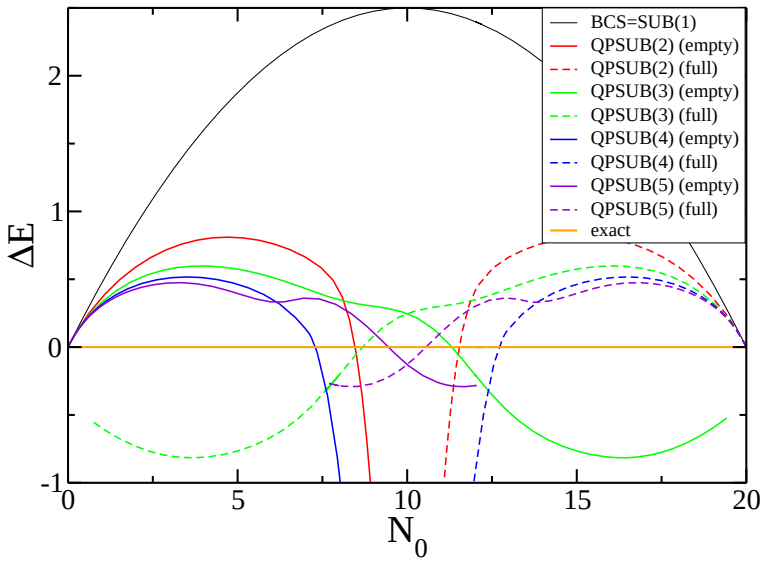

Figure 4.9: Plot of $\Delta E = E_0 - E_0^{exact}$ vs N_0 for quasi-particle QPSUB(2)-SUB(5) ECCM solutions using $\Omega = 10$ and $G = 1$. We compare different orders of approximation using either empty ($\big|0\big\rangle$) or full ($\big|\mathrm{HF}\big\rangle$) model states.

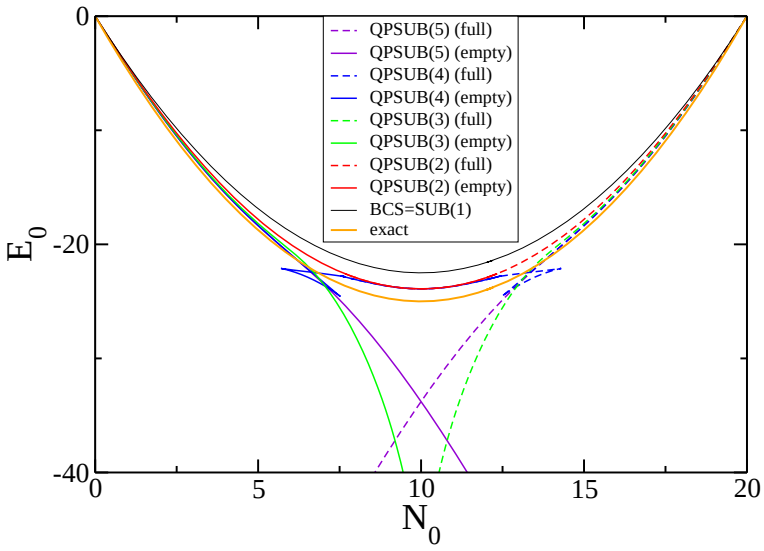

Figure 4.10: Plot of E_0 vs N_0 for quasi-particle QPSUB(2)-QPSUB(5) NCCM solutions using $\Omega = 10$ and $G = 1$. We compare different orders of approximation using either empty ($\big|0\big\rangle$) or full ($\big|\mathrm{HF}\big\rangle$) model states.

4.2.5 RPA Calculation (Solution Stability Analysis)

In order to see how stable the ECCM solutions are for our single-shell pairing model, we need to calculate the harmonic fluctuations of the system about the equilibrium point - i.e. we wish to perform an RPA calculation for the different solutions. We outline the quasi-particle case here since it is more complicated than that of the particle picture. As established in chapter 2, the most straightforward way of doing this is from a time-dependent bivariational principle, which we may derive from the (constrained) action functional

$$A = \int_{-\infty}^{+\infty} dt \big\langle \tilde{\varphi}_0 \big| e^{\hat{\tilde{S}}} e^{-\hat{S}} \left(\hat{H}_{qp} - \lambda \big(\hat{N}_{qp} - N_0 \big) - i \frac{\partial}{\partial t} \right) e^{\hat{S}} \big| \varphi_0 \big\rangle. \tag{4.42}$$

Here, the cluster operators $\hat{S}$ and $\hat{\tilde{S}}$ only contain terms of order QPSUB(2) or higher and our *time-dependent* quasi-particle ket and bra vacuum state wave functions respectively take the usual form

$$\big| \varphi_0 \big\rangle = e^{\hat{S}_1(t)} \big| 0 \big\rangle,$$

$$\big\langle \tilde{\varphi}_0 \big| = \big\langle \Phi_0 \big| e^{\hat{\tilde{S}}_1(t)} e^{-\hat{S}_1(t)}.$$

We make the *harmonic assumption* as stipulated in chapter 2 and write our cluster amplitudes as

$$s_I \left(t \right) = e_I e^{-i \omega_I t}, \tag{4.43}$$

$$\tilde{s}_I \left(t \right) = f_I e^{-i \omega_I t}. \tag{4.44}$$

Therefore, we want to evaluate the RPA frequency ω_I (or excitation energy relative to the ground-state, i.e. $\omega_I = \varepsilon_I - E_0$ where ε_I is an excited-state energy) for each physical solution branch we obtained in our previous calculations, in order to determine how stable the ground-state solution is (of course the frequencies ω_I will only correspond to states having the same symmetry as that of the ground-state).

Evaluating the action of equation (4.42) is more difficult than usual however, since both the states $\big| \varphi_0 \big\rangle$ and $\big\langle \tilde{\varphi}_0 \big|$ as well as the *operators* which make up $\hat{S}$ and $\hat{\tilde{S}}$ depend on time (usually in time-dependent CCM problems, the cluster amplitudes $s_I \left(t \right)$ and $\tilde{s}_I \left(t \right)$ carry all of the time-dependence). We already have an expression for the expectation value of the constrained Hamiltonian

$$\big\langle \hat{H} \big\rangle = \big\langle \tilde{\varphi}_0 \big| e^{\hat{\tilde{S}}} e^{-\hat{S}} \Big(\hat{H}_{qp} - \lambda \big(\hat{N}_{qp} - N_0 \big) \Big) e^{\hat{S}} \big| \varphi_0 \big\rangle$$

up to QPSUB(5). Therefore, we may write the action of equation (4.42) as

$$A = \int_{-\infty}^{+\infty} dt \Big(\big\langle \hat{H} \big\rangle - \big\langle \tilde{\varphi}_0 \big| e^{\hat{\tilde{S}}} e^{-\hat{S}} \Big(i \frac{\partial}{\partial t} \Big) e^{\hat{S}} \big| \varphi_0 \big\rangle \Big),$$

and we thus wish to evaluate the expression

$$\langle\tilde{\varphi}_0|e^{\hat{\tilde{S}}}e^{-\hat{S}}\Big(i\frac{\partial}{\partial t}\Big)e^{\hat{S}}|\varphi_0\rangle, \tag{4.45}$$

in order to derive our RPA solutions.

4.2.5.1 Time Derivatives

Firstly, we write down the linked-cluster expansion for the object $e^{-\hat{S}}i\partial_t e^{\hat{S}}$

$$e^{-\hat{S}}i\partial_t e^{\hat{S}} = i\partial_t + \Big[i\partial_t, \hat{S}\Big] + \frac{1}{2!}\Big[\Big[i\partial_t, \hat{S}\Big], \hat{S}\Big] + \ldots, \tag{4.46}$$

where we use the shorthand notation $\partial_t = \frac{\partial}{\partial t}$ and the $\hat{S}$ and $\hat{\tilde{S}}$ operators are labeled explicitly by

$$\hat{S} = \hat{S}_2 + \hat{S}_2 + \ldots + \hat{S}_n,$$
$$\hat{\tilde{S}} = \hat{\tilde{S}}_2 + \hat{\tilde{S}}_3 + \ldots + \hat{\tilde{S}}_n.$$

Hence, in detail we have

$$e^{-\hat{S}}i\partial_t e^{\hat{S}} = i\partial_t + \Big[i\partial_t, \Big(\hat{S}_2 + \hat{S}_3 + \ldots + \hat{S}_n\Big)\Big]$$

$$+\frac{1}{2!}\Big[\Big[i\partial_t, \Big(\hat{S}_2 + \hat{S}_3 + \ldots + \hat{S}_n\Big)\Big], \Big(\hat{S}_2 + \hat{S}_3 + \ldots + \hat{S}_n\Big)\Big] + \ldots,$$

where all operators act to the right on $|\varphi_0\rangle$ as usual. Consider the j^{th} element of the first commutator

$$\Big[i\partial_t, \hat{S}_j\Big].$$

Specifically what this really means is

$$\Big[i\partial_t, \hat{S}_j\Big]|\varphi_0\rangle$$

$$= i\partial_t\hat{S}_j|\varphi_0\rangle - \hat{S}_j i\partial_t|\varphi_0\rangle$$
$$= i\partial_t\big(\hat{S}_j\big)|\varphi_0\rangle + \hat{S}_j i\partial_t|\varphi_0\rangle - \hat{S}_j i\partial_t|\varphi_0\rangle$$
$$= i\dot{\hat{S}}_j|\varphi_0\rangle.$$

We may therefore break up the general matrix element of equation (4.45) as

$$\langle\tilde{\varphi}_0|e^{\hat{\tilde{S}}}e^{-\hat{S}}\big(i\partial_t\big)e^{\hat{S}}|\varphi_0\rangle = \langle\tilde{\varphi}_0|e^{\hat{\tilde{S}}}e^{-\hat{S}}\big(i\partial_t e^{\hat{S}}\big)_{LC}|\varphi_0\rangle + \langle\tilde{\varphi}_0|e^{\hat{\tilde{S}}}i\partial_t|\varphi_0\rangle, \tag{4.47}$$

where the label LC stands for "linked-cluster" as before. The last term of this expression is the most simple to evaluate so we begin from there. Since our quasi-particle ket

vacuum state wave function is given by

$$\big|\varphi_0\big\rangle = e^{\hat{S}_1(t)}\big|0\big\rangle = e^{s(t)\hat{\Delta}^\dagger}\big|0\big\rangle,$$

the time derivative is given by

$$\begin{aligned}\partial_t\Big(e^{s(t)\hat{\Delta}^\dagger}\big|0\big\rangle\Big) &= \partial_t\Big(s\left(t\right)\hat{\Delta}^\dagger\Big)e^{s(t)\hat{\Delta}^\dagger}\big|0\big\rangle \\ &= \dot{s}\left(t\right)\hat{\Delta}^\dagger e^{s(t)\hat{\Delta}^\dagger}\big|0\big\rangle \\ &= \dot{s}\left(t\right)\hat{\Delta}^\dagger\big|\varphi_0\big\rangle,\end{aligned}$$

i.e. we have

$$\partial_t\big|\varphi_0\big\rangle = \dot{s}\left(t\right)\hat{\Delta}^\dagger\big|\varphi_0\big\rangle. \tag{4.48}$$

We now write $\hat{\Delta}^\dagger$ in terms of quasi-particle operators

$$\hat{\Delta}^\dagger_{qp} = \tilde{s}\left(t\right)\left(\Omega - \hat{n}\right) - \tilde{s}\left(t\right)^2\hat{\delta} + \hat{\delta}^\dagger.$$

Although this introduces an *implied* time dependence into the operator $\hat{\Delta}^\dagger$, it does *not* mean that $\hat{\Delta}^\dagger$ is actually time dependent. Evaluating the second matrix element in equation (4.47) we thus have

$$\begin{aligned}\big\langle\tilde{\varphi}_0\big|e^{\hat{\tilde{S}}}i\partial_t\big|\varphi_0\big\rangle &= i\big\langle\tilde{\varphi}_0\big|e^{\hat{\tilde{S}}}\dot{s}\left(t\right)\left(\tilde{s}\left(t\right)\left(\Omega - \hat{n}\right) - \tilde{s}\left(t\right)^2\hat{\delta} + \hat{\delta}^\dagger\right)\big|\varphi_0\big\rangle \\ &= i\dot{s}\left(t\right)\tilde{s}\left(t\right)\Omega.\end{aligned}$$

The first part of the matrix element in equation (4.47) may be broken further into two terms

$$\begin{aligned}&\big\langle\tilde{\varphi}_0\big|e^{\hat{\tilde{S}}}e^{-\hat{S}}\big(i\partial_t e^{\hat{S}}\big)_{LC}\big|\varphi_0\big\rangle = \\ &\big\langle\tilde{\varphi}_0\big|e^{\hat{\tilde{S}}}\sum_{m=2}\frac{1}{m!}\left(i\partial_t s_m\left(t\right)\right)\hat{\delta}^{\dagger m}\big|\varphi_0\big\rangle + \big\langle\tilde{\varphi}_0\big|e^{\hat{\tilde{S}}}\sum_{n=1}\frac{1}{n!}\left[\sum_{m=2}\frac{1}{m!}s_m\left(t\right)i\partial_t\big(\hat{\delta}^{\dagger m}\big),\hat{S}\right]_{n-1}\big|\varphi_0\big\rangle, \\ &= \big\langle\hat{D}_1\big\rangle + \big\langle\hat{D}_2\big\rangle,\end{aligned} \tag{4.49}$$

where the label on the commutator $n-1$ means the linked-cluster expansion includes the first order term of $\partial_t\big(\frac{1}{m!}s_m\left(t\right)\hat{\delta}^{\dagger m}\big)$. The first term in equation (4.49), $\big\langle\hat{D}_1\big\rangle$, can be evaluated by methods we have previously developed for our CCM calculations. The second term is somewhat more complicated however.

We must first calculate the time derivative of the quasi-particle pairing creation operator $\hat{\delta}^\dagger$, thus we need to write $\hat{\delta}^\dagger$ in terms of the original (time-independent) particle operators $\hat{a}^\dagger_k$ and $\hat{a}_k$. We therefore have

$$\hat{\delta}^{\dagger} = \hat{d}_{k}^{\dagger}\hat{d}_{\bar{k}}^{\dagger} = \sum_{k}\big((1-\tilde{s}\,(t)\,s\,(t))\,\hat{a}_{k}^{\dagger} - \tilde{s}\,(t)\,\hat{a}_{\bar{k}}\big)\big((1-\tilde{s}\,(t)\,s\,(t))\,\hat{a}_{\bar{k}}^{\dagger} - \tilde{s}\,(t)\,\hat{a}_{k}\big),$$

and we may write the time derivative of this as

$$\partial_{t}\hat{\delta}^{\dagger} = \partial_{t}\big(\hat{d}_{k}^{\dagger}\hat{d}_{\bar{k}}^{\dagger}\big) = \partial_{t}\big(\hat{d}_{k}^{\dagger}\big)\hat{d}_{\bar{k}}^{\dagger} + \hat{d}_{k}^{\dagger}\partial_{t}\big(\hat{d}_{\bar{k}}^{\dagger}\big).$$

With some simple algebraic manipulation we may show that

$$\partial_{t}\hat{\delta}^{\dagger} = -2\dot{s}\,(t)\,\tilde{s}\,(t)\,\hat{\delta}^{\dagger} + \big(\dot{\tilde{s}}\,(t) + \tilde{s}\,(t)^{2}\,\dot{s}\,(t)\big)\,(\hat{n}-\Omega)\,. \tag{4.50}$$

Using this relation we may further derive that $\partial_{t}\hat{\delta}^{\dagger m}$ is given by

$$\partial_{t}\hat{\delta}^{\dagger m} = -2\dot{s}\,(t)\,\tilde{s}\,(t)\,m\hat{\delta}^{\dagger m} + \big(\dot{\tilde{s}}\,(t) + \tilde{s}\,(t)^{2}\,\dot{s}\,(t)\big)\hat{\delta}^{\dagger m}m\big(\hat{n}-\Omega+m-1\big), \tag{4.51}$$

which in turn can be used to evaluate $\big\langle\hat{D}_{2}\big\rangle$ from equation (4.49). Thus we may finally show that

$$\begin{aligned}\big\langle\hat{D}_{2}\big\rangle = i\sum_{m=2} -\frac{1}{m-1!}s_{m}\,(t)\,\Bigg(&2\tilde{s}\,(t)\,\dot{s}\,(t)\,\big\langle\tilde{\varphi}_{0}\big|e^{\hat{\tilde{S}}}\hat{\delta}^{\dagger m}\big|\varphi_{0}\big\rangle \\ &+\big(\dot{\tilde{s}}\,(t) + \tilde{s}\,(t)^{2}\,\dot{s}\,(t)\big)\big(\Omega-m+1\big)\big\langle\tilde{\varphi}_{0}\big|e^{\hat{\tilde{S}}}\hat{\delta}^{\dagger m-1}\big|\varphi_{0}\big\rangle\Bigg) \\ +i\big(\dot{\tilde{s}}\,(t) + \tilde{s}\,(t)^{2}\,\dot{s}\,(t)\big)\sum_{m,q>1}\frac{s_{m}\,(t)\,s_{q}\,(t)}{(m-1)!(q-1)!}&\big\langle\tilde{\varphi}_{0}\big|e^{\hat{\tilde{S}}}\hat{\delta}^{\dagger m+q-1}\big|\varphi_{0}\big\rangle.\end{aligned} \tag{4.52}$$

We therefore now have all the information required to evaluate the action functional of equation (4.42).

4.2.5.2 RPA Results

We choose to evaluate the RPA calculations for the two most general approximations we have used, namely the particle and quasi-particle ECCM approaches. Figure (4.11) displays the solutions of the RPA frequencies for particle ECCM calculations between SUB(2) and SUB(5) approximation with $\Omega = 10$ and $G = 1$. Figure (4.12) displays the analogous solutions for the quasi-particle ECCM calculations between QPSUB(2) and QPSUB(5). These pictures should be viewed in combination with the particle and quasi-particle solutions shown in figures (4.4) and (4.9) respectively, which highlight the variations between the various CCM solutions and the exact ground-state energy. Only results up to a half-filled shell are shown in figures (4.11) and (4.12).

The RPA frequencies appear in pairs $\pm\omega$ for a given solution branch, although we are only concerned with the positive values for physical excitations. In both sets

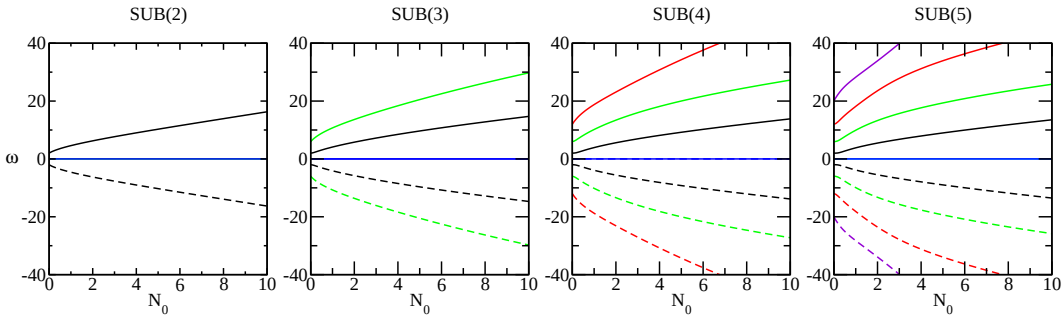

Figure 4.11: Plot of RPA frequencies ω vs N_0 for particle SUB(2)-SUB(5) ECCM solutions using $\Omega = 10$ and $G = 1$.

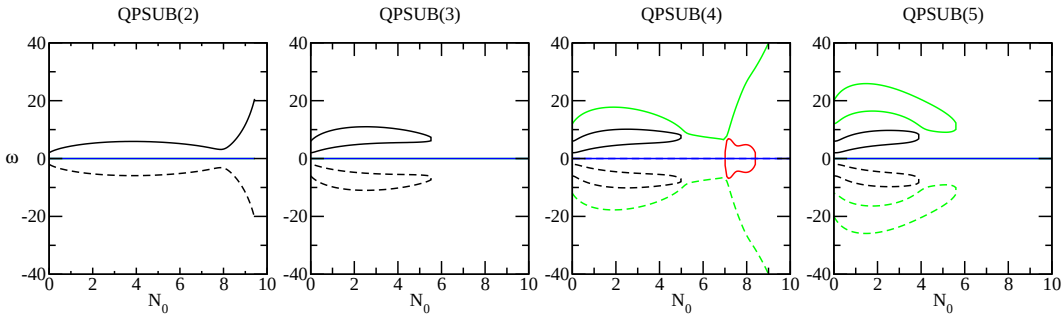

Figure 4.12: Plot of RPA frequencies ω vs N_0 for quasi-particle QPSUB(2)-QPSUB(5) ECCM solutions using $\Omega = 10$ and $G = 1$.

of pictures we observe zero-mode solutions for ω which are doubly-degenerate - these stem from the excitations which break particle number but remain "along" the ground-state solution branch. As was explained for the quartic anharmonic oscillator model in chapter 3, the higher the SUB(n) approximation, the more modes (or higher level excitation energies) we will see - this pattern is clearly observed again in the particle ECCM case. Note that there is little variation in the first excited-state (black line) across the SUB(2)-SUB(5) particle ECCM pictures although the second (green) and third (red) excited-states show a much stronger pattern of convergence - this shows that lower RPA frequencies (excitation energies) are already fairly accurate to low order ECCM truncation and have a much smaller dependence on high order cluster correlations compared to higher RPA frequencies.

Although these modes all have real frequencies, they also break particle number since they show nonzero excitation energy for a completely empty shell - although we have constrained the particle number for the ground-state, as soon as we expand about the ground-state (which is the basis of the RPA approach) we will no longer conserve particle number. Notice that both schemes produce the same RPA frequencies at $N_0 = 0$ - this is because the two different approaches are identical at this point.

The strange pictures of the quasi-particle case go some way to explaining the convergence patterns shown earlier. To even order QPSUB(n) we see a collapse of the RPA frequencies at mid-shell and this collapse seems to happen for smaller N_0 as the order

of approximation is increased (i.e. it happens further away from mid-shell the higher we truncate n). To odd order QPSUB(n) we see that all nonzero RPA frequencies collide in pairs and go off into the complex plane. These properties combined represent a total breakdown of the quasi-particle approach.

The collapse at mid-shell for even order QPSUB(n) ground-state solutions we saw in figure (4.8) is echoed in the RPA frequencies of even order QPSUB(n) (the excitation energies of the states with the same symmetry as the ground-state all collapse at mid-shell). Figure (4.8) showed a convergence of sorts for odd order QPSUB(n) ground-state solutions - this seems to be due to there being an even number of (nonzero) RPA modes which collide and become complex, thus the collapse from a single RPA mode is not observed.

4.3 Discussion

In this chapter we have studied an idealised and exactly solvable pairing model of a finite number of fermions confined to a finite space. We have primarily completed studies of the model using ECCM techniques - using either particle or quasi-particle operators for our calculations - as well as performing a limited number of quasi-particle NCCM calculations for comparative purposes. Each one of our methods seems to have some failing. For a large number of states Ω (or equivalently, a large number of particles N_0) the particle ECCM seems to show the most promise at the SUB(2) level, however for a small number of states it derails quite badly as a reliable technique by SUB(4) order. Since the SUB(2) result worked particularly well up to mid-shell, we decided to break our calculations into two pieces and work from either "end" of the shell, until each result met in the middle. Such an approach showed a slow convergence of the ECCM solution to the ground-state energy, although there was clearly a limit as to how close we could get to the true ground-state solution.

The quasi-particle ECCM also showed some promise initially, but only for odd order QPSUB(n) approximations. Quite surprisingly the quasi-particle NCCM fares particularly well at some points as well - for instance the QPSUB(2) calculation for large degeneracy Ω - before producing some very odd results at QPSUB(4). It is difficult to comprehend why these techniques fail as badly as they do in certain places. The RPA calculation of the excitation energies shows that the standard particle ECCM is rather stable, yet we see some very odd behavior coming from the quasi-particle ECCM.

The overall failure of these approaches is perhaps linked to the fact that the model has an exactly solvable form. Thus perhaps the tools we are using to study the problem may simply be too technical and too advanced in order to recreate the model's simple and exact ground-state energy expression. For a more realistic system and working in a larger model space, we would expect some of the problems demonstrated in our

results to be less dominant and less pronounced. As appealing as the quasi-particle scheme first was, we conclude this chapter by admitting that the quasi-particle ECCM or high order quasi-particle NCCM results, coupled with the information from the RPA frequencies, are not stable enough to be trusted - the initial idea of using quasi-particle operators to study pairing seemed attractive but as the results show, low order (e.g. SUB(2)) particle ECCM calculations are far more reliable.

Chapter 5

Pairing between Fermionic Atoms of an Ultracold Dilute Gas confined in an Ellipsoidal Harmonic Trap

The model of single-shell pairing discussed in the previous chapter provided us with a useful insight into ways of applying CCM techniques to pairing problems. Ultimately, the fact that the model was "idealised" - exactly solvable and considered in a relatively small finite space - seems to have been our downfall. We concluded that the standard particle ECCM arguably gave the most stable results to low order - with this in mind, we now proceed to look at a different model of pairing in this limit. As a means to study the BCS and BEC regimes of an ultracold dilute atomic gas, we propose to study a system of paired fermionic atoms confined within an ellipsoidal harmonic trap. A model such as this may be used to represent an idealised system in which BCS-BEC crossover may be observed [95, 96, 97]. After introducing the basic formalism of the model we calculate the normal and abnormal densities of the standard SUB(1) (particle) ECCM approach in order to investigate the ground-state properties of the trapped condensate. Solving the ECCM equations for this system proves to be rather complicated, thus we write a computer code in C++. This in itself is somewhat more problematic than first anticipated and so we simplify our equations by assuming a diagonal form and seek a solution using Mathematica. By plotting graphs of single-particle occupation probabilities versus single-particle energies we prove the existence of both quantum degeneracy and pairing in either regime. Ideally we would have liked to increase the order of our approximation to SUB(2) in order to see what happens beyond the SUB(1) (mean-field) solution. Since this has not been possible, we instead outline what would have been our approach to study the collective modes of the system in either the BCS or BEC limit.

5.1 The Model

We are interested in studying the pairing between ultracold fermionic atoms in a superfluid state, i.e. a state where the atoms form correlated s-wave Cooper pairs in **k**-space and there is a relatively weak attraction between pairs [92]. We assume this superfluid to be confined within a trap (produced, for example, by a magnetic field or a laser) and dilute enough so that the collisions in the superfluid may be described solely in terms of s-wave scattering [92]. By applying an external (variable) magnetic field to the system it is possible to tune the s-wave scattering length a_s of the two-body potential between a BCS-like superfluid ($a_s < 0$) and a BEC composed of diatomic molecules ($a_s > 0$) across a so-called *Feshbach resonance* [146] (which in essence corresponds to the point at which the energy of two scattering atoms is equal to that of a bound diatomic molecule of the pair [94]). Although we will assume certain properties that will simplify our model, we choose the trap to be ellipsoidal to retain some generality (and also because most experimentalists tend to utilise nonspherical traps to begin with [95, 96, 97]).

The model we propose to study consists of N_0 identical fermionic atoms of arbitrary half-integer spin[1] that are held at zero temperature, confined within a harmonic trap and interacting via a two-body force. We consider the system in 3-dimensions and for convenience we neglect any isospin-dependence of the atoms. We write the Hamiltonian for such a system as

$$\hat{H} = \sum_{\alpha,\sigma} \varepsilon_\alpha \hat{a}^\dagger_{\alpha,\sigma} \hat{a}_{\alpha,\sigma} + \sum_{\alpha,\beta,\gamma,\delta} V_{\alpha\beta\gamma\delta} \hat{a}^\dagger_{\alpha,\uparrow} \hat{a}^\dagger_{\beta,\downarrow} \hat{a}_{\delta,\downarrow} \hat{a}_{\gamma,\uparrow}, \tag{5.1}$$

where σ is the fermion spin (either $\uparrow$ or $\downarrow$).

The operators $\hat{a}^\dagger_{\alpha,\sigma}$ and $\hat{a}_{\alpha,\sigma}$ are single-particle creation and annihilation operators respectively, defined relative to the bare particle vacuum $\left|0\right\rangle$ and obeying the usual fermionic anticommutation relations

$$\left\{\hat{a}_{\alpha,\sigma}, \hat{a}^\dagger_{\beta,\sigma'}\right\} = \delta_{\alpha,\beta}\delta_{\sigma,\sigma'},$$

$$\left\{\hat{a}_{\alpha,\sigma}, \hat{a}_{\beta,\sigma'}\right\} = 0 = \left\{\hat{a}^\dagger_{\alpha,\sigma}, \hat{a}^\dagger_{\beta,\sigma'}\right\}.$$

The label α is an index used to represent the set of quantum numbers (n_x, n_y, n_z) which arise from each of the three independent 1-dimensional harmonic oscillator potentials that make up the total trap, hence

$$\alpha = \{n_x, n_y, n_z\}, \tag{5.2}$$

[1] we do not specify any particular species and hence a value of total atomic spin.

and summation in equation (5.1) is therefore over harmonic oscillator shells. Writing our fermion operators explicitly we have

$$\left\{\hat{a}_{n_x n_y n_z,\sigma}, \hat{a}^{\dagger}_{n'_x n'_y n'_z,\sigma'}\right\} = \delta_{n_x,n'_x}\delta_{n_y,n'_y}\delta_{n_z,n'_z}\delta_{\sigma,\sigma'},$$

$$\left\{\hat{a}_{n_x n_y n_z,\sigma}, \hat{a}_{n'_x n'_y n'_z,\sigma'}\right\} = 0 = \left\{\hat{a}^{\dagger}_{n_x n_y n_z,\sigma}, \hat{a}^{\dagger}_{n'_x n'_y n'_z,\sigma'}\right\},$$

where the operators $\hat{a}^{\dagger}_{n_x n_y n_z}$ and $\hat{a}_{n_x n_y n_z}$ are formally given by the tensorial products of one-body fermionic creation and annihilation operators respectively, i.e.

$$\hat{a}^{\dagger}_{n_x n_y n_z} = \hat{a}^{\dagger}_{n_x} \otimes \hat{a}^{\dagger}_{n_y} \otimes \hat{a}^{\dagger}_{n_z},$$

$$\hat{a}_{n_x n_y n_z} = \hat{a}_{n_x} \otimes \hat{a}_{n_y} \otimes \hat{a}_{n_z}.$$

The Hamiltonian of equation (5.1) may be considered as consisting of two parts

$$\hat{H} = \hat{H}_0 + \hat{H}_1. \tag{5.3}$$

The first part is composed of one-body terms - the kinetic energy of the atoms and the trapping potential they are subject to. The second part is the two-body interaction between the atoms - we choose to describe this with a Gaussian function.

5.1.1 One-Body Term $\hat{H}_0$

The single-particle eigenstates of the one-body term $\hat{H}_0$ are defined to be

$$\left|\phi_{\alpha,\sigma}\right\rangle = \hat{a}^{\dagger}_{\alpha,\sigma}\left|0\right\rangle. \tag{5.4}$$

Excluding spin, we may write these states in 3-dimensional coordinate representation as

$$\begin{aligned}\left\langle \mathbf{r}|\phi_{n_x n_y n_z}\right\rangle &= \phi_{n_x,n_y,n_z}(x,y,z) = \phi_{n_x}(x)\,\phi_{n_y}(y)\,\phi_{n_z}(z)\\ &= \sqrt{\frac{1}{n_x!2^{n_x}}}\left(\frac{1}{\pi b_x^2}\right)^{\frac{1}{4}}\exp\left(-\frac{x^2}{2b_x^2}\right)H_{n_x}\left(\frac{x}{b_x}\right)\\ &\times\sqrt{\frac{1}{n_y!2^{n_y}}}\left(\frac{1}{\pi b_y^2}\right)^{\frac{1}{4}}\exp\left(-\frac{x^2}{2b_y^2}\right)H_{n_y}\left(\frac{x}{b_y}\right)\\ &\times\sqrt{\frac{1}{n_z!2^{n_z}}}\left(\frac{1}{\pi b_z^2}\right)^{\frac{1}{4}}\exp\left(-\frac{x^2}{2b_z^2}\right)H_{n_z}\left(\frac{x}{b_z}\right),\end{aligned}$$

where

$$b_x = \sqrt{\frac{\hbar}{m\omega_x}};\; b_y = \sqrt{\frac{\hbar}{m\omega_y}};\; b_z = \sqrt{\frac{\hbar}{m\omega_z}},$$

and H_n are Hermite polynomials [2]. Similarly in coordinate representation, the 3-dimensional harmonic trap potential $\hat{V}_{\text{ho}}$ [92] is given by

$$\hat{V}_{\text{ho}} = \frac{1}{2}m\big(\omega_x^2 x^2 + \omega_y^2 y^2 + \omega_z^2 z^2\big), \tag{5.5}$$

and the energy eigenvalues ε_α of the states $\big|\phi_{\alpha,\sigma}\big\rangle$ are therefore given by

$$\varepsilon_\alpha = \sum_{\tau=1}^{3} \hbar\omega_\tau\Big(n_\tau + \frac{1}{2}\Big)$$

$$= \hbar\omega_x\Big(n_x + \frac{1}{2}\Big) + \hbar\omega_y\Big(n_y + \frac{1}{2}\Big) + \hbar\omega_z\Big(n_z + \frac{1}{2}\Big). \tag{5.6}$$

The angular frequency ω_τ is often denoted as the "trap frequency" [92].

The energy of equation (5.6) is the sum of the 3 independent oscillator energies that make up the total trap (one for each direction x, y and z) and each oscillator has an independent angular frequency. For an *isotropic* (i.e. spherical) harmonic trap, all oscillators share the same angular frequency

$$\omega_x = \omega_y = \omega_z = \omega,$$

thus the energy eigenvalues of equation (5.6) are reduced to

$$\varepsilon_\alpha = \hbar\omega\Big(n_x + n_y + n_z + \frac{3}{2}\Big). \tag{5.7}$$

However, we will be mainly considering the more general *anisotropic* (i.e. nonspherical) trap in our calculations, where there is axial symmetry between x and y coordinates. In which case, both x and y directions of the trap will share the same value of angular frequency

$$\omega_x = \omega_y = \omega_\perp,$$

but the z direction will take a different value to $\omega_\perp$

$$\omega_z \neq \omega_\perp.$$

This means that the energy eigenvalues of equation (5.6) are reduced to

$$\varepsilon_\alpha = \hbar\omega_\perp\Big(n_x + n_y + 1\Big) + \hbar\omega_z\Big(n_z + \frac{1}{2}\Big). \tag{5.8}$$

Comparing equation (5.5) with the standard Cartesian equation of an ellipsoid

$$\frac{x^2}{a^2} + \frac{y^2}{b^2} + \frac{z^2}{c^2} = 1, \tag{5.9}$$

it may be shown that a trap with $\omega_z > \omega_\perp$ is an *oblate* spheroid ("disc" shaped - see figure (5.1)) and a trap with $\omega_z < \omega_\perp$ is a *prolate* spheroid ("cigar" shaped - see figure (5.2)). The trap shape is usually described in terms of the dimensionless *deformation parameter* λ [92]

$$\lambda = \frac{\omega_z}{\omega_\perp}, \tag{5.10}$$

thus traps with $\lambda > 1$ are disk shaped and traps with $\lambda < 1$ are cigar shaped[2]. We will be investigating BCS-BEC crossover in both of these trap shapes.

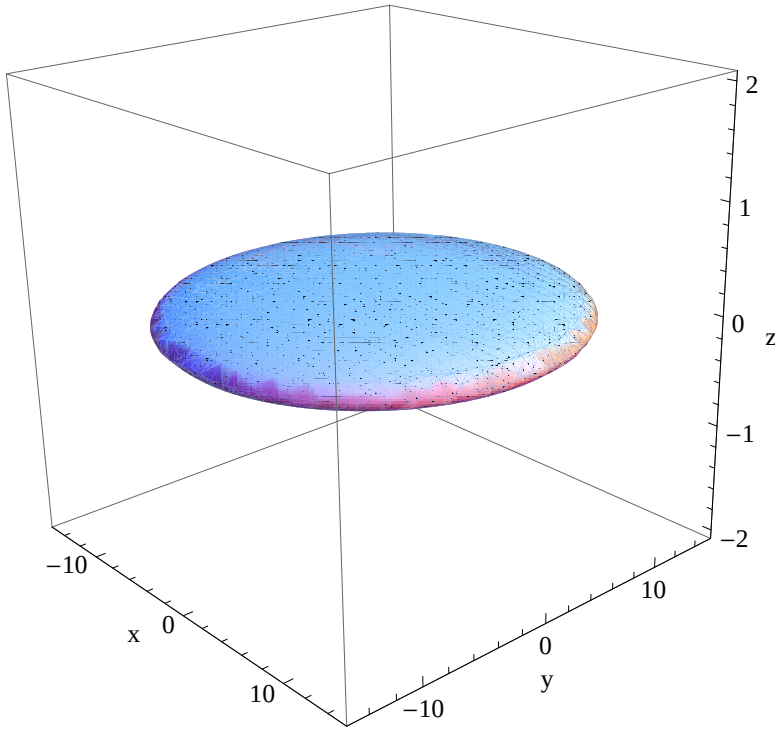

Figure 5.1: Plot of a disk shaped trap potential $\hat{V}_{\text{ho}} = \frac{1}{2}m\left(\omega_\perp^2 x^2 + \omega_\perp^2 y^2 + \omega_z^2 z^2\right) = 1$, with $m = 1$, $\omega_\perp = \frac{1}{10}$ and $\omega_z = 4$.

[2]it is common for traps to be specified solely by a value for the perpendicular (radial) frequency $\omega_\perp$ and the deformation parameter λ [94, 95, 97].

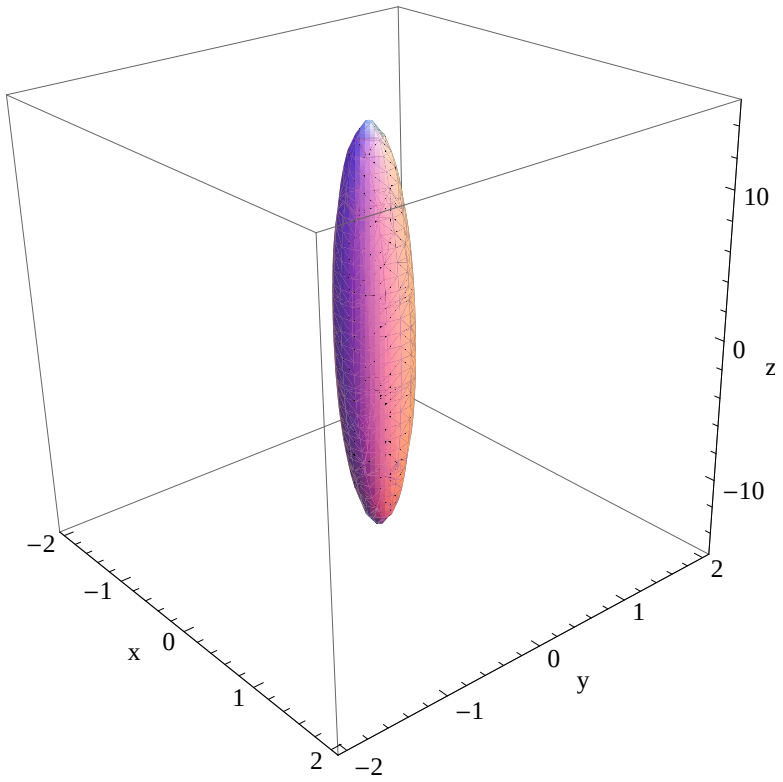

Figure 5.2: Plot of a cigar shaped trap potential $\hat{V}_{\text{ho}} = \frac{1}{2}m\left(\omega_\perp^2 x^2 + \omega_\perp^2 y^2 + \omega_z^2 z^2\right) = 1$, with $m = 1$, $\omega_\perp = 4$ and $\omega_z = \frac{1}{10}$.

5.1.2 Two-Body Term $\hat{H}_1$

The coefficients $V_{\alpha\beta\gamma\delta}$ of the two-body interaction given in equation (5.1) are given by the matrix elements

$$V_{\alpha\beta\gamma\delta} = \left\langle \phi_{\alpha,\uparrow}\phi_{\beta,\downarrow}\middle|\hat{V}\middle|\phi_{\gamma,\uparrow}\phi_{\delta,\downarrow}\right\rangle, \tag{5.11}$$

where we choose to write our (Gaussian) potential operator as

$$\hat{V} = V_0\left(\frac{1}{\sqrt{2\pi}}\right)^3 \frac{1}{\sigma^3}\exp\left(-\frac{1}{2\sigma^2}\left((x-x')^2 + (y-y')^2 + (z-z')^2\right)\right). \tag{5.12}$$

The Gaussian is centered at the point $\mathbf{r}' = (x', y', z')$ and the standard deviation (width) of the distribution is σ. The potential operator $\hat{V}$ of equation (5.12) is obviously composed of three independent terms, one for each direction in 3-dimensional space. The overall strength of the potential is given by V_0 and the indices α, β, γ and δ of equation (5.11) are explicitly given by

$$\alpha = \left\{n_x^{(1)}, n_y^{(1)}, n_z^{(1)}\right\},$$

$$\beta = \left\{n_x^{(2)}, n_y^{(2)}, n_z^{(2)}\right\},$$
$$\gamma = \left\{n_x^{(3)}, n_y^{(3)}, n_z^{(3)}\right\},$$
$$\delta = \left\{n_x^{(4)}, n_y^{(4)}, n_z^{(4)}\right\}.$$

By altering the width σ of the two-body Gaussian potential and the strength of the potential V_0 we can alter the s-wave scattering length a_s of the atomic gas - or said another way - for a fixed value of σ we can tune the system between BCS and BEC regimes (alter a_s between negative and positive values) by changing V_0.

In order to evaluate the coefficients given in equation (5.11), we need only evaluate the matrix element for one term (for example, the x coordinate) since all three expressions are the same, except for the specific coordinate label (x, y or z). Thus we need to evaluate the matrix element

$$\left\langle \phi_{n_x^{(1)},\uparrow}\phi_{n_{x'}^{(2)},\downarrow}\right|\exp\left(\frac{-(x-x')^2}{2\sigma^2}\right)\left|\phi_{n_x^{(3)},\uparrow}\phi_{n_{x'}^{(4)},\downarrow}\right\rangle, \tag{5.13}$$

or equivalently the integral

$$I_x = \int_{-\infty}^{+\infty}\int_{-\infty}^{+\infty} \phi_{n_x^{(1)}}(x)\,\phi_{n_{x'}^{(2)}}(x')\exp\left(\frac{-(x-x')^2}{2\sigma^2}\right)\phi_{n_x^{(3)}}(x)\,\phi_{n_{x'}^{(4)}}(x')\,dxdx', \tag{5.14}$$

where we initially neglect normalisation for the sake of convenience. Evaluating equation (5.14) is most easily achieved by writing the Hermite polynomials which make up the single-particle wave functions as generating functions. Thus, I_x of equation (5.14) becomes

$$I_x = \int_{-\infty}^{+\infty}\int_{-\infty}^{+\infty} H_{n_x^{(1)}}(x)\,H_{n_x^{(3)}}(x)\,e^{-x^2}H_{n_{x'}^{(2)}}(x')\,H_{n_{x'}^{(4)}}(x')\,e^{-x'^2}\exp\left(\frac{-(x-x')^2}{2\sigma^2}\right)dxdx', \tag{5.15}$$

where the generating function for Hermite polynomials is given by

$$H_n(x) = \left(\frac{1}{\sqrt{2}}\frac{d}{dz}\right)^n \frac{1}{\pi^{\frac{1}{4}}}\exp\left(-z^2+2xz\right). \tag{5.16}$$

We can evaluate equation (5.15) analytically but to check we have the correct answer we write a Mathematica code - we may hence show

$$I_x = N\sum_{m_{13}=0}^{\min(n_1,n_3)}\sum_{m_{24}=0}^{\min(n_2,n_4)} \frac{(-1)^m}{(\sigma^2+2)^{n+1/2}}\frac{(2n-1)!!}{lm_{24}!m_{13}!}, \tag{5.17}$$

where

$$l = (n_1-m_{13})!(n_2-m_{24})!(n_3-m_{13})!(n_4-m_{24})!,$$

$$m = m_{13} + m_{24},$$

$$n = (n_1 + n_2 + n_3 + n_4)/2 - m,$$

$$N = (-1)^{(n_1 - n_2 + n_3 - n_4)/2} \sigma \sqrt{n_1! n_2! n_3! n_4!}.$$

The summations run up to the smallest value of integers in the pairs $\left(n_1, n_3\right)$ or $\left(n_2, n_4\right)$, which we write as $\min(n_1, n_3)$ or $\min(n_2, n_4)$. We may therefore write our *normalised* 3-dimensional coefficients $V_{\alpha\beta\gamma\delta}$ as

$$V_{\alpha\beta\gamma\delta} = \widetilde{V}_0 I_x I_y I_z, \tag{5.18}$$

where $\widetilde{V}_0$ is given by

$$\widetilde{V}_0 = V_0 \left(\frac{1}{\sqrt{2\pi}} \right)^3 \frac{1}{\sigma^3},$$

and the terms I_y and I_z are simply given by equation (5.17) with the x label replaced with y or z (since they are all given by the same expression).

5.2 Extended Coupled Cluster Method

Having calculated the exact forms of both ε_α and $V_{\alpha\beta\gamma\delta}$ from the Hamiltonian of equation (5.1), we are now in a position to begin our ECCM calculations.

5.2.1 SUB(1) Calculation

For a model that is rather more complicated than any we have studied previously, it is sensible to begin from the lowest order approximation we can make, i.e. we would like to see what the mean-field approach predicts for the ground-state properties of this model. We therefore perform a simple BCS/SUB(1) ECCM calculation first - we can justify this approach based on the fact BCS theory offers a relatively good *qualitative* description of BCS-BEC crossover [92] (unfortunately it does not offer a similarly good *quantitative* description of the crossover however [92]). We use precisely the same approach as described in chapter 2 for the s-wave pairing problem, choosing our model state $\left|\Phi_0\right\rangle$ as the bare particle vacuum $\left|0\right\rangle$ and writing our SUB(1) pairing cluster correlation operators as

$$\hat{S}_1 = \sum_{\alpha,\beta} s^{(1)}_{\alpha\beta} \hat{a}^\dagger_{\alpha,\uparrow} \hat{a}^\dagger_{\beta,\downarrow}, \tag{5.19}$$

$$\hat{\tilde{S}}_1 = \sum_{\alpha,\beta} \tilde{s}^{(1)}_{\alpha\beta} \hat{a}_{\beta,\downarrow} \hat{a}_{\alpha,\uparrow}. \tag{5.20}$$

We are now assuming that the cluster amplitudes will depend on the 3-dimensional harmonic energy quantum numbers (n_x, n_y, n_z) and so we denote SUB(1) terms with a superscript, in order to avoid needlessly complicated notation where SUB(n) terms are denoted with subscripts alongside single-particle labels α and β. The cluster amplitudes are no longer numbers in this case but are (square) matrices - the greater the number of particles we put into our trap the more oscillator shells we must include and hence the larger $s^{(1)}_{\alpha\beta}$ and $\tilde{s}^{(1)}_{\alpha\beta}$ will become.

As was the case with the single-shell pairing model in chapter 4, in the ECCM approach we require an expression for the constrained ground-state energy functional

$$E\big(\{s_I, \tilde{s}_I\}\big) = \big\langle \Phi_0 \big| e^{\hat{\tilde{S}}} e^{-\hat{S}} \big(\hat{H} - \lambda\big(\hat{N} - N_0\big)\big) e^{\hat{S}} \big| \Phi_0 \big\rangle,$$

where λ is the chemical potential and N_0 is the average number of fermionic atoms. Due to the construction of the Hamiltonian in equation (5.1), the ECCM functional may be split as

$$\begin{aligned} E\big(\{s_I, \tilde{s}_I\}\big) = \big\langle \Phi_0 \big| e^{\hat{\tilde{S}}} e^{-\hat{S}} \big(\hat{H}_0 - \lambda\big(\hat{N} - N_0\big)\big) e^{\hat{S}} \big| \Phi_0 \big\rangle \\ + \big\langle \Phi_0 \big| e^{\hat{\tilde{S}}} e^{-\hat{S}} \hat{H}_1 e^{\hat{S}} \big| \Phi_0 \big\rangle, \end{aligned} \tag{5.21}$$

where the linked-cluster expansions truncate at second order in $\hat{H}_0$ and $\hat{N}$ and fourth order in $\hat{H}_1$, in typical fashion. For the case of single-shell pairing in chapter 4 we could solve these commutators in a very simple way, due to the SU(2) quasi-spin algebra inherent to that model. Unfortunately, no such simplification exists for our trap model and so we will need to explicitly evaluate all of the matrix elements in equation (5.21). We already know a straightforward way of doing this however, namely evaluating the normal and abnormal densities of HFB theory (as shown in chapter 2).

5.2.1.1 Normal Density

The normal density is defined by the matrix elements

$$\rho_{\alpha\sigma,\beta\sigma'} = \big\langle \tilde{\varphi}_0 \big| \hat{a}^{\dagger}_{\beta,\sigma'} \hat{a}_{\alpha,\sigma} \big| \varphi_0 \big\rangle, \tag{5.22}$$

where, to SUB(1) approximation for our trap model, the quasi-particle vacuum states $\big|\varphi_0\big\rangle$ and $\big\langle\tilde{\varphi}_0\big|$ are given by

$$\big|\varphi_0\big\rangle = e^{\hat{S}_1} \big|0\big\rangle, \tag{5.23}$$

$$\big\langle\tilde{\varphi}_0\big| = \big\langle 0 \big| e^{\hat{\tilde{S}}_1} e^{-\hat{S}_1}. \tag{5.24}$$

We proceed to evaluate the normal density exactly as was demonstrated previously in chapter 2. For this system it may be shown that the only contributions to $\rho_{\alpha\sigma,\beta\sigma'}$ are

given by

$$\rho_{\alpha\sigma,\beta\sigma'} = \big\langle 0\big| e^{\hat{\tilde{S}}_1} \Big[\hat{a}^\dagger_{\beta,\sigma'}\hat{a}_{\alpha,\sigma}, \hat{S}_1\Big] \big|0\big\rangle,$$

and thus we have

$$\rho_{\alpha\sigma,\beta\sigma'}\left(s^{(1)}, \tilde{s}^{(1)}\right) = \delta_{\sigma,\sigma'} \sum_{\mu} \big(\delta_{\sigma,\uparrow}\tilde{s}^{(1)}_{\beta\mu}s^{(1)}_{\alpha\mu} + \delta_{\sigma,\downarrow}\tilde{s}^{(1)}_{\mu\beta}s^{(1)}_{\mu\alpha}\big). \tag{5.25}$$

5.2.1.2 Abnormal Densities

The abnormal and conjugate abnormal densities are defined by the matrix elements

$$\kappa_{\alpha\sigma,\beta\sigma'} = \big\langle \tilde{\varphi}_0\big|\hat{a}_{\beta,\sigma'}\hat{a}_{\alpha,\sigma}\big|\varphi_0\big\rangle, \tag{5.26}$$

$$-\kappa^\star_{\alpha\sigma,\beta\sigma'} = \big\langle \tilde{\varphi}_0\big|\hat{a}^\dagger_{\beta,\sigma'}\hat{a}^\dagger_{\alpha,\sigma}\big|\varphi_0\big\rangle. \tag{5.27}$$

Starting with the abnormal density $\kappa_{\alpha\sigma,\beta\sigma'}$, the only contributions are given by

$$\kappa_{\alpha\sigma,\beta\sigma'} = \big\langle 0\big| \Big[\hat{a}_{\beta,\sigma'}\hat{a}_{\alpha,\sigma}, \hat{S}_1\Big] \big|0\big\rangle + \big\langle 0\big|\frac{1}{2}e^{\hat{\tilde{S}}_1} \Big[\Big[\hat{a}_{\beta,\sigma'}\hat{a}_{\alpha,\sigma}, \hat{S}_1\Big], \hat{S}_1\Big] \big|0\big\rangle,$$

which may be shown to give

$$\kappa_{\alpha\sigma,\beta\sigma'} = \delta_{\sigma,\uparrow}\delta_{\sigma',\downarrow}\big(s^{(1)}_{\alpha\beta} - \sum_{\pi,\mu}\tilde{s}^{(1)}_{\pi\mu}s^{(1)}_{\pi\beta}s^{(1)}_{\alpha\mu}\big) - \delta_{\sigma,\downarrow}\delta_{\sigma',\uparrow}\big(s^{(1)}_{\beta\alpha} - \sum_{\pi,\mu}\tilde{s}^{(1)}_{\pi\mu}s^{(1)}_{\pi\alpha}s^{(1)}_{\beta\mu}\big). \tag{5.28}$$

The conjugate abnormal density $-\kappa^\star_{\alpha\sigma,\beta\sigma'}$ has a very simple form since there is only one contributing term

$$-\kappa^\star_{\alpha\sigma,\beta\sigma'} = \big\langle 0\big|\hat{\tilde{S}}_1\hat{a}^\dagger_{\beta,\sigma'}\hat{a}^\dagger_{\alpha,\sigma}\big|0\big\rangle,$$

which gives

$$-\kappa^\star_{\alpha\sigma,\beta\sigma'} = -\big(\delta_{\sigma,\uparrow}\delta_{\sigma',\downarrow}\tilde{s}^{(1)}_{\alpha\beta} - \delta_{\sigma,\downarrow}\delta_{\sigma',\uparrow}\tilde{s}^{(1)}_{\beta\alpha}\big). \tag{5.29}$$

We may compare the normal and abnormal densities given in equations (5.25), (5.28) and (5.29) of this problem with those of the "BCS form" (i.e. no hole states) as given in equation (2.111) of chapter 2. All three expressions are identical in each case, excluding the important fact that the cluster amplitudes defined for our trap model are now dependent on the 3-dimensional harmonic energy quantum numbers (n_x, n_y, n_z) - thus we must take into account that, for example, the terms $\tilde{s}^{(1)}_{\alpha\beta}$ and $\tilde{s}^{(1)}_{\beta\alpha}$ are different (i.e. the cluster amplitudes are *not* diagonal, as in the previous case). We must also keep the tilde terms on the left of the expressions (where they enter the matrix elements) since they represent matrices in this case, not just numbers.

5.2.1.3 Ground-State Energy Functional and ECCM Equations

As was shown in chapter 2, using the HFB method we may write down the (unconstrained) ground-state energy functional for the Hamiltonian of equation (5.1) in terms of the normal and abnormal densities

$$E\big(\{\rho,\kappa\}\big) = \sum_{\alpha,\sigma} \varepsilon_\alpha \rho_{\alpha\sigma,\alpha\sigma} + \sum_{\alpha,\beta,\gamma,\delta} V_{\alpha\beta\gamma\delta}\big(\rho_{\gamma\uparrow,\alpha\uparrow}\rho_{\delta\downarrow,\beta\downarrow} - \rho_{\alpha\uparrow,\delta\downarrow}\rho_{\beta\downarrow,\gamma\uparrow}\big)$$

$$- \sum_{\alpha,\beta,\gamma,\delta} V_{\alpha\beta\gamma\delta}\kappa^{\star}_{\beta\downarrow,\alpha\uparrow}\kappa_{\gamma\uparrow,\delta\downarrow}. \tag{5.30}$$

Evaluating each of these densities in turn we have

$$\rho_{\alpha\sigma,\alpha\sigma} = \sum_{\mu}\big(\tilde{s}^{(1)}_{\alpha\mu}s^{(1)}_{\alpha\mu} + \tilde{s}^{(1)}_{\mu\alpha}s^{(1)}_{\mu\alpha}\big),$$

$$-\kappa^{\star}_{\beta\downarrow,\alpha\uparrow} = \tilde{s}^{(1)}_{\alpha\beta},$$

$$\kappa_{\gamma\uparrow,\delta\downarrow} = s^{(1)}_{\gamma\delta} - \sum_{\pi,\mu}\tilde{s}^{(1)}_{\pi\mu}s^{(1)}_{\pi\delta}s^{(1)}_{\gamma\mu},$$

$$\rho_{\gamma\uparrow,\alpha\uparrow} = \sum_{\mu}\tilde{s}^{(1)}_{\alpha\mu}s^{(1)}_{\gamma\mu},$$

$$\rho_{\delta\downarrow,\beta\downarrow} = \sum_{\mu}\tilde{s}^{(1)}_{\mu\beta}s^{(1)}_{\mu\delta},$$

$$\rho_{\alpha\uparrow,\delta\downarrow} = \rho_{\beta\downarrow,\gamma\uparrow} = 0.$$

Thus we may show that the ground-state energy functional is given by

$$E\big(\{s^{(1)},\tilde{s}^{(1)}\}\big) = \sum_{\alpha}\varepsilon_\alpha\Bigg(\sum_{\mu}\big(\tilde{s}^{(1)}_{\alpha\mu}s^{(1)}_{\alpha\mu} + \tilde{s}^{(1)}_{\mu\alpha}s^{(1)}_{\mu\alpha}\big)\Bigg)$$

$$+ \sum_{\alpha,\beta,\gamma,\delta} V_{\alpha\beta\gamma\delta}\Bigg(\sum_{\mu}\tilde{s}^{(1)}_{\alpha\mu}s^{(1)}_{\gamma\mu}\sum_{\pi}\tilde{s}^{(1)}_{\pi\beta}s^{(1)}_{\pi\delta}\Bigg) + \sum_{\alpha,\beta,\gamma,\delta} V_{\alpha\beta\gamma\delta}\tilde{s}^{(1)}_{\alpha\beta}\Bigg(s^{(1)}_{\gamma\delta} - \sum_{\pi,\mu}\tilde{s}^{(1)}_{\pi\mu}s^{(1)}_{\pi\delta}s^{(1)}_{\gamma\mu}\Bigg). \tag{5.31}$$

However, we have thus far neglected the number conserving term $-\lambda\big(\hat{N} - N_0\big)$. This simply amounts to adding the terms

$$\lambda N_0 - \lambda\sum_{\mu}\big(\tilde{s}^{(1)}_{\alpha\mu}s^{(1)}_{\alpha\mu} + \tilde{s}^{(1)}_{\mu\alpha}s^{(1)}_{\mu\alpha}\big),$$

to the functional of equation (5.31) since the matrix elements of the number operator

$$\hat{N} = \sum_{\alpha=1}^{M}\hat{a}^{\dagger}_{\alpha,\sigma}\hat{a}_{\alpha,\sigma}, \tag{5.32}$$

are given by the normal density (M here is the total number of states in the system). Thus the *complete* ground-state energy functional is given by

$$E\big(\{s^{(1)},\tilde{s}^{(1)}\}\big) = \lambda N_0 + \sum_{\alpha}\big(\varepsilon_\alpha - \lambda\big)\Bigg(\sum_{\mu}\big(\tilde{s}^{(1)}_{\alpha\mu}s^{(1)}_{\alpha\mu} + \tilde{s}^{(1)}_{\mu\alpha}s^{(1)}_{\mu\alpha}\big)\Bigg)$$

$$+ \sum_{\alpha,\beta,\gamma,\delta} V_{\alpha\beta\gamma\delta}\Bigg(\sum_{\mu}\tilde{s}^{(1)}_{\alpha\mu}s^{(1)}_{\gamma\mu}\sum_{\pi}\tilde{s}^{(1)}_{\pi\beta}s^{(1)}_{\pi\delta}\Bigg) + \sum_{\alpha,\beta,\gamma,\delta} V_{\alpha\beta\gamma\delta}\tilde{s}^{(1)}_{\alpha\beta}\Bigg(s^{(1)}_{\gamma\delta} - \sum_{\pi,\mu}\tilde{s}^{(1)}_{\pi\mu}s^{(1)}_{\pi\delta}s^{(1)}_{\gamma\mu}\Bigg). \quad (5.33)$$

Having calculated the SUB(1) ground-state energy functional, we now wish to solve the ECCM equations for $s^{(1)}$ and $\tilde{s}^{(1)}$. We differentiate equation (5.33) with respect to the general cluster amplitudes $s^{(1)}_{ij}$ and $\tilde{s}^{(1)}_{ij}$, and, after some manipulation (involving relabeling of summation variables and factorising some terms as ρ or κ) we obtain the SUB(1) ECCM equations

$$\frac{\partial}{\partial s^{(1)}_{ij}}E\big(\{s^{(1)},\tilde{s}^{(1)}\}\big) = \big(\varepsilon_i + \varepsilon_j - 2\lambda\big)\tilde{s}^{(1)}_{ij}$$

$$+\sum_{\alpha,\beta} V_{\alpha\beta ij}\tilde{s}^{(1)}_{\alpha\beta} + \sum_{\alpha,\beta,\gamma} V_{\alpha\beta\gamma j}\Big(\rho_{\gamma\uparrow,\alpha\uparrow}\tilde{s}^{(1)}_{i\beta} - \tilde{s}^{(1)}_{\alpha\beta}\rho_{\gamma\uparrow,i\uparrow}\Big)$$

$$+\sum_{\alpha,\beta,\gamma} V_{\alpha\beta i\gamma}\Big(\tilde{s}^{(1)}_{\alpha j}\rho_{\gamma\downarrow,\beta\downarrow} - \tilde{s}^{(1)}_{\alpha\beta}\rho_{\gamma\downarrow,j\downarrow}\Big) = 0,$$

$$\frac{\partial}{\partial \tilde{s}^{(1)}_{ij}}E\big(\{s^{(1)},\tilde{s}^{(1)}\}\big) = \big(\varepsilon_i + \varepsilon_j - 2\lambda\big)s^{(1)}_{ij}$$

$$+\sum_{\gamma,\delta} V_{ij\gamma\delta}\kappa_{\gamma\uparrow,\delta\downarrow} - \sum_{\alpha,\beta,\gamma,\delta} V_{\alpha\beta\gamma\delta}\tilde{s}^{(1)}_{\alpha\beta}s^{(1)}_{i\delta}s^{(1)}_{\gamma j}$$

$$+\sum_{\beta,\gamma,\delta}\Big(V_{\beta j\gamma\delta}\rho_{\gamma\uparrow,\beta\uparrow}s^{(1)}_{i\delta} + V_{i\beta\gamma\delta}s^{(1)}_{\gamma j}\rho_{\delta\downarrow,\beta\downarrow}\Big) = 0. \quad (5.34)$$

We also have the constraint condition

$$\frac{\partial}{\partial\lambda}E\big(\{s^{(1)},\tilde{s}^{(1)}\}\big) = N_0 - \sum_{\alpha,\mu}\big(\tilde{s}^{(1)}_{\alpha\mu}s^{(1)}_{\alpha\mu} + \tilde{s}^{(1)}_{\mu\alpha}s^{(1)}_{\mu\alpha}\big) = 0, \quad (5.35)$$

which trivially fixes N_0 as

$$N_0 = \sum_{\alpha,\mu}\big(\tilde{s}^{(1)}_{\alpha\mu}s^{(1)}_{\alpha\mu} + \tilde{s}^{(1)}_{\mu\alpha}s^{(1)}_{\mu\alpha}\big).$$

These equations are considerably more difficult than any we have solved previously. As such, we write a C++ code in order to solve them, as it is doubtful Mathematica would be able to handle such a task.

5.2.1.4 C++ Code (Solving the ECCM Equations)

In order to solve the ECCM equations in (5.34) subject to the particle number constraint in (5.35), we write a C++ code and utilise a multiple root-finding routine from the GNU Scientific Library (GSL). At the start of a calculation we manually set the total number of particles and hence oscillator shells as well as the standard deviation of the two-body Gaussian potential σ (which we center at the point $\mathbf{r}' = (0, 0, 0)$) and the various trap frequencies $\omega_\perp$ and ω_z. Similar to the anharmonic oscillator studies presented in chapter 3, we work with the natural units $m = \hbar = 1$. We must choose σ to be considerably smaller than our harmonic oscillator bath in order to correctly model a *dilute* condensate (i.e. the range of the two-body interaction must be considerably smaller than the parameters of the harmonic oscillator trap). We feed values for the harmonic oscillator quantum numbers (n_x, n_y, n_z) into the two-body potential in order to evaluate the potential coefficients $V_{\alpha\beta\gamma\delta}$. A random number generator is used to initialise the cluster amplitude matrices $s^{(1)}_{\alpha\beta}$ and $\tilde{s}^{(1)}_{\alpha\beta}$ with small numbers in each element.

Although the overall code is rather more complicated than that used for any of our previous models, the method of solution we employ is fairly simple. By coding the SUB(1) ECCM equations of (5.34) and (5.35) and initialising the cluster amplitudes with small numbers, we employ a "steepest-descent" approach. By finding the gradient of the ECCM equations and then gradually "walking" along them, we attempt to find the minimum of the gradient, and thus the values of the cluster amplitudes which satisfy equations (5.34) and (5.35).

A rather unfortunate problem we encounter with this technique is the sensitivity of the solution method to the starting conditions - it is not obvious *a priori* what the best starting values for the cluster amplitudes should be. When we first began to solve the equations, we employed a random number generator to initialise the cluster amplitudes. If we initialise our problem (unknowingly) with an unphysical solution however, solving the ECCM equations will produce an unphysical answer (the unphysical initial condition naturally converges to a unphysical solution branch). The ECCM answer is unphysical in the sense that it gives state occupation probabilities greater than 1 (in fact, it will pack all N_0 particles into a single oscillator shell). Unfortunately, we have no means to determine an initial set of values for $s^{(1)}_{\alpha\beta}$ and $\tilde{s}^{(1)}_{\alpha\beta}$ that we know for certain are definitely physical and will (hopefully) converge to a physical answer.

Coupled with this, the equations become increasingly more complicated to solve once we factor in a large number particles (which is an absolute necessity in order to accurately model our superfluid condensate). This in turn leads to a summation over a large number of oscillator shells and hence working with increasingly large cluster amplitude matrices. We did not attempt to make use of the *physical subspace condition*

we introduced in the formalism of chapter 2 due to the complicated structure of our abnormal densities. At this stage of our work, the ECCM equations are simply too intractable to solve completely - we must find a way to somehow simplify our approach in order to obtain any meaningful insight.

5.2.1.5 Mathematica Code (Diagonal Approximation)

In order to make some headway into our trap problem we consider taking a step back from solving the full problem using our C++ code. Instead, we attempt to solve the ECCM equations for a simplified case using Mathematica[3]. By assuming that our cluster correlation operators are now diagonal, i.e.

$$\hat{S}_1 = \sum_{\alpha} s^{(1)}_{\alpha\alpha} \hat{a}^{\dagger}_{\alpha,\uparrow} \hat{a}^{\dagger}_{\alpha,\downarrow},$$

$$\hat{\tilde{S}}_1 = \sum_{\alpha} \tilde{s}^{(1)}_{\alpha\alpha} \hat{a}_{\alpha,\downarrow} \hat{a}_{\alpha,\uparrow},$$

then we can greatly simplify computation of the ECCM equations. This is a rather basic approximation to make - indeed it is highly likely there are off-diagonal terms in these matrices that are important - however, we simplify our calculations in this manner in order to obtain a *simple* insight into the problem, without the need for excessive or elaborate computer coding and algebraic manipulation.

In the diagonal approximation, the constrained ground-state energy functional of equation (5.33) simplifies to

$$E\big(\{s^{(1)}, \tilde{s}^{(1)}\}\big) = \lambda N_0 + 2\sum_{\alpha} \big(\varepsilon_\alpha - \lambda\big) \tilde{s}^{(1)}_{\alpha\alpha} s^{(1)}_{\alpha\alpha}$$

$$+ \sum_{\alpha,\beta} V_{\alpha\beta\alpha\beta} \tilde{s}^{(1)}_{\alpha\alpha} s^{(1)}_{\alpha\alpha} \tilde{s}^{(1)}_{\beta\beta} s^{(1)}_{\beta\beta} + \sum_{\alpha,\beta} V_{\alpha\alpha\beta\beta} \tilde{s}^{(1)}_{\alpha\alpha} \big(s^{(1)}_{\beta\beta} - \tilde{s}^{(1)}_{\beta\beta} s^{(1)}_{\beta\beta} s^{(1)}_{\beta\beta}\big), \tag{5.36}$$

and we can now clearly see the equivalence of this matrix form with the ground-state energy functional of equation (2.125) in chapter 2. The SUB(1) ECCM equations are now reduced to

$$\frac{\partial}{\partial s^{(1)}_{ii}} E\big(\{s^{(1)}, \tilde{s}^{(1)}\}\big) = 2\big(\varepsilon_i - \lambda\big) \tilde{s}^{(1)}_{ii}$$

$$+ \sum_{\alpha} V_{i\alpha i\alpha} \tilde{s}^{(1)}_{ii} \rho_{\beta\downarrow,\beta\downarrow} + \sum_{\alpha} V_{\alpha i\alpha i} \rho_{\alpha\uparrow,\alpha\uparrow} \tilde{s}^{(1)}_{ii}$$

$$+ \sum_{\alpha} V_{\alpha\alpha ii} \tilde{s}^{(1)}_{\alpha\alpha} \big(1 - 2\tilde{s}^{(1)}_{ii} s^{(1)}_{ii}\big) = 0,$$

[3] we use Mathematica at this point as a relatively quick and easy way to resolve our previous computational difficulties.

$$\frac{\partial}{\partial \tilde{s}_{ii}^{(1)}} E\big(\{s^{(1)}, \tilde{s}^{(1)}\}\big) = 2\big(\varepsilon_i - \lambda\big) s_{ii}^{(1)}$$
$$+ \sum_{\alpha} V_{i\alpha i\alpha} s_{ii}^{(1)} \rho_{\alpha\downarrow,\alpha\downarrow} + \sum_{\alpha} V_{\alpha i\alpha i} \rho_{\alpha\uparrow,\alpha\uparrow} s_{ii}^{(1)}$$
$$+ \sum_{\alpha} V_{ii\alpha\alpha} \kappa_{\alpha\uparrow,\alpha\downarrow} - \sum_{\alpha} V_{\alpha\alpha ii} \tilde{s}_{\alpha\alpha}^{(1)} s_{ii}^{(1)} s_{ii}^{(1)} = 0, \tag{5.37}$$

and we are now able to find solutions for the trapped condensate by iteration.

An evaluation of the SUB(1) ground-state energy for this model is not of much concern to us, rather, we are more interested in the ground-state *properties* that we can observe from our simplified SUB(1) ECCM solutions. Solving the set of equations in (5.37) *is* important however, since we require the (physically correct) values of the cluster amplitudes $s_{\alpha\alpha}^{(1)}$ and $\tilde{s}_{\alpha\alpha}^{(1)}$ to generate our ECCM wave functions (from which we can derive the aforementioned ground-state properties). At this point there is one final but crucial aspect of these calculations we have yet to discuss - the s-wave scattering length of collisions within the condensate.

s-wave Scattering Length

The most important parameter throughout all of our calculations in this problem is the s-wave scattering length a_s. To be more precise, it is usually the dimensionless parameter $1/k_F a_s$ that is studied in the literature [92, 93] (when considering infinite systems), k_F being the wave number at the Fermi surface. The limits $1/k_F a_s \to \pm\infty$ correspond to BEC and BCS regimes respectively, with the point $1/k_F a_s = 0$ corresponding to the so-called *unitarity* regime, directly in the middle of the crossover where a_s becomes divergent [92]. It is by altering a_s between negative and positive values that will allow us to model the BCS-BEC crossover in our trapped condensate.

In order to actually calculate a_s for our two-body Gaussian potential we use a form of Kohn's variational method, as given in [147]. This entails solving the radial Schrödinger equation for the s-wave wave function $u(r)$ (with a reduced mass of $\frac{1}{2}$ since we are using natural units for $\hbar$ and m). By using a trial form of $u(r)$ that obeys some specific boundary conditions [147] we can determine a_s via a variational calculation.

Figure (5.3) shows a plot of the s-wave scattering length $a_s(V_0, \sigma)$ as a function of the potential strength and the Gaussian width - in fact, we have plotted the variables $-V_0\sigma^2$ against σ/a_s for a fixed value of σ. In calculating $a_s(V_0, \sigma)$ it becomes apparent that the scattering length actually scales as $\sigma f(V_0\sigma^2)$ where f is some function of the product between potential strength and Gaussian width squared. The plot of figure (5.3) remains the same independent of the value of σ and we utilise it in order to determine the strength of the potential V_0 for a given value of a_s. Taking a_s as positive or negative will give us the correct values of V_0 required by our Mathematica code in order to compute quantities in either the BEC or BCS regimes respectively. In order

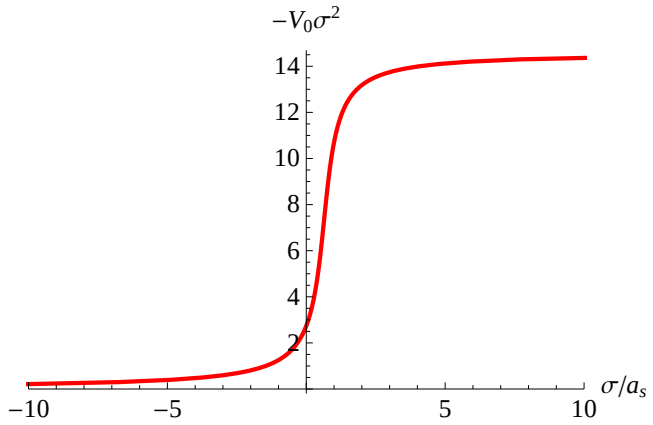

Figure 5.3: Plot of Gaussian potential strength $-V_0\sigma^2$ vs the s-wave scattering length σ/a_s for $\sigma = 0.01$. For a predetermined value of a_s we can find the corresponding strength V_0 from this graph.

to incorporate a_s into the main Mathematica code we actually fit an arctan function to the plot of figure (5.3) and use this to find the necessary values for V_0.

5.2.1.6 Diagonal Approximation Results

The experiments used to investigate BCS-BEC crossover in dilute Fermi gases typically use a large number of either ^6Li [96, 115] or ^{40}K [94, 95, 97] atoms (N_0 is usually of the order 10^6 [94, 96]) and the trap deformation parameter λ is often quite small (usually of the order 0.01 [94, 96, 97]). Given the simplicity of our approach, it is not possible to use values of this order in our equations with any success. Instead, we solve the problem for a sensible set of parameters to describe a dilute quantum degenerate condensate as best possible.

In order to test for evidence of quantum degeneracy we study single-particle occupation probabilities v_k^2 (calculated using the BCS/SUB(1) wave functions) in conjunction with the number of harmonic oscillator shells each calculation uses - we expect to find a high population of particles occupying the lowest shells with the higher shells containing progressively fewer particles until there is zero occupation in the outermost shell. If this pattern is not observed then we modify either N_0 or the number of shells used in each calculation until we can discern an obvious Fermi surface. In the absence of pairing, the Fermi surface appears as a step function when plotted as occupation probability v_k^2 vs single-particle energy ϵ_k, indicating a complete occupation of all levels up to the Fermi energy ϵ_{k_F} [26]. In the presence of pairing however, the sharp edges of this step function become fuzzy on either side - the width of this dispersion indicates the pairing gap Δ_k [26].

Figure (5.4) shows the diagonal BCS/SUB(1) results for a cigar shaped trap containing 100 particles. In the BCS regime, for single-particle energies up to $\epsilon_k = 4$ or so we find a complete occupation of states (oscillator shells) to good approximation and

past single-particle energies of $\epsilon_k = 8$ there is essentially zero occupation. We take this a proof that the Fermi gas is exhibiting quantum degenerate effects (namely that we can observe an almost full Fermi sea). Depletion of the Fermi sea is clearly evident for single-particle energies between $\epsilon_k = 4$ and $\epsilon_k = 8$ and hence constitutes evidence for pairing [26]. Due to the presence of the harmonic trap potential, the lowest single-particle energy is no longer zero[4], thus the overall plot is shifted away from the y-axis by at least an energy factor of 1.7255 when compared with standard BCS theory [26].

In the BEC regime we see a total depletion of all states below the Fermi sea, as opposed to just within the vicinity of the Fermi level for the BCS case. This is evidence to suggest pairing is now taking place throughout all of the states and not simply at the Fermi level [92, 93]. The BEC side also tends to have a rather long tail, meaning a far greater number of oscillator shells need to be taken into account before zero occupation can be observed. At first glance, the top two pictures from either regime appear similar in shape - this is the very hallmark of a crossover and evidence that the condensate does not change abruptly between each limit (as would be expected if the system were to undergo a phase transition between BCS and BEC sides). The bottom picture shows a snapshot of the deep BEC regime - depletion of the Fermi sea is even more apparent here. For comparative purposes, figure (5.5) shows the diagonal BCS/SUB(1) results for a disk shaped trap containing 100 particles[5].

The plots given in figures (5.4) and (5.5) may in some sense be compared with studies of momentum distribution across the BCS-BEC crossover in an infinite system [148, 149]. Whilst figures (5.4) and (5.5) are the BCS/SUB(1) results for *energy* distributions in a finite system, the results for momentum distributions in [148, 149] are in principle alike, and the two separate set of results should be expected to show some similarities. BEC depletion in both of these figures does not appear to be quite as dramatic as that shown in the literature, however, this is likely to be a consequence of working in a relatively small finite system.

It is not possible to push the Mathematica code too far with regards to a larger number of atoms - incorporating more atoms and hence more oscillator shells increases computation time a great deal with either little or no improvement over the results shown (and can lead to the code simply crashing) - nevertheless, we have been able show clear evidence of ground-state pairing effects and BCS-BEC crossover in our model, even when we have reduced the initial nontrivial problem to a simplified case that makes use of a rather crude approximation scheme.

[4] the zeroth energy level of the system is reset to $\epsilon_0 = 1.6 \times 1 + 0.251 \times 0.5 = 1.7255$.

[5] where the zeroth energy level of the system is now reset to $\epsilon_0 = 0.61 \times 1 + 1.6 \times 0.5 = 1.41$.

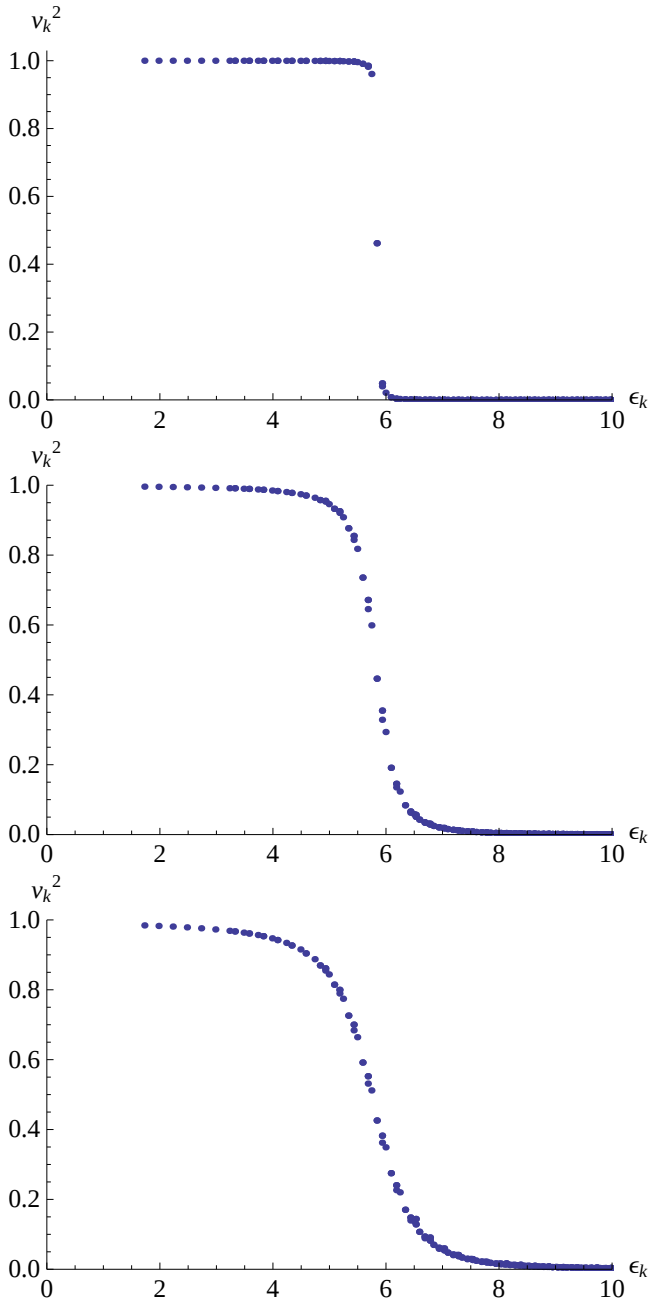

Figure 5.4: Plot of occupation probability v_k^2 vs single-particle energy ϵ_k in a cigar shaped trap ($\omega_\perp = 1.6$, $\omega_z = 0.251$, $\lambda = 0.16$) for $N_0 = 100$ particles and $\sigma = 0.05$. The top picture shows the BCS regime ($\sigma/a_s = -0.5$), the middle picture shows the BEC regime shortly after crossover ($\sigma/a_s = 1$) and the bottom picture shows the deep BEC regime ($\sigma/a_s = 100$).

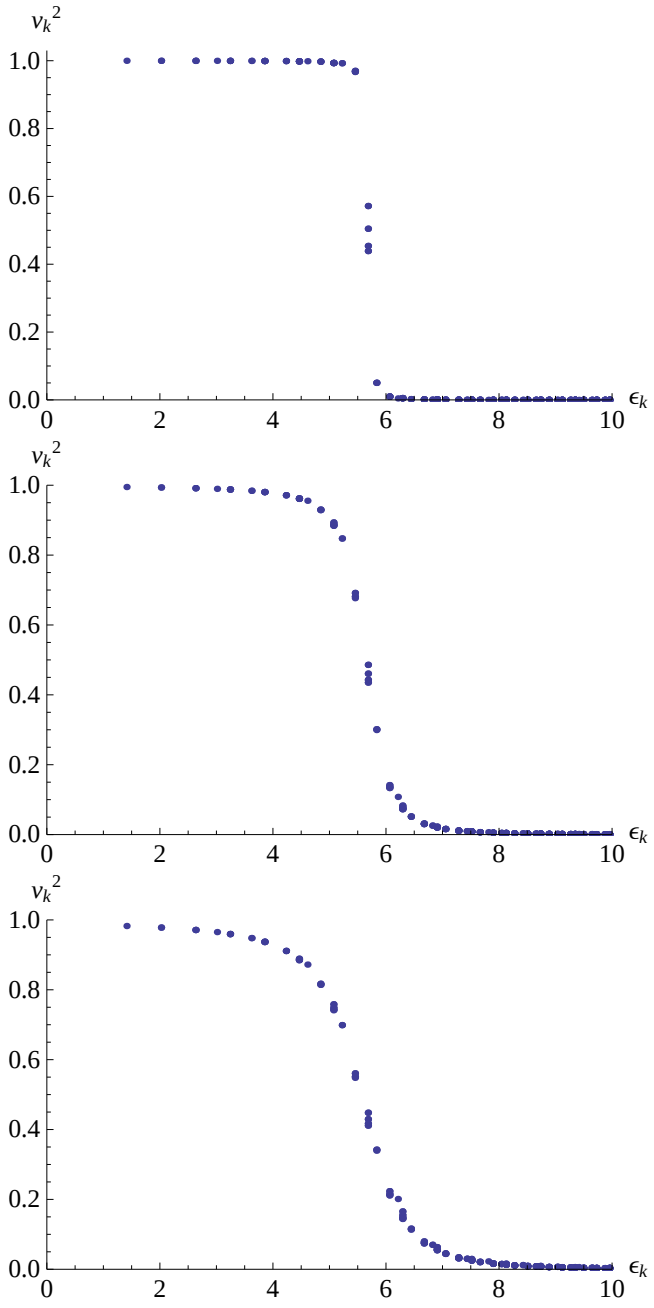

Figure 5.5: Plot of occupation probability v_k^2 vs single-particle energy ϵ_k in a disk shaped trap ($\omega_\perp = 0.61$, $\omega_z = 1.6$, $\lambda = 2.62$) for $N_0 = 100$ particles and $\sigma = 0.05$. The top picture shows the BCS regime ($\sigma/a_s = -0.5$), the middle picture shows the BEC regime shortly after crossover ($\sigma/a_s = 1$) and the bottom picture shows the deep BEC regime ($\sigma/a_s = 100$).

5.3 Collective Modes

As we have just shown, it has not been possible to obtain results for the *complete* BCS/SUB(1) ECCM ground-state energy - instead, we have solved the (simplified) diagonal BCS/SUB(1) problem as a means to investigate ground-state properties of the BCS-BEC crossover. As such, it is obviously not possible to give results for any higher order (complete) ECCM calculations - we could attempt to perform a diagonal second order calculation for the system but it is not obvious whether this would yield anything of great interest (ultimately, a complete second order ECCM calculation would hold much more worth than another simplified calculation). Instead, we will now briefly outline what our approach to calculating the collective modes of this model would have been, provided we had been able to solve the complete BCS/SUB(1) problem.

5.3.1 SUB(2) Calculation

Collective modes in the BCS-BEC crossover are typically studied using the (time-dependent) superfluid hydrodynamic equations [92, 93, 116]. It has been shown recently that BCS theory cannot account for important quantitative details in the collective modes of dilute Fermi gases however [115], and thus methods which go beyond mean-field theory are now being developed to calculate collective modes [116]. Going beyond mean-field in the ECCM approach naturally implies performing a SUB(2) calculation. In this case we would use the cluster correlation operators given by

$$\hat{S}_2 = \frac{1}{2} \sum_{\alpha,\beta,\gamma,\delta} s^{(2)}_{\alpha\beta\gamma\delta} \hat{a}^\dagger_{\alpha,\downarrow} \hat{a}^\dagger_{\beta,\uparrow} \hat{a}^\dagger_{\gamma,\downarrow} \hat{a}^\dagger_{\delta,\uparrow}, \tag{5.38}$$

$$\hat{\tilde{S}}_2 = \frac{1}{2} \sum_{\alpha,\beta,\gamma,\delta} \tilde{s}^{(2)}_{\alpha\beta\gamma\delta} \hat{a}_{\delta,\uparrow} \hat{a}_{\gamma,\downarrow} \hat{a}_{\beta,\uparrow} \hat{a}_{\alpha,\downarrow}, \tag{5.39}$$

and evaluate the ground-state energy functional in the usual fashion.

Clearly from just glancing at these terms we can appreciate how involved the SUB(2) ECCM calculation would be, especially in comparison to the SUB(1) case of equation (5.33) (which itself was already much more complicated than our SUB(1) single-shell pairing functional of equation (4.16)). The SUB(2) cluster operators are now constructed from four single-particle operators and the cluster amplitudes are dependent on four sets of harmonic energy indices - this would result in a large number of extra terms in the ground-state energy functional and an even more complicated set of ECCM equations to solve. It would likely take a substantial amount of time and effort to solve the complete SUB(2) problem, given the difficulties we faced in attempting to solve the initial SUB(1) problem.

In order to calculate the RPA frequencies to SUB(2) and hence the collective excita-

tions of a trapped fermionic atom gas, we would use the (constrained) action functional

$$A = \int_{-\infty}^{+\infty} dt \langle \Phi_0 | e^{\hat{\tilde{S}}(t)} e^{-\hat{S}(t)} \left(\hat{H} - \lambda(\hat{N} - N_0) - i\frac{\partial}{\partial t} \right) e^{\hat{S}(t)} | \Phi_0 \rangle,$$

and write down our time-dependent cluster amplitudes as varying harmonically with respect to time (the *harmonic assumption*). Provided a reliable SUB(2) solution had been obtained for $\langle \hat{H} \rangle$, this step would be relatively straightforward (since all the time-dependence is contained within the cluster amplitudes themselves). By altering the strength of the potential V_0 in relation to the sign of the s-wave scattering length a_s as before, it would be possible to calculate the collective modes of the system in both BCS and BEC limits. Were we able to produce a computer code that was robust enough, i.e. we were able to perform successful calculations for a very large number of atoms, altering the shape of the harmonic trap (varying $\omega_\perp$ and ω_z) to specific values would allow us to make a comparison of our results with recent calculations that utilise a beyond mean-field perturbative approach to collective modes [116].

5.4 Discussion

In this chapter we have presented calculations for a model of fermionic atom pairing, where the atoms are confined in an ellipsoidal harmonic trap at zero temperature. It is designed as a rather simple approximation to model an ultracold dilute gas of trapped fermionic atoms in which BCS-BEC crossover may be observed. Our initial goal was to solve the BCS/SUB(1) ECCM problem for the system using standard particle formalism, in order to investigate ground-state properties either side of the crossover. To overcome some of the initial computational difficulties we encountered for the complete SUB(1) problem, we reduced our calculations to a simplistic diagonal approximation of the ECCM - in essence we solved a simplified mean-field problem (supported by the fact that mean-field theory is known to give a good qualitative description over all regimes of the crossover).

Our results for the diagonal SUB(1) approximation provided strong evidence for pairing in the BCS regime (state depletion and a pairing gap either side of the Fermi surface) as well as in the BEC regime (total depletion of shell occupation, especially notably in the deep BEC regime). Even though our system was relatively small and we were unable to set parameters to the order used in experiments on BCS-BEC crossover (for example, using realistic values for the trapping frequencies and a large number of atoms), we were able to demonstrate BCS-BEC crossover in our model in a transparent manner. Unfortunately, a similar calculation for the collective excitations of the trapped condensate has not been realised. Nevertheless, we have discussed in principle how we would have continued our investigation where possible. Such a

conclusion is regrettable, however, we do believe our work has been fruitful and the foundations of possible future calculations have been laid in place throughout this chapter.

Chapter 6

Summary and Conclusions

The underlying goal of this thesis was to find an optimal formulation of the Coupled Cluster Method engineered towards the study of pairing problems in quantum many-body theory. We have used the standard "particle" form of Extended CCM (albeit in a slightly simplified manner) as well as "quasi-particle" forms of both the Normal and Extended CCM (again there have been certain simplifications used in these approaches). These methods have all been applied to a rather straightforward case study which we termed "single-shell pairing". An attempt to use the Extended CCM to study pairing within a more realistic model (an ultracold dilute gas of fermionic atoms confined within a harmonic trap) has only been partially successful - we have solved a simplified "particle" Extended CCM problem and have provided evidence for BCS-BEC crossover in the model, however, we have been unable to perform a calculation for the collective modes of this system due to time constraints.

Nevertheless, we have uncovered a great deal of useful information from our work on the single-shell pairing model, as demonstrated throughout chapter 4. Our initial research was focused on the use of quasi-particle states and operators in the ECCM formalism. It was our belief that using this picture - as opposed to that of ordinary particle states and operators or the NCCM formalism - we would naturally incorporate a greater number of particle correlations that were present within a many-body system and we could thus produce results which were more accurate than an equivalent particle ECCM approach to the same order of approximation. We chose a completely generic model of pairing between fermions within a finite space (or "shell") - by ensuring that this model had an SU(2) quasi-spin algebra associated with it, and was thus exactly solvable, we would be able to compare and contrast various CCM approaches with the *exact* answer for the model.

The lowest order or SUB(1) approximation of the ECCM is nothing more than the standard mean-field picture. When this calculation is performed relative to a bare particle vacuum $|0\rangle$, it can be made identical to a BCS calculation with a relabeling of cluster amplitudes in terms of the variational BCS parameters u_k and v_k. With that

in mind, we redefined the particle SUB(1) ECCM result as the quasi-particle vacuum. We then introduced a bi-canonical quasi-particle basis, constructed from the actions of the SUB(1) particle operators $\left(\hat{a}_k^\dagger, \hat{a}_k\right)$ (of both normal and time-reversed states) on the SUB(1) ECCM ground-state wave function $\left|\varphi_0\right\rangle$. This was covered separately in the formalism of chapter 2. Although we had also shown that the ECCM could be written in terms of the normal and abnormal densities of the HFB method, evaluating the matrix elements which make up the ground-state energy functional for the single-shell pairing case was rather simple, due to the inherent SU(2) quasi-spin algebra of the model.

Before we attempted to calculate the quasi-particle ECCM solutions, we utilised the particle ECCM formalism, as a test of sorts for our computational techniques and to obtain an understanding of what we might expect from the quasi-particle approach. Going beyond the BCS/SUB(1) mean-field solution we saw the usual multiple solution branches that the CCM produces. By following particle number fluctuation concurrently, we were able to determine any branches which became unphysical (i.e. had a negative particle number fluctuation). Up to the middle of the shell, the physical SUB(2) solution made a marked improvement over the BCS/SUB(1) result. For a large state degeneracy Ω we saw the SUB(2) result become increasingly closer to the exact answer, although the improvement was always better from the empty shell to mid-shell, as opposed to mid-shell to full shell. We therefore decided to focus on particle calculations relative to a bare particle vacuum $\left|0\right\rangle$ between empty and mid-shell and hole calculations relative to a filled Hartree-Fock state $\left|\mathrm{HF}\right\rangle$ working backwards from the full shell to mid-shell. Continuing up to SUB(4) approximation with this scheme using $\Omega = 10$ we saw a gradual convergence towards the exact ground-state energy, although there was clearly a limit as to how much we could improve our ECCM estimate.

At the SUB(4) level of the particle ECCM where the degeneracy of states Ω was equal to n (which also coincides with the SUB(4) NCCM for this model) we saw a rather odd occurrence - we observed only four solution branches (there were a great deal more for the SUB(3) case) and although we saw solutions which matched the correct answer, they all occurred on different branches. Since we would usually like to assume that a physical CCM solution must be smoothly and continuously connected to the model state, which is clearly not seen for this particular case, we used this as evidence to support our initial idea of using a quasi-particle approach, instead of a standard particle one.

Since the particle SUB(1) ECCM acts as the vacuum to our quasi-particle formalism, the lowest natural truncation we can make in the quasi-particle picture is the QPSUB(2) approximation (also known as the use of "Brueckner orbitals" in quantum chemistry). By rewriting the initial Hamiltonian in terms of quasi-particle operators, as well as altering the resultant SU(2) quasi-spin algebra to reflect this change of opera-

tors, it was relatively simple to convert previous particle calculations into quasi-particle calculations. One immediate difference of using quasi-particles became apparent - it was not possible to find all real solution branches between QPSUB(2) and QPSUB(4) as it had been for the particle case. The equations were simply too ill-behaved and the solutions too numerous in order to achieve this. Not only that, there were some worrying signs to come from the lowest order solution - whereas the particle SUB(2) case had shown an improved estimate for the ground-state energy for increasing Ω, the quasi-particle QPSUB(2) case, although stable for small Ω, began to show a collapse at mid-shell - the branch simply plummets towards negative infinity. This was to become worse the greater Ω became.

This collapse was not observed for the QPSUB(3) solution although it was seen again at QPSUB(4) - a strange pattern was to develop showing a convergence of solutions at odd order approximations and a mid-shell collapse of solutions at even order approximations. At this stage we had no clear understanding of why this was happening. Dropping down to a quasi-particle NCCM picture, we were quite surprised to find a rather stable QPSUB(2) solution, which became increasingly better for larger Ω - there was still a minor discrepancy at mid-shell but this was not unphysical, i.e. the particle number fluctuation did not become negative, and it was certainly not as pronounced as the problem of the QPSUB(2) ECCM solution. Regrettably, when increasing truncation in the NCCM quasi-particle picture past QPSUB(2), we again found a collapse of the solutions around mid-shell.

As a possible means of determining why the quasi-particle ECCM formalism failed in the way it did, we sought to calculate the excitation spectrum of the model, relative to the ground-state solution. Hence we performed an RPA calculation for both particle and quasi-particle ECCM cases, focusing on excited-states possessing the same symmetry as the ground-state. The RPA frequencies (excitation energies) in the particle case were rather uninteresting - this is arguably a testament to the stability of the approach. On the other hand, the RPA frequencies in the quasi-particle case were very curious - at even orders of truncation we see an odd number of modes which collapse around mid-shell (excluding zero modes) but for odd orders of truncation we see an even number of modes meet in pairs and become complex (again, excluding zero modes). The higher the QPSUB(n) approximation becomes, the further these collapses are observed from the mid-shell. These results go some way to explaining the observed even/odd pattern of quasi-particle ECCM solutions collapsing/converging for the ground-state energy.

Ultimately we have reached the conclusion that the quasi-particle ECCM approach should not be trusted - low order (e.g. SUB(2)) particle ECCM calculations as well as low order (e.g. QPSUB(2)) quasi-particle NCCM calculations show encouraging signs, especially when analysed concurrently with particle number fluctuation, which allows

us to easily determine unphysical solutions. Although all of the different approaches are not without their own problems or limitations, it is these two cases - particularly low order particle ECCM - which have been shown to perform rather admirably. It is our belief that in applying these particular approaches to more realistic models of pairing in larger model spaces (which, unfortunately, we have been unable to do) the issues and defects we have exposed will not be as important.

Further Work

Although much of the work presented in chapter 3 has already been performed by others previously, it is to the author's best knowledge that no ECCM calculations of anharmonic oscillator models, particularly the double-well oscillator model stipulated in chapter 3, have been published. Due to time constraints it was not possible to complete ECCM studies of these models past the SUB(2) approximation, nor was it possible to investigate the use of translationally shifted model states, as a means to calculate the energy level splittings associated with double-well oscillators. Implementing a solution following routine and focusing on the physical solution branches at high order SUB(n) for this problem could be rather interesting. There is clearly room for further investigation of this model using ECCM techniques.

Quite obviously, the initial work laid out in chapter 5 remains incomplete. First and foremost, the complete BCS/SUB(1) ECCM calculation for the ground-state energy of our model would need to be concluded. Although this would simply represent a mean-field result, it would be intriguing to compare the CCM result to those of other quantum many-body methods for similar models (for example, quantum Monte Carlo techniques). Following this, a complete SUB(2) calculation would then be required - this would provide the basis on which a SUB(2) RPA calculation could be performed. Ultimately we would have liked to have accomplished the solutions for this scheme as it would represent the first application of CCM techniques to the rather modern study of collective modes in the BCS-BEC crossover problem. Nevertheless, it is the author's belief that we have laid a suitable foundation upon which further investigations of this problem can be built.

Bibliography

[1] A. Einstein, *Über einen die Erzeugung und Verwandlung des Lichtes betreffenden heuristischen Gesichtspunkt (On a Heuristic Point of View Concerning the Generation and Conversion of Light*), Ann. der Phys. **17** (1905) 132

[2] S. Gasiorowicz, *Quantum Physics* (John Wiley & Sons, Inc., Second Edition, 1996)

[3] M. Planck, *Über das Gesetz der Energieverteilung im Normalspektrum (On the Law of Distribution of Energy in the Normal Spectrum)*, Ann. der Phys. **4** (1901) 553

[4] N. Bohr, *On the Constitution of Atoms and Molecules*, I. Phil. Mag. **26** (1913) 1

[5] N. Bohr, *On the Quantum Theory of Line-spectra*, D. KGL. Danske Vidensk. Selsk. Skrifter, naturvidensk. og mathem. Afd. 8. Raekke, **IV**.1 (1918) 1

[6] A. H. Compton, *A Quantum Theory of the Scattering of X-rays by Light Elements*, Phys. Rev. **21** (1923) 483

[7] L. de Broglie, *Ondes et Quanta (Waves and Quanta*), Compt. Ren. **177** (1923) 507

[8] W. Heisenberg, *Über quantentheoretische Umdeutung kinematischer und mechanischer Beziehungen (Quantum Theoretical Re-interpretation of Kinematic and Mechanical Relations)*, Zeits. f. Phys. **33** (1925) 879; M. Born and P. Jordan, *Zur Quantenmechanik (On Quantum Mechanics*), Zeits. f. Phys. **34** (1925) 858; M. Born, W. Heisenberg, P. Jordan, *Zur Quantenmechanik II (On Quantum Mechanics* II), Zeits. f. Phys. **35** (1926) 557

[9] E. Schrödinger, *Quantizierung als Eigenwertproblem (Erste Mitteilung) (Quantization as a Problem of Proper Values. Part I.)*, Ann. der Phys. **79** (1926) 361

[10] E. Schrödinger, *Über das Verhältnis der Heisenberg Born Jordanischen Quantenmechanik zu der meinen (On the Relation Between the Quantum Mechanics of Heisenberg, Born, and Jordan, and that of Schrödinger)*, Ann. der Phys. **79** (1926) 734

[11] P.A. M. Dirac, *The Fundamental Equations of Quantum Mechanics*, Proc. Roy. Soc. **109** (1925) 642

[12] P. A. M. Dirac, *A New Notation for Quantum Mechanics*, Proc. Camb. Phil. Soc. **35** (1939) 416

[13] P. A. M. Dirac, *The Quantum Theory of the Electron*, Proc. Roy. Soc. **A 117** (1928) 610; **A 118** (1928) 351

[14] A. I. M. Rae, *Quantum Mechanics* (Institute of Physics, Fourth Edition, 2002)

[15] M. Maggiore, *A Modern Introduction to Quantum Field Theory* (Oxford University Press, 2005)

[16] P. A. Martin and F. Rothen, *Many-Body Problems and Quantum Field Theory* (Springer, Second Edition, 2004)

[17] R. F. Bishop, *The Coupled Cluster Method*, in "Lecture Notes in Physics", Microscopic Quantum-Many Body Theories and their Applications, **Vol. 510/1998**, (Springer Berlin / Heidelberg 1998) 1

[18] R. F. Bishop and H. G. Kümmel, *The coupled-cluster method*, Phys. Today **40** (3) (1987) 52

[19] K. Emrich and J. G. Zabolitzky, *Coupled cluster equations for superconducting systems*, in "Lecture Notes in Physics", **Vol. 198**, (1984) 271

[20] K. Emrich and J. G. Zabolitzky, *Electron correlations in the Bogoljubov coupled-cluster formalism*, Phys. Rev. B **30** (1984) 2049

[21] R. F. Bishop and W. A. Lahoz, *Two-component Fermi systems. I. Fluid coupled cluster theory*, J. Phys. A: Math. Gen. **20** (1987) 4203

[22] R. F. Bishop and W. A. Lahoz, *Two-component Fermi systems. II. Superfluid coupled cluster theory*, Z. Phys. B **73** (1988) 363

[23] R. D. Mattuck, *A Guide to Feynman Diagrams in the Many-body Problem* (Dover, Second Edition, 1992)

[24] J. Bardeen, L. N. Cooper and J. R. Schrieffer, *Microscopic Theory of Superconductivity*, Phys. Rev. **106** (1957) 162

[25] J. Bardeen, L. N. Cooper and J. R. Schrieffer, *Theory of Superconductivity*, Phys. Rev. **108** (1957) 1175

[26] P. Ring and P. Schuck, *The Nuclear Many-Body Problem* (Springer, Study Edition, 2004)

[27] B. Mihaila and J. H. Heisenberg, *Microscopic Calculation of the Inclusive Electron Scattering Structure Function in* ^{16}O, Phys. Rev. Lett. **84** (2000) 1403

[28] A. L. Fetter and J. D. Walecka, *Quantum theory of many-particle systems* (Dover Publications, Inc., 2003 - reprinting of the seventh printing of the 1971 McGraw-Hill Book Company published edition)

[29] E. Caliceti, M. Meyer-Hermann, P. Ribeca, A. Surzhykov, U. D. Jentschura, *From useful algorithms for slowly convergent series to physical predictions based on divergent perturbative expansions*, Phys Rep. **446** (2007) 1

[30] J. Goldstone, *Derivation of the Brueckner Many-Body Theory*, Proc. Roy. Soc. A **239** (1957) 267

[31] B. D. Day, *Elements of the Brueckner-Goldstone Theory of Nuclear Matter*, Rev. Mod. Phys. **39** (1967) 719

[32] A. Szabo and N. S. Ostlund, *Modern Quantum Chemistry: Introduction to Advanced Electronic Structure Theory* (Dover Publications, Inc., 1996)

[33] D. Binosi and L. Theußl, *JaxoDraw: A graphical user interface for drawing Feynman diagrams*, Comput. Phys. Commun. **161** (2004) 76

[34] K. A. Brueckner, *Many-Body Problem for Strongly Interacting Particles. II. Linked Cluster Expansion*, Phys. Rev. **100** (1955) 36

[35] J. S. Arponen, *Independent-cluster methods as mappings of quantum theory into classical mechanics*, Theor. Chim. Acta **80** (1990) 149

[36] J. S. Arponen and R. F. Bishop, *Independent-Cluster Parametrizations of Wave Functions in Model Field Theories. I. Introduction to Their Holomorphic Representations*, Ann. Phys. **207** (1991) 171

[37] J. S. Arponen and R. F. Bishop, *Independent-Cluster Parametrizations of Wave Functions in Model Field Theories. II. Classical Mappings and Their Algebraic Structure*, Ann. Phys. **227** (1993) 275

[38] J. S. Arponen and R. F. Bishop, *Independent-Cluster Parametrizations of Wave Functions in Model Field Theories. III. The Coupled-Cluster Phase Spaces and Their Geometrical Structure*, Ann. Phys. **227** (1993) 334

[39] H. G. Kümmel, *A Biography of the Coupled Cluster Method*, Int. J. Mod. Phys. B **17** (2003) 5311

[40] R. K. Nesbet, *Brueckner's Theory and the Method of Superposition of Configurations*, Phys. Rev. **109** (1958) 1632

[41] R. J. Bartlett and M. Musial, *Coupled-cluster theory in quantum chemistry*, Rev. Mod. Phys. **79** (2007) 219

[42] J. Arponen, *Variational principles and Linked-Cluster expS expansions for static and dynamic Many-Body problems*, Ann. Phys. **151** (1983)

[43] F. Coester, *Bound states of a many-particle system*, Nucl. Phys. **7** (1958) 421

[44] F. Coester and H. Kümmel, *Short-range correlations in nuclear wave functions*, Nucl. Phys. **17** (1960) 477

[45] J. Čížek, *On the Correlation Problem in Atomic and Molecular Systems. Calculation of Wavefunction Components in Ursell-Type Expansion Using Quantum-Field Theoretical Methods*, J. Chem. Physics **45** (1966) 4256

[46] J. Čížek and J. Paldus, *Correlation Problems in Atomic and Molecular Systems III. Rederivation of the Coupled-Pair Many-Electron Theory Using the Traditional Quantum Chemical Methods*, Int. J. Quantum Chem. **5** (1971) 359

[47] J. Paldus, J. Čížek and I. Shavitt, *Correlation Problems in Atomic and Molecular Systems. IV. Extended Coupled-Pair Many-Electron Theory and Its Application to the BH_3 Molecule*, Phys. Rev. A **5** (1972) 50

[48] J. Hubbard, *The Description of Collective Motions in Terms of Many-Body Perturbation Theory*, Proc. Roy. Soc. A **240** (1957) 539

[49] N. M. Hugenholtz, *Perturbation approach to the Fermi gas model of heavy nuclei*, Physica **23** (1957) 481

[50] N. M. Hugenholtz, *Perturbation theory of large quantum systems*, Physica **23** (1957) 533

[51] R. F. Bishop, *A tribute to Hermann Kümmel on his 80th birthday*, Int. J. Mod. Phys. B **17** (2003) 5295

[52] M. Gari, H. Kümmel and J. G. Zabolitzky, *Short-range correlations and parity impurities*, Nucl. Phys. **A161** (1971) 625

[53] H. Kümmel, *Theory of many-body wave functions with correlations*, Nucl. Phys. **A176** (1971) 205

[54] H. Kümmel and K. H. Lührmann, *Equations for linked clusters and the energy variational principle*, Nucl. Phys. **A191** (1972) 525

[55] K. H. Lührmann and H. Kümmel, *Equations for linked clusters and Brueckner-Bethe theory*, Nucl. Phys. **A194** (1972) 225

[56] H. Kümmel and J. G. Zabolitzky, *Fully Self-Consistent Brueckner-Hartree-Fock and Renormalized Brueckner-Hartree-Fock Calculation for* ^4He *and* ^{16}O, Phys. Rev. C **7** (1973) 547

[57] R. Offermann, W. Ey and H. Kümmel, *Degenerate many fermion theory in expS form*, Nucl. Phys. **A273** (1976) 349

[58] R. Offermann, *Degenerate many fermion theory in expS form (II). Comparison with perturbation theory*, Nucl. Phys. **A273** (1976) 368

[59] W. Ey, *Degenerate many fermion theory in expS form (III). Linked valence expansions*, Nucl. Phys. **A296** (1978) 189

[60] K. H. Lührmann, *Equations for Subsystems*, Ann. Phys. **Vol. 103** (1977) 253

[61] H. J. Lipkin, N. Meshkov and A. J. Glick, *Validity of many-body approximation methods for a solvable system (I). Exact Solutions and Perturbation Theory*, Nucl. Phys. **62** (1965) 188

[62] N. Meshkov, A. J. Glick and H. J. Lipkin, *Validity of many-body approximation methods for a solvable system (II). Linearization Procedures*, Nucl. Phys. **62** (1965) 199

[63] A. J. Glick, H. J. Lipkin and N. Meshkov *Validity of many-body approximation methods for a solvable system (III). Diagram Summations*, Nucl. Phys. **62** (1965) 211

[64] P. Hoodbhoy and J. W. Negele, *Time-dependent coupled-cluster approximation to nuclear dynamics. I. Application to a solvable model*, Phys. Rev. C **18** (1978) 2380

[65] E. Dalgaard and H. J. Monkhurst, *Some aspects of the time-dependent coupled-cluster approach to dynamic response functions*, Phys. Rev. A **28** (1983) 1217

[66] H. Kümmel, K. H. Lührmann and J. G. Zabolitzky, *Many-fermion theory in expS (or coupled cluster) form*, Phys. Rep. **36**C (1978) 1

[67] R. F. Bishop and K. H. Lührmann, *Electron correlations: I. Ground-state results in the high-density regime*, Phys. Rev. B **17** (1978) 3757

[68] R. F. Bishop and K. H. Lührmann, *Electron correlations: II. Ground-state results at low and metallic densities*, Phys. Rev. B **26** (1982) 5523

[69] K. Emrich, *An extension of the coupled cluster formalism to excited states (I)*, Nucl. Phys. **A351** (1981) 379

[70] K. Emrich, *An extension of the coupled cluster formalism to excited states (II) Approximations and tests*, Nucl. Phys. **A351** (1981) 397

[71] K. Emrich and J. G. Zabolitzky, *Negative parity states in ^{16}O from coupled-cluster equations*, Nucl. Phys. **A351** (1981) 439

[72] B. D. Day and J. G. Zabolitzky, *Coupled-cluster calculation for nuclear matter and comparison with the hole-line expansion*, Nucl. Phys. **A366** (1981) 221

[73] J. Arponen and J. Rantakivi, *The Lipkin pseudospin model in the variational expS formalism*, Nucl. Phys. **A407** (1983) 141

[74] J. S. Arponen, R. F. Bishop and E. Pajanne, *Extended coupled cluster method I. Generalised coherent bosonization as a mapping of quantum theory into classical Hamiltonian mechanics*, Phys. Rev. A **36** (1987) 2519

[75] J. S. Arponen, R. F. Bishop and E. Pajanne, *Extended coupled cluster method II. Excited states and generalized random-phase approximation*, Phys. Rev. A **36** (1987) 2539

[76] J. S. Arponen, R. F. Bishop, E. Pajanne and N. I. Robinson, *Extended coupled cluster method III. Zero-temperature hydrodynamics of a condensed Bose fluid*, Phys. Rev. A **37** (1988) 1065

[77] N. I. Robinson, R. F. Bishop and J. Arponen, *Extended coupled cluster method IV. An excitation energy functional and applications to the Lipkin model*, Phys. Rev. A **40** (1989) 4256

[78] U. Kaulfuss, *Renormalization of the coupled cluster equations in three-dimensional ϕ^4 quantum field theory*, Phys. Rev. D **32** (1985) 1421

[79] C. S. Hsue, H. Kümmel and P. Ueberholz, *Coupled cluster description of field theories: Procedures and their applications to the vacuum sector in (1+1)-dimensional Φ^4 field theories*, Phys. Rev. D **32** (1985) 1435

[80] U. B. Kaulfuss and M. Altenbokum, *Anharmonic oscillator as a test of the coupled cluster method*, Phys. Rev. D **33** (1986) 3658

[81] G. Sanyal, S. H. Mandal and D. Mukherjee, *Thermal averaging in quantum many-body systems: a non-perturbative thermal cluster cumulant approach*, Chem. Phys. Lett. **192** (1992) 55

[82] J. H. Heisenberg and B. Mihaila, *Ground state correlations and mean field in ^{16}O*, Phys. Rev. C **59** (1999) 1440

[83] B. Mihaila and J. H. Heisenberg, *Center-of-mass corrections reexamined: A many-body expansion approach*, Phys. Rev. C **60** 054303 (1999)

[84] B. Mihaila and J. H. Heisenberg, *Ground state correlations and mean field in ^{16}O II. Effects of a three-nucleon interaction*, Phys. Rev. C **61** 054309 (2000)

[85] K. Kowalski, D. J. Dean, M. Hjorth-Jensen, T. Papenbrock and P. Piecuch, *Coupled Cluster Calculations of Ground and Excited States of Nuclei*, Phys. Rev. Lett. **92** 132501 (2004)

[86] D. J. Dean and M. Hjorth-Jensen, *Coupled-cluster approach to nuclear physics*, Phys. Rev. C **69** 054320 (2004)

[87] M. Wloch, D. J. Dean, J. R. Gour, M Hjorth-Jensen, K. Kowalski, T. Papenbrock and P. Piecuch, *Ab-Initio Coupled-Cluster Study of ^{16}O*, Phys. Rev. Lett. **94** 212501 (2005)

[88] J. R. Gour, P. Piecuch, M. Hjorth-Jensen, M. Wloch and D. J. Dean, *Coupled-cluster calculations for valence systems around ^{16}O*, Phys. Rev. C **74** 024310 (2006)

[89] T. Papenbrock, D. J. Dean, J. R. Gour, G. Hagen, M. Hjorth-Jensen, P. Piecuch and M. Wloch, *Coupled-cluster theory for nuclei*, Int. J. Mod. Phys. B **20** (2006) 5338

[90] G. Hagen, T. Papenbrock, D. J. Dean, A. Schwenk, A. Nogga, M. Wloch and P. Piecuch, *Coupled-cluster theory for three-body Hamiltonians*, Phys. Rev. C **76** 034302 (2007)

[91] G. Hagen, T. Papenbrock, D. J. Dean, M. Hjorth-Jensen and B. Velamur Asokan, *Ab initio computation of neutron-rich oxygen isotopes*, Phys. Rev. C **80** 021306 (2009)

[92] S. Giorgini, L. P. Pitaevskii and S. Stringari, *Theory of ultracold atomic Fermi gases*, Rev. Mod. Phys. **80** (2008) 1215

[93] W. Ketterle and M. W. Zwierlein, *Making, probing and understanding ultracold Fermi gases*, e-print arXiv:0801.2500 (2008)

[94] C. A. Regal, C. Ticknor, J. L. Bohn and D. S. Jin, *Creation of ultracold molecules from a Fermi gas of atoms*, Nature **424** (2003) 47

[95] M. Greiner, C. A. Regal and D. S. Jin, *Emergence of a molecular Bose-Einstein condensate from a Fermi gas*, Nature **426** (2003) 537

[96] M. W. Zwierlein, C. A. Stan, C. H. Schunck, S. M. F. Raupach, S. Gupta, Z. Hadzibabic and W. Ketterle, *Observation of Bose-Einstein Condensation of Molecules*, Phys. Rev. Lett. **91** 250401 (2003)

[97] C. A. Regal, M. Greiner and D. S. Jin, *Observation of Resonance Condensation of Fermionic Atom Pairs*, Phys. Rev. Lett. **92** 040403 (2004)

[98] M. W. Zwierlein, J. R. Abo-Shaeer, A. Schirotzek, C. H. Schunck and W. Ketterle, *Vortices and superfluidity in a strongly interacting Fermi gas*, Nature **435** (2005) 1047

[99] D. J. Dean and M. Hjorth-Jensen, *Pairing in nuclear systems: from neutron stars to finite nuclei*, Rev. Mod. Phys. **75** (2003) 607

[100] L. N. Cooper, *Bound electron pairs in a Fermi gas*, Phys. Rev. **104** (1956) 1189

[101] J. F. Annett, *Superconductivity, Superfluids and Condensates* (Oxford University Press, 2004)

[102] A. J. Leggett, *Quantum Liquids: Bose Condensation and Cooper Pairing in Condensed-Matter Systems* (Oxford University Press, 2007)

[103] F. Dalfovo, S. Giorgini, L. P. Pitaevskii and S. Stringari, *Theory of Bose-Einstein condensation in trapped gases*, Rev. Mod. Phys. **71** (1999) 463

[104] A. Bohr, B. R. Mottelson and D. Pines, *Possible Analogy between the Excitation Spectra of Nuclei and Those of the Superconducting Metallic State*, Phys. Rev. **110** (1958) 936

[105] L. N. Cooper, R. L. Mills and A. M. Sessler, *Possible Superfluidity of a System of Strongly Interacting Fermions*, Phys. Rev. **114** (1959) 1377

[106] A. K. Kerman, R. D. Lawson and M. H. Macfarlane, *Accuracy of the Superconductivity Approximation for Pairing Forces in Nuclei*, Phys. Rev. **124** (1961) 162

[107] M. H. Anderson, J. R. Ensher, Mr. R. Matthews and C. E. Wieman, *Observation of Bose-Einstein Condensation in a Dilute Atomic Vapor*, Science **269** (1995) 198

[108] K. B. Davis, M. O. Mewes, M. R. Andrews, N. J. van Druten, D. S. Durfee, D. M. Kurn and W. Ketterle, *Bose-Einstein Condensation in a Gas of Sodium Atoms*, Phys. Rev. Lett. **75** (1995) 3969

[109] B. DeMarco and D. S. Jin, *Onset of Fermi Degeneracy in a Trapped Atomic Gas*, Science **285** (1999) 1703

[110] D. M. Eagles, *Possible Pairing without Superconductivity at Low Carrier Concentrations in Bulk and Thin-Film Superconducting Semiconductors*, Phys. Rev. **186** (1969) 456

[111] A. J. Leggett, *Cooper pairing in spin-polarized Fermi systems*, J. Phys. **41** (1980) C7

[112] P. Nozières, S. Schmitt-Rink, *Bose Condensation in an Attractive Fermion Gas: From Weak to Strong Coupling Superconductivity*, J. Low. Temp. Phys. **59** (1985) 195

[113] C. A. R. Sá de Melo, M. Randeria and J. R. Engelbrecht, *Crossover from BCS to Bose Superconductivity: Transition Temperature and Time-Dependent Ginzburg-Landau Theory*, Phys. Rev. Lett. **71** 3202 (1993)

[114] M. Bartenstein, A. Altmeyer, S. Riedl, S. Jochim, C. Chin, J. Hecker Denschlag and R. Grimm, *Collective Excitations of a Degenerate Gas at the BEC-BCS Crossover*, Phys. Rev. Lett. **92** 203201 (2004)

[115] A. Altmeyer, S. Riedl, C. Kohstall, M. J. Wright, R. Geursen, M. Bartenstein, C. Chin, J. Hecker Denschlag and R. Grimm, *Precision Measurements of Collective Oscillations in the BEC-BCS Crossover*, Phys. Rev. Lett. **98** 040401 (2007)

[116] S. Cao, Y. L. Ma and G. Huang, *Collective modes of trapped superfluid Fermi gases in the BCS-BEC crossover beyond the mean-field approximation*, Phys. Rev. A **79** 013620 (2009)

[117] H. Kümmel, *Origins of the Coupled Cluster Method*, Theor. Chim. Acta **80** (1991) 81

[118] R. F. Bishop, *An overview of coupled cluster theory and its applications in physics*, Theor. Chim. Acta **80** (1991) 95

[119] M. Gell-Mann and F. Low, *Bound states in quantum field theory*, Phys. Rev. **84** (1951) 350

[120] J. B. Marion and S. T. Thornton, *Classical dynamics of particles and systems* (Harcourt College Publishers, Fourth Edition, 1995)

[121] J. Arponen, *Constrained Hamiltonian approach to the phase space of the coupled cluster method*, Phys. Rev. A **55** (1997) 2686

[122] C. M. Bender and T. T. Wu, *Anharmonic Oscillator*, Phys. Rev. **184** (1969) 1231

[123] R. Balsa, M. Plo, J. G. Esteve and A. F. Pacheco, *Simple procedure to compute accurate energy levels of a double-well anharmonic oscillator*, Phys. Rev. D **28** (1983) 1945

[124] C. E. Reid, *Energy eigenvalues and matrix elements for the quartic oscillator*, J. Mol. Spectrosc. **36** (1970) 183

[125] R. F. Bishop and M. F. Flynn, *Variational and coupled cluster calculations of the spectra of anharmonic oscillators*, Phys. Rev. A **38** (1988) 2211

[126] R. F. Bishop, M. C. Bosca and M. F. Flynn, *An energy-replicating class of non-renormalisable supercoherent states*, Phys. Lett. A **132** (1988) 440

[127] R. F. Bishop, M. C. Bosca and M. F. Flynn, *Nonuniqueness in the energy spectra of anharmonic oscillators using the coupled cluster method*, Phys. Rev. A **40** (1989) 3484

[128] S.J. Chang, *Quantum fluctuations in a φ^4 field theory. I. Stability of the vacuum*, Phys. Rev. D **12** (1975) 1071

[129] F. J. Dyson, *Divergence of Perturbation theory in Quantum Electrodynamics*, Phys. Rev. **85** (1952) 631

[130] J. J. Loeffel, A. Martin, B. Simon and A. S. Wightman, *Pade approximants and the anharmonic oscillator*, Phys. Lett. **30B** (1969) 656

[131] S. Graffi, V. Grecchi and B. Simon, *Borel summability: Application to the anharmonic oscillator*, Phys. Lett. **32B** (1970) 631

[132] C. S. Hsue and J. L. Chern, *Two-step approach to one-dimensional anharmonic oscillators*, Phys. Rev. D **29** (1984) 643

[133] K. Banerjee and S. P. Bhatnagar, *Two-well oscillator*, Phys. Rev. D **18** (1978) 4767

[134] C. Schwartz, *A study of some approximation schemes in quantum mechanics*, Ann. Phys. **32** (1965) 277

[135] E. M. Harrell, *Double Wells*, Commun. Math. Phys. **75** (1980) 239

[136] S. K. Bhattacharya, *Modified semiclassical quantisation for double minimum potentials: Applications to anharmonic oscillators*, Phys. Rev. A **31** (1985) 1991

[137] E. Gildener and A. Patrascioiu, *Pseudoparticle contributions to the energy spectrum of a one-dimensional system*, Phys. Rev. D **16** (1977) 423

[138] R. J. W. Hodgson and Y. P. Varshni, *Splitting in a double-minimum potential with almost twofold degenerate lower levels*, J. Phys. A **22** (1989) 61

[139] C. S. Park, M. G. Jeong, S-K. Yoo and D. K. Park, *Double-well potential: The WKB approximation with phase loss and anharmonicity effect*, Phys. Rev. A **58** (1998) 3443

[140] M. R. M. Witwit, *Energy levels of double-well potentials in a three-dimensional system*, J. Math. Phys. **36** (1995) 187

[141] F. Arias de Saavedra and E. Buendía, *Perturbative-variational calculations in two-well anharmonic oscillators*, Phys. Rev. A **42** (1990) 5073

[142] R. W. Richardson, *A restricted class of exact eigenstates of the pairing-force Hamiltonian*, Phys. Lett. **3** (1963) 277

[143] R. W. Richardson and N. Sherman, *Exact eigenstates of the pairing-force Hamiltonian*, Nucl. Phys. **52** (1964) 221

[144] A. K. Kerman, *Pairing Forces and Nuclear Collective Motion*, Ann. Phys. **12** (1961) 300

[145] H. F. Jones, *Groups, representations and physics* (Institute of Physics, Second Edition, 2003)

[146] H. Feshbach, *A Unified Theory of Nuclear Reactions II*, Ann. Phys. **19** (1962) 287

[147] T. Ohmura, *Variational Method for Scattering Length*, Phys. Rev. **124** (1961) 130

[148] L. Viverit, S. Giorgini, L. P. Pitaevskii and S. Stringari, *Momentum distribution of a trapped Fermi gas with large scattering length*, Phys. Rev. A **69** 013607 (2004)

[149] C. A. Regal, M. Greiner, S. Giorgini, M. Holland and D. S. Jin, *Momentum Distribution of a Fermi Gas of Atoms in the BCS-BEC Crossover*, Phys. Rev. Lett. **95** 250404 (2005)